OPTIMAL CONTROL OF A STEPPING MOTOR

Melvin E. Steele, M.Sc.

Ph.D. Thesis

September, 1974.

Department of Electrical Engineering

THE UNIVERSITY OF ASTON IN BIRMINGHAM.

SUMMARY

Over the past few years the stepping motor has been the subject of detailed study by manufacturers, users and research workers. This interest arises from the rapidly increasing demand for digital actuators, particularly in the machine tool and computer peripheral industries. The optimal control of a stepping motor is expected to play an important role in producing high performance positioning systems for these and other types of applications. Therefore the object of this thesis is to study some of the problems facing the systems engineer who has to design this type of system.

After a general introductory chapter which reviews selected topics thought to be directly relevant to the production of an optimum system the work falls, broadly, into two parts.

The first part (chapters 2-4) presents a method of modelling stepping motors in terms of electrical and magnetic equivalent circuits. 'Exact' and simplified models for a permanent magnet motor are presented, and simple linear and non-linear models are used to theoretically optimise the input variables.

The second part (chapters 5-6) is devoted to the drive circuit and the control of stepping motors. A thyristor inverter circuit is presented, which could possibly be used to drive a power stepping motor, and which can be readily used for closed-loop control of the machine. Optical and electronic methods of phase angle control are discussed and a digital method of accurate phase angle control is developed. Finally, a computer controlled stepping motor drive system is described in which the computer is able to delegate various duties. Particularly the important function of switching in an optimal way to a simple smaller local controller.

INDEX

LIST OF PRINCIPAL SYMBOLS

a	=	phase angle of I w.r.t. Cw
A_o, A_1...	=	position logic signals
β	=	impedance angles
B	=	switching matrix
γ	=	phase angle of V w.r.t. Cw
C	=	e.m.f. constant
CB	=	control logic signals
CL	=	current logic signals
CLK	=	clock logic signals
δ	=	phase angle of I_m w.r.t. Cw
D	=	driving signals
ε	=	phase angle of V_m w.r.t. Cw
E,e	=	e.m.f.
EC	=	electrical circuit
ζ	=	damping factor
F	=	'forward' logic signal
F,f	=	constant and instantaneous value of m.m.f.
G	=	thyristor gate signals
η	=	efficiency
h	=	control transition matrix
I,i	=	constant and instantaneous value of current
K,k,ℓ	=	constants
λ	=	Lagrangian multipliers, eigenvalues
Λ	=	permeance
L	=	inductance
$\mathcal{L}$	=	transference
μ	=	permeability
MC	=	magnetic circuit
m	=	number of phases, number of pulses generated in time t_r

N = effective series turns per phase

N_p = turns per pole

n = No. of identical sections

n_s = No. of identical sections wound in series

θ_e, θ_m = electrical and mechanical angular position of rotor respectively

θ_w = angular width of pulse

P = power

PA,PB = optical signals

PC = checked values of PH

PH = signals derived from photo transistor

PL = latched value of PH

σ = eigenvalue real part

R = resistance, 'reverse' logic signal, input transition matrix

$R_o, R_1 \ldots$ = input logic signals from local controller

r = integer, input

$S_o, S_1 \ldots$ = output logic signals to local controller

S_2 = number of rotor teeth

SB = switching decision logic signal

S_c = scaling factor

SD = sequence detection logic signal

SN = sign of position logic signal

τ = time constant

t = time

t_r = reset clock period

T = torque, input pulse period

$\not{\Phi}, \not{\phi}$ = transition matrices

$\not{\phi}$ = instantaneous value of flux

Ψ = flux linkages

$\hat{\Psi}$ = saturating value of flux linkages

U,V,W,X,Y,Z	=	phase angle logic signals
UD	=	direction logic signal
ω	=	electrical angular frequency
ω_m	=	mechanical angular velocity
ω_n	=	natural frequency
ω_s	=	stepping frequency
W	=	energy
x,$\underline{x}$	=	state variable, state vector
y	=	admittance
ZD	=	zero position detection logic signal

Suffixes

a,b	=	phase winding A and B
a,b,c	=	inverter conditions
c_u	=	copper loss
d	=	d.c. supply quantity
e	=	e.m.f.
F_e	=	iron loss
g	=	air gap quantities
L	=	total losses
ℓ	=	approximate leakage flux path quantities
m	=	approximate main flux path quantities
o	=	optimum
oc	=	open circuit
p	=	pole quantities
pm	=	permanent magnet quantities
r	=	input
rC_c	=	rotor core quantities, circumferential
rC_r	=	rotor core quantities, in radial direction
rt	=	rotor tooth quantities

s	=	switching quantities
SC_a	=	stator core quantities, in axial direction
SC_c	=	stator core quantities, circumferential
S	=	stator leakage flux path quantities
Sr	=	stator rotor leakage flux path quantities
St	=	stator tooth quantities
Sx	=	stator cross leakage flux path quantities
w	=	winding quantities

Operators etc.

$\oplus$	=	Exclusive OR function
$\hat{}$	=	peak or maximum value
$\bar{}$	=	vector
$\bar{}$	=	logical inverse
$\mathfrak{R}$	=	real part
$*$	=	conjugate

Logic symbols:- In view of their widespread acceptance in this country American standard logic symbols have been used.

1. INTRODUCTION

1.1 The Stepping Motor.

The electrical stepping motor can be defined as an incremental actuator which converts electrical pulse inputs to mechanical output motion. Other forms of stepping motor include hydraulic and pneumatic types and the motion of any of these types can be either rotary or linear. Of the various types of stepping motor[42] the electrical rotary type is by far the most common and is the type considered here. The two main variations of this type of machine (excluding solenoid ratchet types) are,

(i) Variable reluctance (VR)

and (ii) Permanent magnet (PM).

Although a permanent magnet type[14] is referred to, much of the work to be presented here can be applied to both types of machine.

The electrical pulse input to the machine is applied by energising and de-energising successive phases of the motor in turn. Operation is bi-directional and reversal of direction is obtained by reversal of the sequence of phase energisation.

Generally a constant angular displacement is produced by each input pulse and any errors at each step are non-cumulative. This makes the machine an excellent device for use in position control systems. Positions can be controlled within an accuracy of a few per cent of one step simply by applying the correct number of pulses. The resulting simplicity of a system which requires no position measuring equipment makes the stepping motor an attractive possibility for many applications.

Although the history of stepping motors can be traced back to the early 1930's it was some 30 years or so later that interest in

these devices began to become significant. This was mainly because of the development of the transistor, and since then the number of publications about stepping motors has increased rapidly. The growth of application in machine tools and later in the computer industry has sustained this interest.

In 1970 the market for stepping motors was described as small, specialised but expanding and according to the ERA was estimated at 19,500 motors (up to 0.075 kw) worth £350,000 for 1969, with an annual growth rate of more than 20% and served by at least 14 suppliers in the UK, though at the time the market was suspected to be greater than this[43].

In 1973 however, the ERA estimated an annual growth of 15% (industrial sources indicate it is greater), but the number of suppliers had increased to 43.

With increasing interest and demand it appears that for a number of years the future market for stepping motors will be one of continued rapid expansion.

1.2 Background to the Project.

At the commencement of this project in October 1970 the general area of digital control of electrical machines was considered. Although very little was known about stepping motors at that time, an initial study of existing literature indicated that there was considerable scope for a project on this subject. A further thorough search of the literature confirmed this. It appeared that further work which would make a contribution to the role of the stepping motor as an element in high performance positioning systems would be most useful, and this became the main objective of the research programme.

Apart from review and introductory type of articles the literature

dealt mainly with the following technical problems:-

(i) Modelling and simulation;- Existing models are surveyed in Section 2.1

and (ii) Computer controlled and closed-loop operation;- Notably the work of Fredriksen[31,36,44,45,46,47] dominated this topic.

Despite the amount of existing literature, to deduce that these areas were adequately covered would have been to under-estimate the importance of these topics.

It was felt that existing models were somewhat idealised for a machine of this type, and if a simpler closed-loop technique could be found this might enhance the possibilities for closed-loop control.

A further area that had barely been touched upon was the subject of the optimal control of stepping motors[48]. This subject can depend heavily upon the above two topics and upon other aspects that will be outlined in Section 1.6. A future trend for high performance systems is likely to be towards 'optimal control'. To study the feasibility of 'optimal' systems for a particular application it is necessary to know the difficulties and the methods available to control the motor in an optimum manner.

An investigation of the areas of work relevant to the optimal control of a stepping motor was taken up as the method to achieve the main objective.

1.3 Defining an Optimum System.

A wide range of problems can confront the engineer who wishes to obtain a suitable stepping motor system which is optimum for his application.

It should be stated at the outset that this work cannot provide a complete solution to such problems. It does not attempt to present

a formula or procedure from which an engineer using a particular index of performance can arrive at the optimum type and size of motor, details of the optimum drive circuit or the optimum configuration for the overall system.

If this were possible the engineer may still have the problem of defining his index of performance. In a general form this would be very complicated, being a function of several variables such as overall cost, motor size, maximum torque, maximum speed, power and settling times under various conditions. It would also include more abstract factors such as accuracy, reliability and degree of resonance. Clearly this is virtually an impossible task.

The problem is better tackled by the engineer who is familiar with the requirements for the application. He can use a knowledge of stepping motors together with certain available techniques to arrive at a solution.

The work therefore attempts to examine areas which are thought most relevant to the optimal control of stepping motors and in which further work might help in some way to inspire a solution to the control problem.

The work is not confined to one particular application and so 'optimum' can only be defined here as that which best meets the users requirements. To attempt to define it more closely would only add to the misuse that the word already receives.

The requirements dealt with however are those which are likely to be useful for a wide range of high performance applications.

1.4 Selecting an Optimal System.

Selecting the optimal system is often reduced to the selection of a suitable motor and drive circuit from manufacturers stock items and is based upon the ability of the engineer to match system require-

ments with manufacturers data. Provided the system meets these requirements it is accepted to be optimum since no further effort is warranted, irrespective of whether other systems could prove to be 'better'.

Although this may seem a straight-forward matter, it does not always provide a satisfactory solution and the system selected may not meet the users requirements. The cause may have been the mis-interpretation of data or simply by having considered the motor completely separate to the drive circuit. The two are closely inter-dependant.

The fact that stepping motors are not yet widely understood accounts for some of the difficulties.

Another cause of difficulty in system selection is that manufacturers data is not standardised[1]. The term stepping motor has been used here since this seemsthe most likely term to be adopted in Britain, but even this is not yet standard and the device is often referred to as a stepper motor or just a stepper.

A common criticism amongst users is a lack of data on the part of the manufacturer. On the other hand the users of a particular motor could be operating under hundreds of different sets of conditions and it is difficult for the manufacturer to supply data to completely cover all these cases. Nevertheless, without complete data relevant to the users operating conditions there will be uncertainty about the system being optimum.

This situation is more acute for stepping motors than for most other types of electrical machine. It is not a simple matter to predict the effect of a change in load inertia, current or stepping frequency upon the torque developed. An approximation for the characteristics under steady state stepping conditions cannot be estimated by using a few simple formula. Even so, the estimation is

no more difficult than that of the transient response of more conventional types of machine.

If important data is not available then either the manufacturer or the user must be prepared to investigate by experiment or by modelling studies.

The synthesis problem - 'What motor and drive circuit best gives the required performance' is not tackled directly. Selecting the optimum system is essentially an iterative procedure consisting of the prediction of performance that can be obtained by various motor-drive circuit combinations until the system requirements are met.

This may seem a lengthy process but may be aided by initially making certain approximations, as may seem necessary, in the prediction of performance[2]. This may yield an acceptable solution to the problem very quickly.

The more stringent the requirements and the higher the demanded performance, then the greater the difficulty in finding a suitable solution. For instance, a stringent control policy may require closed-loop control, or even computer control, with perhaps the use of adaptive control techniques. A more accurate model, special manufacture of a machine, or special drive circuits may be necessary.

An important matter to be established is whether the stepping motor with its digital compatability, open-loop simplicity yet with fast slewing capabilities (particularly when in a closed-loop) is the most suitable choice. If there is any doubt other possibilities should also be considered.

For a majority of present applications the optimum system may be found by the procedure already outlined. Whilst these can present some difficulties it is usually possible to find an acceptable solution.

For the remaining applications some of the above considerations will be necessary and these will be dealt with further, in the following sections.

1.5 Survey of Literature.

A literature survey is given, where appropriate, in each main section and the resulting list of references thought to be most relevant to this work is given in Section 9. If required, a more comprehensive bibliography may be used for reference so.

As was indicated in Section 1.2, a reasonable amount of literature has been available though many of these have been review and introductory types of articles for the growing numbers of engineers, and others, requiring some familiarity with stepping motors. During recent years there has also been a growing number of engineers requiring more specialised knowledge in this field.

This fact has been recognised by the recent organisation of conferences held specifically for this subject, in the U.S.A., by the University of Illinois in 1972, 1973 and 1974, and later in Europe, in 1974, by the University of Leeds, England. These are now international events to be held annually and have started to produce a growth of literature that the engineer with a more specialist interest can refer to, or contribute to.

This recent 'explosion' of interest later confirmed the initial indications of considerable scope for a project on this subject.

1.6 Objectives of the Project.

In Section 1.1 it was stated that the main objective was to make a contribution to the role of the stepping motor, as an element in high performance positioning systems. It was also stated that the method of reaching this would be by investigation of areas of work relevant to the optimal control of a stepping motor.

Consideration of the outstanding problems led to other objectives, as follows:-

(i) Modelling:- In order to effectively control a stepping motor, the dynamics of the machine should first be fully understood. It is foreseen that future work in this field could use adaptive control methods which may depend heavily upon an accurate model. For these reasons, an initial objective was to arrive at a satisfactory mathematical model of the machine which would adequately represent its performance over a wide range of operating conditions. These include operation at different levels of saturation and transient conditions.

(ii) Input Optimisation:- In a practical system constraints are present a) on the level of available forcing (i.e. voltage) and b) upon the extent to which the machine can be forced. (i.e. temperature, mechanical considerations). The effects upon temperature rise due to various types of forcing should therefore be considered. If maximum torque, subject to a given value of losses is used as an index of performance, a sinusoidal voltage waveform might appear to be the optimum choice. The simplicity resulting from using forcing function signals that have been derived digitally would usually impose the restriction of a pulsed supply. Another objective was therefore to establish the conditions to give maximum torque subject to fixed losses when the machine is operated from both sinusoidal and from pulsed supplies.

(iii) Drive Circuits:- When operated from a pulsed supply the power requirements of most stepping motors can be handled by transistors and this is the standard method used. Suitable drive circuits for applications involving large stepping motors, and in cases where considerable forcing is to be used, are not sufficiently developed and the thyristor may then be a more suitable device. A further objective was to develop a drive circuit that would be suitable for stepping motors.

(iv) Closed Loop Control:- Established methods of closed-loop control

give control of torque and not control of speed because they do not accurately control the 'phase angle' and would become complicated and expensive if adapted to do so. A closed-loop method that will give close control of the phase angle would find application in many optimal systems especially if the method were relatively simple. Another objective was therefore to establish such a method.

(v) Optimal Controller:- The final objective was to develop a bang-bang type of controller, capable of optimum switching from maximum acceleration to maximum decelleration, for time optimal control. The controller being designed to adjust the control action for a varying load.

The most basic of the above objectives is the modelling of stepping motors which is the subject of Section 2. The aim was to produce an electrical equivalent circuit model that could be used to predict the machine performance over a wide range of operating conditions. Such models are commonly used by electrical engineers throughout industry as a convenient method of analysis. Linear and non-linear versions of the equivalent circuit model were then used, and described in Sections 3 and 4, to maximise the torque by controlling the input voltage.

Section 5 describes the type of drive circuits that were used and the additional data and equipment that was required to achieve closed-loop control. Finally Section 6 describes how an optimal controller is designed and used in a practical system.

2. EQUIVALENT CIRCUIT MODELS FOR A STEPPING MOTOR

2.1 Introduction

An early attempt to define a transfer function for the stepping motor was made in 1961 by O'Donahue[3] and the model proposed was equivalent to a second order linear system. This enabled the machine performance to be compared with the type of system familiar to the control engineer. Such a simple model is useful for preliminary study although it does have many limitations.

Alternative models have also been derived, generally by using one of the following approaches:-

(i) Although it is recognised that the machine is non-linear the previous approach is still persued and machine performance is approximated to that of a second or third order linear system[4,5], depending upon the assumptions made. Multi-step operation of the machine is modelled by storing values of angular velocity and position at the completion of each step and these are used as the initial conditions for the following step, when the positional error has been updated. This can be done by using either analogue or digital simulation methods as described in the literature[6,7].

(ii) The machine is regarded as non-linear in that the torque is expressed as a sinusoidal function of position. This results in a second order non-linear differential equation and the phase-plane is a convenient method of analysis. These techniques can be applied to multi-step operation and have also been described in the literature[8,9,10]. If winding inductance is not negligible (or if a switched current source cannot be assumed) the phase plane method is not applicable and the analysis is consequently more difficult[11].

Unfortunately, the sinusoidal form of the torque characteristic is not the only non-linearity present in the machine. One recent model[13] does include some harmonics but it would be useful to have available a model which could account for saturation and armature reaction.

With the increased stepping rates which can now be achieved consideration must also be given to the iron losses within the machine.

The increasing demands upon stepping motor performance require not only more sophisticated control techniques but also an accurate model for use in the assessment of the control method, and the machine parameters.

These machines are broadly classified as either permanent magnet or variable reluctance types, but there are a number of different versions of each and even some 'novel' machines which may be classed as stepping motors. In proposing an equivalent circuit model no attempt has been made to cover all types, however the general procedure outlined can be readily applied to any electromagnetic configuration.

The structure of any model can be derived by study of the magnetic circuit and it is the aim of this section to demonstrate the importance of this approach for developing suitable equivalent circuit models.

The field of usefulness of the model may be extended to the prediction of the single step response, the multi-stepping performance in terms of pull-in and pull-out frequencies or other possible characteristics if the type of driving circuit and load are known. All these important operating characteristics can be predicted accurately if the motor torque prediction is satisfactory. The static torque characteristic has therefore been selected as a basis for model verification and comparison.

Whereas previous models may have been unrealistic in certain respects a very accurate model must usually be of the distributed parameter type and would consequently require considerable computational effort to establish and use.

In the example given the model chosen gave reasonable agreement with experimental results up to and beyond the normal operating current. Although accuracy is not exceptional the model could be considered to be

useful as the necessary compromise, which is often difficult to achieve, between model simplicity and accuracy.

2.2. The Magnetic Equivalent Circuit

In order to obtain a realistic model, the starting point should be a detailed study of the magnetic circuit. This differs widely from one machine to another and will have a considerable influence on the structure of the model. We cannot therefore expect the same electrical equivalent circuit for all stepping motors.

The example considered is a permanent magnet machine of a very popular type which originated in the U.S.A. as a synchronous inductor motor[14]. The machine is also known as a hybrid vernier type of stepping motor. Fig. 2.1 shows a two-phase, 4 pole machine with 8 main stator teeth and 42 rotor teeth, the stator fine teeth being set at a pitch corresponding to 40 teeth. The permanent magnet is magnetised in an axial direction. The two rotor sections are offset by half the rotor tooth pitch and the stator sections have a common winding. A corresponding conventional synchronous machine would have 84 poles.

The basic magnetic circuit is contained in a sector which includes 4 consecutive main stator teeth and spans 2π radians, electrical ($n = 2$). Consider the magnetic paths of one such sector in terms of cylindrical co-ordinates. The magnetic circuit for each sector may be considered to consist of 5 sub-circuits in each half (Fig.2.2a). The flux will have axial, radial and circumferential components as shown in the magnetic circuit of Fig.2.2b. The magnetic sub-circuits for a pole, MC_p and that for the permanent magnet, MC_{pm} are shown in Figs. 2.2b and 2.2c. The paths to various fluxes are defined in Fig.2.3.

The flux ϕ_{pm} is a non-linear function of the m.m.f., f_{pm}, as determined by the characteristics of the permanent magnet (see Fig.2.4).

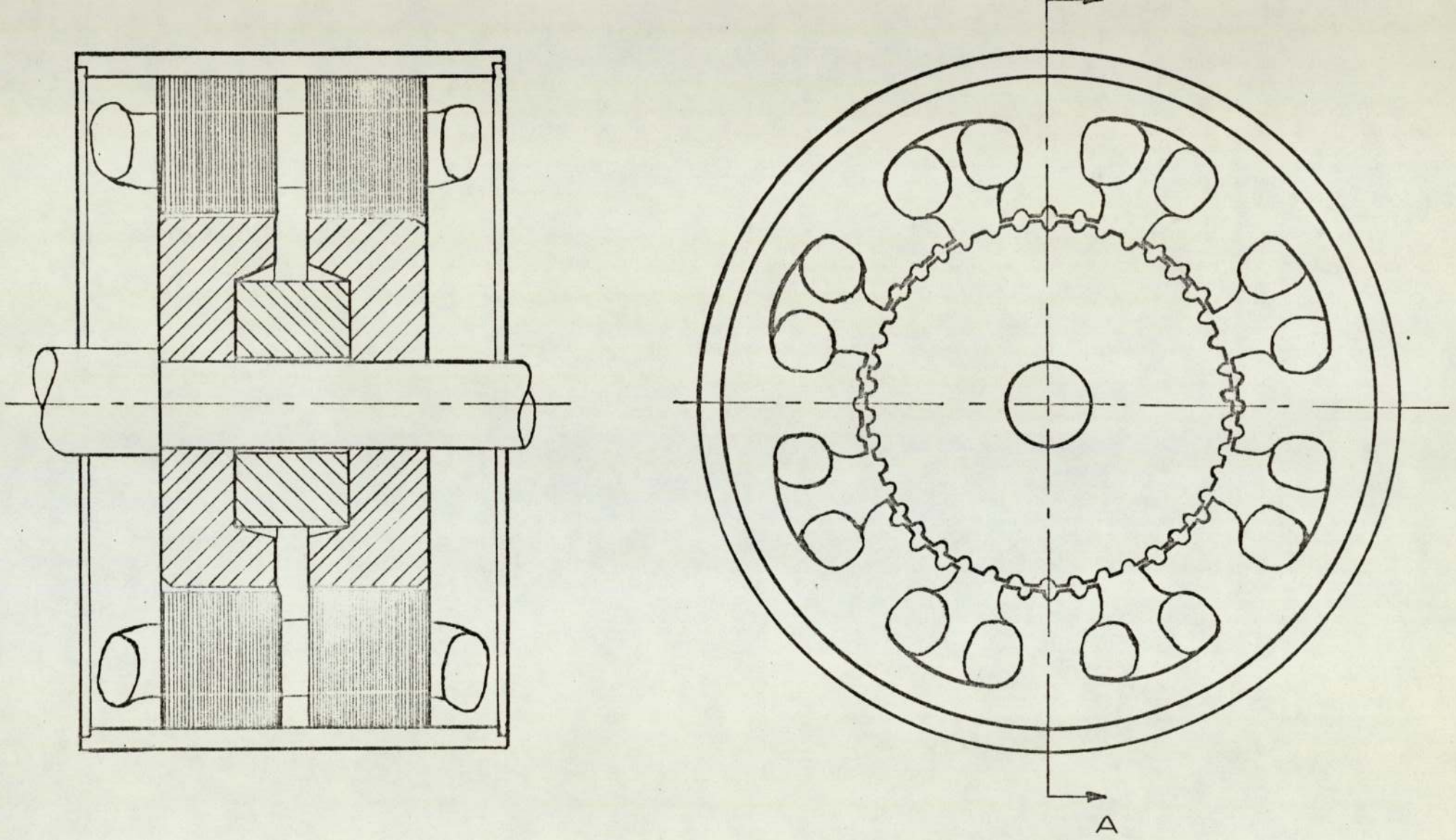

(a) Side elevation through section AA

(b) Front elevation

Fig.2.1 Cross-section of stepping motor stator rotor assembly

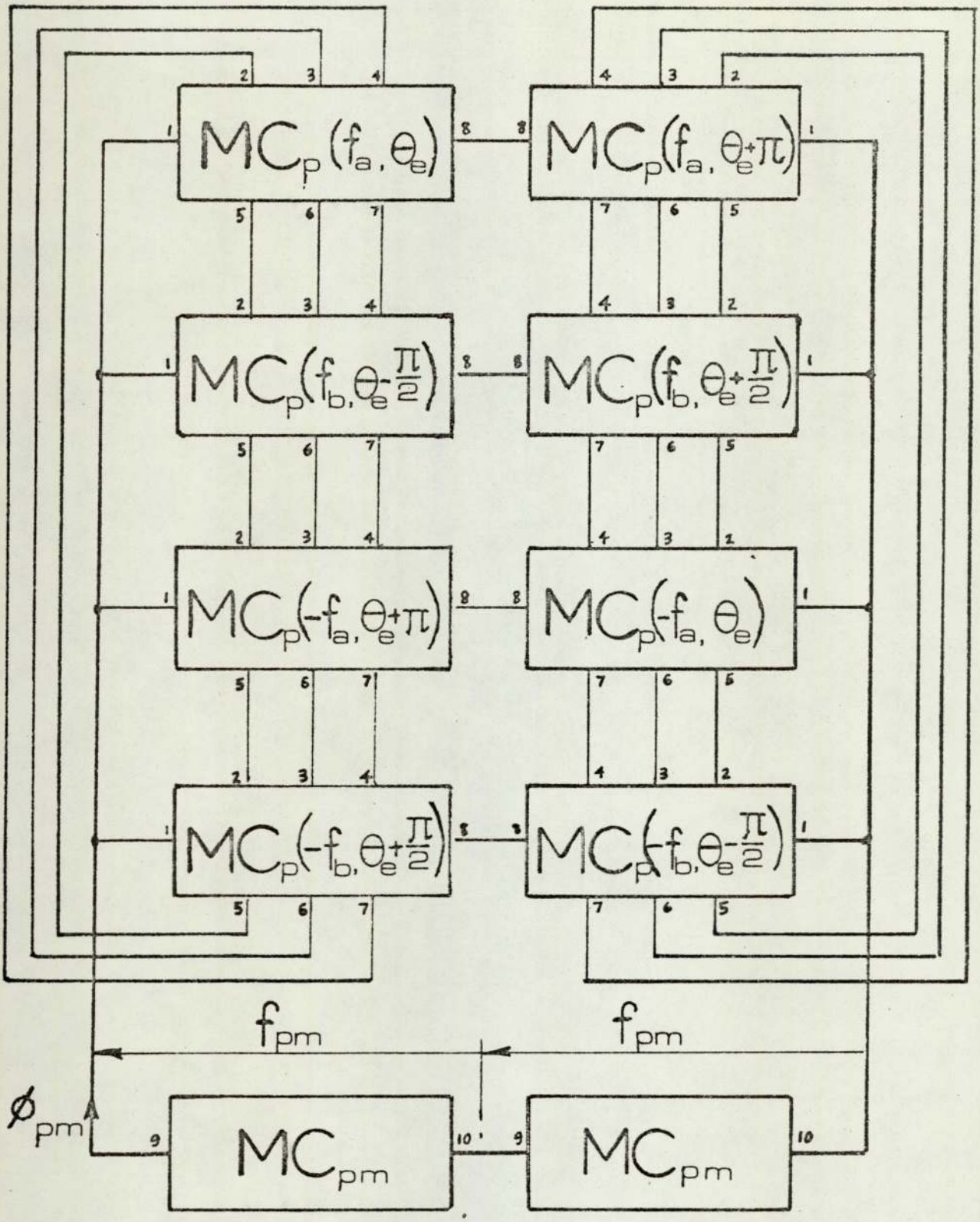

Fig.2.2(a) Magnetic equivalent circuit.

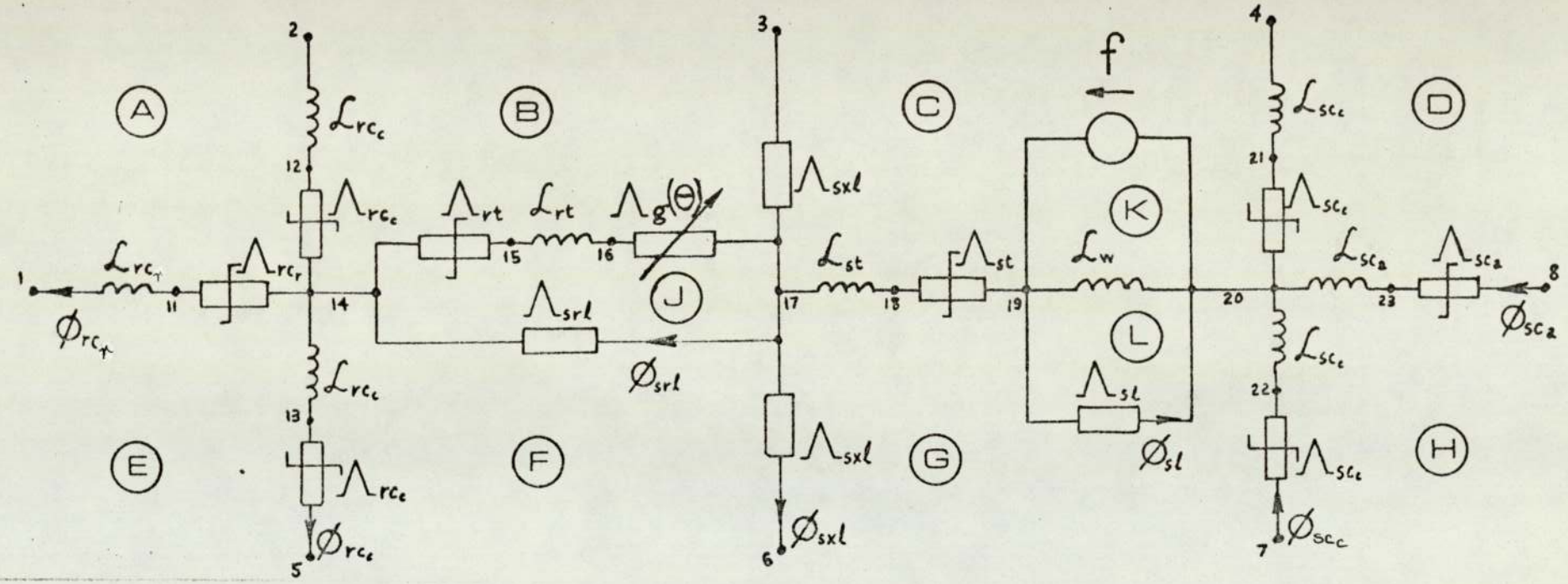

Fig.2.2(b) Magnetic sub-circuit $MC_p(f,\theta)$

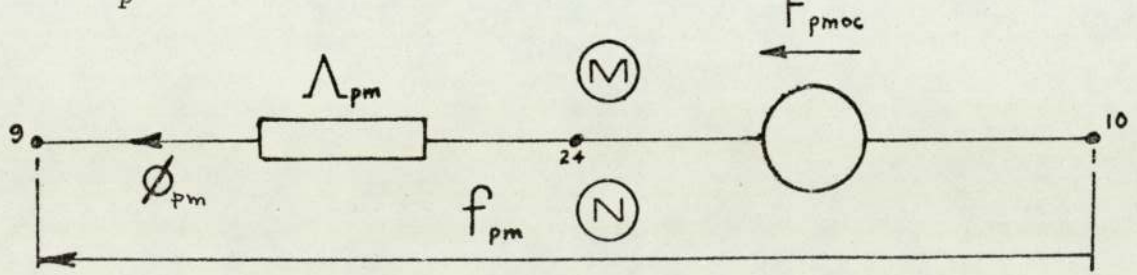

Fig.2.2(c) Magnetic sub-circuit MC_{pm}

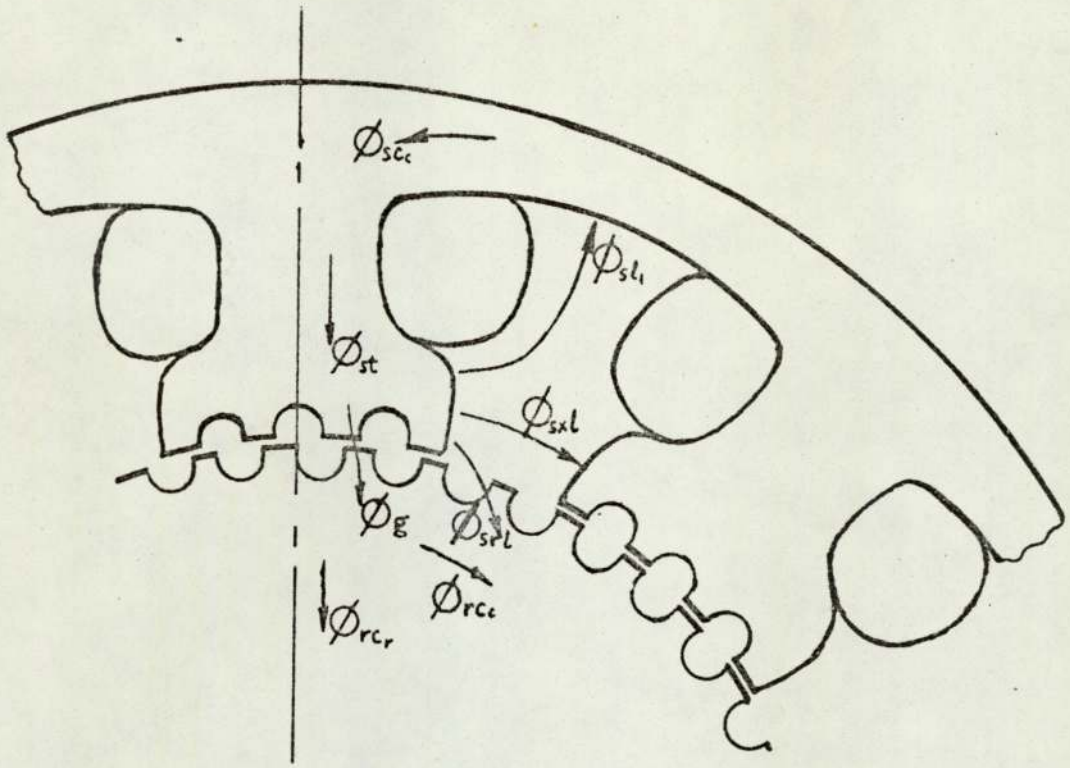

Fig.2.3(a) Main pole and leakage flux paths.

Total leakage flux $\phi_s = \phi_{s\,1} + \phi_{s\,2}$

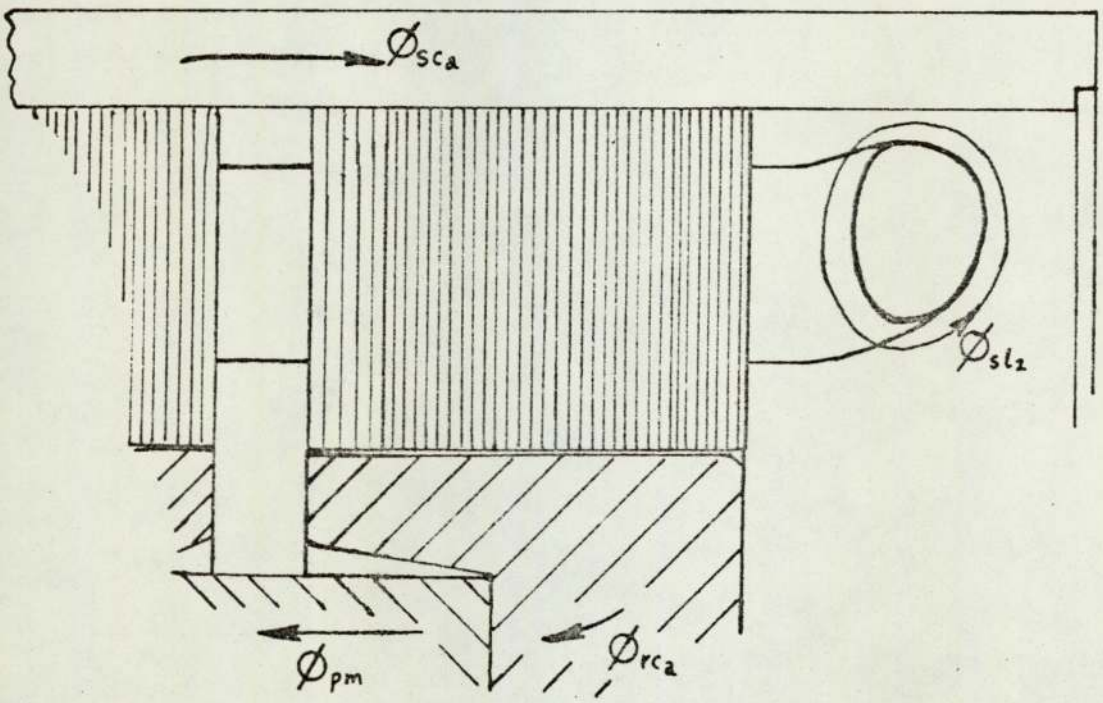

Fig.2.3(b) Axial and end leakage flux paths.

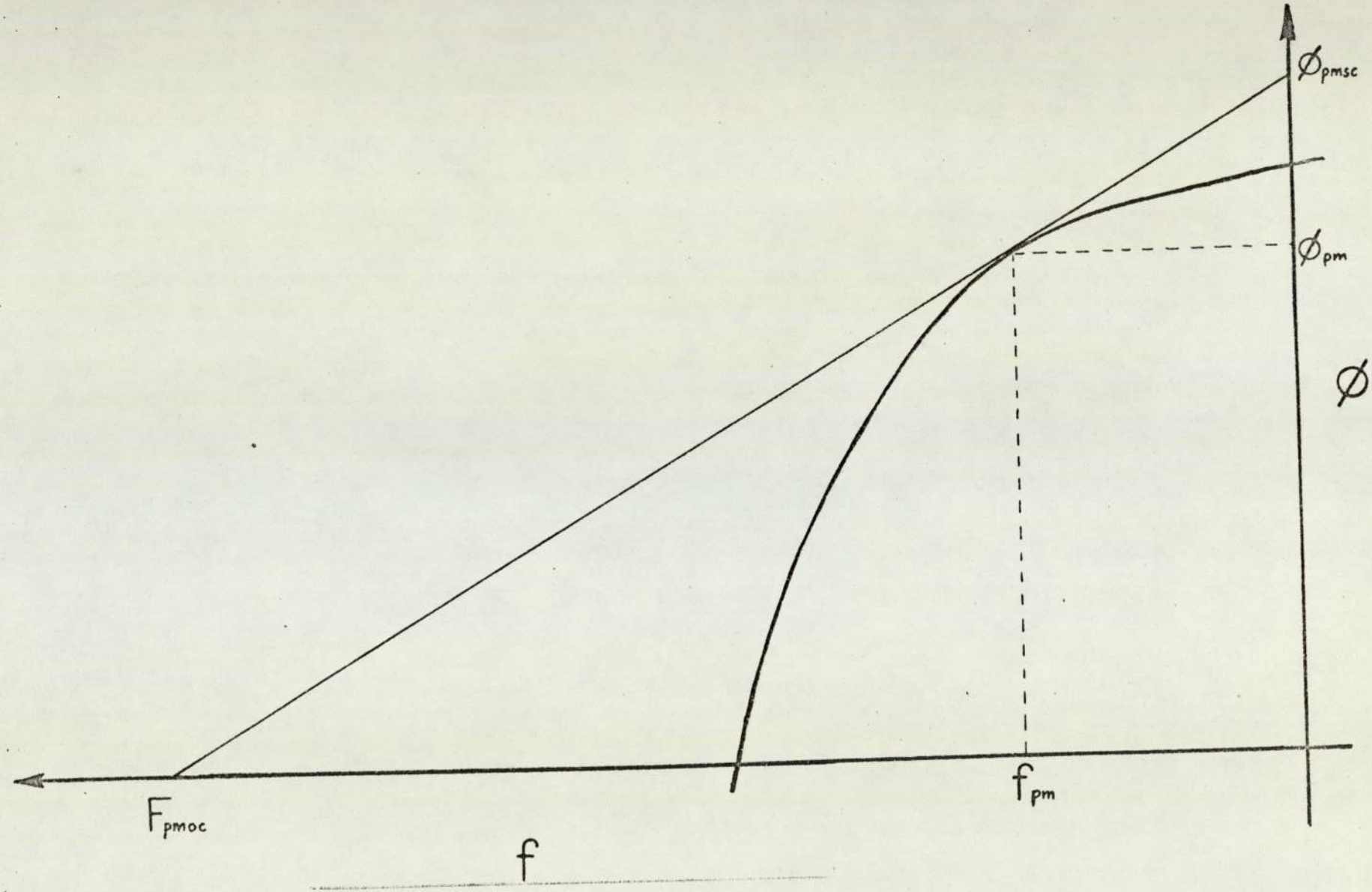

Fig.2.4 Permanent magnet characteristic

A linear approximation to this characteristic, about an appropriate operating point can be made, and this may be sufficiently accurate for moderate changes in f_{pm}. The representation used is that described by Slemon[15] of a constant m.m.f. source, F_{pmoc} in series with a reluctance of $1/\Lambda_{pm}$, shown in Fig.2.2c. Alternatively Λ_{pm} could represent the incremental internal permeance of the m.m.f. source, and would in this case be a non-linear function of f_{pm}. The total permanent magnet circuit in each half can be considered as n sub-circuits MC_{pm} in parallel.

2.3 THE ELECTRICAL EQUIVALENT CIRCUIT

2.3.1 Formation of Dual Circuit

It is now proposed to obtain the electrical equivalent circuit by using the principle of duality[16].

It is of interest to note that it is not possible to form an exact dual electrical equivalent circuit directly. This is because of the topological properties of the magnetic equivalent circuit. It was first shown by Whitney[17] that no geometrical dual exists for a non-planar graph.

A 'physical' dual however can be obtained by the introduction of ideal transformers into the circuit and some methods of doing this have been reviewed by Bloch[18]. Using this approach the electrical equivalent of Fig.2.5a is obtained as the dual of the magnetic circuit of Fig.2.2a. The electrical sub-circuit for a pole EC_p and that for the permanent magnet EC_{pm} are shown in Figs.2.5b and 2.5c. The circuits are interconnected by ideal transformers.

The procedure for forming the dual electric circuit from the magnetic circuit of Figs 2.2b and 2.2c is as follows.

(i) Nodes and inter-nodal spaces are defined by the encircled symbols shown.

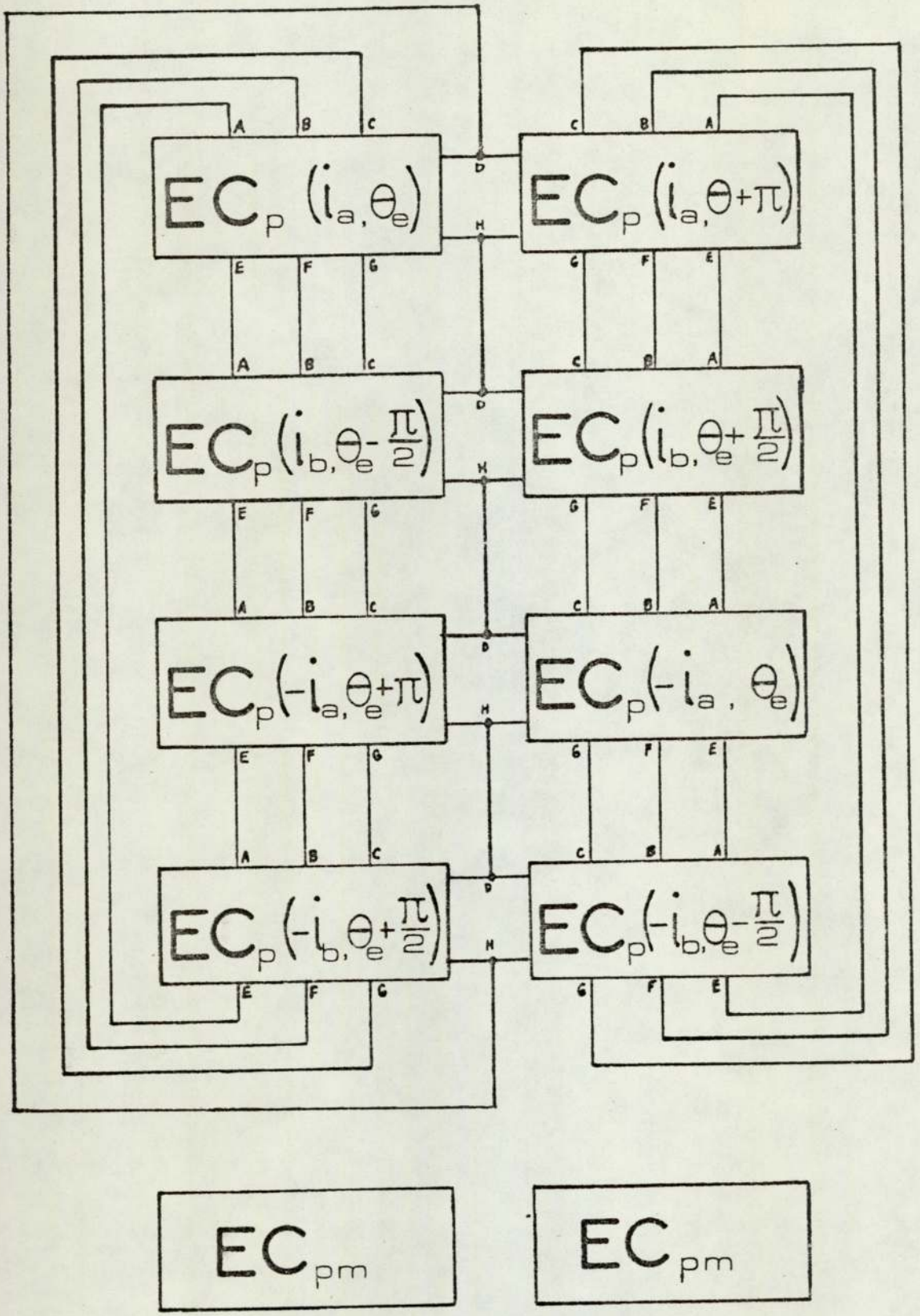

Fig.2.5(a) Electrical equivalent circuit.

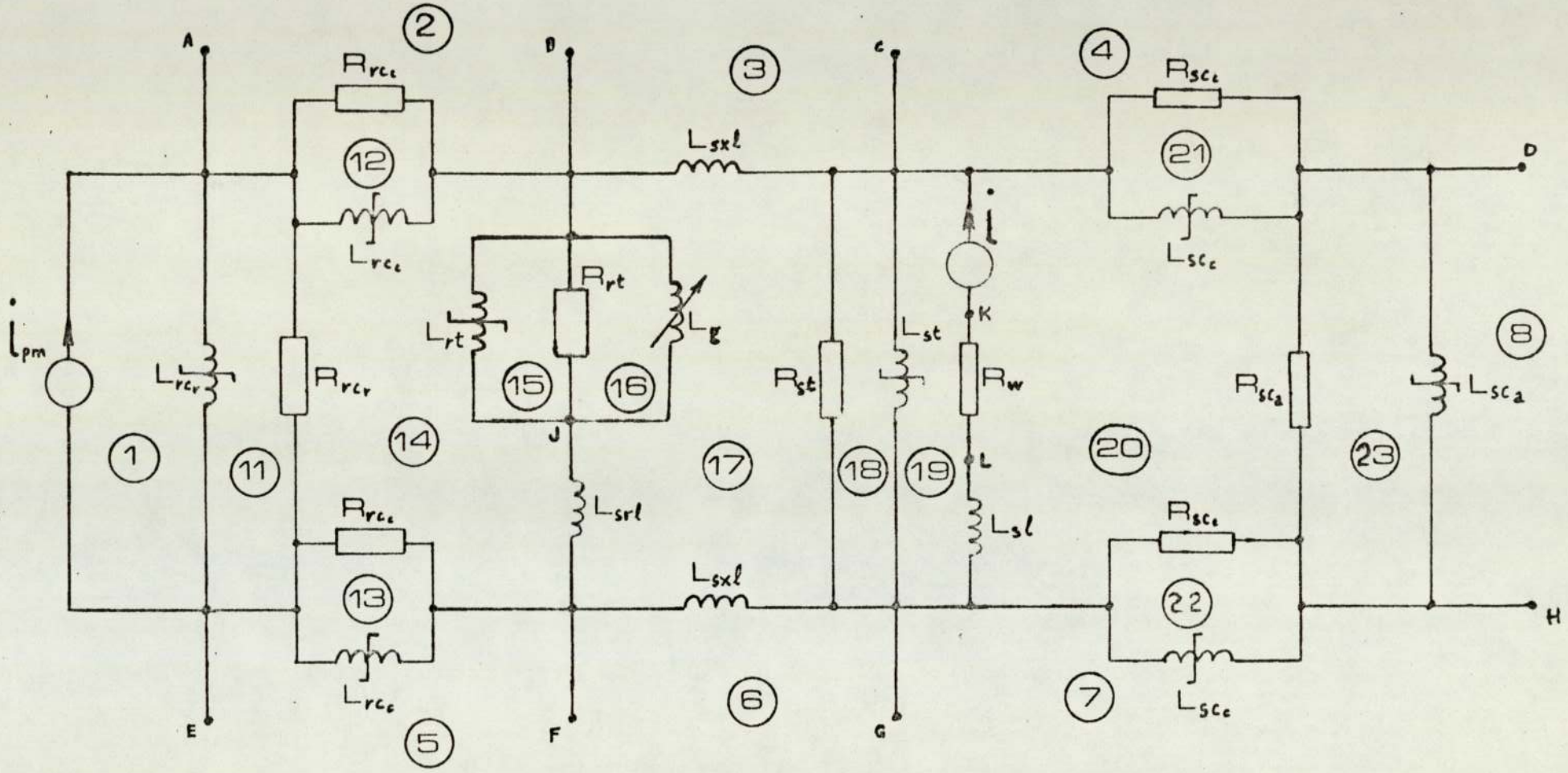

Fig.2.5(b) Electrical sub-circuit $EC_p(i,\theta)$

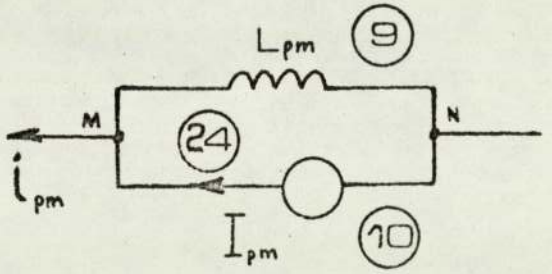

Fig.2.5(c) Electrical sub-circuit EC_{pm}

(ii) Nodes in the magnetic circuit are transformed to inter-nodal spaces in the electric circuit.

(iii) Inter-nodal spaces in the magnetic circuit are transformed to nodes in the electric circuit.

(iv) Magnetic circuit elements lying between adjacent internodal spaces are therefore transformed to elements connected between corresponding nodes in the electric circuit. The same magnetic circuit elements connected between nodes, when transformed, will lie between corresponding inter-nodal spaces in the electric circuit.

(v) Permeances in the magnetic circuit transform to inductances in the electric circuit, where

$$L = N^2 \Lambda \qquad \ldots\ldots\ldots\ldots \quad (2\text{-}1)$$

(vi) Transferences[19], or magnetic inductances[20], in the magnetic circuit transform to resistances in the electric circuit, where

$$R = \frac{N^2}{\mathcal{L}} \qquad \ldots\ldots\ldots\ldots \quad (2\text{-}2)$$

(vii) M.M.F's in the magnetic circuit transform to currents in the electric circuit, where

$$i = f/N \qquad \ldots\ldots\ldots\ldots \quad (2\text{-}3)$$

(viii) Fluxes in the magnetic circuit transform to voltages in the electric circuit, where

$$v = N \frac{d\phi}{dt} \qquad \ldots\ldots\ldots\ldots \quad (2\text{-}4)$$

The resulting current sources is, in Fig.2.5b, at the input terminals is not one of constant current and should be regarded merely as a source which drives a current i into the machine. A voltage controlled source v can be substituted if this is desirable (corresponding to a flux source $\int \frac{v}{N} dt$ instead of the m.m.f source in Fig.2.2b).

2.3.2 Armature Reaction

The interaction between the field due to the permanent magnet and that due to the winding is clearly accounted for in the model. The resulting flux in the gap is determined in terms of the flux in the poles of each phase, and not as a vector quantity which is usual for synchronous machines. Not only does the presence of winding currents considerably change the distribution of flux in the gap, but the m.m.f., f_{pm}, due to the permanent magnet may also vary.

2.3.3 Inter-action between Phases

If an alternating current were flowing in phase Winding A then an e.m.f. would be induced in winding B.

Interaction between phases occurs because of

i) Variations in f_{pm} due to winding currents.

ii) The flow of rotor circumferential flux ϕ_{rc_c}. This source of interaction varies with rotor position. Null positions occur when θ_e is a multiple of $\pi/_2$.

2.4 APPROXIMATE NON-LINEAR MODEL

2.4.1 Approximate Equivalent Circuit

In the form of Fig.2.5a the model may well be more complex than is required. However, having arrived at a general model, this can be easily simplified to suit the differing needs of the user, from machine designer to control engineer.

As an example, let us now assume that the reluctance of each magnetic circuit in the stator and rotor core is sufficiently small to be neglected and that the stator and rotor iron losses can be represented as dissipated in the components $\mathcal{L}_{st}$ and $\mathcal{L}_{rt}$ only. This would often be a reasonable assumption since the reluctance of these circuits will be much smaller than those of the air gap and

saturation will occur to a greater extent in the teeth than in the cores.

Although the permeances Λ_{slx} are associated with cross leakage flux, the net flux crossing between phases along these paths is now zero (see Fig.2.2b).

Phases are now separable, and if ϕ_{sxl} is small it may be either neglected or combined with ϕ_{sl} or ϕ_{srl}.

R_{st} and L_{st}, shown in Fig.2.5b form the stator tooth impedance, R_{rt} and L_{rt} form the rotor tooth impedance and L_g is the gap inductance. An approximate equivalent circuit, shown in Fig.2.6b can be formed by considering these inductances to be combined in parallel and the corresponding magnetic impedances to be in series. The combined magnetising inductance is a function of the current i_m, and of θ_e.

i.e. $$\frac{1}{L_m(i_m,\theta_e)} \triangleq \frac{1}{L_{st}(i_{ms})} + \frac{1}{L_{rt}(i_{mr})} + \frac{1}{L_g(\theta_e)} \quad \ldots\ldots (2\text{-}5)$$

Leakage impedances can now also be combined as shown, where

$$L_l \triangleq L_{sl} + L_{srl} \quad \ldots\ldots\ldots\ldots (2\text{-}6)$$

The physical significance of this arrangement is that the leakage flux which was previously considered to have branched from the main flux is now considered to flow in a separate circuit. Since the leakage paths now considered contain iron, the consequence of L_l remaining constant is that effects known as 'saturation of leakage reactance' are not accounted for in the approximate model. Saturation in the main flux paths however is more significant and cannot easily be neglected, although the complexity of the model is greater if this is included. This complexity can be reduced if the inductance $L_m(i_m,\theta_e)$ is expressed by an appropriate function.

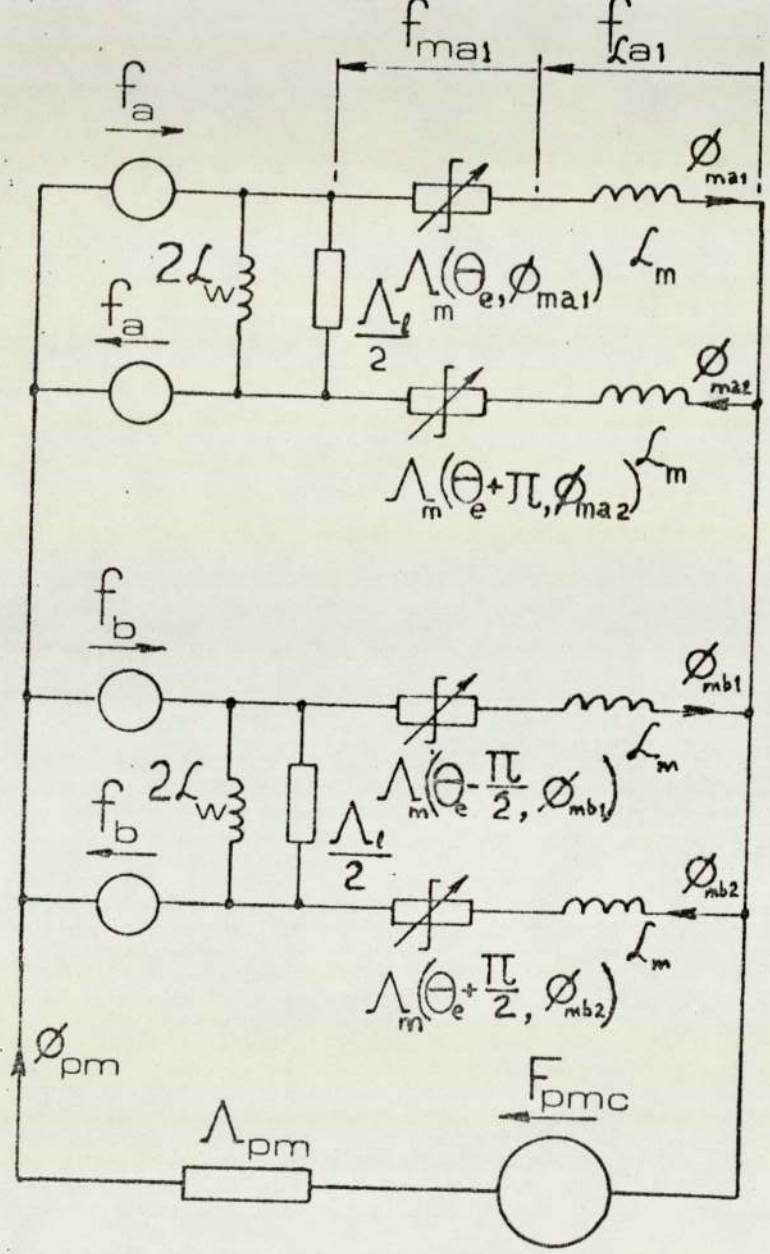

Fig.2.6(a) Approximate magnetic equivalent circuit

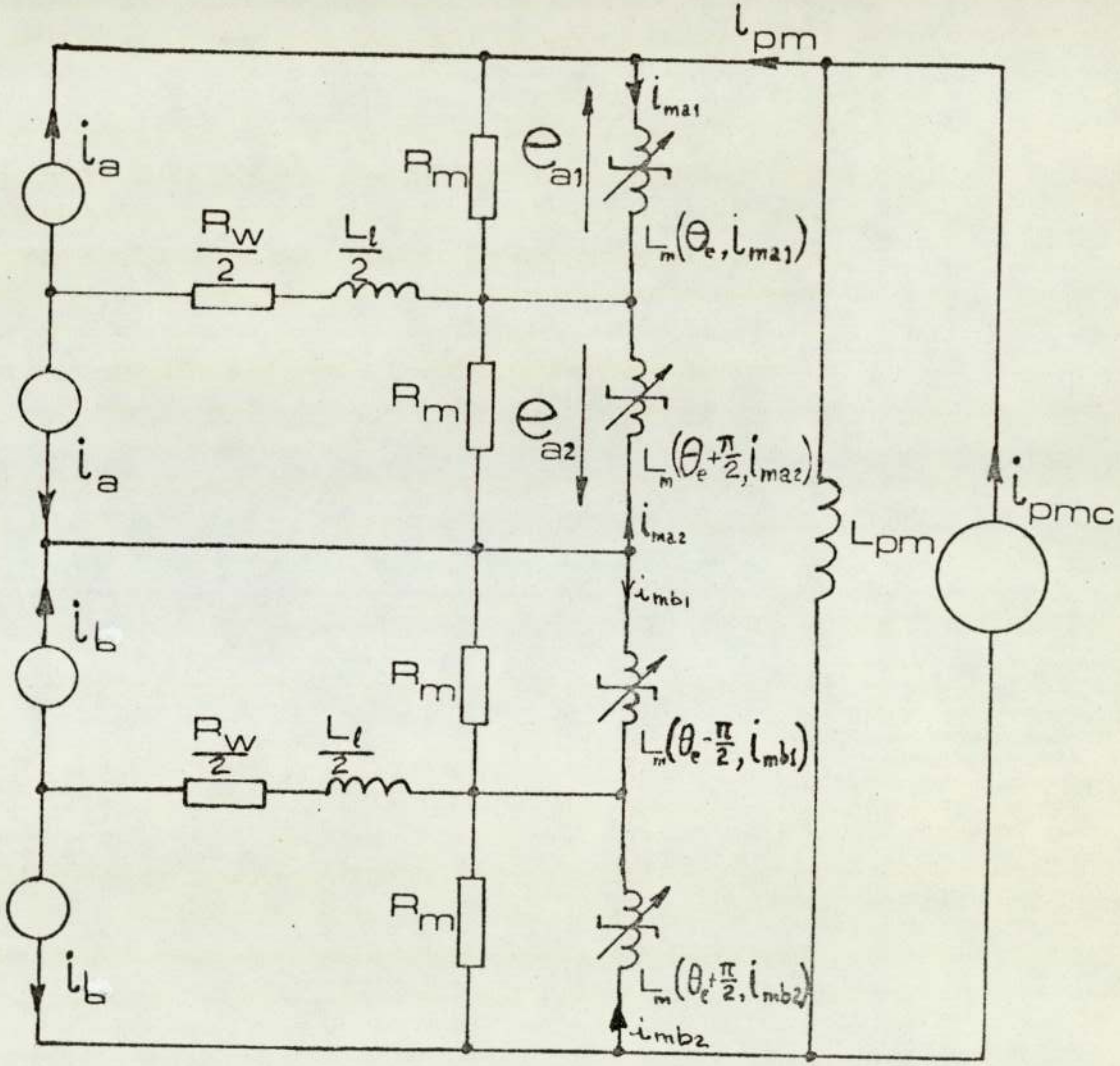

Fig.2.6(b) Approximate electrical equivalent circuit

The following approximation is now proposed. Let the flux associated with $\Lambda_m(i_m,\theta_e)$ have a saturating value $\hat{\phi}_m$ and when this value is not reached, let ϕ_m assume an unsaturated value determined by assuming the permeances Λ_m as primarily functions of θ_e only.

This gives the piecewise linear approximation as shown in Fig.2.7.

thus,

$$\phi_m = \hat{\phi}_m \Big|_{f_m \Lambda_m(\theta_e) \geqslant \hat{\phi}_m} \qquad \ldots\ldots\ldots\ldots \quad (2\text{-}7)$$

$$\phi_m = f_m \Lambda_m(\theta_e) \Big|_{-\hat{\phi}_m < f_m \Lambda_m(\theta_e) < \hat{\phi}_m} \qquad \ldots\ldots\ldots \quad (2\text{-}8)$$

$$\phi_m = -\hat{\phi}_m \Big|_{f_m \Lambda_m(\theta_e) \leqslant -\hat{\phi}_m} \qquad \ldots\ldots\ldots \quad (2\text{-}9)$$

2.4.2 Operation in Unsaturated Conditions

The mechanical torque produced at the shaft is given by

$$T = \frac{\partial W_{mech}}{\partial \theta_m} \quad (f,\theta) \qquad \ldots\ldots\ldots\ldots \quad (2\text{-}10)$$

The total mechanical energy is obtained from the energy balance equation

$$W_{mech} = W_{elect} - W_{stored} - W_{loss} \qquad \ldots\ldots\ldots\ldots \quad (2\text{-}11)$$

in terms of the magnetic circuit, Fig.2.6a.

$$W_{mech} = \sum \left[(f_m + f_\ell)\, \phi_m - \frac{f_m \phi_m}{2} - f_\ell\, \phi_m \right] \ldots\ldots \quad (2\text{-}12)$$

$$T = \frac{\partial}{\partial \theta_m} \sum \frac{f_m \phi_m}{2} \qquad \ldots\ldots\ldots\ldots \quad (2\text{-}13)$$

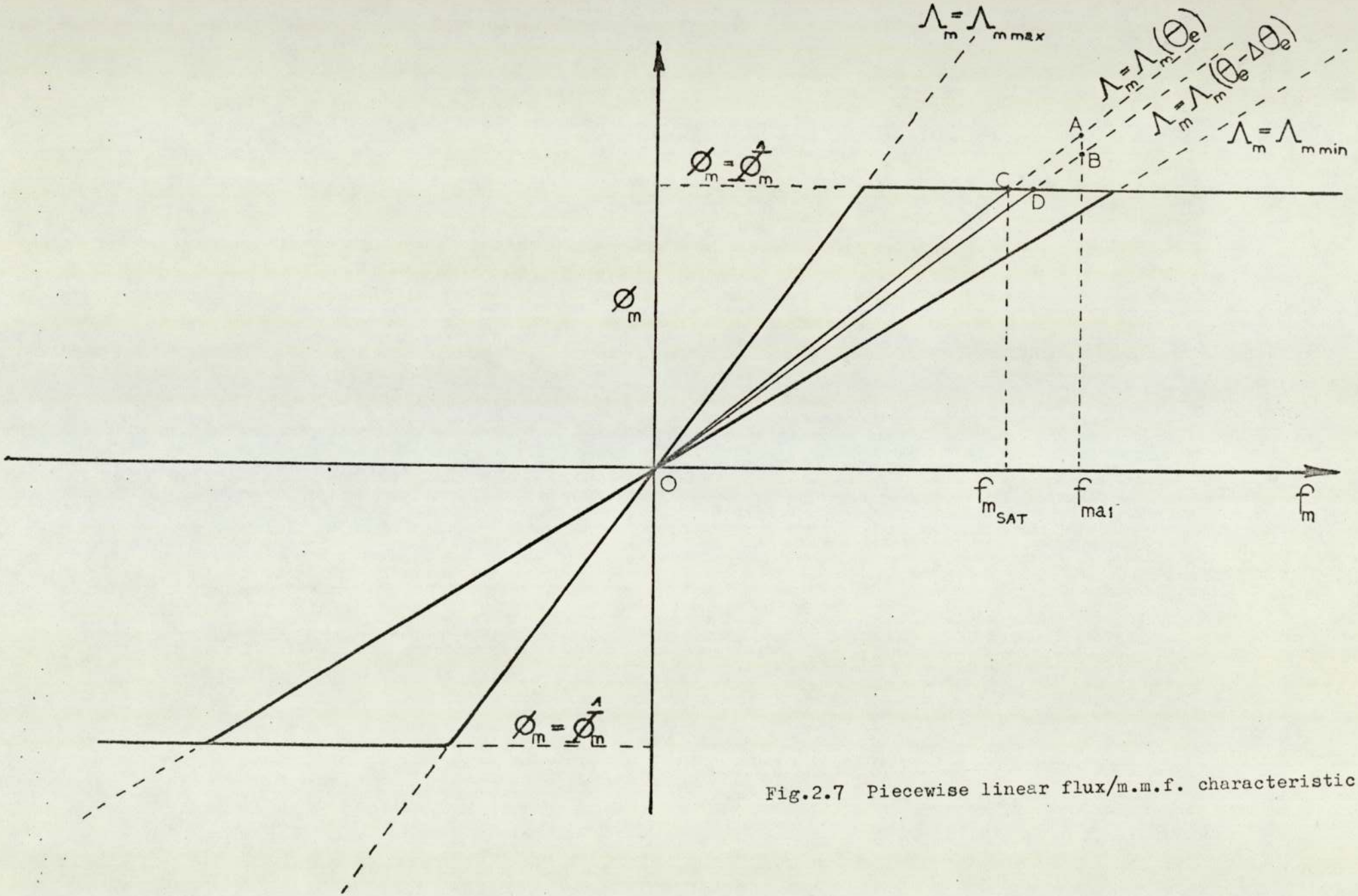

Fig.2.7 Piecewise linear flux/m.m.f. characteristic

$$T = \frac{S_2 n}{2}\left[f_{mal}^{\,2}\ \frac{d\Lambda_m(\theta_e)}{d\theta_e} + f_{ma2}^{\,2}\ \frac{d\Lambda_m(\theta_e+\pi)}{d\theta_e} + f_{mbl}^{\,2}\ \frac{d\Lambda_m(\theta_e-\pi/2)}{d\theta_e} + f_{mb2}^{\,2}\ \frac{d\Lambda_m(\theta_e+\pi/2)}{d\theta_e}\right] \quad \ldots\ldots\ldots\ldots\ (2\text{-}14)$$

similarly, in terms of the electrical circuit, Fig.2.6b.

$$T = \frac{S_2 n}{2}\left[i_{mal}^{\,2}\ \frac{dL_m(\theta_e)}{d\theta_e} + i_{ma2}^{\,2}\ \frac{dL_m(\theta_e+\pi)}{d\theta_e} + i_{mbl}^{\,2}\ \frac{dL_m(\theta_e-\pi/2)}{d\theta_e} + i_{mb2}^{\,2}\ \frac{dL_m(\theta_e+\pi/2)}{d\theta_e}\right] \quad \ldots\ldots\ldots\ldots\ (2\text{-}15)$$

The induced e.m.f.'s are given by,

$$e = e_1 + e_2 = N\left(\frac{d\phi_{m1}}{dt} + \frac{d\phi_{m2}}{dt}\right) \quad \ldots\ldots\ldots\ldots\ (2\text{-}16)$$

thus, $$e_a = N\left[S_2\left(f_{mal}\ \frac{d\Lambda_m(\theta_e)}{d\theta_e} + f_{ma2}\ \frac{d\Lambda_m(\theta_e+\pi)}{d\theta_e}\right)\frac{d\theta_m}{dt} + \Lambda_m(\theta_e)\ \frac{df_{mal}}{dt} + \Lambda_m(\theta_e+\pi)\ \frac{df_{ma2}}{dt}\right] \quad \ldots\ldots\ldots\ldots\ (2\text{-}17)$$

$$e_b = N\left[S_2\ \left(f_{mbl}\ \frac{d\Lambda_m(\theta_e-\pi/2)}{d\theta_e} + f_{mb2}\ \frac{d\Lambda_m(\theta_e+\pi/2)}{d\theta_e}\right)\frac{d\theta_m}{dt} + \Lambda_m(\theta_e-\pi/2)\ \frac{df_{mbl}}{dt} + \Lambda_m(\theta_e+\pi/2)\ \frac{df_{mb2}}{dt}\right] \quad \ldots\ldots\ (2\text{-}18)$$

and, $$e_a = \left[S_2\ \left(i_{mal}\frac{dL_m(\theta_e)}{d\theta_e} + i_{ma2}\ \frac{dL_m(\theta_e+\pi)}{d\theta_e}\right)\ \frac{d\theta_m}{dt} + L_m(\theta_e)\ \frac{di_{mal}}{dt} + L_m(\theta_e+\pi)\ \frac{di_{ma2}}{dt}\right]n_s \quad \ldots\ldots\ldots\ (2\text{-}19)$$

$$e_b = \left[S_2 \left(i_{mb1} \frac{dL_m(\theta_e - \pi/2)}{d\theta_e} + i_{mb2} \frac{dL_m(\theta_e + \pi/2)}{d\theta_e} \right) \frac{d\theta_m}{dt} \right.$$

$$\left. + L_m(\theta_e - \pi/2) \frac{di_{mb1}}{dt} + L_m(\theta_e + \pi/2) \frac{di_{mb2}}{dt} \right] \eta_s \quad \ldots\ldots\ldots\ldots \quad (2\text{-}20)$$

2.4.3 Operation in Saturation

If saturation occurs then the torque is no longer given by equations (2-14) or (2-15), but it can be obtained by considering the points on the $\phi_m - f_m$ diagram for small increments in θ_e. In the absence of saturation, the torque is proportional to the incremental area OAB, shown in Fig.2.7, as θ_e changes to a new value $\theta_e + \Delta\theta_e$.

$$\text{Area OAB} = \frac{f_m^2}{2} \frac{d\Lambda_m(\theta_e)}{d\theta_e} \quad \ldots\ldots\ldots\ldots\ldots\ldots \quad (2\text{-}21)$$

In the presence of saturation the effective incremental area is shown by the shaded element in Fig.2.7, where,

$$\text{Area OCD} = \frac{f_m^2}{2} \frac{d\Lambda_m(\theta_e)}{d\theta_e} \times \left(\frac{f_{msat}}{f_m} \right)^2 \quad \ldots\ldots\ldots \quad (2\text{-}22)$$

Comparison of equations (2-14) and (2-21) will show that the constant of proportionality is

$$\frac{S_2 n}{2} \quad \text{and} \quad f_{m\,sat} = \frac{\hat{\phi}_m}{\Lambda_m(\theta_e)} \quad \ldots\ldots\ldots\ldots \quad (2\text{-}23)$$

The torque and e.m.f. contributed by a saturated pole are then given, for pole A1 saturating, by using equations (2-22) and (2-23)

$$T_{a1} = \frac{S_2 n}{2} \left(\frac{\hat{\phi}_m}{\Lambda_m(\theta_e)} \right)^2 \frac{d\Lambda_m(\theta_e)}{d\theta_e} \quad \ldots\ldots\ldots\ldots \quad (2\text{-}24)$$

$$\text{or,} \quad T_{a1} = \frac{S_2 n}{2} \left(\frac{\hat{\Psi}_m}{L_m(\theta_e)} \right)^2 \frac{dL_m(\theta_e)}{d\theta_e} \quad \ldots\ldots\ldots\ldots \quad (2\text{-}25)$$

and $e_{al} = 0$ ..... (2-26)

These expressions are then substituted for the appropriate terms in equations (2-14 to 2-20) given in section 2.4.2.

2.4.4 Open Circuit Characteristic

From equations (2-17) and (2-18), the open circuit e.m.f.'s when the machine is driven at constant speed ω_m, are given by

$$e_a = N f_{pm} S_2 \omega_m \left(\frac{d\Lambda_m(\theta_e)}{d\theta_e} - \frac{d\Lambda_m(\theta_e + \pi)}{d\theta_e}\right) \quad \text{..... (2-27)}$$

$$e_b = N f_{pm} S_2 \omega_m \left(\frac{d\Lambda_m(\theta_e - \pi/2)}{d\theta_e} - \frac{d\Lambda_m(\theta_e + \pi/2)}{d\theta_e}\right) \quad \text{.... (2-28)}$$

or from equations (2-19) and (2-20)

$$e_a = i_{pm} S_2 \omega_m \eta_s \left(\frac{dL_m(\theta_e)}{d\theta_e} - \frac{dL_m(\theta_e + \pi)}{d\theta_e}\right) \quad \text{..... (2-29)}$$

$$e_b = i_{pm} S_2 \omega_m \eta_s \left(\frac{dL_m(\theta_e - \pi/2)}{d\theta_e} - \frac{dL_m(\theta_e + \pi/2)}{d\theta_e}\right) \quad \text{..... (2-30)}$$

Let the unsaturated permeance distribution $\Lambda_m(\theta_e)$ be expressed by

$$\Lambda_m(\theta_e) = \Lambda_{mo} + \Lambda_{m1}\cos\theta_e + \Lambda_{m2}\cos 2\theta_e + \Lambda_{m3}\cos 3\theta_e + \text{.....} \quad \text{(2-31)}$$

thus $$L_m(\theta_e) = L_{mo} + L_{m1}\cos\theta_e + L_{m2}\cos 2\theta_e + L_{m3}\cos 3\theta_e + \text{.....} \quad \text{(2-32)}$$

using equations (2-27), (2-28) and (2-31) we have,

$$e_a = -2N f_{pm} S_2 \omega_m (\Lambda_{m1}\sin\theta_e + 3\Lambda_{m3}\sin 3\theta_e + 5\Lambda_{m5}\sin 5\theta_e + \text{.....} \quad \text{(2-33)}$$

$$e_b = 2N f_{pm} S_2 \omega_m (\Lambda_{m1} \cos \theta_e - 3\Lambda_{m3} \cos 3\theta_e + 5\Lambda_{m5} \cos 5\theta_e - \ldots) \ldots\ldots \quad (2\text{-}34)$$

similarly,

$$e_a = -2 i_{pm} S_2 \omega_m (L_{m1} \sin \theta_e + 3L_{m3} \sin 3\theta_e + 5L_{m5} \sin 5\theta_e + \ldots) n_s \ldots\ldots \quad (2\text{-}35)$$

$$e_b = 2 i_{pm} S_2 \omega_m (L_{m1} \cos \theta_e - 3L_{m3} \cos 3\theta_e + 5L_{m5} \cos 5\theta_e - \ldots) n_s \ldots\ldots \quad (2\text{-}36)$$

Thus only odd harmonics are present in the e.m.f. waveform.

2.4.5 Static Torque Characteristics

With constant phase currents I_a and I_b insufficient to cause saturation, the torque equations (2-14) and (2-15) may be rewritten as

$$T = \frac{S_2 n}{2} \left[(F_a + f_{pm})^2 \frac{d\Lambda_m(\theta_e)}{d\theta_e} + (F_a - f_{pm})^2 \frac{d\Lambda_m(\theta_e + \pi)}{d\theta_e} \right.$$

$$\left. + (F_b + f_{pm})^2 \frac{d\Lambda_m(\theta_e - \pi/2)}{d\theta_e} + (F_b - f_{pm})^2 \frac{d\Lambda_m(\theta_e + \pi/2)}{d\theta_e} \right] \ldots\ldots \quad (2\text{-}37)$$

and,

$$T = \frac{S_2 n}{2} \left[(I_a + i_{pm})^2 \frac{dL_m(\theta_e)}{d\theta_e} + (I_a - i_{pm})^2 \frac{dL_m(\theta_e + \pi)}{d\theta_e} \right.$$

$$\left. + (I_b + i_{pm})^2 \frac{dL_m(\theta_e - \pi/2)}{d\theta_e} + (I_b - i_{pm})^2 \frac{dL_m(\theta_e + \pi/2)}{d\theta_e} \right] \ldots\ldots \quad (2\text{-}38)$$

Using equations (2-31) and (2-32)

$$T = S_2 n \left\{ 2 f_{pm} \left[F_b (\Lambda_{m1} \cos \theta_e - 3\Lambda_{m3} \cos 3\theta_e + 5\Lambda_{m5} \cos 5\theta_e - \ldots) \right.\right.$$

$$\left. - F_a (\Lambda_{m1} \sin \theta_e + 3\Lambda_{m3} \sin 3\theta_e + 5\Lambda_{m5} \sin 5\theta_e - \ldots) \right]$$

$$+ (F_b^2 + f_{pm}^2) (2\Lambda_{m2} \sin 2\theta_e - 4\Lambda_{m4} \sin 4\theta_e + 6\Lambda_{m6} \sin 6\theta_e - \ldots)$$

$$-(F_a^2+f_{pm}^2)\ (2\Lambda_{m2}\sin 2\theta_e + 4\Lambda_{m4}\sin 4\theta_e + 6\Lambda_{m6}\sin 6\theta_e ---)\Big\} \ldots \quad (2\text{-}39)$$

and

$$T = S_2 n\Big\{ 2i_{pm}\Big[I_b(L_{m1}\cos\theta_e - 3L_{m3}\cos 3\theta_e + 5L_{m5}\cos 5\theta_e ---)$$

$$- I_a(L_{m1}\sin\theta_e + 3L_{m3}\sin 3\theta_e + 5L_{m5}\sin 5\theta_e ----)\Big]$$

$$+ (I_b^2+i_{pm}^2)\ (2L_{m2}\sin 2\theta_e - 4L_{m4}\sin 4\theta_e + 6L_{m6}\sin 6\theta_e ---)$$

$$- (I_a^2+i_{pm}^2)\ (2L_{m2}\sin 2\theta_e + 4L_{m4}\sin 4\theta_e + 6L_{m6}\sin 6\theta_e ---)\Big\} \ldots . \quad (2\text{-}40)$$

Thus in addition to the fundamental torque there are

(i) Odd harmonic torques, which are also proportional to the phase currents.

(ii) Harmonic torques of order $2(2r-1)$, where $r = 1,2,3$ --- etc, which disappear when $I_a = I_b$.

(iii) Harmonic torques of order $4r$, which are always present, even when the machine is unenergised.

Thus the expression for detent torque,

$$T_{det} = -8S_2 n f_{pm}^2\ (\Lambda_{m4}\sin 4\theta_e + 2\Lambda_{m8}\sin 8\theta_e ---) \quad \ldots\ldots \quad (2\text{-}41)$$

or,

$$T_{det} = -8S_2 n i_{pm}^2\ (L_{m4}\sin 4\theta_e + 2L_{m8}\sin 8\theta_e ---) \quad \ldots\ldots\ldots \quad (2\text{-}42)$$

The stable rotor positions of neutral torque correspond to the positions of maximum permeance for the flux paths of each pole.

If it is not admissable to take f_{pm} as being constant, it is found from

$$f_{pm} = \frac{F_{pmoc}\Lambda_{pm}}{\Lambda_{pm} + \sum\Lambda_m} \quad \ldots\ldots\ldots\ldots\ldots\ldots \quad (2\text{-}43)$$

where,

$$\sum\Lambda_m = \Lambda_m(\theta_e) + \Lambda_m(\theta_e+\pi) + \Lambda_m(\theta_e-\pi/2) + \Lambda_m(\theta_e+\pi/2) \ldots . \quad (2\text{-}44)$$

or,

$$\sum \Lambda_m = 4 (\Lambda_{mo} + \Lambda_{m4} \cos 4\theta_e + \Lambda_{m8} \cos 8\theta_e \text{ ---}) \quad \ldots\ldots\ldots \quad (2\text{-}45)$$

Thus permeance harmonics of order 4r directly contribute to variations in the impedance presented to the permanent magnet circuit.

The extent of magnetisation or demagnetisation of the permanent magnet due to the phase currents can be deduced.

2.4.6 Parameter Measurement

Most parameters for the approximate model can be obtained from design data or measurement. The estimation of permeance harmonics by the former method has been mentioned but this is complicated by the fact that saturation of some areas of the teeth, particularly the corners, will affect the value of the unsaturated permeance. If the permeance harmonics are obtained by measurement this effect will be accounted for.

Estimates for the odd harmonics can be made from the open circuit e.m.f. but special provision must be made to measure the even harmonics. In the experimental machine search coils were fitted as follows:-

1) A search coil wound around a main stator pole in one section only.
2) A search coil wound circumferentially between the two stator sections.

The e.m.f. induced in search coil (1) contains both even and odd harmonics, and if f_{pm} can be assumed constant the permeance harmonics are easily deduced. In the absence of phase currents the variations in f_{pm} should be small, but we may wish to check this.

Variations in ϕ_{pm}, and therefore in f_{pm}, will be indicated by the e.m.f. in search coil (2). These can if necessary be used to correct the measurements obtained from search coil (1).

E.M.f. waveforms for the experimental machine are shown in Fig.2.8. and the harmonics measured are listed in Table 2.1. For this

a)

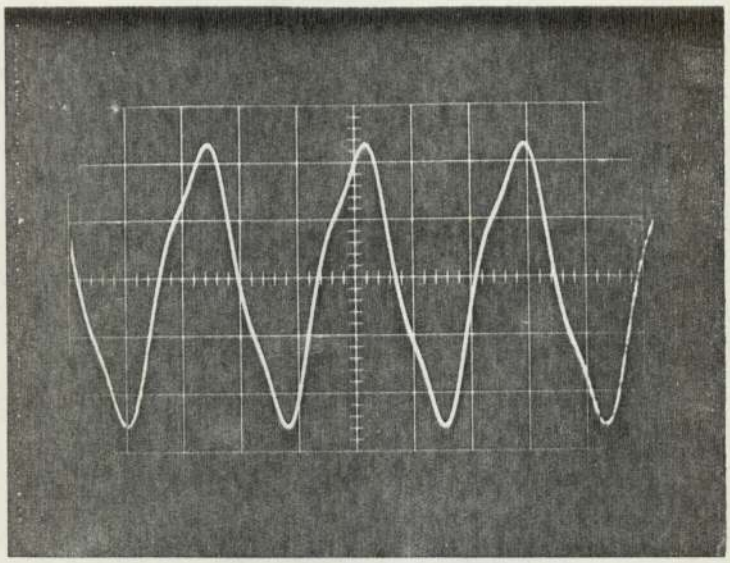

b)

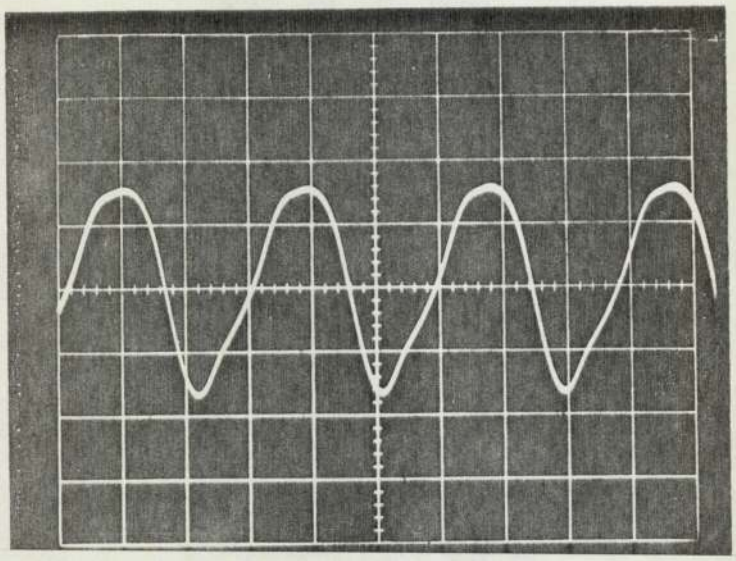

c)

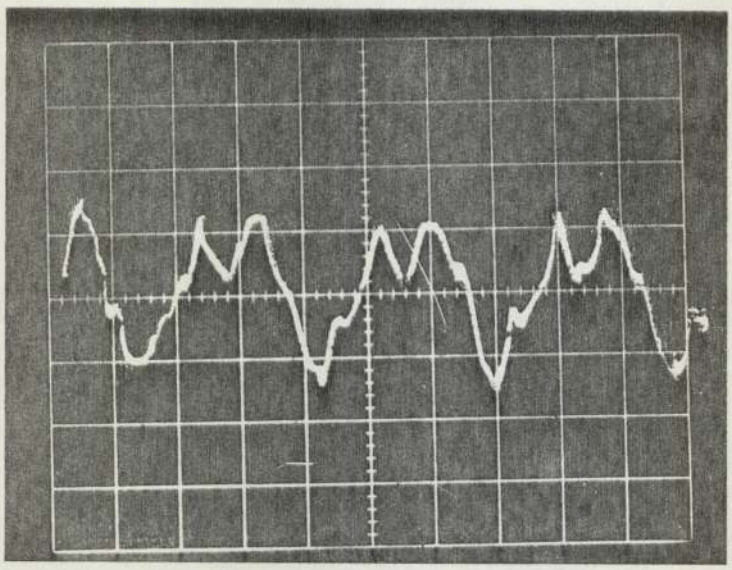

Fig.2.8 VERTICAL SCALE (a) 40V/div. (b) 0.1V/div. (c) 10mV/div.
HORIZONTAL SCALE (a) 0.2ms/div. (b) 5ms/div. (c) 1ms/div.

HARMONIC	PHASE WINDING E.M.F. (% OF FUNDAMENTAL)	STATOR POLE	CIRCUMFERENTIAL
		SEARCH COIL E.M.F.'s (%OF POLE SEARCH COIL) FUNDAMENTAL ‡	
1	100	100	2.8
2	0	20	0.5
3	12	12	0.5
4	0	0	1.8
5	4.5	4.5	0
6	0	4.0	0.2
7	0	0	0
8	0	0	0.6
9 to 15	0	0	0
16	0	0	0.15

TABLE2.1. E.M.F. HARMONICS

‡ BOTH SEARCH COILS HAVE THE SAME NUMBER OF TURNS.

machine the corrections due to variations in f_{pm} did not significantly affect the estimation of the permeance harmonics.

The presence of harmonics which are not of order 4r, in search coil (2) is believed to be due to a slightly non-uniform air-gap.

2.5 MODEL SELECTION

2.5.1 Model Accuracy

It is difficult to state in general the accuracy that can be obtained using the models mentioned so far since this depends upon the type and size of a particular machine.

In the absence of a large amount of experimental results on a wide range of machines, it is suggested that a simple model be adopted at first. A more complex model can be used as required. If the complexity of the models of Fig.2.2 and Fig.2.5 are inadequate, a distributed parameter model may be used and the principle of duality will still apply.

A prime requirement of the model is the accurate prediction of the static torque characteristic, which must be satisfied before consideration can be given to dynamic behaviour. The following example is given to show what can be achieved using the very simple steady state model shown in Fig.2.9.

For a motor of the type considered here, the following parameters were obtained from design data and measurement:-

$\Lambda_{pm} = 0.201\ \mu Wb/AT$ $\qquad$ $\Lambda_{m2} = 0.09\ \mu Wb/AT$

$F_{pmoc} = 6534\ AT$ $\qquad$ $\hat{\phi}_m = 0.638\ mWb$

$\Lambda_{mo} = 2.2\ \mu Wb/AT$ $\qquad$ $N = 100$

$\Lambda_{m1} = 0.9\ \mu Wb/AT$ $\qquad$ $n = 4$

Rated continuous current = 0.6A.

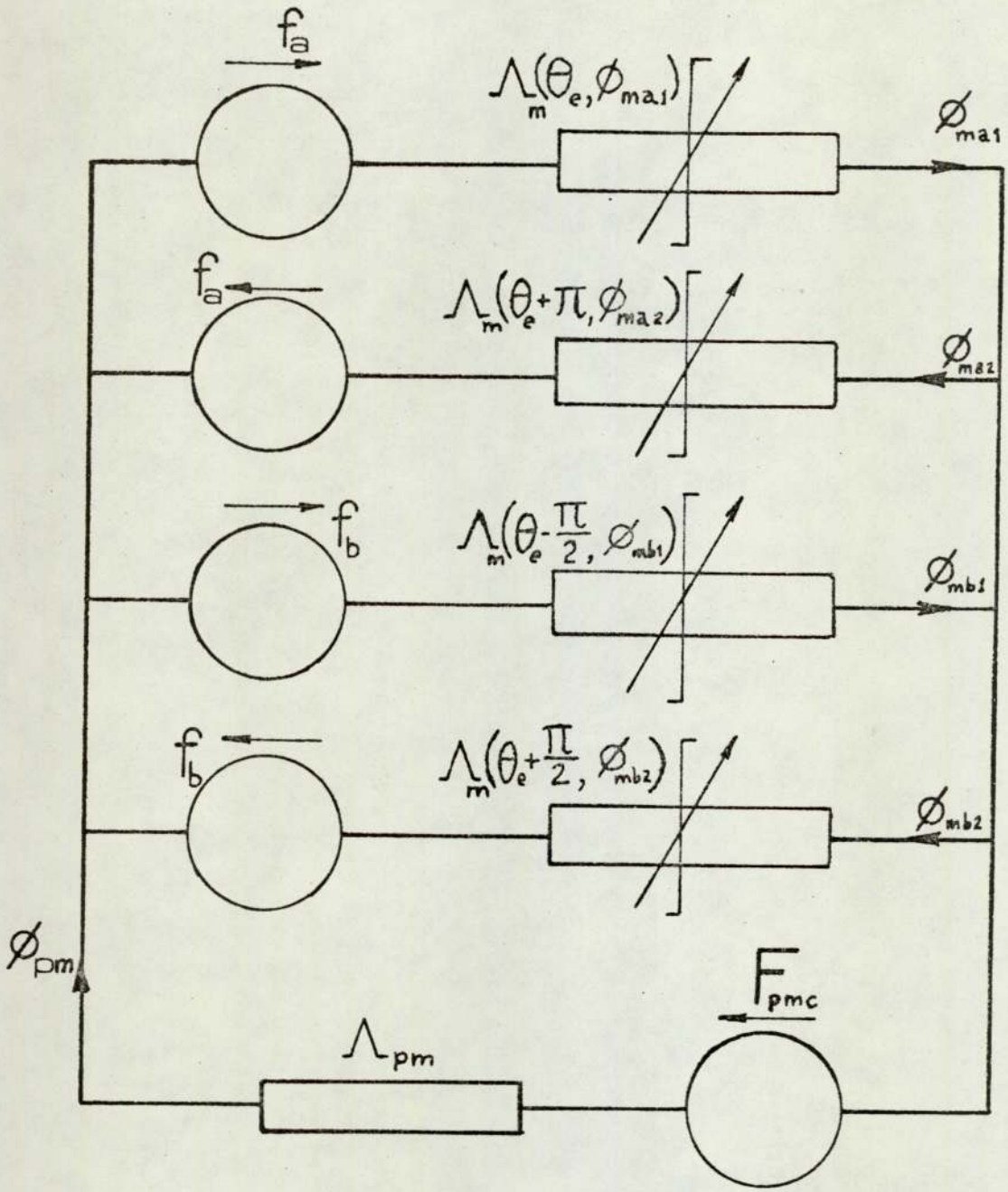

Fig.2.9. Simple Steady State Model.

Λ_1 and higher harmonic terms of Λ_m are neglected.

The results, shown in Fig.2.10. give a good approximation to the experimental static torque curves. The comparison has been continued beyond the useful operating range of the machine (up to $2\frac{1}{2}$ times full load current), where an increase in current produces a reduction in torque. At these current levels the predicted and measured values diverge rapidly.

The reduction in net torque at higher currents is due to,

(i) Saturation of the poles where winding m.m.f. aids the m.m.f. due to the permanent magnet.

(ii) A reduction of flux in the poles where the winding m.m.f. opposes that due to the permanent magnet.

These effects combine to reduce the net flux linkages in the machine.

2.5.2 Comparison with Rotating Field Model

The resulting flux in the gap is modelled in terms of the actual flux flowing in each pole. The usefulness of such a direct approach may at first be doubted when compared to the well established theory of the conventional synchronous machine, to which the stepping motor is related. The approach is however, completely in accordance with the theory of pulsating field machines[12].

For a magnetically linear machine with a sinusoidally distributed winding operating from a sinusoidal supply, which gives rise to a sinusoidal m.m.f. distribution, a rotating vector of flux is a convenient concept. Such ideal conditions are seldom applicable to the stepping motor.

To draw a comparison with rotating field models, saturation must be neglected and a sinusoidally distributed permeance assumed. The assumption that f_{pm} remains constant is implied since the magnetic load impedance presented to the permanent magnet is now constant.

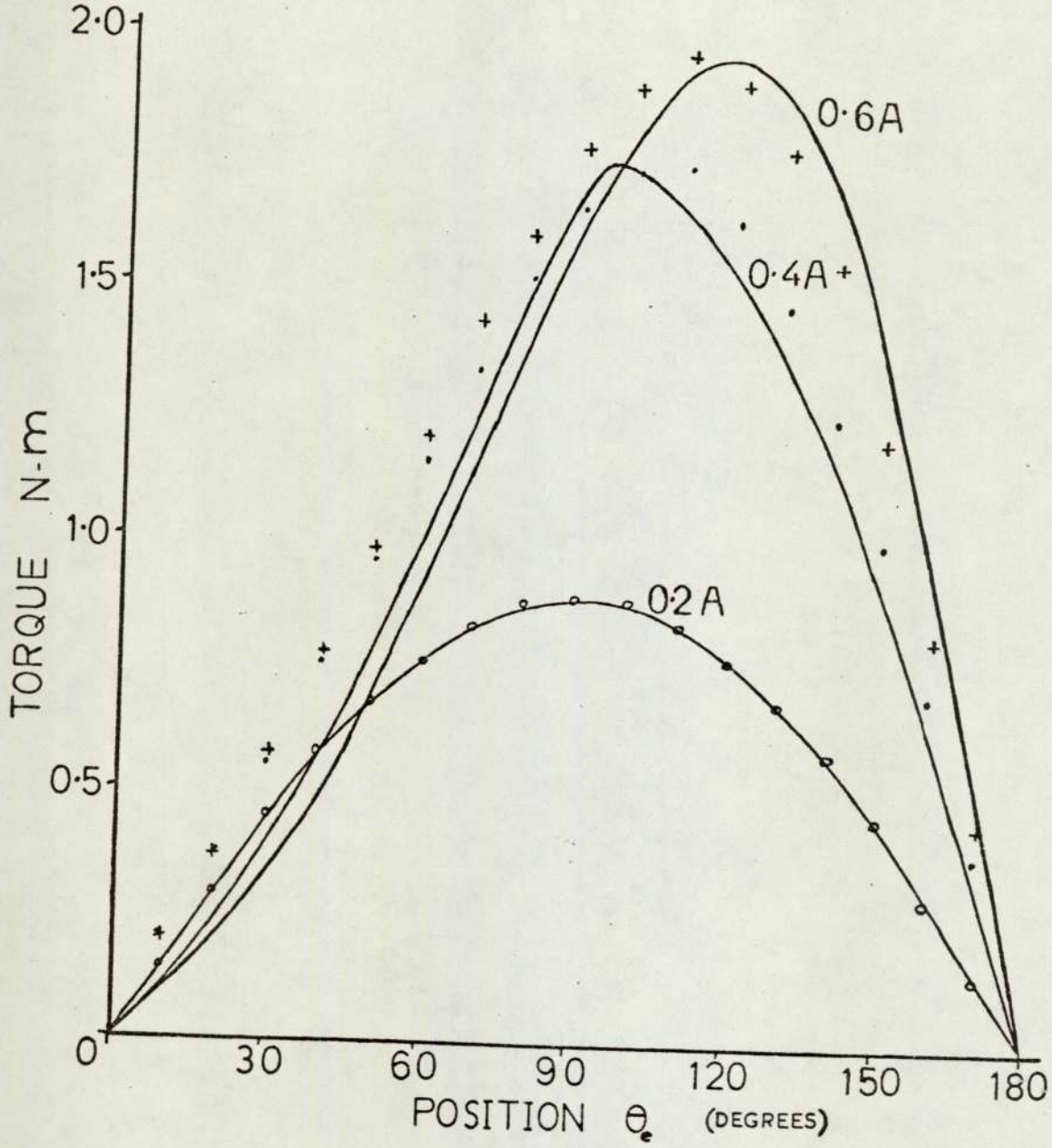

Fig.2.10(a) Static torque characteristics

I = 0.2A, 0.4A, 0.6A

o . + experimental

____ theoretical

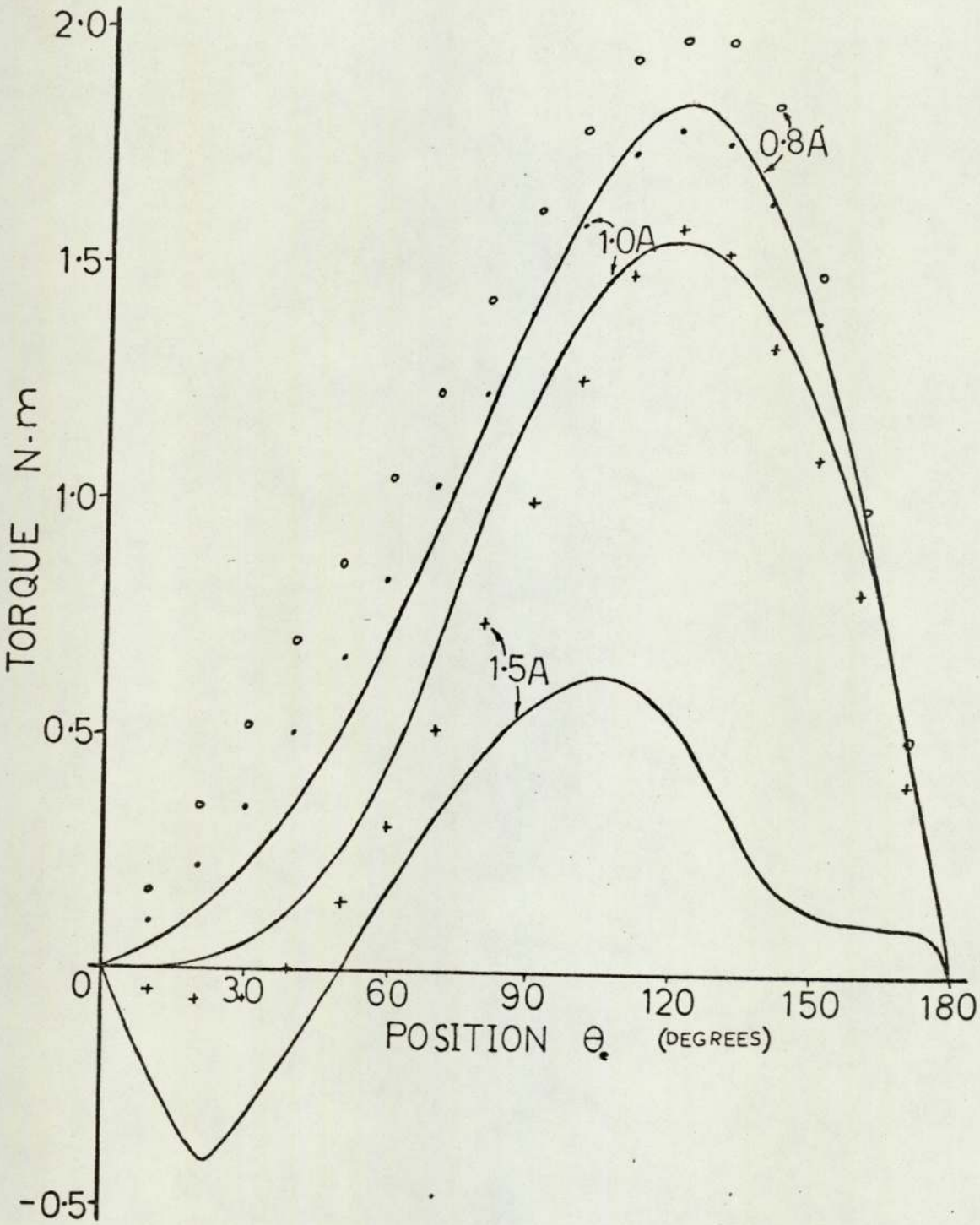

Fig.2.10(b) Static torque characteristics

I = 0.8A, 1.0A, 1.5A.

o . + experimental

_____ theoretical

Equations (2-35), (2-36) and (2-40) now give open circuit e.m.f.'s and torque as

$$e_{aoc} = -2i_{pm}L_{ml}S_2\omega_m \sin\theta_e \quad \ldots\ldots\ldots\ldots\ldots\ldots \quad (2\text{-}46)$$

$$e_{boc} = 2i_{pm}L_{ml}S_2\omega_m \cos\theta_e \quad \ldots\ldots\ldots\ldots\ldots\ldots \quad (2\text{-}47)$$

$$T = 2i_{pm}nL_{ml}S_2(i_b \cos\theta_e - i_a \sin\theta_e) \quad \ldots\ldots\ldots \quad (2\text{-}48)$$

General expressions for the e.m.f. are obtained from equations (2-19) and (2-20) as

$$e_a = \eta_s\left[2L_{mo}\frac{di_a}{dt} - 2i_{pm}L_{ml}S_2\omega_m \sin\theta\right] \quad \ldots\ldots\ldots\ldots \quad (2\text{-}49)$$

$$e_b = \eta_s\left[2L_{mo}\frac{di_b}{dt} + 2i_{pm}L_{ml}S_2\omega_m \sin\theta\right] \quad \ldots\ldots\ldots\ldots \quad (2\text{-}50)$$

Each e.m.f. was derived from two components shown in Fig.2.6b. Considering phase 'a' to be supplied by a voltage source v connected to ideal transformers as in Fig.2.11(a). Equivalent sub-circuits presented to each transformer are shown connected in series in Fig. 2.11(b).

It can be seen from equations (2-14), (2-46) and (2-49) that the circuit of Fig.2.11(c) can replace the series connection of the component voltages e_{a1} and e_{a2}. The combined circuit in Figs.2.11(b) and (c) may be compared to the circuit shown in Fig.2.11(d). With the iron loss component neglected this idealised model can be compared with that used by other authors[4,5,10,11,21] and which can be transformed to d-q axis variables, as for a cylindrical rotor synchronous machine[11].

Although permeance harmonics can be included in a rotating field model these are not easily combined with methods accounting for the harmonics due to saturation[40].

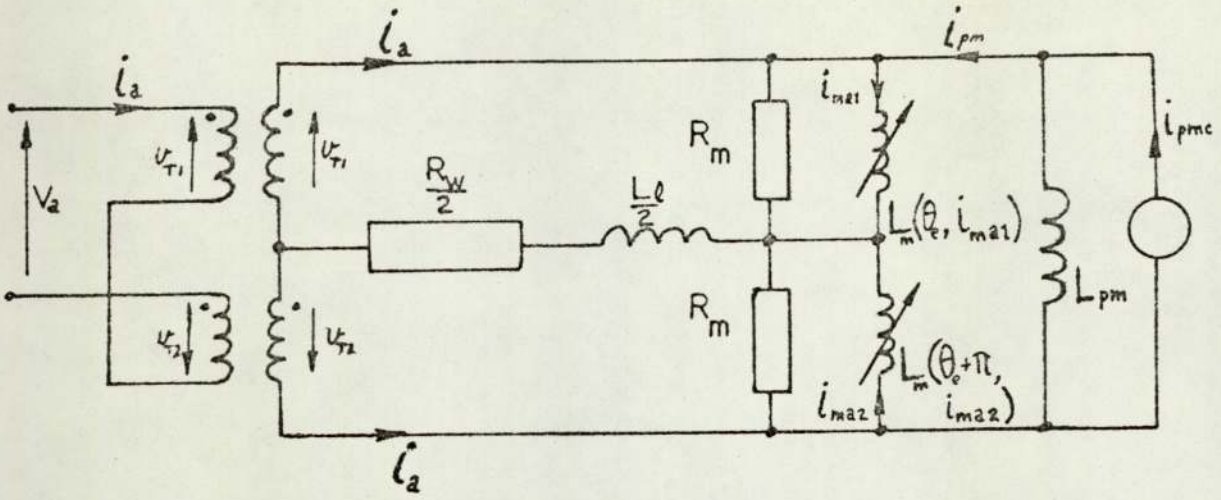

(a) Approximate electrical equivalent circuit using ideal transformers (one phase).

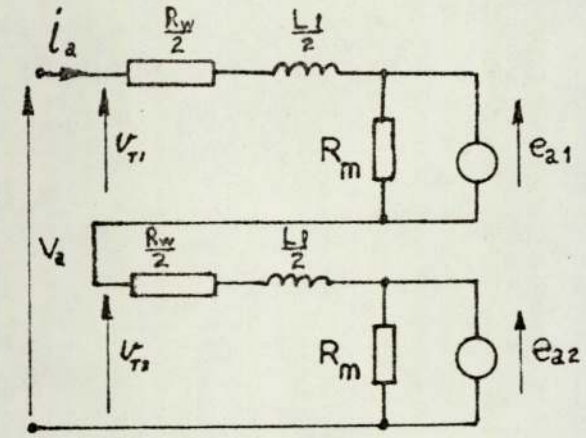

(b) Approximate equivalent circuit presented to phase winding.

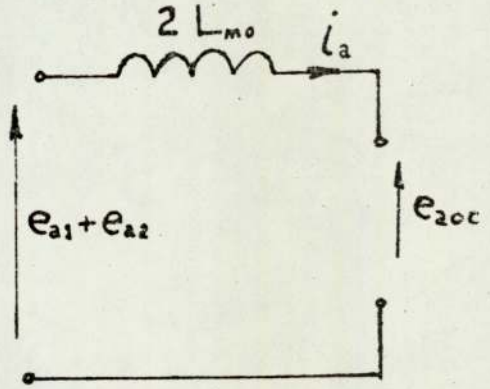

(c) E.m.f. representation.

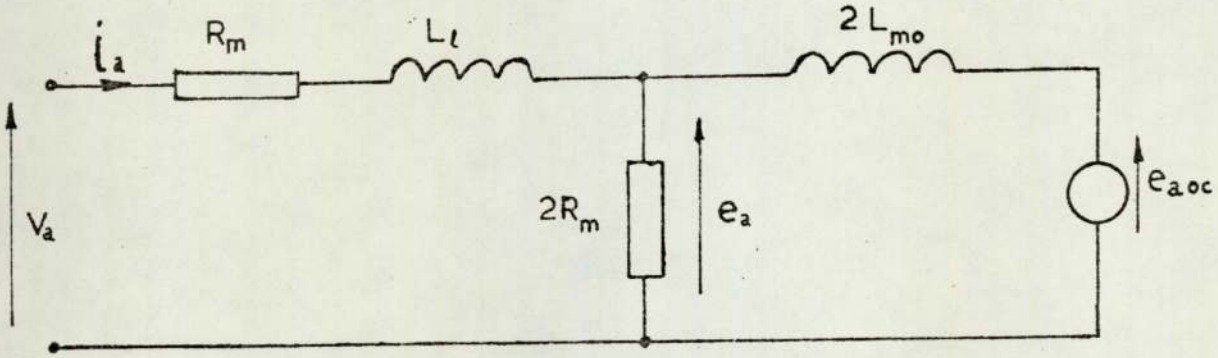

(d) Equivalent circuit derived by combining (b) and (c).

Fig.2.11 Comparison with rotating field model.

2.6 CONCLUSIONS

The electrical and magnetic equivalent circuit models that have been derived show how to take into account iron losses, permeance harmonics, saturation and the interactions between winding and permanent magnet which occur within the machine.

The forming of a magnetic equivalent circuit in addition to, or instead of an electrical equivalent circuit, is a very powerful tool in the modelling of electromagnetic systems. Recent work[20] in this area has aimed to relate this approach to generalised machine theory. Its application to the stepping motor has provided a more realistic model and indicates that the approach can be of advantage for pulsating field machines.

Although this modelling technique is applicable to other types of electrical machine it is not usually adopted or required. From an early stage the Engineer learns to associate a particular electrical circuit with a certain type of machine and the equivalence tends to be 'taken for granted' without formal derivation.

The models presented here are for a popular type of stepping motor but the diversity of other possible electromagnetic configurations requires familiarity with a modelling technique, rather than with a particular model. For a given arrangement of iron and copper it seems far easier to realise the magnetic equivalent circuit than the electrical equivalent circuit, though many engineers may prefer to deal with the latter which may be interpreted through duality.

It is anticipated that the model can be applied to the prediction of the single and multi-step responses, pull in and pull out performance and other possible relationships if the driving circuit and load are known. All these important operating characteristics can be predicted if the motor torque is known with sufficient accuracy.

Whereas a very simple model is inaccurate in the presence of severe saturation, the accuracy is acceptable where moderate saturation is present. For the machine tested, which is typical of its type, the range was up to two and a half times full load current and is a substantial improvement over

models that assume the torque to be approximately proportional to current.

Model simplification thus reduces what would otherwise be an extremely complex problem into a more easily managed form. The simplified linear and non-linear model that has been derived is used for the optimisation procedures in the following section.

3. INPUT OPTIMISATION USING A LINEAR MODEL

3.1 Introduction

To obtain accurate results a digital computer would be used to investigate one of the non-linear models presented in Section 2. If an analytical solution is required then a linear model, such as that derived in Section 2.5.2, must be adopted.

Although magnetic saturation and harmonics have been neglected in its derivation such a model can be very useful in gaining an initial understanding of the machine and is used for the following optimisation studies.

Conditions are restricted to constant speed operation. The phase angle, degree of forcing and (for pulsed supplies) pulse width are to be optimised to give maximum torque with the constraint of limited machine losses.

The equations derived using this performance index also give the optimum conditions, at a given speed, for all possible values of acceleration, including constant speed operation. This is because either the torque or the losses may be fixed, so the same equations can also define the conditions for minimum losses subject to a given torque.

General expressions are derived which enable the conditions for which either the copper loss or the iron loss is a minimum. Of particular interest is the condition for which the total of these losses is a minimum.

If a drive circuit has an effective series resistance this may be included in the term Rw denoting winding resistance. The proportion of the copper losses to be minimised will then depend upon the relative importance of the heat lost in the drive circuit and that lost in the machine.

All these conditions may be obtained by suitable values of the

variable λ in the performance index.

For sinusoidal supplies the optimisation is carried out in terms of the load angle, then in terms of voltage and current phase angles.

Similar procedures are then carried out using pulsed supplies.

3.2 Operation from Sinusoidal Supplies

3.2.1 Circuit Equations

Using a two-port representation for the circuit in Fig.2.11(d) the admittance matrix is given by,

$$\left[y(s)\right] = \frac{1}{2sL_{mo} + (R_w+sL_L)\left(1+\frac{sL_{mo}}{R_m}\right)} \begin{bmatrix} 1 + \frac{sL_{mo}}{R_m} & -1 \\ 1 & -(1+\frac{R_w+sL_L}{2R_m}) \end{bmatrix} \quad \ldots (3\text{-}1)$$

let, $z_1 \angle \beta_1 = 2j\omega L_{mo} + (R_w+j\omega L_L)\left(1+\frac{j\omega L_{mo}}{R_m}\right)$

$$z_2 \angle \beta_2 = 2\,(R_m + j\omega L_{mo})$$

$$z_3 \angle \beta_3 = 2\,R_m + R_w + j\omega L_L \qquad \ldots\ldots (3\text{-}2)$$

thus, $$\begin{bmatrix} I(j\omega) \\ I_m(j\omega) \end{bmatrix} = \frac{1}{z_1 \angle \beta_1} \begin{bmatrix} \frac{z_2}{2R_m}\angle \beta_2 & -1 \\ 1 & \frac{-z_3}{2R_m}\angle \beta_3 \end{bmatrix} \begin{bmatrix} V(j\omega) \\ E(j\omega) \end{bmatrix} \quad \ldots\ldots (3\text{-}3)$$

also, let,

$$\left.\begin{aligned} e_\alpha &= \hat{E}\cos\theta_e \quad \text{and} \quad e = \hat{V}_m \cos\theta_e \\ \text{where} \quad \hat{E} &= C\omega \\ C &= 2s_2 L_{m1} i_{pm} \\ \text{and} \quad v &= \hat{V}\cos(\theta_e+\gamma) \end{aligned}\right\} \quad \ldots (3\text{-}4)$$

considering the e.m.f. as the reference phase,

i.e. $E(j\omega) = \hat{E}\angle 0 \qquad I_m(j\omega) = \hat{I}_m\angle\delta$

$V(j\omega) = \hat{V}\angle\gamma \qquad I(j\omega) = \hat{I}\angle\alpha$ .... (3-5)

The torque developed can be obtained from

$$\omega T = \frac{m}{2}\,\mathrm{Re}\left(E(j\omega).\ I_m^{*}(j\omega)\right) \qquad \text{.... (3-6)}$$

where m is the number of phases and * denotes conjugate.

thus $$T = \frac{m\,C\,\hat{I}_m}{2}\cos\delta \qquad \text{.... (3-7)}$$

or in terms of V and γ,

$$T = \frac{mC}{2z_1}\left(\hat{V}\cos(\beta_1-\gamma) - \frac{Cwz_3}{2R_m}\cos(\beta_1-\beta_3)\right) \qquad \text{.... (3-8)}$$

Subject to the single constraint, $\hat{V} \leqslant \hat{V}_{max}$ .... (3-9)

the conditions for maximum torque would be,

$$\hat{V}_o = \hat{V}max \qquad \text{.... (3-10)}$$

and γ_o, the optimum values for γ, would be

$$\gamma_{oF} = \beta_1 \quad \text{and} \quad \gamma_{oR} = \beta_1 - \pi \qquad \text{.... (3-11)}$$

for 'forward' and 'reverse' torques. These would lie within the range 0 to $\pi/2$ and $-\pi$ to $-\pi/2$ respectively and would be functions of speed.

δ_o would be constant, having values of 0 and π respectively.

If losses are considered, the optimisation is not as simple and in general δ_o is not constant.

3.2.2 Optimisation in terms of I_m and δ

The copper and iron losses are given by,

$$P_{cu} = \frac{m}{2} \hat{I}^2 R_w \qquad \ldots\ (3\text{-}12)$$

and

$$P_{Fe} = \frac{m}{4} \frac{\hat{V}_m^2}{R_m} \qquad \ldots\ (3\text{-}13)$$

Considering the vector diagram of Fig.3.1

$$\hat{I}^2 = \hat{I}_m^2 + \left(\frac{\hat{V}_m}{2R_m}\right)^2 + \frac{\hat{I}_m \hat{V}_m}{R_m} \cos(\varepsilon - \delta) \qquad \ldots\ (3\text{-}14)$$

$$\hat{V}_m^2 = (c\omega)^2 + (2\hat{I}_m \omega L_{mo})^2 - 4\hat{I}_m c\omega^2 L_{mo} \cos\left(\delta - \frac{\pi}{2}\right) \qquad \ldots\ (3\text{-}15)$$

and,

$$\frac{\sin\left(\frac{\pi}{2} - \delta\right)}{\hat{V}_m} = \frac{\sin\left(\frac{\pi}{2} - \varepsilon + \delta\right)}{c\omega} \qquad \ldots\ (3\text{-}16)$$

hence,

$$P_{cu} = \frac{m}{2}\left(\hat{I}_m^2 + \left(\frac{\hat{V}_m}{2R_m}\right)^2 + \frac{\hat{I}_m c\omega}{R_m} \cos\delta\right) R_w \qquad \ldots\ (3\text{-}17)$$

and,

$$P_{Fe} = \frac{m}{4} \cdot \frac{(c\omega)^2 + (2\hat{I}_m \omega L_{mo})^2 - 4\hat{I}_m c\omega^2 L_{mo} \sin\delta}{R_m} \qquad \ldots\ (3\text{-}18)$$

The input power is given by,

$$P_{in} = \omega T + P_{cu} + P_{Fe} \qquad \ldots\ (3\text{-}19)$$

Now let,

$$F(\hat{I}_m, \delta) = T + \lambda_1 P_{cu} + \lambda_2 P_{Fe} \qquad \ldots\ (3\text{-}20)$$

where λ_1 and λ_2 are Lagrangian multipliers.

The losses are expressed in the form,

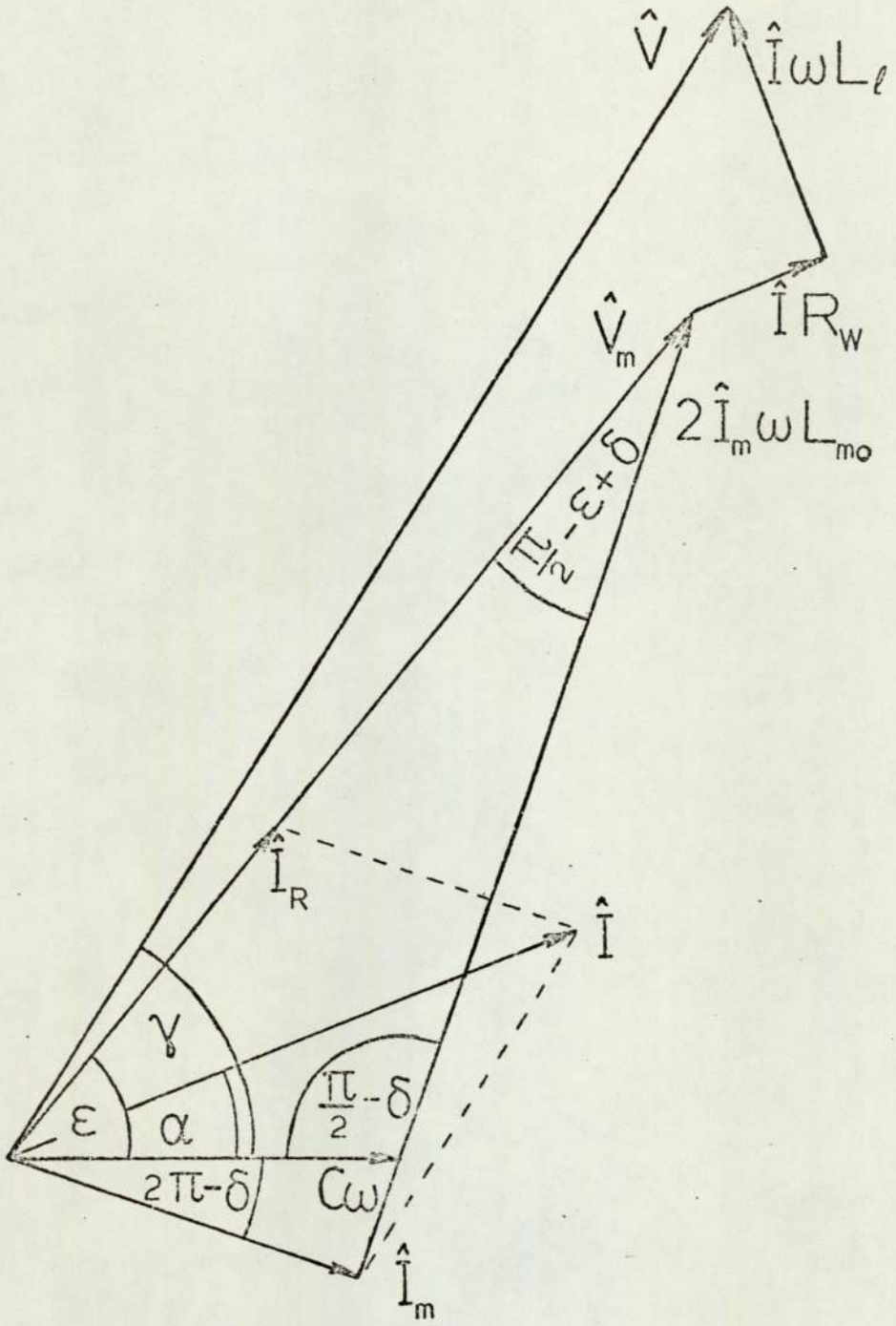

Fig.3.1 Vector Diagram

$$P_L = P_{cu} + \lambda P_{Fe} \qquad \ldots\ (3\text{-}21)$$

where,

$$\lambda = \frac{\lambda_2}{\lambda_1} \qquad \ldots\ (3\text{-}22)$$

T, P_{cu} and P_{Fe} in equation (3-20) are given by equations (3-7), (3-17) and (3-18), the solution being obtained by putting,

$$\frac{\partial F}{\partial \hat{I}_m} = 0 \quad \text{and} \quad \frac{\partial F}{\partial \delta} = 0 \qquad \ldots\ (3\text{-}23)$$

Note that the form chosen for equation (3-20) is not the only possibility, since minimising $F = T + \lambda P_L$ gives the same conditions as minimising, $F = \omega T + \lambda P_L$,

$$F = P_L + \lambda(T-k),$$

or, $F = P_{in} + \lambda(P_L - k)$ and so on.

For these conditions, $\hat{I}_m = \hat{I}_{mo}$ and $\delta = \delta_o$

giving,

$$\hat{I}_{mo} \sin \delta_o = \frac{2\omega^2 L_{mo} C\,(R_w + \lambda 2R_m)}{(2R_m)^2 R_w + (2\omega L_{mo})^2 (R_w + \lambda 2R_m)} \qquad \ldots\ (3\text{-}24)$$

thus for minimum P_{cu},

$(\lambda = 0)$ $$\hat{I}_{mo} \sin \delta_o = \frac{2\omega^2 L_{mo} C}{(2R_m)^2 + (2\omega L_{mo})^2} \qquad \ldots\ (3\text{-}25)$$

for minimum P_{Fe},

$(\lambda \to \infty)$ $$\hat{I}_{mo} \sin \delta_o = \frac{C}{2 L_{mo}} \qquad \ldots\ (3\text{-}26)$$

i.e. v_m is in phase with i_m

and for minimum $(P_{cu} + P_{Fe})$,

$(\lambda = 1)$ $$\hat{I}_{mo} \sin \delta_o = \frac{2\omega^2 L_{mo} C(R_w + 2R_m)}{(2R_m)^2 R_w + (2\omega L_{mo})^2 (R_w + 2R_m)} \qquad \ldots\ (3\text{-}27)$$

3.2.3 Optimisation in terms of V and γ

The input power is given by,

$$P_{in} = \frac{m}{2} \mathcal{R} \left(V(jw)\, I^{*}(jw) \right) \qquad \ldots\ (3\text{-}28)$$

I(jw) is given by equation (3-3)

thus,

$$P_{in} = \frac{m}{2} \frac{\hat{V}}{z_1} \left(\frac{\hat{V} z_2}{2R_m} \cos(\beta_1 - \beta_2) - C\omega \cos(\gamma + \beta_1) \right) \qquad \ldots\ (3\text{-}29)$$

from equations (3-8), (3-19) and (3-29),

the total losses are given by,

$$P_{cu}+P_{Fe} = \frac{m}{2z_1} \left(\frac{\hat{V}^2 z_2 \cos(\beta_1-\beta_2) + (C\omega)^2 z_3 \cos(\beta_3-\beta_1)}{2R_m} - 2\hat{V}C\omega \cos\beta_1 \cos\gamma \right) \qquad \ldots\ (3\text{-}30)$$

from equations (3-3) and (3-5),

$$I(j\omega) = \frac{1}{z_1} \left(\frac{\hat{V} z_2}{2R_m} \angle \gamma + \beta_2 - \beta_1 \; - C\omega \angle -\beta_1 \right) \qquad \ldots\ (3\text{-}31)$$

hence using equation (3-12),

$$P_{cu} = \frac{m}{2} \left(\left(\frac{\hat{V} z_2}{2R_m} \right)^2 + (C\omega)^2 - \frac{\hat{V} C\omega z_2}{R_m} \cos(\gamma+\beta_2) \right) \frac{R_w}{z_1^2} \qquad \ldots\ (3\text{-}32)$$

and from equations (3-30) and (3-32),

$$P_{Fe} = \frac{m}{2z_1} \left(\frac{\hat{V}^2 z_2}{2R_m} \left(\cos(\beta_1-\beta_2) - \frac{z_2 R_w}{2R_m z_1} \right) + (C\omega)^2 \left(\frac{z_3 \cos(\beta_3-\beta_1)}{2R_m} - \frac{R_w}{z_1} \right) \right.$$

$$\left. + \hat{V}\, C\omega \left(\frac{z_2 R_w}{z_1 R_m} \cos(\gamma+\beta_2) - 2\cos\beta_1 \cos\gamma \right) \right) \qquad \ldots\ (3\text{-}33)$$

now let,

$$F(\hat{V}, \gamma) = T + \lambda_1 P_{cu} + \lambda_2 P_{Fe} \qquad \ldots\ (3\text{-}34)$$

where T, P_{cu} and P_{Fe} are given by equations (3-8), (3-32) and (3-33) and a procedure similar to that used for equation (3-20) is carried out.

This gives,

$$\hat{V}_o \sin(\gamma_o-\beta_1) = \frac{-R_m C\omega(z_2R_w(1-\lambda)\sin(\beta_1+\beta_2)+R_m z_1 \lambda \sin(2\beta_1))}{z_2(z_2R_w(1-\lambda)+R_m z_1 \lambda \cos(\beta_1-\beta_2)} \quad \ldots. (3\text{-}35)$$

thus, for minimum P_{cu},

$$(\lambda = 0) \qquad \hat{V}_o \sin(\gamma_o-\beta_1) = -\frac{R_m C\omega}{z_2} \sin(\beta_1+\beta_2) \quad \ldots. (3\text{-}36)$$

for minimum P_{Fe},

$$(\lambda \to \infty)$$

$$\hat{V}_o \sin(\gamma_o-\beta_1) = \frac{-R_m C\omega(R_m z_1 \sin(2\beta_1) - R_w z_2 \sin(\beta_1+\beta_2))}{z_2(R_m z_1 \cos(\beta_1-\beta_2)-R_w z_2)} \quad \ldots. (3\text{-}37)$$

and for minimum $(P_{cu}+P_{Fe})$,

$$(\lambda = 1) \qquad \hat{V}_o \sin(\gamma_o-\beta_1) = \frac{-R_m C\omega \sin(2\beta_1)}{z_2 \cos(\beta_1-\beta_2)} \quad \ldots. (3\text{-}38)$$

3.2.4 Optimisation in terms of I and α

From equation (3-3), using hybrid parameters,

$$\begin{bmatrix} V(j\omega) \\ I_m(j\omega) \end{bmatrix} = \frac{2R_m}{z_2 \angle \beta_2} \begin{bmatrix} z_1 \angle \beta_1 & 1 \\ 1 & \frac{-1}{2R_m} \end{bmatrix} \begin{bmatrix} I(j\omega) \\ E(j\omega) \end{bmatrix} \quad \ldots. (3\text{-}39)$$

from equations (3-5), (3-6) and (3-39),

$$T = \frac{m C}{2z_2}(2R_m \hat{I} \cos(\alpha-\beta_2) - C\omega \cos\beta_2) \quad \ldots. (3\text{-}40)$$

from equations (3-28) and (3-39),

$$P_{in} = \frac{mR_m \hat{I}}{z_2}(\hat{I}z_1 \cos(\beta_1-\beta_2) + C\omega \cos(\alpha+\beta_2)) \quad \ldots. (3\text{-}41)$$

P_{cu} is given by (3-12)

using (3-12), (3-19), (3-40) and (3-41)

$$P_{Fe} = \frac{m}{2}\left(\hat{I}^2\left(\frac{2R_m z_1}{z_2}\cos(\beta_1-\beta_2)-R_w\right)+\frac{C\omega R_m}{z_2^2}\left(C\omega - 4\hat{I}\sin\alpha\sin\beta_2\right)\right) \quad \ldots. (3\text{-}42)$$

letting $F(\hat{I}, \alpha) = T + \lambda_1 P_{cu} + \lambda_2 P_{Fe}$ .... (3-43)

and solving for $\hat{I}_o$ and α_o gives,

$$\hat{I}_o \sin(\alpha_o - \beta_2) = \frac{R_m C\omega\lambda\sin(2\beta_2)}{R_w z_2(1-\lambda)+2R_m z_1\lambda\cos(\beta_1-\beta_2)} \quad \ldots. (3\text{-}44)$$

thus for minimum P_{cu},

($\lambda = 0$)

$$\alpha_{oF} = \beta_2 \quad \text{and} \quad \alpha_{oR} = \beta_2 - \pi \quad \ldots. (3\text{-}45)$$

this would also be the condition for maximum torque, subject to the constraint,

$$\hat{I} \leq \hat{I}max \quad \ldots. (3\text{-}46)$$

whereupon I_o would be,

$$\hat{I}_o = \hat{I}max \quad \ldots. (3\text{-}47)$$

for minimum P_{Fe},

($\lambda \to \infty$)

$$\hat{I}_o\sin(\alpha_o-\beta_2) = \frac{R_m C\omega\sin(2\beta_2)}{2R_m z_1\cos(\beta_1-\beta_2)-R_w z_2} \quad \ldots. (3\text{-}48)$$

and for minimum $(P_{cu} + P_{Fe})$,

($\lambda = 1$)

$$\hat{I}_o\sin(\alpha_o-\beta_2) = \frac{C\omega\sin(2\beta_2)}{2z_1\cos(\beta_1-\beta_2)} \quad \ldots. (3\text{-}49)$$

Otherwise, subject to the single constraint,

$$\hat{I} \leq \hat{I}_{max} \qquad \ldots\ (3\text{-}50)$$

the conditions for maximum torque would be,

$$\hat{I}_o = \hat{I}_{max} \qquad \ldots\ (3\text{-}51)$$

$$\alpha_{oF} = \beta_2 \quad \text{or} \quad \alpha_{oR} = \beta_2 - \pi \qquad \ldots\ (3\text{-}52)$$

corresponding to the condition

$$\delta = \delta_o \qquad \ldots\ (3\text{-}53)$$

which has values of 0 and π respectively.

3.3 OPERATION FROM PULSED SUPPLIES

3.3.1 System Equations

The state equation for the system shown in Fig.3.2 is

$$\begin{bmatrix} \dot{V} \\ \dot{r} \\ \dot{x}_1 \\ \dot{x}_2 \\ \dot{i} \\ \dot{i}_m \end{bmatrix} = \begin{bmatrix} 0 & 0 & 0 & 0 & 0 & 0 \\ 0 & 0 & 0 & 0 & 0 & 0 \\ 0 & 0 & 0 & 1 & 0 & 0 \\ 0 & 0 & -\omega^2 & 0 & 0 & 0 \\ 0 & \frac{1}{L_L} & 0 & 0 & \frac{-1}{\tau_1}\frac{-1}{\tau_2} & \frac{1}{\tau_2} \\ 0 & 0 & \frac{-C\omega}{2L_{mo}} & 0 & \frac{1}{\tau_3} & \frac{-1}{\tau_3} \end{bmatrix} \begin{bmatrix} V \\ r \\ x_1 \\ x_2 \\ i \\ i_m \end{bmatrix} \qquad \ldots\ (3\text{-}54)$$

where,

$$\tau_1 = \frac{L_L}{R_w}$$

$$\tau_2 = \frac{L_L}{2R_m} \qquad \ldots\ (3\text{-}55)$$

$$\tau_3 = \frac{L_{mo}}{R_m}$$

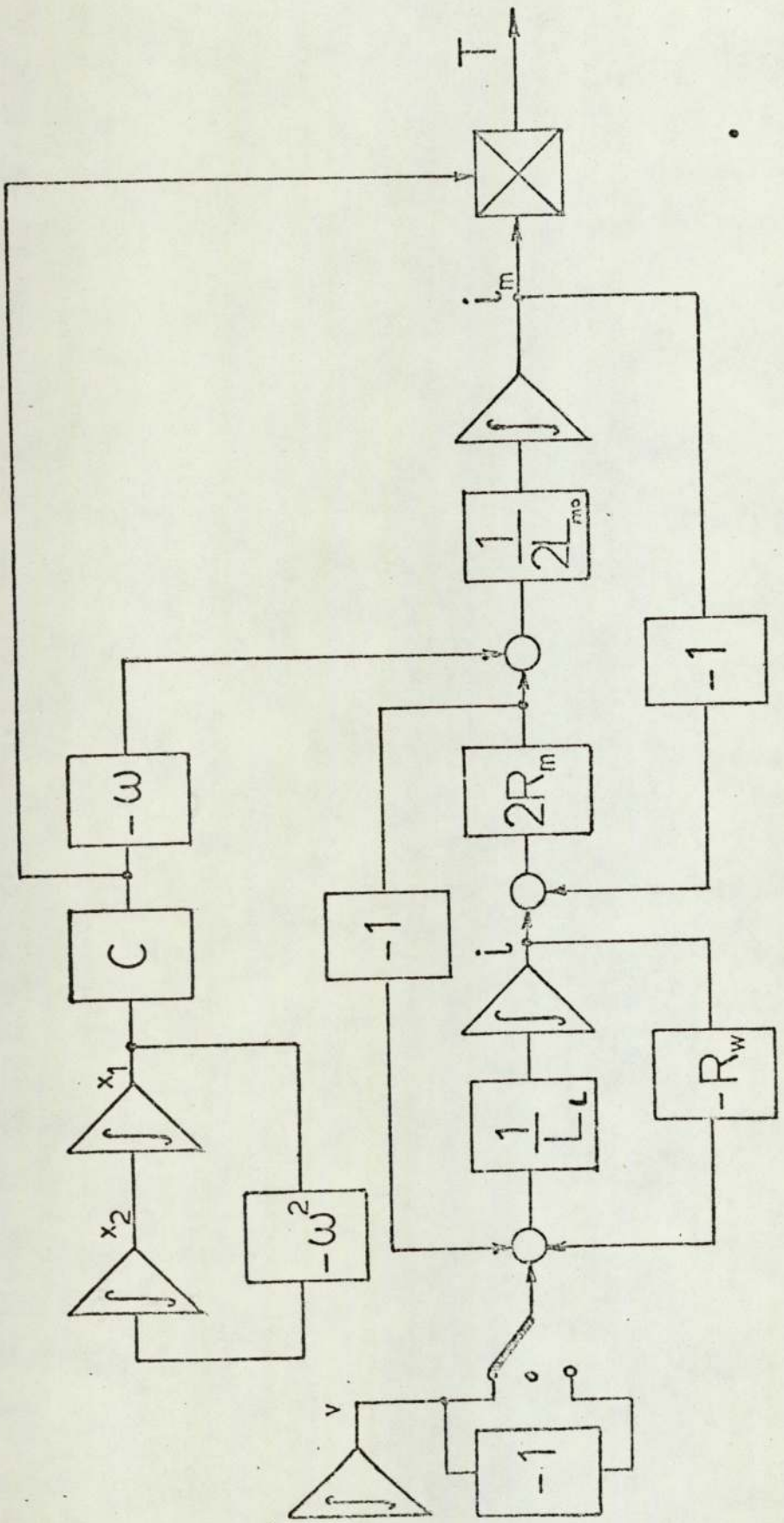

Fig.3.2 State Diagram

Let the overall transition matrix[41] be partitioned as follows,

$$\underline{\phi}(t)=\begin{bmatrix} 1 & 0 & 0 & 0 \\ 0 & 1 & 0 & 0 \\ 0 & 0 & R_e(t) & 0 \\ 0 & h_v(t) & h_e(t) & \phi_c(t) \end{bmatrix} \qquad \ldots\ (3\text{-}56)$$

$R_e(t)$, the e.m.f. 'input' transition matrix is given by,

$$R_e(t) = \begin{bmatrix} \cos \omega t & \frac{\sin \omega t}{\omega} \\ -\omega \sin \omega t & \cos \omega t \end{bmatrix} \qquad \ldots\ (3\text{-}57)$$

$h_v(t)$ and $h_e(t)$ are control transition matrices, associated with input voltage and e.m.f. respectively. These are given by,

$$h_v(t)= \frac{1}{L_L} \begin{bmatrix} \frac{1}{\sigma_1\sigma_2\tau_3} + \frac{1}{\sigma_1-\sigma_2}\left\{\left(1+\frac{1}{\sigma_1\tau_3}\right)e^{\sigma_1 t} - \left(1+\frac{1}{\sigma_2\tau_3}\right)e^{\sigma_2 t}\right\} \\ \frac{1}{\tau_3}\left\{\frac{1}{\sigma_1\sigma_2} + \frac{1}{\sigma_1-\sigma_2}\left(\frac{e^{\sigma_1 t}}{\sigma_1} - \frac{e^{\sigma_2 t}}{\sigma_2}\right)\right\} \end{bmatrix}$$

$\ldots\ (3\text{-}58)$

and,

$$h_e(t)= \frac{C\omega}{2L_{mo}(\sigma_1-\sigma_2)}\left\{\frac{-e^{\sigma_1 t}}{\omega^2+\sigma_1^2}\begin{bmatrix} \sigma_1/\tau_2 & 1/\tau_2 \\ \sigma_1(\sigma_1+1/\tau_1+1/\tau_2) & \sigma_1+1/\tau_1+1/\tau_2 \end{bmatrix}\right.$$

$$+\frac{e^{\sigma_2 t}}{\omega^2+\sigma_2^2}\begin{bmatrix} \sigma_2/\tau_2 & 1/\tau_2 \\ \sigma_2(\sigma_2+1/\tau_1+1/\tau_2) & \sigma_2+1/\tau_1+1/\tau_2 \end{bmatrix}$$

$$+\frac{\sin(\omega t+\theta_1)}{\omega(\omega^2+\sigma_1^2)}\begin{bmatrix} \sigma_1/\tau_2 & 1/\tau_2 \\ 0 & \sigma_1+1/\tau_1+1/\tau_2 \end{bmatrix} - \frac{\sin(\omega t+\theta_2)}{\omega(\omega^2+\sigma_2^2)}\left.\begin{bmatrix} \sigma_2/\tau_2 & 1/\tau_2 \\ 0 & \sigma_2+1/\tau_1+1/\tau_2 \end{bmatrix}\right.$$

$$+ \frac{\cos(\omega t+\theta_1)}{\omega^2+\sigma_1^2}\begin{bmatrix} 0 & 0 \\ \sigma_1+1/\tau_1+1/\tau_2 & 0 \end{bmatrix} - \frac{\cos(\omega t-\theta_2)}{\omega^2+\sigma_2^2}\begin{bmatrix} 0 & 0 \\ \sigma_2+1/\tau_1+1/\tau_2 & 0 \end{bmatrix}\Bigg\}$$

..... (3-59)

$$\phi_c(t) = \frac{1}{\sigma_1-\sigma_2}\begin{bmatrix} (\sigma_1+1/\tau_3)e^{\sigma_1 t} - (\sigma_2+1/\tau_3)e^{\sigma_2 t} & 1/\tau_2(e^{\sigma_1 t} - e^{\sigma_2 t}) \\ 1/\tau_3(e^{\sigma_1 t} - e^{\sigma_2 t}) & (\sigma_1+1/\tau_1+1/\tau_2)e^{\sigma_1 t} - (\sigma_2+1/\tau_1+1/\tau_2)e^{\sigma_2 t} \end{bmatrix}$$

..... (3-60)

σ_1 and σ_2 in the above equations are the eigenvalues given by the solution of the characteristic equation.

$$\sigma^2 + (1/\tau_1+1/\tau_2+1/\tau_3)\,\sigma + \frac{1}{\tau_1\tau_3} = 0 \qquad \text{..... (3-61)}$$

also, $\theta_1 = \tan^{-1}\frac{\omega}{\sigma_1}$ and $\theta_2 = \tan^{-1}\frac{\omega}{\sigma_2}$

3.3.2 Operation from Pulsed Voltage Supplies

If $t - t_o = \dfrac{\theta_e + \gamma + \frac{\theta w}{2}}{\omega}$ ..... (3-62)

where θw is the width of the pulse for a 3-level pulse sequence, such that

$$r = V \;\Big|\; -\gamma - \tfrac{\theta w}{2} \leqslant \theta_e < -\gamma + \tfrac{\theta w}{2}$$

$$r = 0 \;\Big|\; -\gamma + \tfrac{\theta w}{2} < \theta_e < -\gamma - \tfrac{\theta w}{2} + \pi \qquad \text{..... (3-63)}$$

and $$r = -V \;\Big|\; -\gamma - \tfrac{\theta w}{2} + \pi \leqslant \theta_e < -\gamma + \tfrac{\theta w}{2} + \pi$$

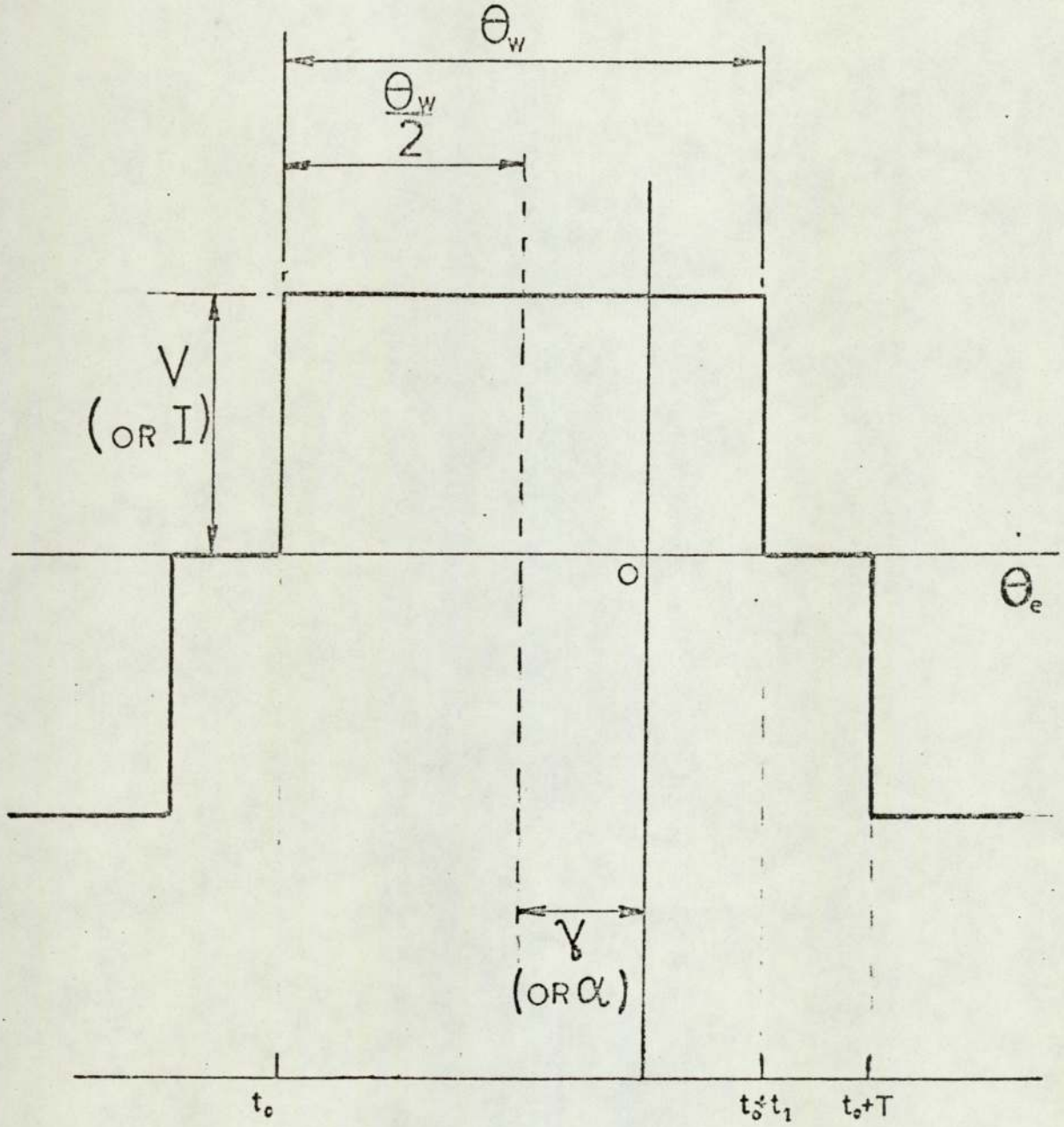

Fig.3.3 Three Level Input Sequence

as shown in Fig.3.3 let, $t_o = \dfrac{-\gamma - \frac{\theta_w}{2}}{\omega}$

$$t_1 = \frac{\theta_w}{\omega}$$

$$t_2 = \frac{\pi - \theta_w}{\omega} \qquad \ldots\ldots (3\text{-}64)$$

$$T = t_1 + t_2$$

The state vector, when half of the switching cycle after $t = t_o$ is completed, is given by,

$$\underline{x}\,(t_o+T) = \phi\,(t_2)\; B_2\; \phi\,(t_1)\; B_1\; \underline{x}(t_o) \qquad \ldots\ldots (3\text{-}65)$$

where the switching matrices, B_1 and B_2 are given by

$$B_1 = \begin{bmatrix} 1 & 0 & 0 & 0 \\ 1 & 0 & 0 & 0 \\ 0 & 0 & I_2 & 0 \\ 0 & 0 & 0 & I_2 \end{bmatrix} \qquad \ldots\ldots (3\text{-}66)$$

$$B_2 = \begin{bmatrix} 1 & 0 & 0 & 0 \\ 0 & 0 & 0 & 0 \\ 0 & 0 & I_2 & 0 \\ 0 & 0 & 0 & I_2 \end{bmatrix} \qquad \ldots\ldots (3\text{-}67)$$

where I_2 is a 2 x 2 unit matrix

similarly, $\underline{x}\,(t_o+2T) = \phi(t_2)\; B_2\; \phi\,(t_1)\; B_3\; \underline{x}(t_o+T) \qquad \ldots\ldots (3\text{-}68)$

where,

$$B_3 = \begin{bmatrix} 1 & 0 & 0 & 0 \\ -1 & 0 & 0 & 0 \\ 0 & 0 & I_2 & 0 \\ 0 & 0 & 0 & I_2 \end{bmatrix} \qquad \ldots\ldots (3\text{-}69)$$

but, $\underline{x}(t_o+T) = -\underline{x}(t_o)$ ..... (3-70)

letting, $\underline{\phi}(t_2)\, B_2\, \underline{\phi}(t_1)\, B_1 = H(T)$ ..... (3-71)

using equations (3-55), (3-64) and (3-65)

$$H(T) = \begin{bmatrix} 1 & 0 & 0 & 0 \\ 0 & 0 & 0 & 0 \\ 0 & 0 & R_e(t_2)R_e(t_1) & 0 \\ 0 & \phi_c(t_2)h_r(t_1) & h_e(t_2)R_e(t_1)+\phi_c(t_2)h_e(t_1) & \phi_c(t_2)\phi_c(t_1) \end{bmatrix}$$

..... (3-72)

The state vector can be calculated for any time t if its value at $t = t_o$ is known.

From equations (3-65), (3-70) and (3-71)

$$-\underline{x}(t_o) = H(T)\, \underline{x}(t_o) \qquad \text{..... (3-73)}$$

Using the properties of the transition matrix, equation (3-72) becomes,

$$H(T) = \begin{bmatrix} 1 & 0 & 0 & 0 \\ 0 & 0 & 0 & 0 \\ 0 & 0 & R_e(T) & 0 \\ 0 & h_v(T)-h_v(t_2) & h_e(T) & \phi_c(T) \end{bmatrix} \qquad \text{..... (3-74)}$$

Only the elements i and i_m are of interest here, and it is convenient to use superposition to obtain these because the components of i and i_m due to the e.m.f. have already been obtained in equation (3-3).

i.e. $$\begin{bmatrix} i(t) \\ i_m(t) \end{bmatrix}_e = \frac{-C\omega}{z_1} \begin{bmatrix} \cos(\omega t-\beta_1) \\ \frac{z_3}{2R_m} \cos(\omega t+\beta_3-\beta_1) \end{bmatrix} \qquad \text{..... (3-75)}$$

The components of i and i_m due to the input r are for

$0 < t - t_o < t_1$,

$$\begin{bmatrix} i(t) \\ i_m(t) \end{bmatrix}_r = \begin{bmatrix} h_v(t-t_o) & \phi_c(t-t_o) \end{bmatrix} \begin{bmatrix} V \\ i(t_o) \\ i_m(t_o) \end{bmatrix}_r \quad \ldots\ (3\text{-}76)$$

and for, $t_1 < t-t_o < t_2$,

$$\begin{bmatrix} i(t) \\ i_m(t) \end{bmatrix}_r = \begin{bmatrix} h_v(t-t_1) & \phi_c(t-t_1) \end{bmatrix} \begin{bmatrix} 0 \\ i(t_1) \\ i_m(t_1) \end{bmatrix}_r \quad \ldots\ (3\text{-}77)$$

but, $i(t_o)$ and $i_m(t_o)$ are yet to be determined.

From equations (3-73) and (3-74)

$$-\begin{bmatrix} i(t_o) \\ i_m(t_o) \end{bmatrix} = \begin{bmatrix} h_v(T)-h_v(t_2) & \phi_c(T) \end{bmatrix} \begin{bmatrix} V \\ i(t_o) \\ i_m(t_o) \end{bmatrix} \quad \ldots\ (3\text{-}78)$$

$$\begin{bmatrix} i(t_o) \\ i_m(t_o) \end{bmatrix} = -(\phi_c(T)+I_2)^{-1}(h_v(T)-h_v(t_2))\ V \quad \ldots\ (3\text{-}79)$$

By combining the components given by equations (3-75) and (3-79)

$$\begin{bmatrix} i(t_o) \\ i_m(t_o) \end{bmatrix} = -(\phi_c(T)+I_2)^{-1}(h_v(T)-h_v(t_2))V - \frac{C\omega}{z_1} \begin{bmatrix} \cos(-\gamma - \frac{\theta w}{2} - \beta_1) \\ \frac{z_3}{2R_m} \cos(-\gamma - \frac{\theta w}{2} + \beta_3 - \beta_1) \end{bmatrix}$$

$\ldots\ (3\text{-}80)$

now $P_{in} = m\ \overline{r\ i}$ $\ldots\ (3\text{-}81)$

using equations (3-75), (3-76) and (3-81)

$$P_{in} = \frac{mVw}{\pi} \left\{ \int_{t_o}^{t_o+t_1} \left[h_{v_{11}}(t-t_o) \quad \phi_{c_{11}}(t-t_o) \quad \phi_{c_{12}}(t-t_o) \right] \begin{bmatrix} V \\ i(t_o) \\ i_m(t_o) \end{bmatrix}_r dt \right.$$

$$\left. - \frac{C}{z_1} \int_{-\gamma-\frac{\theta w}{2}}^{-\gamma+\frac{\theta w}{2}} \cos(\theta_e - \beta_1).d\theta_e \right\} \quad \ldots\ldots (3\text{-}82)$$

where $i(t_o)$ and $i_m(t_o)$ are given by equation (3-79)

$$P_{in} = \frac{mV\omega}{\pi} \left(V\, f(\theta w) - \frac{2C}{z_1} \cos(\gamma+\beta_1) \sin\left(\frac{\theta w}{2}\right) \right) \quad \ldots\ldots (3\text{-}83)$$

where,

$$f(\theta w) = \int_{t_o}^{t_o+t_1} \left[h_{v_{11}}(t-t_o) \quad \phi_{c_{11}}(t-t_o) \quad \phi_{c_{12}}(t-t_o) \right] \begin{bmatrix} 1 \\ -(\phi_c(T)+I_2)^{-1}(h_v(T)-h_v(t_2)) \end{bmatrix} dt$$

$\ldots\ldots (3\text{-}84)$

The mean torque is given by,

$$\overline{T} = \frac{m\,C}{2z_1} \left(\hat{V}_1 \cos(\gamma-\beta_1) - \frac{C\omega z_3}{2R_m} \cos(\beta_3-\beta_1) \right) \quad \ldots\ldots (3\text{-}85)$$

(c.f. equation (3-8)).

$\hat{V}_1$, the fundamental component of r is given by,

$$\hat{V}_1 = \frac{4V}{\pi} \sin\left(\frac{\theta w}{2}\right) \quad \ldots\ldots (3\text{-}86)$$

now,

$$P_{cu} = \frac{mRw}{\pi} \int_{-\gamma-\frac{\theta w}{2}}^{-\gamma-\frac{\theta w}{2}+\pi} i^2 . \, d\theta_e \qquad \ldots\ldots (3\text{-}87)$$

and using equations (3-75), (3-76), (3-79) and (3-86)

$$P_{cu} = \frac{mRw}{\pi} \left(f_2(\theta w) V^2 + \frac{\pi}{2} \left(\frac{C\omega}{z_1}\right)^2 + \frac{VC\omega}{z_1} f_1(\theta w) \right) \qquad \ldots\ldots (3\text{-}88)$$

where,

$$f_1(\theta w) = \int_{t_o}^{t_o+t_1} g(t) . \cos(\omega t - \beta_1) . \, dt \qquad \ldots\ldots (3\text{-}89)$$

$$f_2(\theta w) = \int_{t_o}^{t_o+t_1} (g(t))^2 \, dt \qquad \ldots\ldots (3\text{-}90)$$

$$g(t) = \left[h_{v_{11}}(t-t_o) \;\; \phi_{c_{11}}(t-t_o) \;\; \phi_{c_{12}}(t-t_o) \right] \begin{bmatrix} 1 \\ -(\phi_c(T)+I_2)^{-1}(h_v(T)-h_v(t_2)) \end{bmatrix} \qquad \ldots\ldots (3\text{-}91)$$

and using equations (3-19), (3-83), (3-85), (3-86) and (3-88)

$$P_{Fe} = m\left\{ \frac{V}{\pi} \left(V(\omega f(\theta w) - R_w f_2(\theta w)) - \frac{4C\omega}{z_1} \sin\left(\frac{\theta w}{2}\right) \cos\beta_1 \cos\gamma \right) + \frac{C\omega}{z_1} \left(\frac{C\omega z_3}{4R_m} \cos(\beta_3 - \beta_1) - R_w \left(\frac{C\omega}{2z_1} + \frac{V}{\pi} f_1(\theta w) \right) \right) \right\} \qquad \ldots\ldots (3\text{-}92)$$

letting $F(V, \gamma, \theta w) = \bar{T} + \lambda_1 P_{cu} + \lambda_2 P_{Fe}$ $\ldots\ldots (3\text{-}93)$

and solving for V_o, γ_o and θw_o gives,

$$\sin(\gamma_o-\beta_1)\left\{2V_o((1-\lambda)\,R_w z_1 f_2(\theta w_o)+\lambda\omega z_1 f(\theta w_o))+(1-\lambda)C\omega R_w f_1(\theta w_o)\right\}$$

$$=-2\,C\omega\lambda\sin\left(\frac{\theta w_o}{2}\right)\sin(2\beta_1) \qquad \ldots\ldots (3\text{-}94)$$

and,

$$\tan\left(\frac{\theta w_o}{2}\right)=\frac{(1-\lambda)R_w\left\{2V_o z_1 f_2(\theta w_o)+C\omega f_1(\theta w_o)\right\}+\lambda 2z_1\omega V_o f(\theta w_o)}{2(1-\lambda)R_w\left\{V_o z_1 f_2'(\theta w_o)+C\omega f_1'(\theta w_o)\right\}+\lambda 2z_1\omega V_o f'(\theta w_o)}$$

$\ldots\ldots (3\text{-}95)$

where $f'(\theta w)$, $f_1'(\theta w)$ and $f_2'(\theta w)$ are the derivatives of $f(\theta w)$, $f_1(\theta w)$ and $f_2(\theta w)$ with respect to θw.

thus for minimum P_{cu},

$$(\lambda=0) \qquad V_o=\frac{-C\omega\, f_1(\theta w_o)}{2z_1\, f_2(\theta w_o)} \qquad \ldots\ldots (3\text{-}96)$$

and,

$$\tan\left(\frac{\theta w_o}{2}\right)=\frac{2V_o z_1 f_2(\theta w_o)+C\omega f_1(\theta w_o)}{2V_o z_1 f_2'(\theta w_o)+2C\omega f_1'(\theta w_o)} \qquad \ldots\ldots (3\text{-}97)$$

for minimum P_{Fe},

$(\lambda\to\infty)$

$$\sin(\gamma_o-\beta_1)\left\{2V_o(\omega z_1 f(\theta w_o)-R_w z_1 f_2(\theta w_o))-C\omega R_w f_1(\theta w_o)\right\}$$

$$=2\,C\omega\sin\left(\frac{\theta w_o}{2}\right)\sin(2\beta_1) \qquad \ldots\ldots (3\text{-}98)$$

and,

$$\tan\left(\frac{\theta w_o}{2}\right)=\frac{2V_o z_1\omega f(\theta w_o)-Rw\left\{2Vz_1 f_2(\theta w_o)+Cwf_1(\theta w_o)\right\}}{2V_o z_1\omega f'(\theta w_o)-2Rw\left\{Vz_1 f_2'(\theta w_o)+Cwf_1'(\theta w_o)\right\}} \qquad \ldots\ldots (3\text{-}99)$$

and for minimum $P_{cu}+P_{Fe}$,

$$(\lambda=1) \qquad V_o\sin(\gamma_o-\beta_1)=\frac{-C\sin\left(\frac{\theta w_o}{2}\right)\sin(2\beta_1)}{z_1 f(\theta w_o)} \qquad \ldots\ldots (3\text{-}100)$$

and,

$$\tan\left(\frac{\theta w_o}{2}\right) = \frac{f(\theta w_o)}{f'(\theta w_o)} \qquad \ldots\ldots (3\text{-}101)$$

3.3.3 Operation from Pulsed Current Supplies

If the current is switched in a 3-level sequence of the form shown in Fig.3.3, with magnitudes of I, 0 and -I defined in a manner similar to that of equation (3-63), the state equation for the system becomes,

$$\begin{bmatrix} \dot{I} \\ \dot{i} \\ \dot{x}_1 \\ \dot{x}_2 \\ \dot{i}_m \end{bmatrix} \begin{bmatrix} 0 & 0 & 0 & 0 & 0 \\ 0 & 0 & 0 & 0 & 0 \\ 0 & 0 & 0 & 1 & 0 \\ 0 & 0 & -\omega^2 & 0 & 0 \\ 0 & 1/\tau_3 & \frac{-C\omega}{2L_{mo}} & 0 & -1/\tau_3 \end{bmatrix} \begin{bmatrix} I \\ i \\ x_1 \\ x_2 \\ i_m \end{bmatrix} \qquad \ldots\ldots (3\text{-}102)$$

Again, let the overall transition matrix be partitioned,

$$\phi(t) = \begin{bmatrix} 1 & 0 & 0 & 0 \\ 0 & 1 & 0 & 0 \\ 0 & 0 & R_e(t) & 0 \\ 0 & h_I(t) & h_e'(t) & \phi_c'(t) \end{bmatrix} \qquad \ldots\ldots (3\text{-}103)$$

Re(t) is given by equation (3-57),

$$h_I(t) = 1 - e^{-\frac{t}{\tau_3}} \qquad \ldots\ldots (3\text{-}104)$$

$$h_e'(t) = \frac{-Cw}{2L_{mo}\left(\omega^2+\left(\frac{1}{\tau_3}\right)^2\right)}\left[\frac{-e^{\frac{t}{\tau_3}}}{\tau_3} + \frac{\cos\omega t}{\tau_3} + \omega\sin\omega t \quad e^{-t/\tau_3} - \cos\omega t + \frac{\sin\omega t}{\omega\tau_3} \right]$$

$$\ldots\ldots (3\text{-}105)$$

and, $$\phi_c'(t) = e^{-t/\tau_3} \qquad \ldots\ldots (3\text{-}106)$$

The component of i_m, due to the input i is,

for $0 < t-t_o < t_1$,

$$i_m(t) = h_I(t-t_o)\, I + \phi_c'(t-t_o)\, i_m(t_o) \qquad \ldots\ldots (3\text{-}107)$$

and for $t_1 < t-t_o < t_2$,

$$i_m(t) = \phi_c'(t-t_o)\, i_m(t_1) \qquad \ldots\ldots (3\text{-}108)$$

Also, by comparison with the previous section, (equations (3-62) to (3-79))

$$i(t_o) = -(\phi_c'(T) + 1)^{-1}(h_I(T) - h_I(t_2))\, I \qquad \ldots\ldots (3\text{-}109)$$

$$i(t_o) = \frac{1 - e^{t_1/\tau_3}}{1 + e^{T/\tau_3}}\, I \qquad \ldots\ldots (3\text{-}110)$$

The component of i_m due to the e.m.f. is obtained from equation (3-39),

i.e.
$$i_m(t) = \frac{-C\omega}{z_2} \cos(\omega t - \beta_2) \qquad \ldots\ldots (3\text{-}111)$$

The mean torque can be obtained by comparison with equation (3-40),

i.e.
$$\bar{T} = \frac{m\,C}{2z_2}\,(2R_m \hat{I}_1 \cos(\alpha - \beta_2) - Cw \cos\beta_2) \qquad \ldots\ldots (3\text{-}112)$$

where $\hat{I}_1$, the fundamental component of i is given by,

$$\hat{I}_1 = \frac{4I}{\pi} \sin\left(\frac{\theta w}{2}\right) \qquad \ldots\ldots (3\text{-}113)$$

now, $$\overline{wT} + P_{Fe} = m \overline{v_m i} \quad \ldots\ldots (3\text{-}114)$$

$$= \frac{mI}{\pi} \int_{-\gamma-\frac{\theta w}{2}}^{-\gamma+\frac{\theta w}{2}} (I - i_m), 2R_m . d\theta_e \quad \ldots\ldots (3\text{-}115)$$

where i_m is the sum of the components given by equations (3-107) and (3-108), giving

$$\overline{wT} + P_{Fe} = \frac{2mR_m I}{\pi} \left(\omega \tau_3 \frac{\left(e^{\frac{\pi}{\omega\tau_3}} + e^{\frac{\theta w}{\omega\tau_3}}\right)\left(1 - e^{\frac{-\theta w}{\omega\tau_3}}\right)}{1 + e^{\frac{\pi}{\omega\tau_3}}} + \frac{2C\omega}{z_2} \cos(\alpha+\beta_2)\sin\left(\frac{\theta w}{2}\right) \right) \quad \ldots\ldots (3\text{-}116)$$

$$P_{Fe} = m\left(\frac{2I^2 R_m g(\theta w)}{\pi} - \frac{16C\omega I R_m^2}{\pi z_2^2} \sin\left(\frac{\theta w}{2}\right) \cos\alpha + \left(\frac{C\omega}{z_2}\right)^2 R_m \right) \quad \ldots (3\text{-}117)$$

where,

$$g(\theta w) = \frac{e^{\frac{\pi}{\omega\tau_3}} + e^{\frac{\theta w}{\omega\tau_3}} - e^{\frac{\pi - \theta w}{\omega\tau_3}} - 1}{1 + e^{\frac{\pi}{\omega\tau_3}}} . \omega\tau_3 \quad \ldots\ldots (3\text{-}118)$$

P_{cu} is given by,

$$P_{cu} = m I^2 R_w \frac{\theta w}{\pi} \quad \ldots\ldots (3\text{-}119)$$

and from equations (3-19), (3-116), (3-118) and (3-119)

$$P_{in} = \frac{m I}{\pi} \left\{ 2R_m \left(I g(\theta w) + \frac{2C\omega}{z_2} \cos(\alpha+\beta_2)\sin\left(\frac{\theta w}{2}\right) \right) + I R_w \theta w \right\} \quad \ldots\ldots (3\text{-}120)$$

letting $F(I, \alpha, \theta w) = \overline{T} + \lambda_1 P_{cu} + \lambda_2 P_{Fe}$ ..... (3-121)

and solving gives,

$$I_o \sin(\alpha_o - \beta_2) = \frac{-2\lambda\, C\omega R_m \sin(\frac{\theta w_o}{2}) \sin(2\beta_2)}{z_2 (R_w \theta w_o + 2\lambda R_m g(\theta w_o)} \quad \ldots\ldots (3\text{-}122)$$

and,

$$\tan(\frac{\theta w_o}{2}) = \frac{\theta w_o R_w + \lambda 2 R_m g(\theta w_o)}{R_w + \lambda 2 R_m g'(\theta w_o)} \quad \ldots\ldots (3\text{-}123)$$

where,

$$g'(\theta w) = \frac{d\, g(\theta w)}{d\theta w} \quad \ldots\ldots (3\text{-}124)$$

thus, for minimum P_{cu} ($\lambda = 0$) the conditions for $\alpha = \alpha_o$ are as given by equation (3-45)

while,

$$\tan(\frac{\theta w_o}{2}) = \theta w_o \quad \ldots\ldots (3\text{-}125)$$

i.e. $\theta w_o \triangleq 2.33$ radians (133^o) ..... (3-126)

for minimum P_{Fe},

($\lambda \to \infty$) $$I_o \sin(\alpha_o - \beta_2) = \frac{-Cw \sin(\frac{\theta w_o}{2}) \sin(2\beta_2)}{z_2\, g(\theta w_o)} \quad \ldots\ldots (3\text{-}127)$$

and,

$$\tan(\frac{\theta w_o}{2}) = \frac{g(\theta w_o)}{g'(\theta w_o)} \quad \ldots\ldots (3\text{-}128)$$

taking limits, $$\lim_{\omega \to 0} \tan(\frac{\theta w_o}{2}) = \infty \quad \ldots\ldots (3\text{-}129)$$

i.e. $$\lim_{\omega \to 0} \theta w_o = \pi \qquad \ldots\ldots (3\text{-}130)$$

and $$\lim_{\omega \to \infty} \tan\left(\frac{\theta w_o}{2}\right) = \theta w_o \qquad \ldots\ldots (3\text{-}131)$$

which is also the condition for minimum P_{cu}, and for minimum $(P_{cu} + P_{Fe})$,

$$(\lambda = 1) \qquad I_o \sin(\alpha_o - \beta_2) = \frac{2 R_m \omega \sin\left(\frac{\theta w_o}{2}\right) \sin(2\beta_2)}{z_2 (R_w \theta w_o + 2 R_m g(\theta w_o))} \qquad \ldots\ldots (3\text{-}132)$$

and,

$$\tan\left(\frac{\theta w_o}{2}\right) = \frac{R_w \theta w_o + 2 R_m g(\theta w_o)}{R_w + 2 R_m g'(\theta w_o)} \qquad \ldots\ldots (3\text{-}133)$$

The value of 133° for θw_o given by equations (3-126) and (3-131) satisfies the conditions which maximise the fundamental component of the pulsed waveform for a given r.m.s. value. Alternatively it is that value of θw which minimises the mean square error between the waveform and a sinusoid.

3.4 DISCUSSION

Equations have been derived in this Section on the assumption that there exists an unlimited range of input level and phase angle combinations which will give the required torque. If the optimum input is calculated to be greater than that which is available, the maximum available input must be regarded as the new optimum and this value should be used in re-calculating the new optimum phase angle.

Similarly, if the pulse width θw of a switched supply is fixed then this value must be regarded as the optimum and used in calculating

the optimum input level and phase angle.

The procedures have been restricted to constant speed operation. The assumption that the iron loss can be represented as dissipated in the component R_m is an approximation even at constant speed and is unlikely to be valid over a wide speed range. Re-calculation of the optimum operating conditions is therefore necessary at different speeds using different values of R_m.

3.5 CONCLUSIONS

Conditions have been derived for optimum operation of a stepping motor on the basis of a linear model. The optimum conditions give the required torque with constraints on machine losses and input level.

Operation from sinusoidal and pulsed sources with variable or fixed pulse width has been considered.

The procedures are applicable to other types of synchronous machine which can be represented by the model.

The simple case of a single constraint on input level is relevant to many stepping motor applications where the strategy used is maximum torque for slewing purposes subject to the current rating of the machine not being exceeded.

Constraints on the losses is thought to be relevant when the performance demanded would otherwise result in excessive temperatures within the machine. This problem is likely to be more severe with large machines and a temperature adaptive controller may provide the solution.

For a machine with such a wide range of operating conditions as the stepping motor constraints on the heat losses within the machine

should be a more realistic consideration than that of the winding current.

If it is necessary to take account of saturation and harmonics a non-linear model has to be used and this procedure is dealt with in the following Section.

4. INPUT OPTIMISATION USING A NON-LINEAR MODEL

4.1 Introduction

When the machine is operating out of saturation the linear model and the results of the previous section are applicable, assuming that the effects due to permeance harmonics are negligible. This assumption is not justified if the machine is operating in saturation.

The torque given by the linear model is limited only by the available level of forcing, or the power dissipated as losses. With a non-linear model there is a limitation on the torque, due to saturation, and this effect must be considered if the machine is required to operate in this region.

Let us pose the question;- 'In order to obtain a certain increase in torque, at what point are the additional losses to be regarded as excessive?'

Merely limiting the losses by a performance index of the form used in Section 3 is not the complete answer. The question is partly resolved due to what at first would perhaps be an unexpected effect, but one which is accounted for in the model and has been demonstrated from the test results presented in Section 2.5.1.

If the rotor is locked in a suitable position and the current in one phase is slowly increased from zero the torque will also increase, approximately in proportion to the current. As would be expected, as saturation occurs and changes in flux linkages become restricted, the increase in torque becomes smaller. After a certain point however, a further increase in current results in a reduction in torque. This is due to the fact that only half of the poles of the phase winding are saturated and the change in flux linkages in the other poles, which normally contribute a smaller opposing torque, cause a reduction in the net torque for that phase.

Thus, there is a value of current which produces a maximum value of torque for each rotor position. Even if machine losses are not

excessive, or if the required torque is not developed at this value of current, there would appear to be no justification in allowing further saturation to take place.

In the following analysis therefore the losses are not constrained, but saturation and permeance harmonics are accounted for.

4.2 EFFECTS OF SATURATION AND PERMEANCE HARMONICS

4.2.1 Torque-Current Characteristic

Expressions for torque in the absence of saturation were derived in Section 2.4.2 and these allowed the inclusion of permeance harmonics. The modification to these expressions, required to account for saturation, was mentioned in Section 2.4.3 and some conclusions were drawn in Section 2.4.5 regarding the torques developed due to the permeance harmonics in unsaturated conditions.

Let us further consider the torque in the presence of saturation and permeance harmonics.

If the current i_m of one phase is insufficient to cause saturation

i.e. $$\frac{\hat{\psi}}{L_m(\theta_e)} > \left|i_m + i_{pm}\right| \quad \text{and} \quad \left|i_m - i_{pm}\right| < \frac{\hat{\psi}}{L_m(\theta_e+\pi)}$$

the torque due to that phase is,

$$T = \frac{S_2}{2}\left\{ (i_m+i_{pm})^2 \frac{dL_m(\theta_e)}{d\theta_e} + (i_m-i_{pm})^2 \frac{dL_m(\theta_e+\pi)}{d\theta_e}\right\} \quad \ldots\ldots \quad (4\text{-}1)$$

but, if i_m is sufficient to cause saturation,

i.e. $$\frac{\hat{\psi}}{L_m(\theta_e)} < \left|i_m+i_{pm}\right| \quad \text{and} \quad \left|i_m-i_{pm}\right| < \frac{\hat{\psi}}{L_m(\theta_e+\pi)}$$

the torque becomes

$$T = \frac{S_2}{2}\left\{\left(\frac{\hat{\psi}}{L_m(\theta_e)}\right)^2 \frac{dL_m(\theta_e)}{d\theta_e} + (i_m - i_{pm})^2 \frac{dL_m(\theta_e+\pi)}{d\theta_e}\right\} \ldots\ldots (4\text{-}2)$$

For a given value of θ_e, such that $\frac{dL_m(\theta_e)}{d\theta_e}$ is positive, there are two possible conditions for the maximum torque to occur:-

either (i) $\frac{\hat{\psi}}{L_m(\theta_e)} > 2\, i_{pm}$ and i_m just causes saturation to occur.

i.e. when $$i_m = \frac{\hat{\psi}}{L_m(\theta_e)} - i_{pm} \quad \ldots\ldots\ldots\ldots (4\text{-}3)$$

with
$$\hat{T} = \frac{S_2}{2}\left\{\left(\frac{\hat{\psi}}{L_m(\theta_e)}\right)^2 \frac{dL_m(\theta_e)}{d\theta_e} + \left(\frac{\hat{\psi}}{L_m(\theta_e)} - 2i_{pm}\right)^2 \frac{dL_m(\theta_e+\pi)}{d\theta_e}\right\} \ldots (4\text{-}4)$$

or, (ii) $\frac{\hat{\psi}}{L_m(\theta_e)} \leqslant 2\, i_{pm}$ and $i_m = i_{pm}$

then
$$T = \frac{S_2}{2}\left(\frac{\hat{\psi}}{L_m(\theta_e)}\right)^2 \frac{dL_m(\theta_e)}{d\theta_e} \quad \ldots\ldots\ldots\ldots\ldots (4\text{-}5)$$

Similarly for $\frac{\hat{\psi}}{L_m(\theta_e+\pi)} < |i_m - i_{pm}|$, $|i_m + i_{pm}| < \frac{\hat{\psi}}{L_m(\theta_e)}$

$$T = \frac{S_2}{2}\left\{(i_m + i_{pm})^2 \frac{dL_m(\theta_e)}{d\theta_e} + \left(\frac{\hat{\psi}}{L_m(\theta_e+\pi)}\right)^2 \frac{dL_m(\theta_e+\pi)}{d\theta_e}\right\} \ldots\ldots (4\text{-}6)$$

with possible conditions of maximum (negative) torque occuring when

either (i) $\frac{\hat{\psi}}{L_m(\theta_e+\pi)} > 2i_{pm}$ and $i_m = i_{pm} - \frac{\hat{\psi}}{L_m(\theta_e+\pi)}$

with
$$\hat{T} = \frac{S_2}{2}\left\{\left(\frac{\hat{\psi}}{L_m(\theta_e+\pi)} - 2i_{pm}\right)^2 \frac{dL_m(\theta_e)}{d\theta_e} + \left(\frac{\hat{\psi}}{L_m(\theta_e+\pi)}\right)^2 \frac{dL_m(\theta_e+\pi)}{d\theta_e}\right\} \ldots (4\text{-}7)$$

or, (ii) $$\frac{\hat{\psi}}{L_m(\theta_e+\pi)} \leqslant 2i_{pm} \quad \text{and} \quad i_m = -i_{pm}$$

then $$\hat{T} = \frac{S_2}{2}\left(\frac{\hat{\psi}}{L_m(\theta_e+\pi)}\right)^2 \frac{dL_m(\theta_e+\pi)}{d\theta_e} \qquad \ldots\ldots\ldots\ldots \quad (4\text{-}8)$$

Similar conditions apply for values of θ_e such that $\frac{dL_m(\theta_e)}{d\theta_e}$ is negative.

Only one further condition remains to be considered though this would not normally be regarded as a region of interest.

If, $$\left|i_m - i_{pm}\right| > \frac{\hat{\psi}}{L_m(\theta_e+\pi)} \quad \text{and} \quad \left|i_m + i_{pm}\right| > \frac{\hat{\psi}}{L_m(\theta_e)}$$

then all poles of this phase are saturated, and

$$T = \frac{S_2}{2}\hat{\psi}^2\left\{\left(\frac{1}{L_m(\theta_e)}\right)^2 \frac{dL_m(\theta_e)}{d\theta_e} + \left(\frac{1}{L_m(\theta_e+\pi)}\right)^2 \frac{dL_m(\theta_e+\pi)}{d\theta_e}\right\} \ldots\ldots \quad (4\text{-}9)$$

Thus the effect is to produce a torque-current characteristic which is represented in the non-linear model by three sections, as shown in Fig.4.1. If permeance harmonics are neglected the characteristic is inverse symmetrical about the torque axis (i.e. $T(i_m) = -T(-i_m)$) and consists of a straight line and two parabolic sections.

4.2.2 Maximum Torque Conditions

As in the case of the linear model, optimisation for maximum torque only is again the simplest case to consider.

In Section 4.2.1 it was shown that for a given value of θ_e there exists some value of current for which the torque is a maximum. The optimum current $i_{mo}(\theta_e)$ will now be defined as the current which will give maximum torque for any value of θ_e.

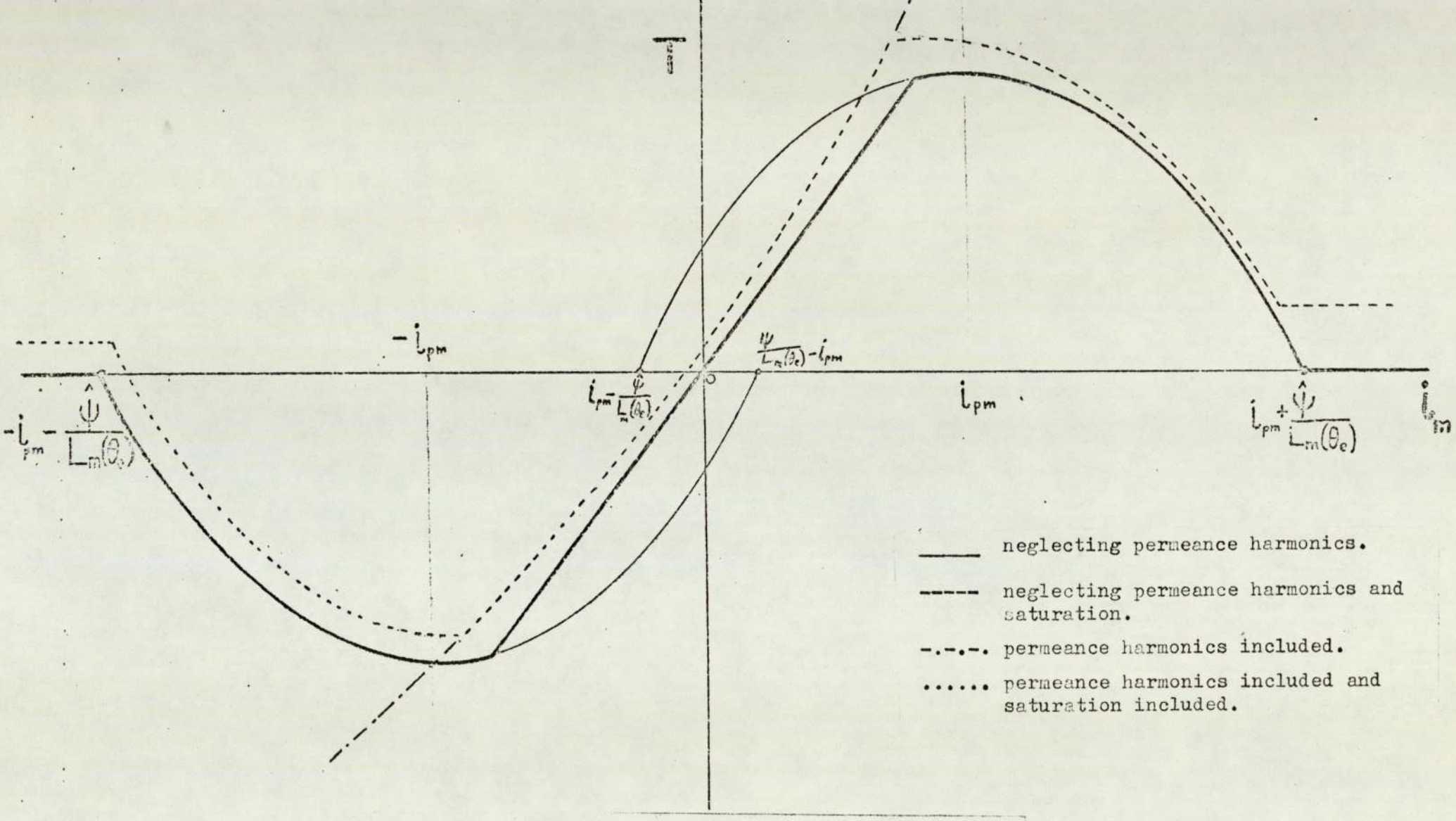

Fig.4.1 Simplified torque-current characteristic

Let $L_m(\theta_e)$ have a maximum value at a single value of θ_e, namely $\theta_e = 0$, then, for $0 \leqq \theta_e < \theta_{es_1}$,

where, $L_m(\theta_{es_1}) = \dfrac{\hat{\psi}}{2i_{pm}}$ ..... (4-10)

then $i_{mo} = i_{pm} - \dfrac{\hat{\psi}}{L_m(\theta_e+\pi)}$ ..... (4-11)

with $T = \dfrac{S_2}{2}\left\{\left(2i_{pm} - \dfrac{\hat{\psi}}{L_m(\theta_e+\pi)}\right)^2 \dfrac{dL_m(\theta_e)}{d\theta_e} - \left(\dfrac{\hat{\psi}}{L_m(\theta_e+\pi)}\right)^2 \dfrac{dL_m(\theta_e+\pi)}{d\theta_e}\right\}$

..... (4-12)

For $\theta_{es_1} \leqq \theta_e < \pi$,

$$i_{mo} = -i_{pm} \quad \text{..... (4-13)}$$

with $\hat{T} = \dfrac{-S_2}{2}\left(\dfrac{\hat{\psi}}{L_m(\theta_e+\pi)}\right)^2 \dfrac{dL_m(\theta_e+\pi)}{d\theta_e}$ ..... (4-14)

For $\pi \leqq \theta_e < \pi+\theta_{es_2}$, where $L_m(\theta_{es_2}) = \dfrac{\hat{\psi}}{2i_{pm}}$ ..... (4-15)

$$i_{mo} = \frac{\hat{\psi}}{L_m(\theta_e)} - i_{pm} \quad \text{..... (4-16)}$$

with the torque given by equation (4-4).

Finally, for $\pi + \theta_{es_2} \leqq \theta_e < 2\pi$,

$$i_{mo} = i_{pm} \quad \text{..... (4-17)}$$

and the torque is given by equation (4-5).

For a machine in which $2i_{pm} L_m(0) < \hat{\psi}$ equations (4-10) and (4-15) cannot be satisfied but θ_{es_1} may be taken as 0.

Also, for a machine in which $2i_{pm}L_m(0) > \hat{\psi}$, θ_{es_2} may be taken as π.

4.2.3 The $\psi - i_m$ Diagram

The $\psi - i_m$ diagram, directly related to the $\phi_m - f_m$ diagram mentioned in Section 2.4.3, is a simple but extremely useful aid to understanding the operation of the machine in the presence of saturation. It also provides a 'graphical' method of solving optimisation problems which are less tractable to solution by purely mathematical means.

Loci for both half phases can be presented on one diagram as shown in Fig.4.2. for the case of maximum torque, considered in Section 4.2.3.

Areas defined by the loci can be interpreted in terms of stored energy, or in terms of co-energy. The mean torque is represented by the areas enclosed by the loci. Areas enclosed by clockwise loci are negative and areas enclosed by anti-clockwise loci are positive. For simplicity i_{pm} is considered to be of constant value I_{pm}.

Using equations (4-4), (4-5), (4-12) and (4-14) the mean value of the maximum torque over the range $\theta_e = 0$ to 2π is given by

$$T = \frac{S_2}{4\pi}\left\{\int_0^{\theta_{es_1}}\left(2I_{pm}-\frac{\hat{\psi}}{L_m(\theta_e+\pi)}\right)^2 dL_m(\theta_e) - \int_0^{\pi}\left(\frac{\hat{\psi}}{L_m(\theta_e+\pi)}\right)dL_m(\theta_e+\pi)\right.$$

$$\left. + \int_{\pi}^{2\pi}\left(\frac{\hat{\psi}}{L_m(\theta_e+\pi)}\right)^2 dL_m(\theta_e) + \int_{+\theta_{es_2}}^{2\pi}\left(\frac{\hat{\psi}}{L_m(\theta_e)} - 2I_{pm}\right)^2 dL_m(\theta_e+\pi)\right\} \quad \ldots\ldots (4\text{-}18)$$

and this is equal to the total shaded area in Fig.4.2 multiplied by the factor S_2.

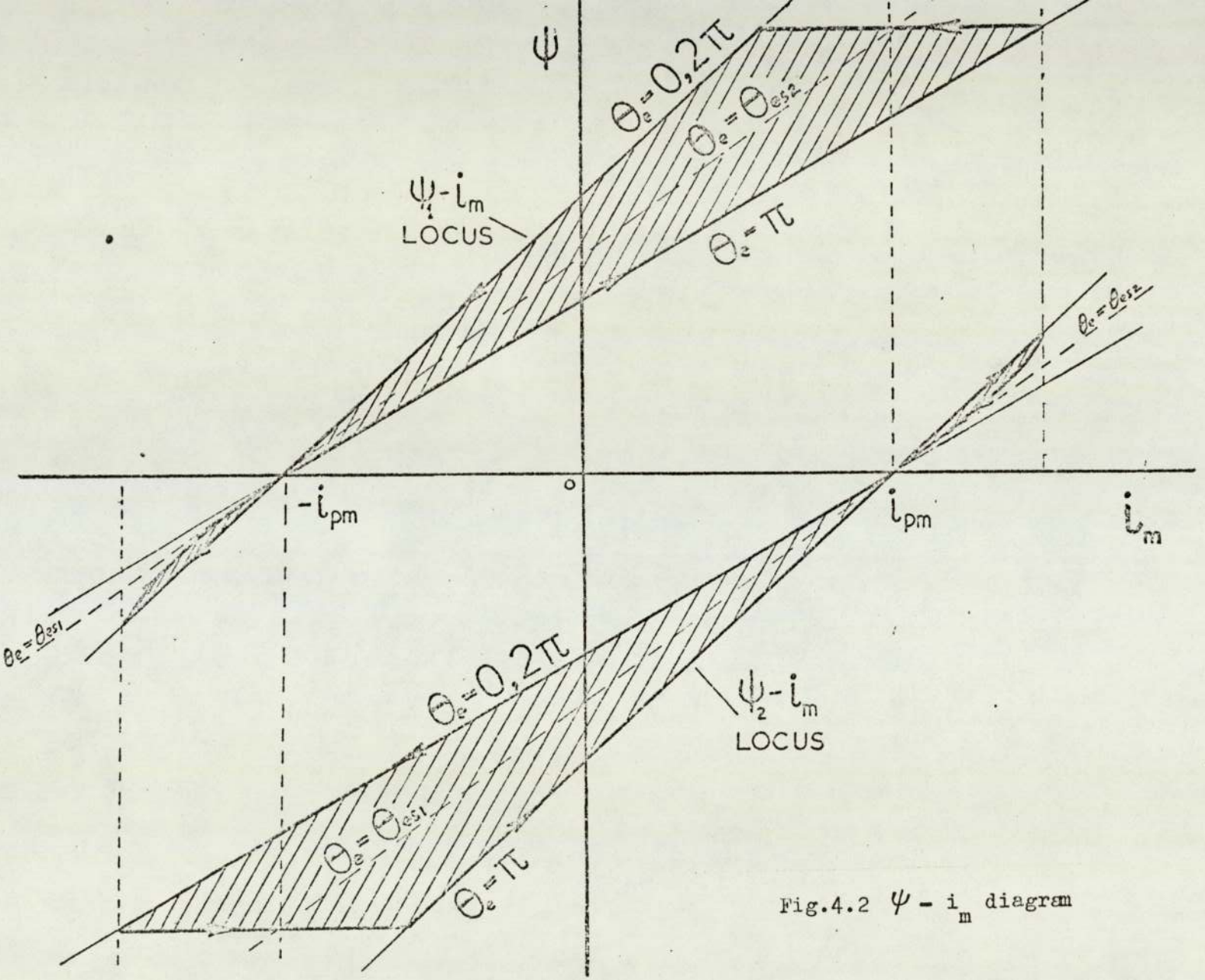

Fig.4.2 $\psi - i_m$ diagram

4.2.4 Production of Harmonic Torques.

Harmonic torques are produced due to the interaction of current and permeance harmonics.

Let $L_m(\theta_e) = L_{mo} + L_{m1} \cos \theta_e + L_{m2} \cos 2\theta_e + L_{m3} \cos 3\theta_e$ .... (4-19)

and let,

$$i_m = -\hat{I}_{m1} \sin (\theta_e+\delta_1) -\hat{I}_{m2} \sin (2\theta_e+\delta_2) -\hat{I}_{m3} \sin (3\theta_e+\delta_3) \text{ .. (4-20)}$$

Using equation (4-1) gives,

$$T = -2S_2 I_{pm} i_m(L_{m1} \sin \theta_e + 3L_{m3} \sin 3\theta_e .....)$$

$$-S_2(i_m^2+I_{pm}^2) (2L_{m1} \sin 2\theta_e + 4L_{m4} \sin 4\theta_e ....) ..... (4-21)$$

Substituting for i_m, given by equation (4-20), into equation (4-21) and expanding shows that:-

(i) Odd permeance harmonics of order p combine with current harmonics of order q to produce harmonic torques, $T_{(p,q)}$, with components of orders p + q and p - q.

These will have a mean value of zero, except when p = q, then

$$T_{(p,p)} = -S_2 I_{pm} \hat{I}_{mp}.pL_{mp} (\cos (2p\theta_e +\delta_p) - \cos \delta_p) ..... (4-22)$$

with a mean value of,

$$\overline{T}_{(p,p)} = S_2 \, p \, I_{pm} \hat{I}_{mp}.L_{mp}.\cos \delta_p \quad ..... (4-23)$$

(ii) Even permeance harmonics of order p combine with current harmonics of orders q1 and q2 to produce harmonic torques, $T_{(p,q1,q2)}$, with components of orders

p, p+2q1, p-2q1, p+2q2, p-2q2,

p+q1+q2, p+q1-q2, p-q1-q2 and p-q1+q2

These harmonic torques could also be regarded as arising from the e.m.f's, $e_{(p,q1)}$ and $e_{(p, q2)}$, and the currents i_{mq1} and i_{mq2} where iq is the harmonic current of order q, and $e_{(p,q)}$ is the e.m.f.

produced due to the permeance harmonic of order p and the current i_q. When p is odd e_p is of order p only and when p is even $e_{(p,q)}$ has components of order p + q and p - q.

The harmonic torques have a mean value of zero, except when p = 2q1, 2q2, q1 + q2 or q2 - q1.

i.e. $$T_{(p,q1,\ q2)}=S_2 p L_{mp}\left[\left(\frac{\hat{I}_{mq1}^{\ 2}+\hat{I}_{mq2}^{\ 2}}{2}+i_{pm}^{\ 2}\right)\sin p\theta_e\right.$$

$$-\frac{\hat{I}_{mq2}^{\ 2}}{4}\left\{\sin\left((p+2q2)\theta_e+2\delta_{q2}\right)+\sin\left((p-2q2)\theta_e-2\delta_{q2}\right)\right\}$$

$$-\frac{\hat{I}_{mq1}^{\ 2}}{4}\left\{\sin\left((p+2q1)\theta_e+2\delta_{q1}\right)+\sin\left((p-2q1)\theta_e-2\delta_{q1}\right)\right\}$$

$$+\frac{\hat{I}_{mq1}\hat{I}_{mq2}}{2}\left(\left\{\sin\left((p+q1-q2)\theta_e+\delta_{q1}-\delta_{q2}\right)+\sin\left((p-q1+q2)\theta_e-\delta_{q1}+\delta_{q2}\right)\right\}\right.$$

$$\left.\left.-\left\{\sin\left((p+q1+q2)\theta_e+\delta_{q1}+\delta_{q2}\right)+\sin\left((p-q1-q2)\theta_e-\delta_{q1}-\delta_{q2}\right)\right\}\right)\right] \quad \ldots\ (4\text{-}24)$$

$$\therefore \overline{T}_{(2q1,q1,-)}=\frac{S_2\ p\ L_{mp}\ \hat{I}_{mq1}^{\ 2}}{4}\sin 2\delta_{q1} \qquad \ldots\ (4\text{-}25)$$

$$\overline{T}_{(2q2,-,q2)}=\frac{S_2\ p\ L_{mp}\ \hat{I}_{mq2}}{4}\sin 2\delta_{q2} \qquad \ldots\ (4\text{-}26)$$

$$\overline{T}_{(q1+q2,q1,q2)}=\frac{S_2\ p\ L_{mp}\ \hat{I}_{mq1}\ \hat{I}_{mq2}}{2}\sin(\delta_{q1}+\delta_{q2}) \qquad \ldots\ (4\text{-}27)$$

and,
$$\overline{T}_{(q2-q1,q1,q2)}=\frac{S_2\ p\ L_{mp}\ \hat{I}_{mq1}\ \hat{I}_{mq2}}{2}\sin(\delta_{q1}-\delta_{q2}) \qquad \ldots\ (4\text{-}28)$$

Hence, non-zero torques are produced from

(i) Odd permeance harmonics and current harmonics of the same order.

(ii) Even permeance harmonics and current harmonics of different orders. For each permeance harmonic of order p, this involves the current harmonic of order p/2 and all pairs of current harmonics with a sum or difference equal to p.

4.3 OPERATION FROM SINUSOIDAL SUPPLIES

Consider the current i_m to be sinusoidal, $\hat{I}_m \angle \delta$ and that the machine is operating at constant speed ω_m.

It is evident from the conclusions of Section 4.2.4 that, if saturation is not reached, the mean torque developed will be independant of all permeance harmonics above the second. An optimisation procedure similar to that applied to the linear model could then be used. From equations (4-23) and (4-25) the mean torque would be

$$\bar{T} = S_2 \hat{I}_m \left(I_{pm} L_{m1} \cos\delta + \frac{\hat{I}_m}{2} L_{m2} \cos 2\delta \right) \quad \ldots\ldots (4\text{-}29)$$

which would be a maximum when $\delta = 0$.

If saturation occurs, the ψ-i_m locus for one half-phase is typically as shown in Fig.4.3, then,

$$\bar{T} = \frac{S_2}{\pi} \left\{ \int_{\theta_{es_2}}^{\theta_{es_1}} \left(I_{pm} - \hat{I}_m \sin(\theta_e + \delta) \right)^2 dL_m(\theta_e) + \int_{\theta_{es_1}}^{\theta_{es_2}} \left(\frac{\hat{\psi}}{L_m(\theta_e)} \right)^2 dL_m(\theta_e) \right\} \ldots (4\text{-}30)$$

giving,

$$\bar{T} = S_2 \left(\left(I_{pm} \hat{I}_m L_{m1} \cos\delta + \frac{\hat{I}_m L_{m2}}{2} \sin 2\delta \right) \left(1 - \frac{\theta_{es_2} - \theta_{es_1}}{\pi} \right) \right.$$

$$+ \frac{1}{\pi} \left[\sum_{p=1}^{n} L_{mp} \left(I_{mp}^2 + \frac{\hat{I}_m^2}{2} \right) \cos p\theta_e - \frac{p}{p+1} I_{pm} \hat{I}_m \sin\left((p+1)\theta_e + \delta \right) \right.$$

$$- \frac{p}{p+2} \frac{\hat{I}_m^2}{4} \cos\left((p+2)\theta_e + 2\delta \right) + \sum_{p=2}^{n} L_{mp} \frac{p}{p-1} I_{pm} \hat{I}_m \sin\left((p-1)\theta_e - \delta \right)$$

$$\left. \left. - \sum_{\substack{p=1 \\ p=2}}^{n} L_{mp} \frac{p}{p-2} \frac{\hat{I}_m^2}{4} \cos\left((p-2)\theta_e - 2\delta \right) - \frac{\psi^2}{L_m(\theta_e)} \right] \right)_{\theta_{es_1}}^{\theta_{es_2}} \quad \ldots\ldots (4\text{-}31)$$

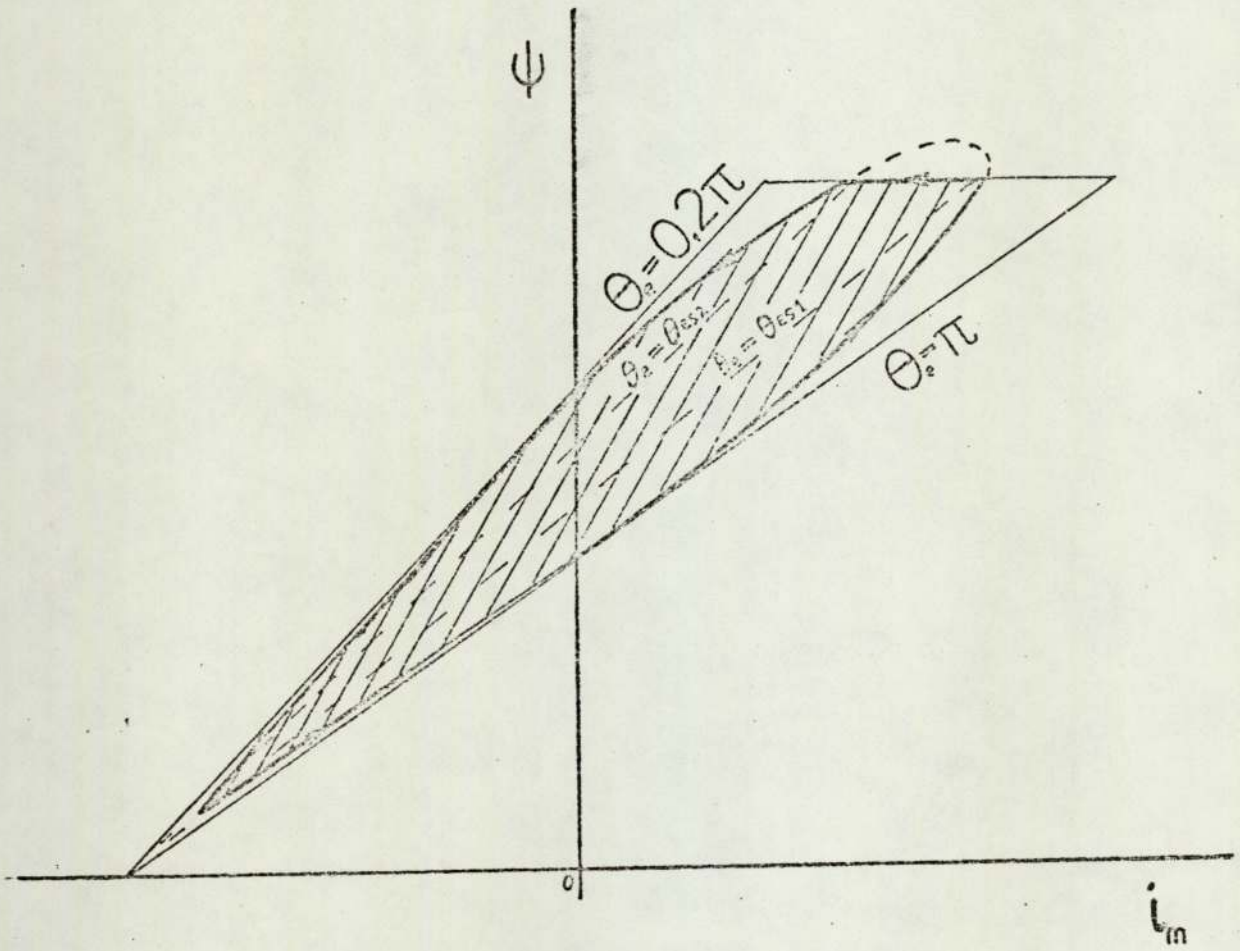

Fig.4.3 Operation from sinusoidal supply.

Maximum mean torque will not in general occur when $\delta = 0$.

4.4 OPERATION FROM PULSED SUPPLIES

If i_m is a three level sequence, as defined in Fig.4.4(a), then the $\psi - i_m$ locus for one half phase is typically as shown in Fig.4.4(b) now,

$$\bar{T} = \frac{S_2}{4\pi}\left\{\int_{\frac{\pi}{2}-\delta-\frac{\theta_W}{2}}^{\frac{\pi}{2}-\delta+\frac{\theta_W}{2}} (I_{pm}-I_m)^2 dL_m(\theta_e) + \int_{-\frac{\pi}{2}-\delta-\frac{\theta_W}{2}}^{\theta_{es}} (I_{pm}+I_m)^2 dL_m(\theta_e) + \int_{\theta_{es}}^{-\frac{\pi}{2}-\delta+\frac{\theta_W}{2}} \left(\frac{\hat{\psi}}{L_m(\theta_e)}\right)^2 dL_m(\theta_e)\right\}$$

..... (4-32)

where,

$$L_m(\theta_{es}) = \frac{\hat{\psi}}{I_{pm}+I_m} \qquad \text{..... (4-33)}$$

$$\bar{T} = \frac{S_2}{2\pi}\left\{(I_{pm}-I_m)^2\left(L_m\left(\frac{\pi}{2}-\delta+\frac{\theta_W}{2}\right) - L_m\left(\frac{\pi}{2}-\delta-\frac{\theta_W}{2}\right)\right) + 2\hat{\psi}(I_{pm}+I_m)\right.$$

$$\left. - (I_{pm}+I_m)^2 L_m\left(-\frac{\pi}{2}-\delta-\frac{\theta_W}{2}\right) - \frac{\hat{\psi}^2}{L_m\left(-\frac{\pi}{2}-\delta+\frac{\theta_W}{2}\right)}\right\} \quad \text{..... (4-34)}$$

Again, the mean torque will not in general have a maximum value for $\delta = 0$.

For a given value of δ the maximum torque conditions can be determined from the $\psi - i_m$ diagram. This occurs at a value of I_m such that sections XY and X' Y' of the locus, in Fig.4.4(b), are of equal length.

i.e. $(I_{pm}-I_m)\left(L_m\left(\frac{\pi}{2}-\delta-\frac{\theta_W}{2}\right)-L_m\left(\frac{\pi}{2}-\delta+\frac{\theta_W}{2}\right)\right) = \hat{\psi}-(I_{pm}+I_m)L_m\left(-\frac{\pi}{2}-\delta-\frac{\theta_W}{2}\right)$ .. (4-35)

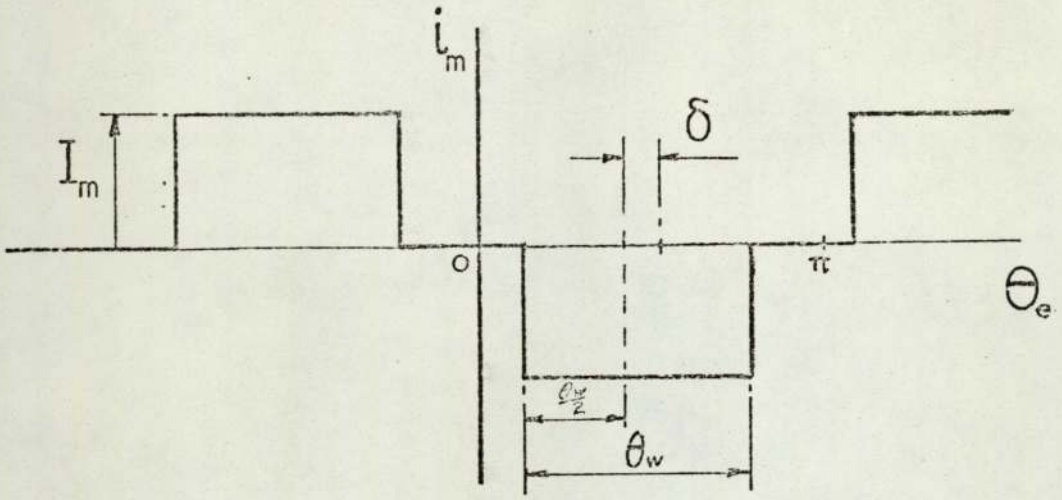

a) Pulsed supply.

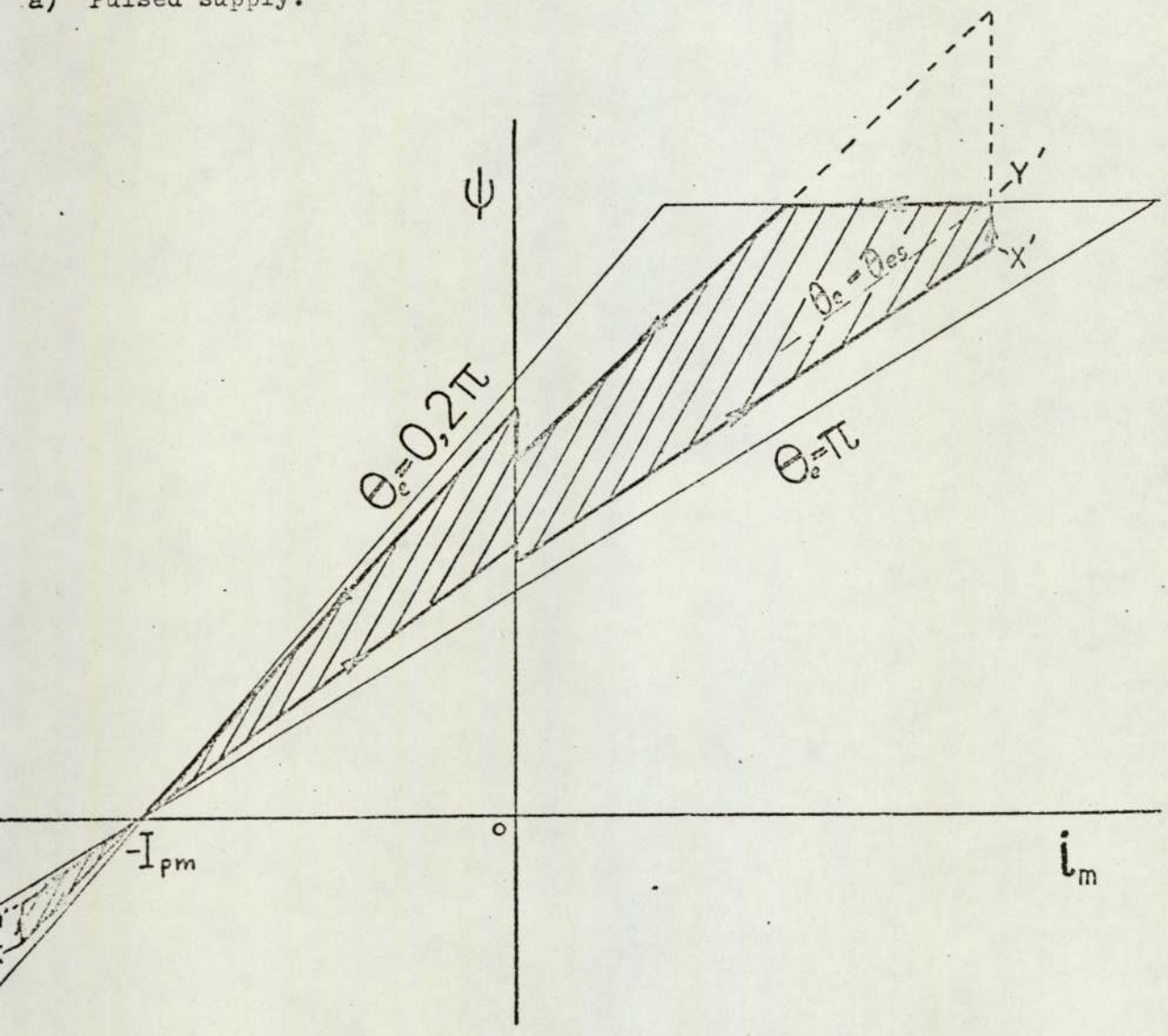

b) $\Psi - i_m$ diagram.

Fig.4.4 Operation from pulsed supply.

$$I_{mo} = \frac{\hat{\psi} + I_{pm}\left(L_m\left(\frac{\pi}{2} - \delta + \frac{\theta_w}{2}\right) - L_m\left(\frac{\pi}{2} - \delta - \frac{\theta_w}{2}\right) - L_m\left(-\frac{\pi}{2} - \delta - \frac{\theta_w}{2}\right)\right)}{L_m\left(\frac{\pi}{2} - \delta + \frac{\theta_w}{2}\right) - L_m\left(\frac{\pi}{2} - \delta - \frac{\theta_w}{2}\right) + L_m\left(-\frac{\pi}{2} - \delta - \frac{\theta_w}{2}\right)} \quad \ldots\ldots\ldots (4\text{-}36)$$

4.5 OPTIMUM STRENGTH OF PERMANENT MAGNET

The M.M.F due to the permanent magnet may be considered as a variable and it may be of interest to determine if conditions exist for this to be an optimum. This is also relevant to machines having a wound field in place of the permanent magnet.

In the case of the pulsed supply for example, considered in Section 4.4, the optimum value of I_{pm}, found by putting

$$\frac{d\bar{T}}{dI_{pm}} = 0 \quad \ldots\ldots\ldots\ldots (4\text{-}37)$$

using equation (4-34) is,

$$I_{pmo} = I_m \frac{L_m\left(\frac{\pi}{2} - \delta + \frac{\theta_w}{2}\right) - L_m\left(\frac{\pi}{2} - \delta - \frac{\theta_w}{2}\right) - L_m\left(-\frac{\pi}{2} - \delta - \frac{\theta_w}{2}\right)}{L_m\left(\frac{\pi}{2} - \delta + \frac{\theta_w}{2}\right) - L_m\left(\frac{\pi}{2} - \delta - \frac{\theta_w}{2}\right) + L_m\left(-\frac{\pi}{2} - \delta - \frac{\theta_w}{2}\right)} \quad \ldots\ldots\ldots (4\text{-}38)$$

This is the optimum constant value of I_{pm} to give maximum mean torque for a given value of δ and I_m. For the mean torque to be a maximum, with a single constraint of the supply current being a limited (constant) level, optimum values of θ_c and δ are:-

$$\theta_{co} = \pi \quad \ldots\ldots\ldots\ldots (4\text{-}39)$$

$$\delta_o = 0 \quad \ldots\ldots\ldots\ldots (4\text{-}40)$$

For $I_m < \left(\frac{\hat{\psi}}{L_m(0)} - I_{pm}\right)$ the machine is unsaturated and the area of the shaded section in Fig.4.5(a) is

$$\text{section area} = \tfrac{1}{2}(L_m(0) - L_m(\pi))(I_m + I_{pm})^2 - \tfrac{1}{2}(L_m(0) - L_m(\pi))(I_m - I_{pm})^2 \ldots (4\text{-}41)$$

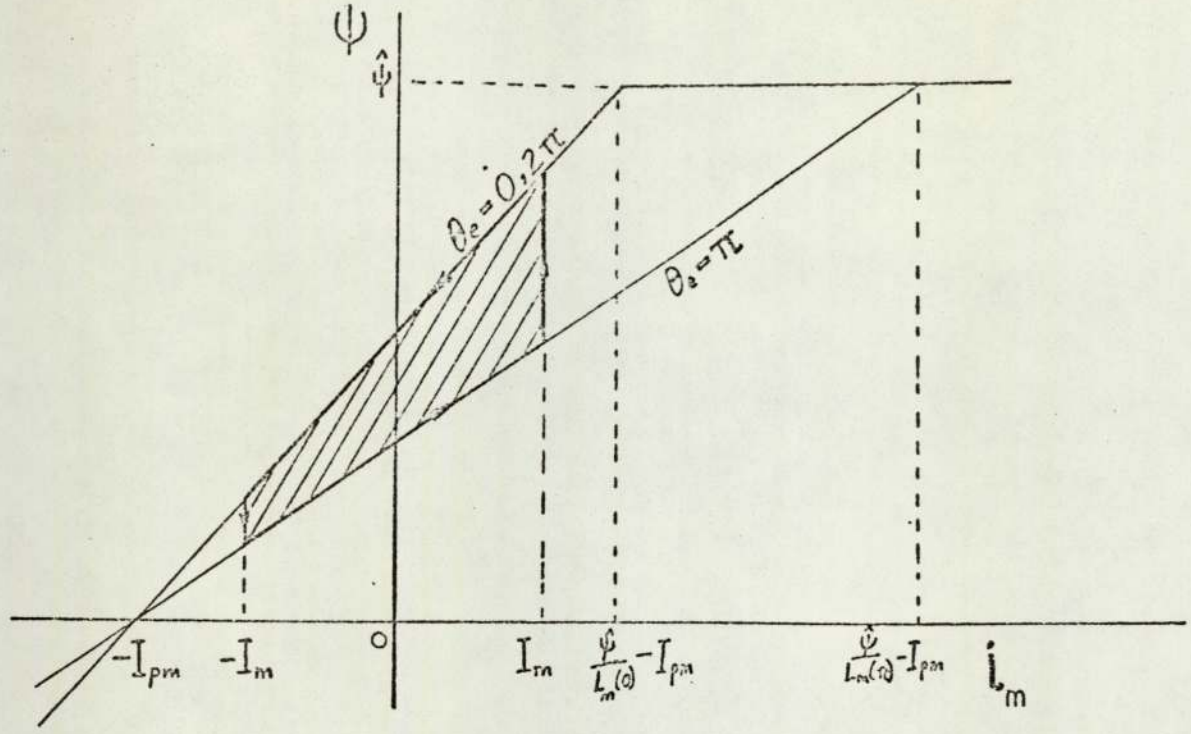

Fig.4.5(a) ψ-i_m diagram:- $I_m < \left(\frac{\hat{\psi}}{L_m(0)} - I_{pm}\right)$

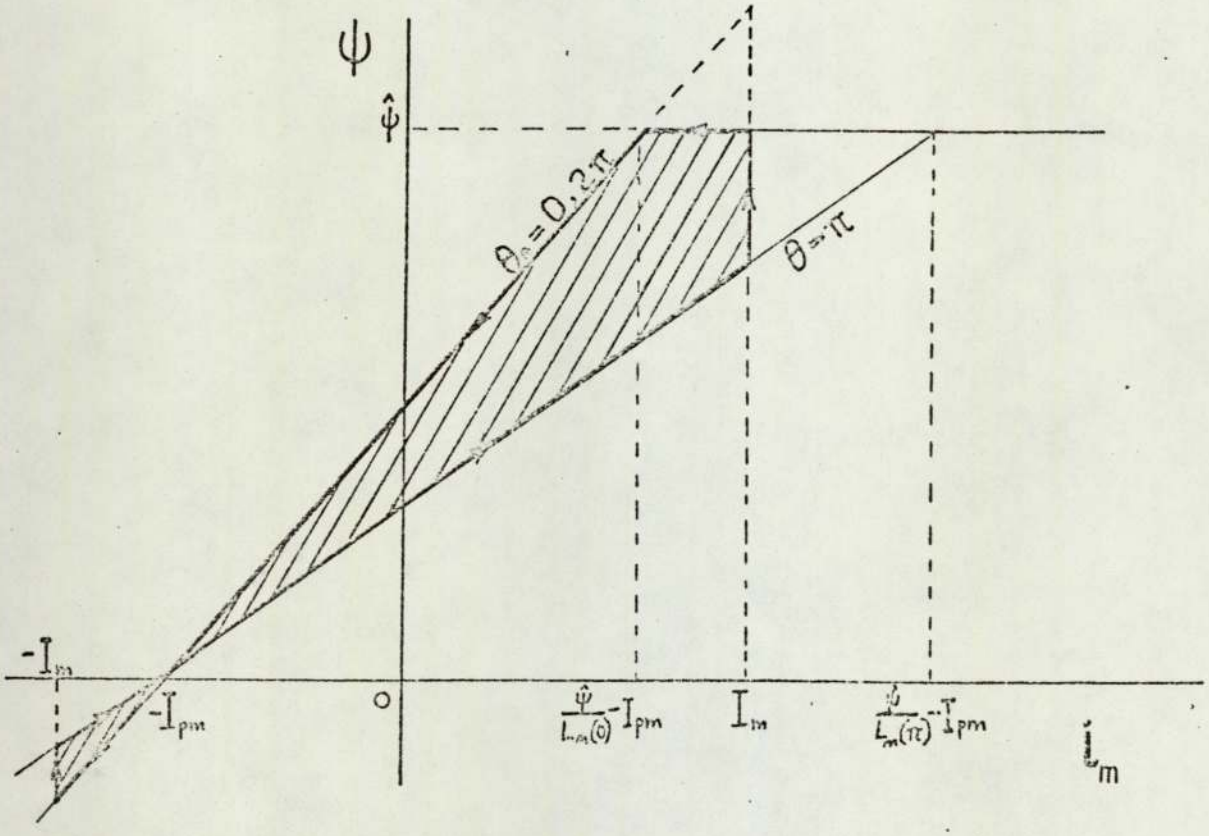

Fig.4.5(b) ψ-i_m diagram:- $\left(\frac{\hat{\psi}}{L_m(0)} - I_{pm}\right) < I_m < \left(\frac{\hat{\psi}}{L_m(\pi)} - I_{pm}\right)$

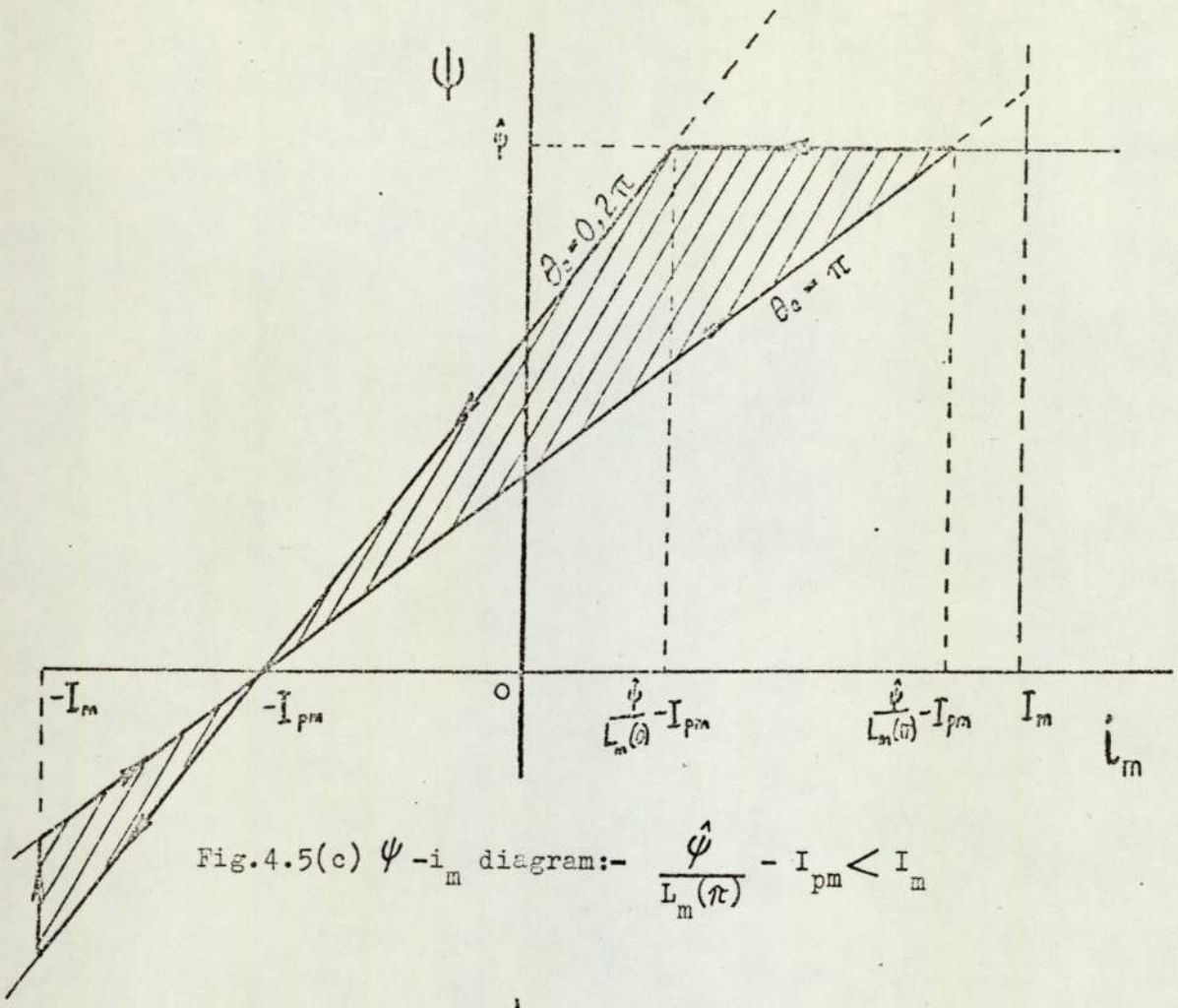

Fig.4.5(c) $\psi - i_m$ diagram:- $\frac{\hat{\psi}}{L_m(\pi)} - I_{pm} < I_m$

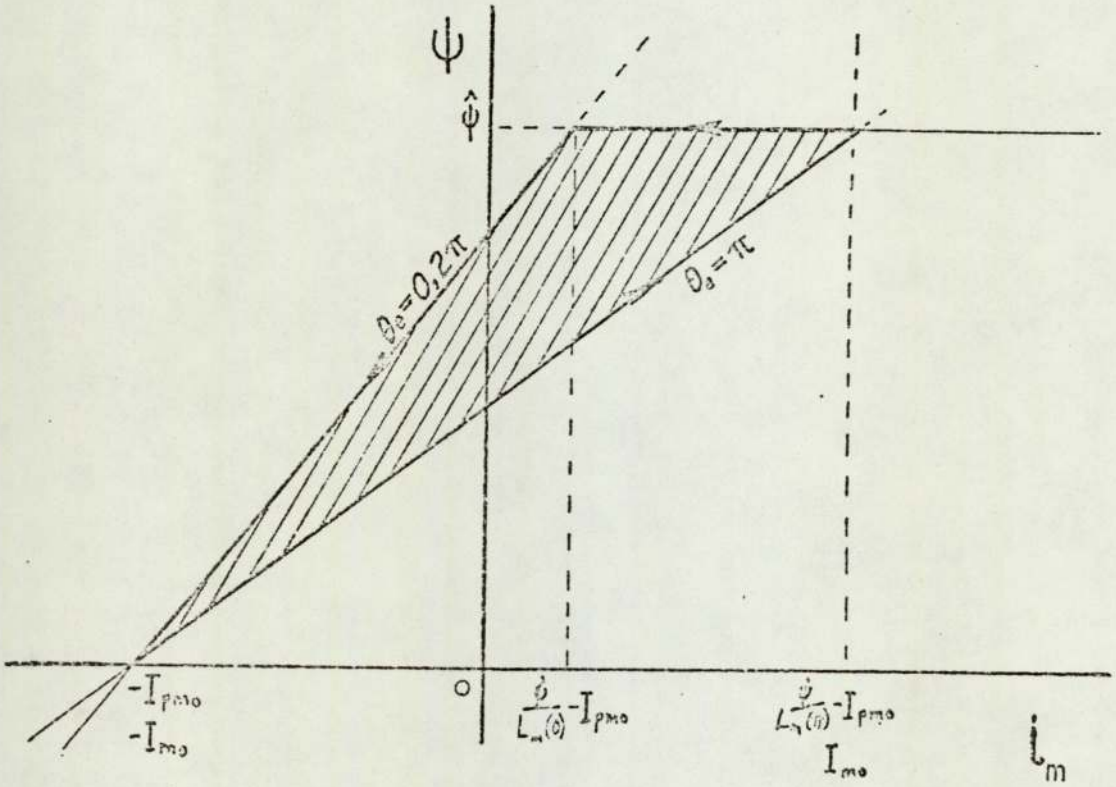

Fig.4.5(d) $\psi - i_m$ diagram:- $I_m = I_{mo}$, $I_{pm} = I_{pmo}$

and the mean torque is, $\bar{T} = 2 S_2 \times$ section area ..... (4-42)

$$\bar{T} = 4 S_2 I_m I_{pm}(L_m(0) - L_m(\pi)) \quad \text{..... (4-43)}$$

For $\left(\frac{\hat{\psi}}{L_m(0)} - I_{pm}\right) < I_m < \left(\frac{\hat{\psi}}{L_m(\pi)} - I_{pm}\right)$ the torque is proportional to the shaded section in Fig.4.5(b).

$$\bar{T} = S_2\left\{4I_m I_{pm}(L_m(0)-L_m(\pi)) - (L_m(0)(I_{pm}+I_m)-\hat{\psi})(I_m - \frac{\hat{\psi}}{L_m(0)}+I_{pm})\right. \quad \text{... (4-44)}$$

and, for $\left(\frac{\hat{\psi}}{L_m(\pi)} - I_{pm}\right) < I_m$, Fig.4.5(c)

$$\bar{T} = S_2\left\{\hat{\psi}^2\left(\frac{1}{L_m(\pi)} - \frac{1}{L_m(0)}\right) - (L_m(o) - L_m(\pi))\,(I_m - I_{pm})\right\} \quad \text{..... (4-45)}$$

In the maximum torque condition, equation (4-44) is applicable, giving,

$$I_{pmo} = I_m + \frac{\hat{\psi} - 2 I_m L_m(\pi)}{L_m(0)} \quad \text{..... (4-46)}$$

as the optimum constant value for I_{pm} to give maximum mean torque for a given value of I_m.

Similarly there is an optimum value of I_m for a given value of I_{pm}, under the same conditions. This is obtained by putting

$$\frac{d\bar{T}}{dI_m} = 0 \quad \text{..... (4-47)}$$

which gives,

$$I_{mo} = I_{pm} + \frac{\hat{\psi} - 2I_{pm}L_m(\pi)}{L_m(0)} \quad \text{..... (4-48)}$$

If I_m and I_{pm} are both optimum, the condition satisfying equations (4-46) and (4-48) is,

$$I_{pmo} + I_{mo} = \frac{\hat{\psi}}{L_m(\pi)} \qquad \ldots\ldots\ldots\ldots\ldots\ldots (4\text{-}49)$$

with

$$I_{mo} = \frac{\hat{\psi}}{2L_m(\pi)} \qquad \ldots\ldots\ldots\ldots\ldots\ldots\ldots (4\text{-}50)$$

and

$$I_{pmo} = \frac{\hat{\psi}}{2L_m(\pi)} \qquad \ldots\ldots\ldots\ldots\ldots\ldots\ldots (4\text{-}51)$$

This condition is shown in Fig.4.5(d).

4.6 DISCUSSION AND CONCLUSIONS

Optimisation procedures using the non-linear model account for the effects of saturation and permeance harmonics and are to some extent complementary to the procedures of Section 3.

A general relationship between current, permeance and torque harmonics, in the absence of saturation has been derived. This can help solve the synthesis problem;-

Given a certain distribution of permeance harmonics, does an optimum input waveform exist?

or;- For a given supply waveform, does an optimum value exist for each permeance harmonic?

It appears that a solution does exist and, for the non-saturating machine, can be obtained by the methods that were applied to the linear model. The solution may however only be useful for matching the driving circuit and the machine over a particular range of speeds. The harmonics in the current waveform will vary with frequency for any system in which the cost of the controller is included in the performance index.

Use of the $\psi - i_m$ diagram has been described This can provide a geometrical solution to many problems involving saturation.

Expressions have been derived for the mean torque developed,

in the presence of saturation, for sinusoidal and pulsed supplies. Unless the current phase angle δ is zero, the condition for maximum torque is best obtained either by a graphical method using the $\psi - i_m$ diagram and a trial and error process, or by a hill climbing procedure on the model.

The case for a current phase angle of $\delta = 0$ is of particular interest, and an example of a pulsed supply with maximum conduction angle $\theta_w = \pi$ was considered. It has been shown that for maximum torque, optimum values exist for both the level of supply current and the M.M.F. due to the permanent magnet, or field winding.

Using the models derived in Section 2, the optimisation covered in Sections 3 and 4 has been for unconstrained maximum torque and for maximum torque constrained by given losses. Similar procedures could be applied to these models for other performance indices if required.

Optimum conditions depend substantially upon the type of drive circuit, the load and, for closed-loop operation, upon which variables are selected to be controlled by feedback. The different types of supply assumed for the optimisation procedures are therefore intended to represent, in general form, alternative drive conditions.

Sections 5 and 6 which follow describe some of these alternatives and the methods which can be used for implementing them.

5. INVERTER DRIVEN CLOSED LOOP STEPPING MOTOR CONTROL SYSTEMS

5.1 Introduction

Present electrical stepping motors are considered to be small in comparison to most other types of electrical machine, but as improvements are made in stepping motor design, and as more effective driving methods are realised, it is likely that larger machines will be produced.

Manufacturers have not yet indicated such a trend, and some reasons that could account for this are:-

(i) The hydraulic stepping motor is already established for 'high-power' applications.

(ii) Instability due to resonance would be less acceptable in larger machines where it would be more important to maintain high overall efficiency.

(iii) Suitable drive circuits for electric power steppers are not yet sufficiently developed.

Given a suitable drive circuit the electric power stepping motor may offer some competition to its hydraulic counterpart.

The cycloinverter drive circuit presented here, although developed for a stepping motor has application in the control of other types of synchronous machine including the synchronous reluctance type which has been of much interest in recent years. It also is likely that some future designs for large stepping motors will stem from this type of machine, which is already well established and capable of being operated as a power stepper.

Drive circuits of the type proposed may also find application to machines of all sizes where relatively large amounts of energy are to be transferred for maximum possible acceleration in a closed loop system. The method of combining these circuits into a closed loop system will therefore also be discussed.

5.2 INVERTER CIRCUITS AND THEIR LIMITATIONS

5.2.1 Choice of Switching Device

Stepping motors can be operated from sinusoidal or switched supplies but the switched supply is the most common method of excitation. This is in accordance with operation as a digital device and also results in less power dissipated in the driving circuit. The power requirements for most stepping motors can therefore be handled by transistors, and at present this is the standard method used. In applications involving large stepping motors, and in cases where considerable forcing is to be used, the thyristor may be found to be a more suitable device.

Since the invention of the thyristor in 1957 it has replaced other devices in a wide range of power circuits, including the control of many types of electrical machine. It is not surprising that the application of this device to the stepping motor has been somewhat neglected, since the basic transistor drive circuit is very simple. Provided with 'diode protection' the transistor can be safely turned 'on' or 'off' at any time, whereas thyristor circuits present special problems which require further discussion.

The price of power transistors is generally lower now than of a few years ago and devices of higher capability have become available, so the thyristor should not be expected to eventually replace the transistor entirely to drive small or medium sized machines. The thyristor is however capable of switching more power, for a single device, and is preferable where higher power levels are involved, especially if commutation can be achieved with fairly simple circuitry.

5.2.2 Types of Inverter

For this application it is important to use an arrangement which will overcome the disadvantage of a limited frequency range generally associated with inverter circuits. The wide range of operating

conditions for the stepping motor requires an inverter to operate from d.c. to several kHz. The facility to vary the output voltage to give similar driving currents at high and low frequencies may also be useful.

At low frequencies the parallel capacitor commutated inverter shown in Fig.5.1 could be used. This circuit was known as early as 1932 using thyratrons and operation on resistive and inductive loads has been analysed by Wagner[22,23]. The circuit has many disadvantages. A large ballast inductance is required to maintain the continuous flow of direct current and to limit voltage overshoots, and in addition a large commutation capacitor is required for operation with inductive loads. The circuit has a limited load range and needs a minimum load to limit the peak voltage across the thyristors. Starting the inverter is also difficult because of the time required to charge the large commutating capacitor.

As in many existing inverter circuits of the past, thyristors were directly substituted for thyratrons, but the better characteristics of the thyristor were not fully utilised by this direct replacement. The addition of diodes, shown dotted in Fig.5.1, gave an improved circuit developed by McMurry and Bedford, which has been analysed by McMurry and Shattuck[24]. The feedback diodes in the circuit return reactive energy associated with inductive loads to the d.c. supply. The capacitor and ballast inductor are no longer required to store this energy and may now be smaller. The improved inverter is less sensitive to changes in load or power factor and can operate over a wider, but still limited, frequency range.

It is necessary to remove the lower frequency limit for use as a stepping motor drive. This is easily achieved by simply omitting the transformer and using a centre tapped 'bifilar' motor phase winding.

Another desirable objective would be to increase the higher

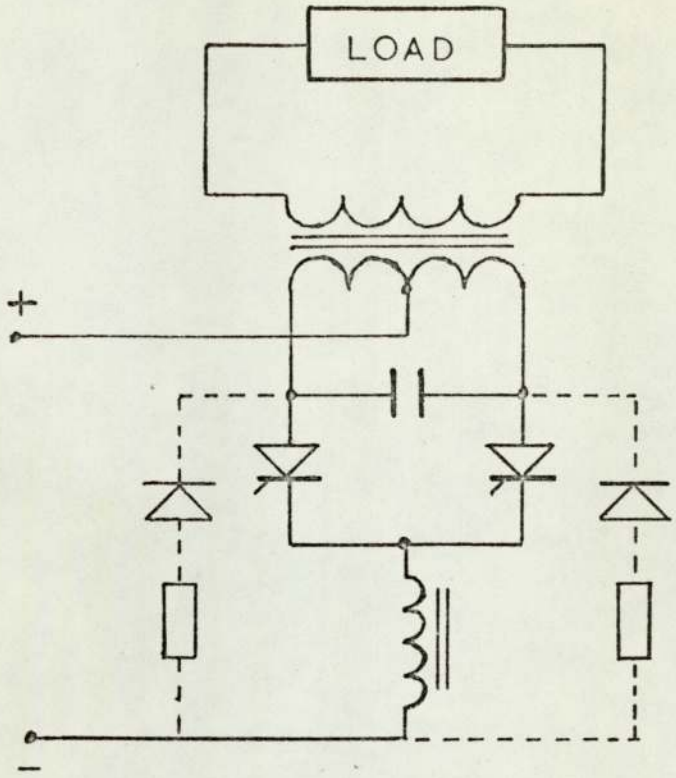

Fig.5.1 Parallel Capacitor Commutated Inverter.

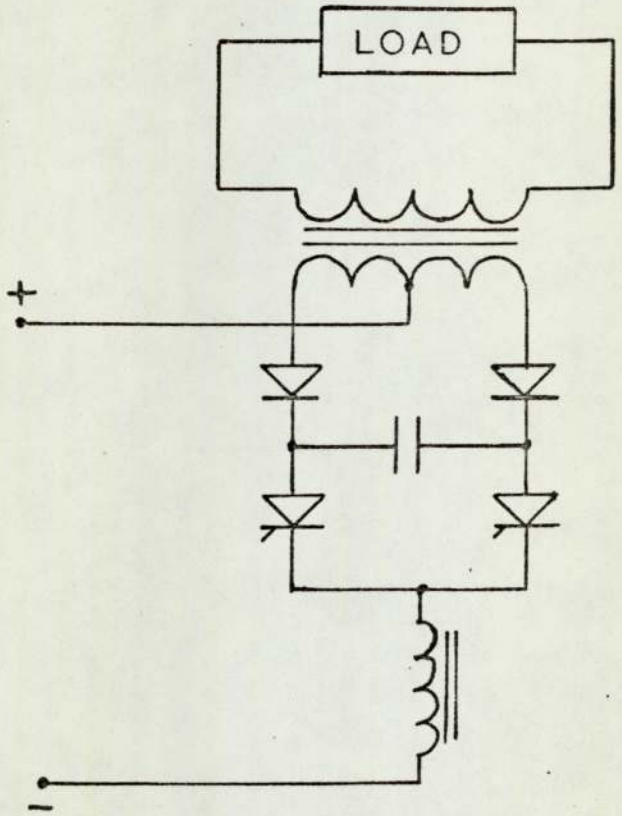

Fig.5.2 Improved Capacitor Commutated Inverter with Wide Frequency Range.

frequency limit, which is determined ultimately by thyristor turn-off time, but commutation losses reduce the efficiency at high frequencies and restrict useful operation to about 1 kHz.

The capacitor must be large enough to apply a reverse voltage across the thyristor during recovery but large currents will be delivered during the remainder of the cycle. It is possible to retain the charge on the capacitor until it is required for commutation by using the circuit of Fig.5.2. This technique has been analysed by Ward[26] and has been shown to be suitable for operation over a wide range of frequency, particularly for drives where load resistance increases with frequency. Although this represents a further improvement, it was concluded that "adjustment of the capacitance as the frequency is varied must be accepted as a necessity and that there is the need to develop the means to do this automatically". No example was given to indicate what frequency range could be achieved in practice and so it may be of interest to consider the views of other later authors as to what constitutes a wide variable frequency.

To some[27], 150 Hz is considered to be a typical maximum frequency which will be improved upon by faster devices, rather than from circuit improvements. Another author[28] could see "no reason to suppose that frequencies up to say 400 Hz are not practical with reasonable efficiency".

High frequency inverters have been developed which are self commutated by resonating the load. These circuits are suitable for use above about 1 kHz because of the need for a resonant circuit which carries full load current. The frequency may be as high as 20 kHz but is basically fixed. Some variation in frequency is possible by firing the thyristors at a lower rate than the resonant frequency of the circuit and a frequency range of 2 to 1 is about the

maximum that can be achieved with a tolerable waveform.

One method, appearing to meet the requirements of operation over a wide frequency, including d.c., is to use a cycloconverter fed from a high frequency supply. For many drives the cycloconverter is an alternative to the d.c. link inverter but for this application the d.c. link must remain since the cycloconverter requires a high frequency input. For operation from the a.c. mains this implies three stages, (i) rectification, (ii) h.f. inversion and (iii) cycloconversion, the latter two stages being referred to as cycloinversion.

A circuit presented in 1969 by Robertson and Hebbar[29], described as 'a tuned circuit commutated inverter' operated as a block fired cycloinverter in which inversion and cycloconversion are not separable stages. It is this type of circuit which will be considered further.

5.3 A NATURALLY COMMUTATED CYCLOINVERTER WITH WIDE FREQUENCY RANGE

5.3.1 Circuit Operation

Consider the circuit shown in Fig.5.3, which operates as a cycloinverter. Let the capacitors have an initial voltage of 1/2 V_d. If pulses are applied to the gates of thyristors TH1 and TH4 current i_d flows through the commutating inductors L_{c_1} and L_{c_4}, capacitors C_2 and C_3 charge and C_1 and C_4 discharge. The voltage across the load rises to a maximum value between V_d and $2V_d$, depending upon the type of load. The load current is then supplied from C_2 and C_3, which also charge C_1 and C_4, while the d.c. supply current i_d reduces to zero and TH1 and TH4 turn off. When the voltage across the load has fallen to a predetermined level, less than the supply, TH1 and TH4 are fired again and the cycle repeats. TH1 and TH4 may

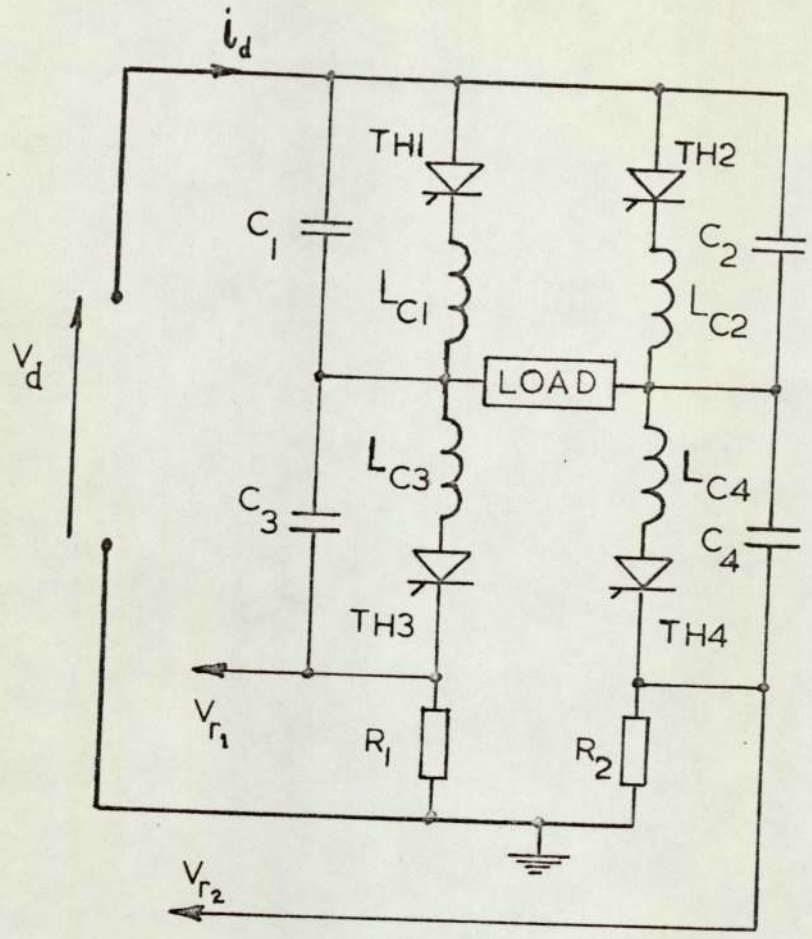

Fig.5.3 Naturally Commutated Cycloinverter (one phase).

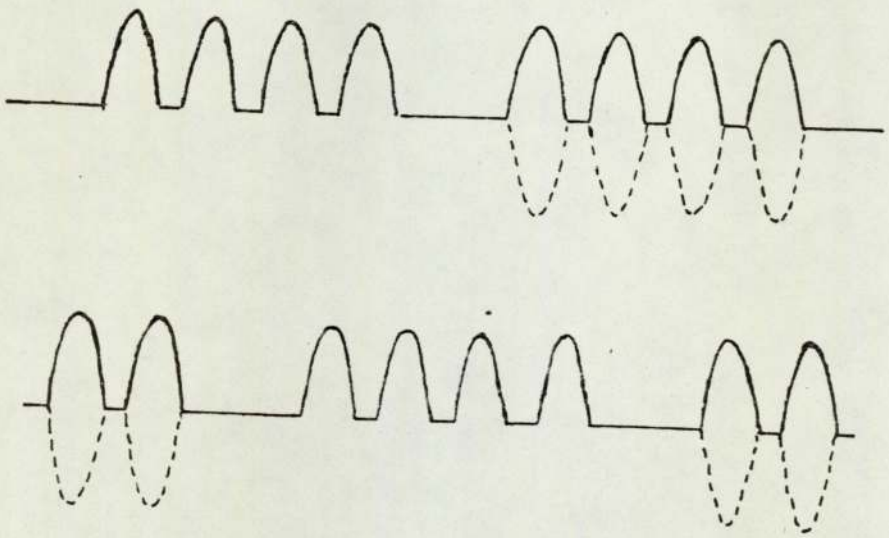

Fig.5.4 Sketch showing typical Input Current Waveform (two phases).

be fired a number of times in this manner.

The load current will be brought to zero if no gate pulses are applied, or can be reversed by firing TH2 and TH3 for a number of cycles.

The inverter output can thus be 'modulated' at a frequency which is much lower than the natural frequency of the commutating circuit, and can easily be varied over a wide frequency range by simply altering the firing sequence. Fig.5.4 shows the form of input current waveform produced by the firing sequence chosen, the output voltage being somewhat smoother. Other forms of modulation are possible which allow selected or general harmonic reduction such as pulse rate modulation. The circuit was used with a two-phase machine so that the sequence in Fig.5.4 produces steps with alternately 'one phase on' and then 'two phases on'.

As the frequency varies, output voltage adjustment is required to give an approximately constant load current and this can be achieved by using a feedback signal proportional to the load current taken from $V_{r_1} - V_{r_2}$. If the firing signals are of a high frequency, these can be inhibited if the load current is greater than a preset value or enabled if it is less than this value. The thyristors then fire at a suitable frequency.

Fig.5.5 shows the voltage waveform across a resistive load as the output frequency is increased, and Fig.5.6 gives the corresponding inverter characteristics. Circuit values used are

$$V_d = 50V$$

Current reference level = 1A

$$R_1 = R_2 = 1\Omega$$

$$C_1 = C_2 = C_3 = C_4 = 6\mu F$$

$$L_{c_1} = L_{c_2} = L_{c_3} = L_{c_4} = 14\mu H$$

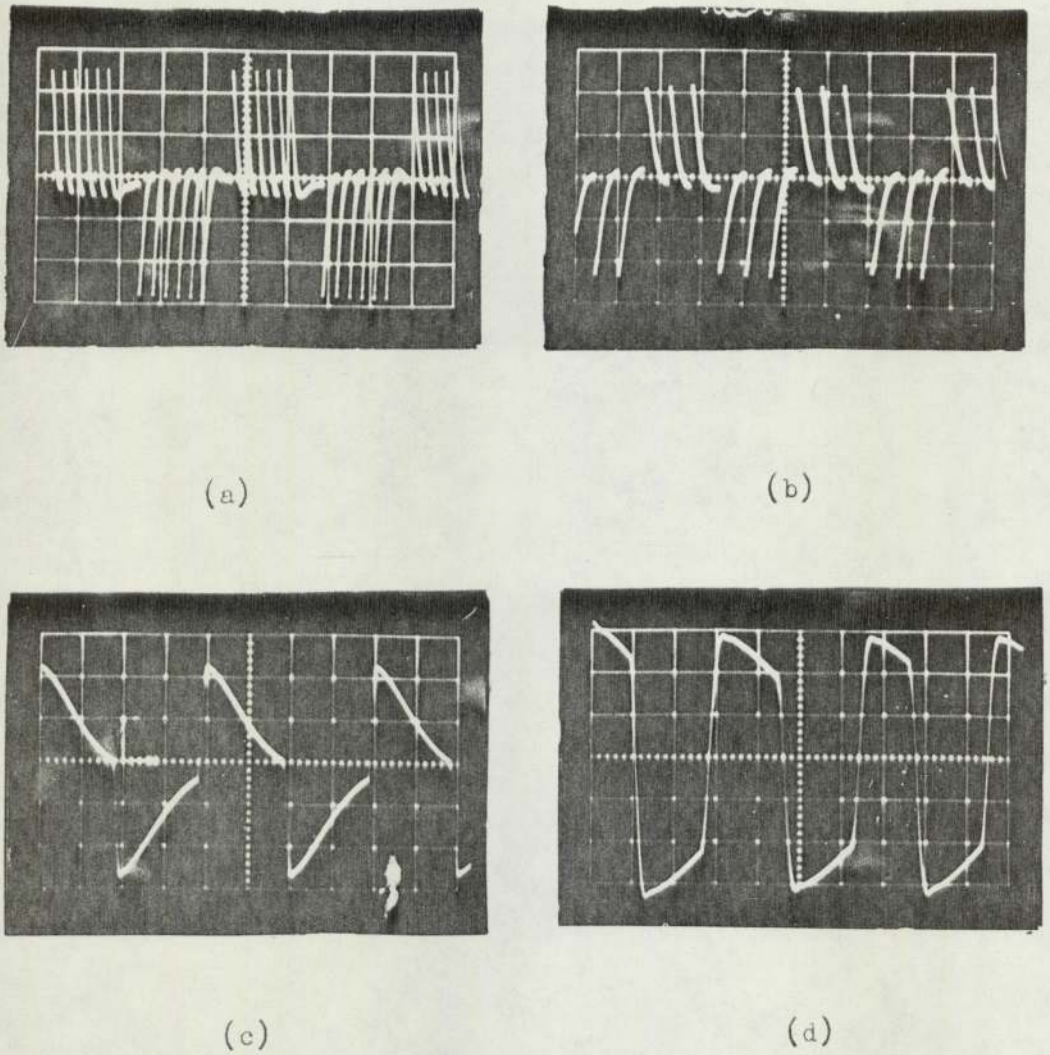

(a) (b)

(c) (d)

Fig.5.5 Output Voltage Waveforms with Resistive Load.

	(a)	(b)	(c)	(d)
Output Frequency, (Hz)	125	300	1,250	3,000
Time scale (ms/div)	2	1	0.2	0.1

V scale = 20V/div

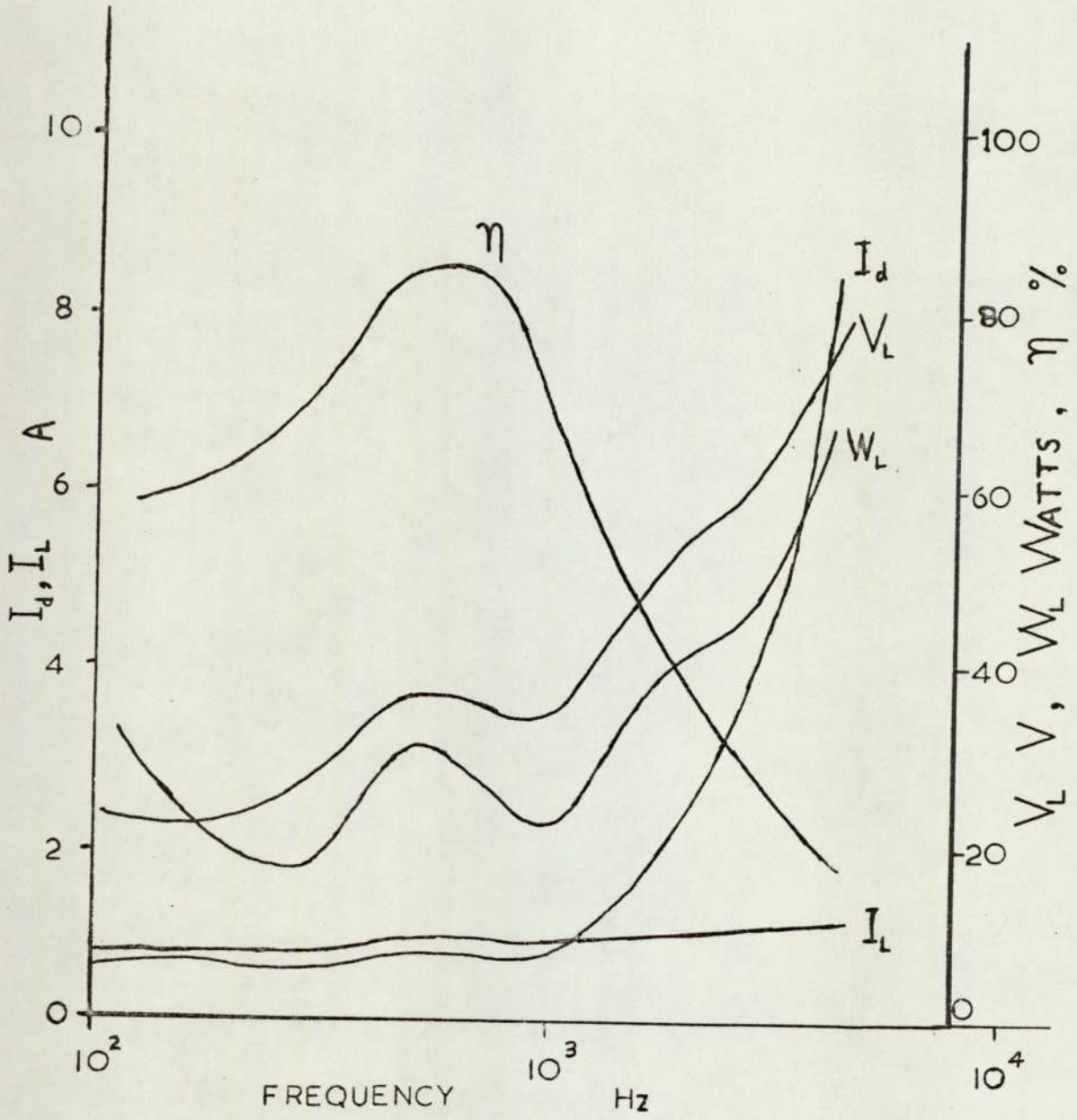

Fig.5.6 Cycloinverter Characteristics with Resistive Load.

Voltage Current

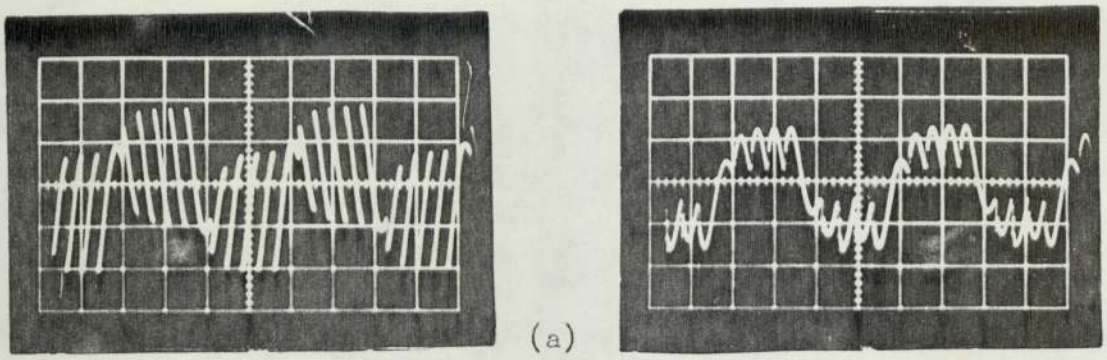

(a)

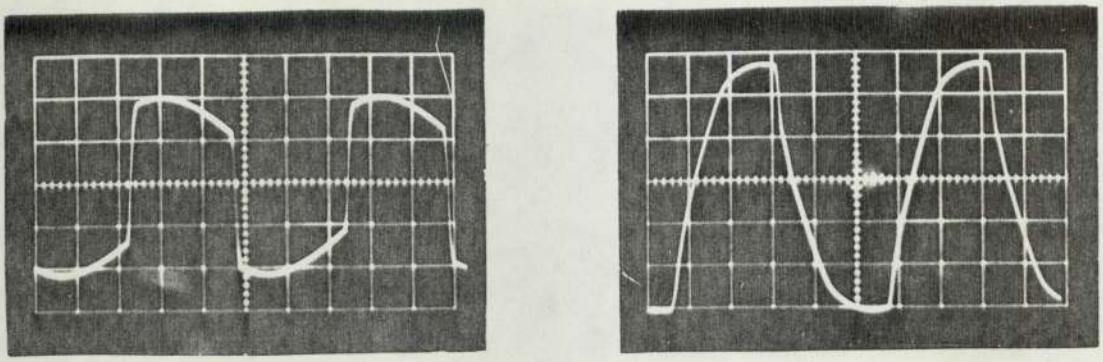

(b)

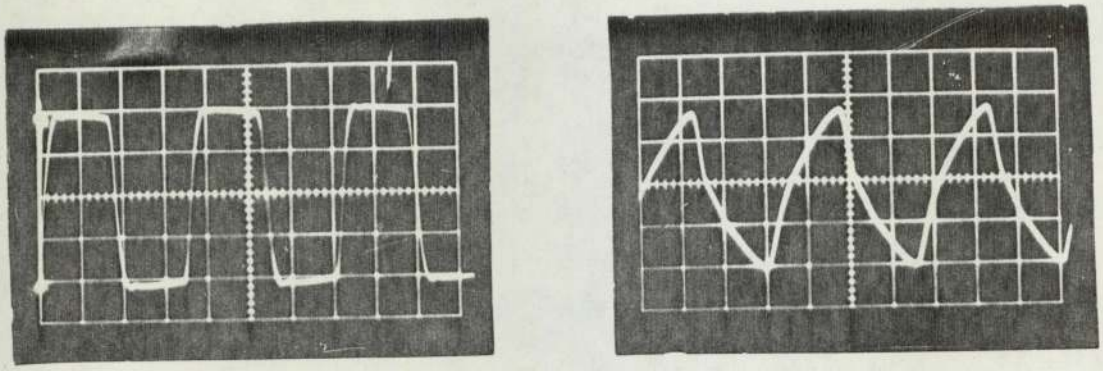

(c)

Fig.5.7 Output Voltage and Current Waveforms with Inductive Load.

	(a)	(b)	(c)
Output frequency (Hz)	125	1,000	3,000
t scale (ms/div)	2	0.2	0.1
V scale (V/div)	20	40	40
I scale (A/div)	0.5	0.5	0.5

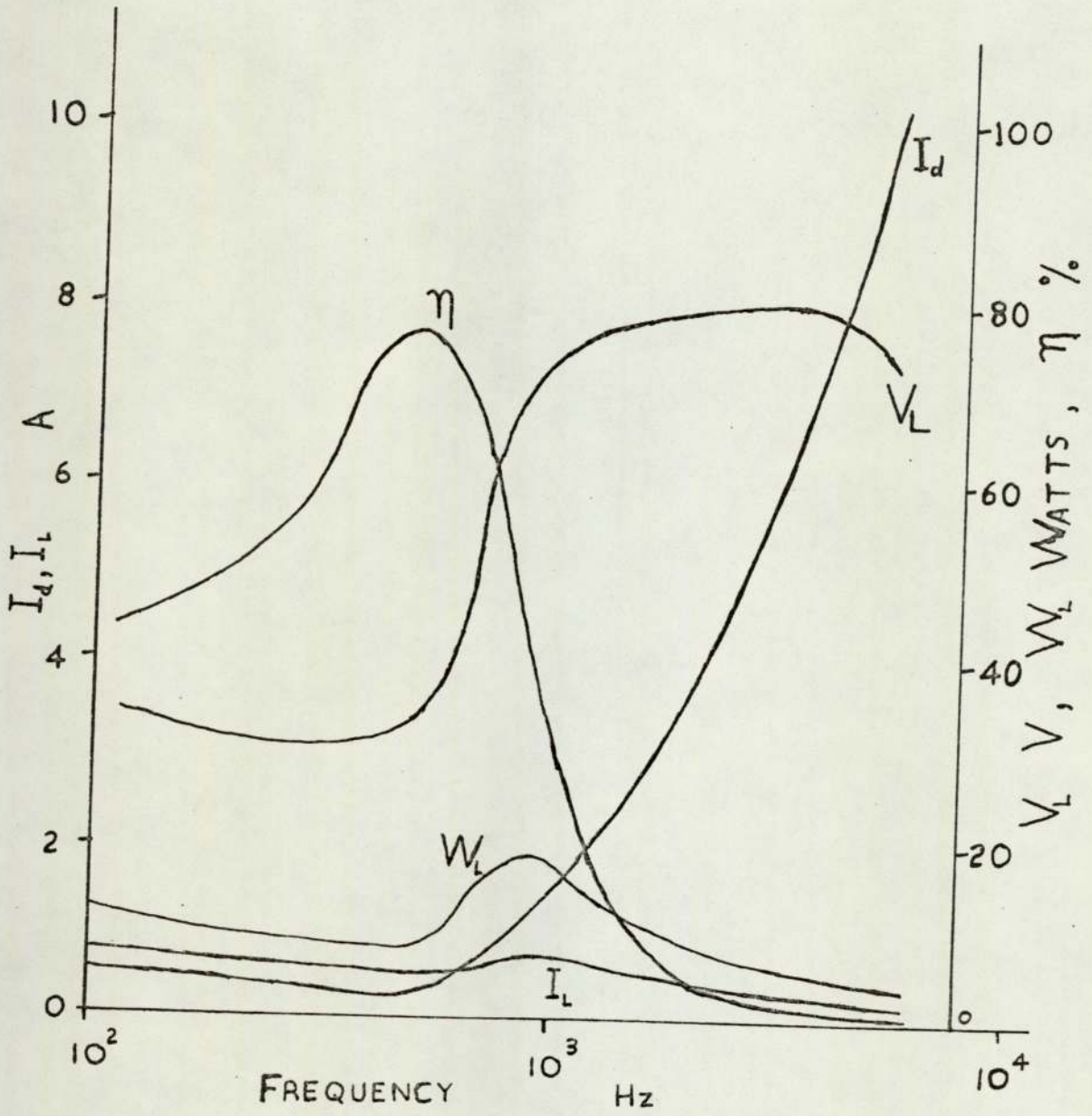

Fig.5.8 Cycloinverter Characteristics with Inductive Load.

With an additional series load inductance of 10 mH the voltage and current waveforms are as shown in Fig.5.7, and the characteristic given in Fig.5.8.

5.3.2 Analysis of Cycloinverter Operation

It can be shown for the purpose of the following analysis that if all capacitors have a value C then the circuit may be modified as shown in Fig.5.9. Operation of the inverter can then be studied by reference to the three conditions of the circuit, represented in Fig.5.10.

a) When TH1 and TH4 are conducting and current i_d flows.

b) When i_d is zero and no thyristors are conducting.

c) When TH2 and TH3 are conducting and current i_d flows.

Neither the thyristor pair TH1 and TH3 nor the thyristor pair TH2 and TH4 should conduct at the same time.

Modulation is achieved by changing the modes of operation of the circuit. These modes are,

A:- The sequence of conditions a - b - a - b - a, for a number of cycles.

B:- The condition b.

C:- The sequence of conditions c - b - c - b - c, for a number of cycles.

There are many possibilities for synthesising output waveforms, but the example used here is the sequence of modes B - A - B - C - B.

Let $L_{c_1} = L_{c_2} = L_{c_3} = L_{c_4} = \frac{L_c}{2}$ ..... (5-1)

and $C_1 = C_2 = C_3 = C_4 = C$ .....

The inverter can be represented by the state diagram shown in Fig.5.11.

Values for ℓ and k are determined by the condition of the circuit as given in Table 5.1.

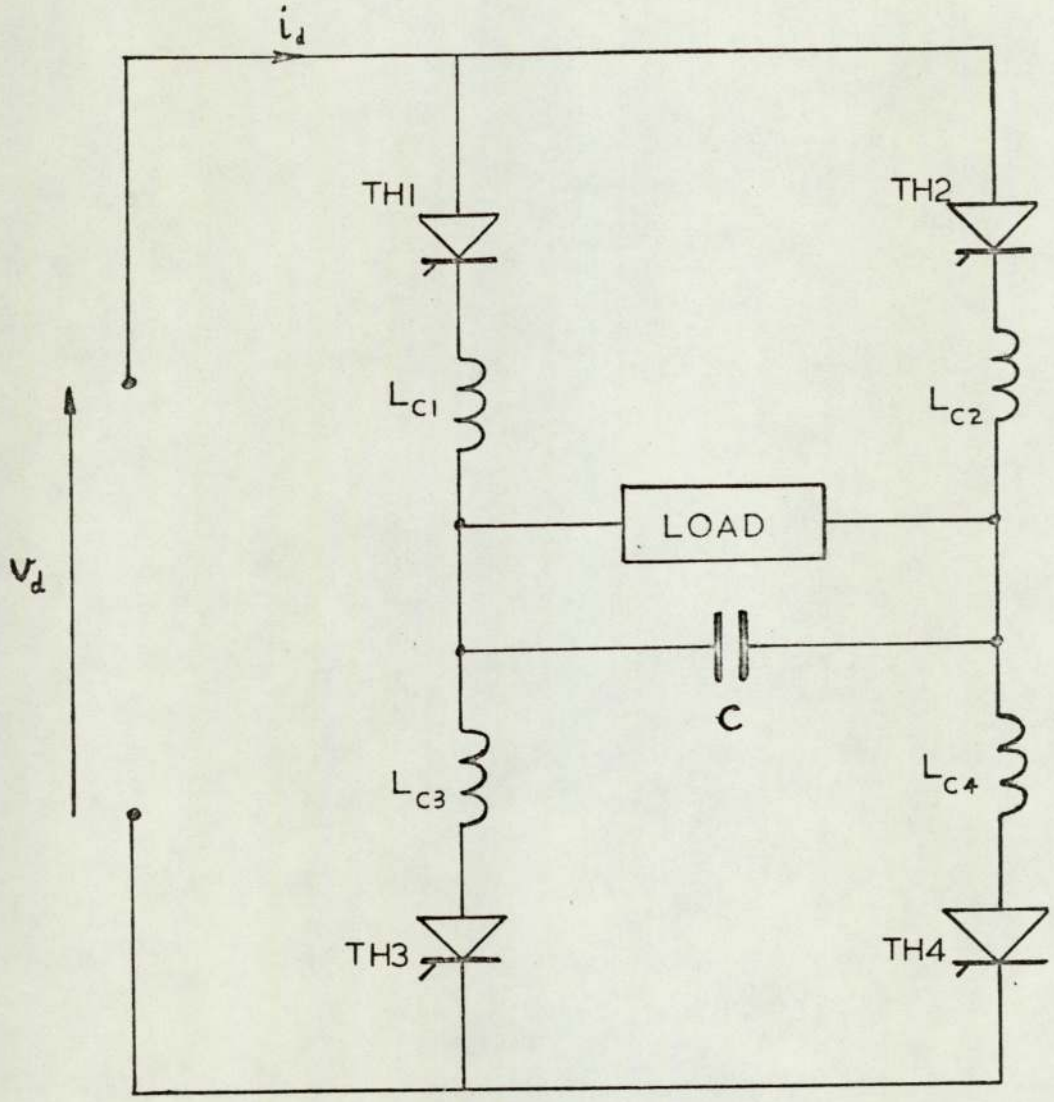

Fig.5.9 Alternative representation for cycloinverter analysis.

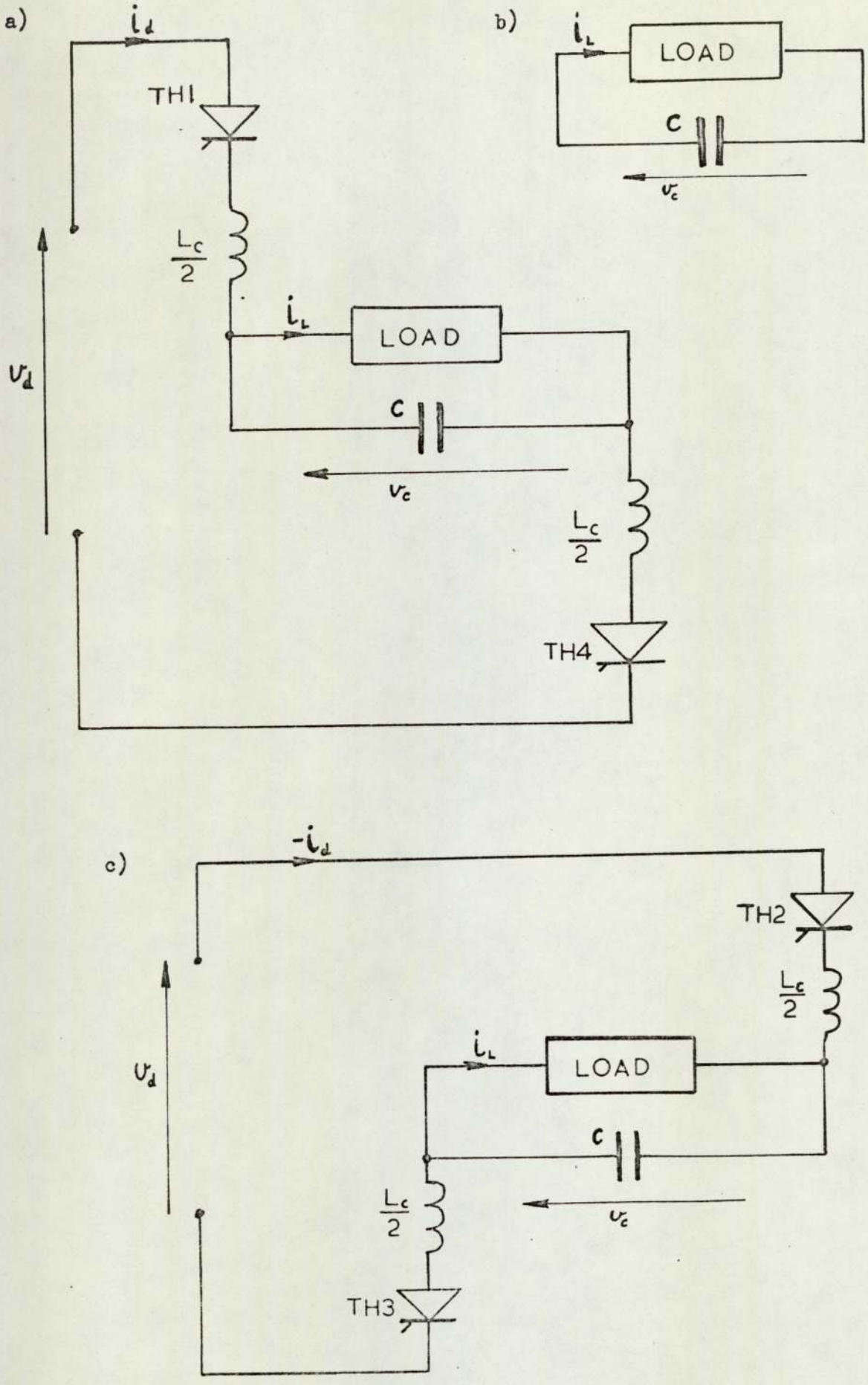

Fig.5.10 Conditions (a) (b) and (c) of cycloinverter.

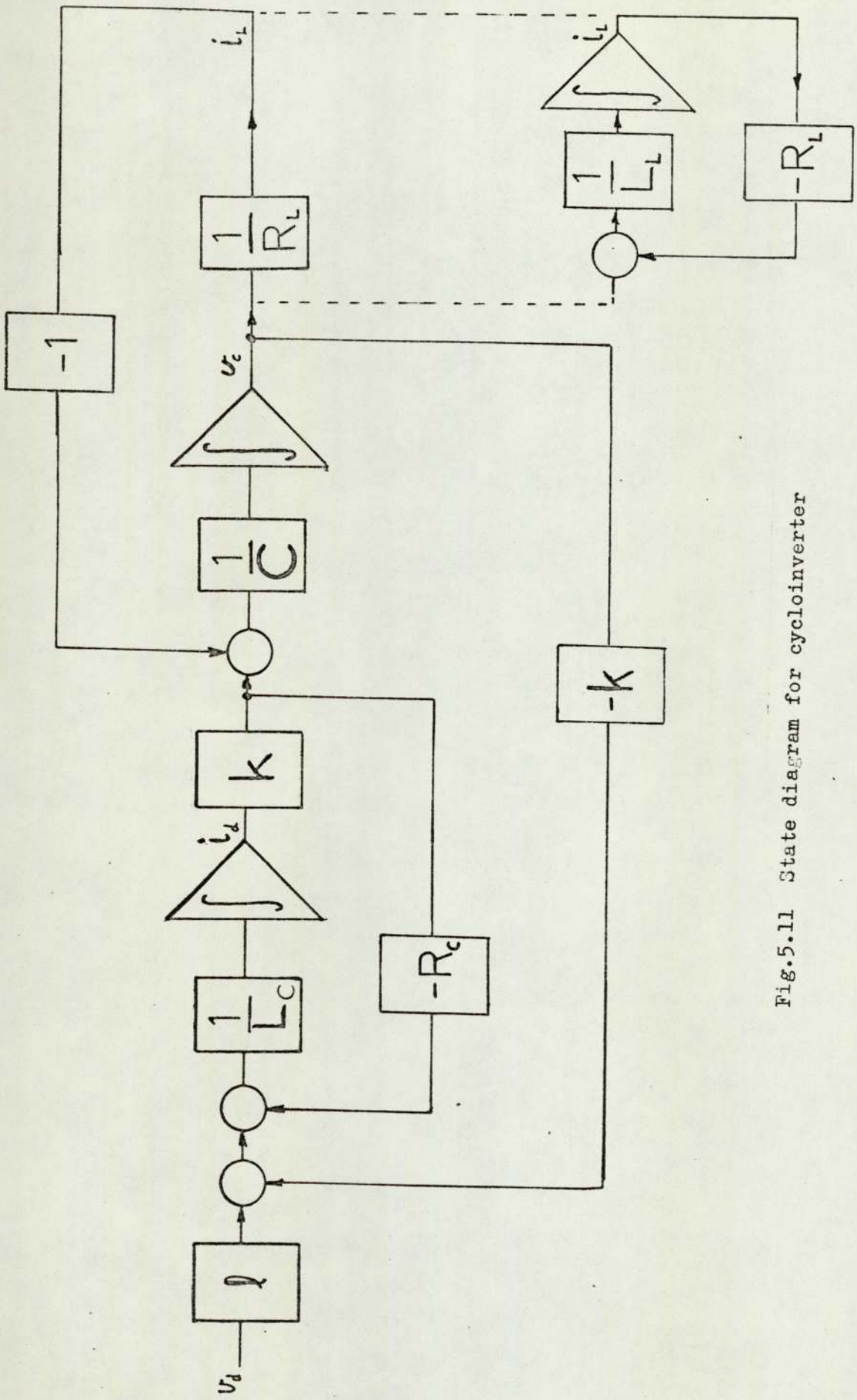

Fig.5.11 State diagram for cycloinverter

	a	b	c
k	1	0	1
ℓ	1	0	-1

Table 5.1

A brief analysis for resistive and inductive loads will be given.

(i) Operation with a resistive load.

With a resistive load R_L, the state equations for the system are

$$\begin{bmatrix} \dot{v}_d \\ \dot{i}_d \\ \dot{v}_c \end{bmatrix} = \begin{bmatrix} 0 & 0 & 0 \\ \frac{\ell}{L_c} & \frac{-k}{\tau_1} & \frac{-k}{L_c} \\ 0 & \frac{k}{C} & \frac{-1}{\tau_2} \end{bmatrix} \begin{bmatrix} v_d \\ i_d \\ v_c \end{bmatrix} \quad \ldots\ldots (5\text{-}2)$$

where,

$$\tau_1 = \frac{L_c}{R_c} \quad \ldots\ldots\ldots \qquad (5\text{-}3)$$

$$\tau_2 = CR_L \quad \ldots\ldots\ldots$$

(the resistnce of the chokes is $\frac{R_c}{2}$)

The overall transition matrix can be expressed as

$$\underline{\phi}(t) = \begin{bmatrix} 1 & 0 \\ h(t) & \phi(t) \end{bmatrix} \quad \ldots\ldots\ldots (5\text{-}4)$$

$\phi(t)$ is the cycloinverter transition matrix, which for conditions a and c is given by

$$\phi_{a,c}(t) = e^{\sigma t} \begin{bmatrix} (\sigma + \frac{1}{\tau_2}) \frac{\sin \omega_a t}{\omega_a} + \cos \omega_a t & \frac{-\sin \omega_a t}{\omega_a L_c} \\ \frac{\sin \omega_a t}{\omega_a C} & (\sigma + \frac{1}{\tau_1}) \frac{\sin \omega_a t}{\omega_a} + \cos \omega_a t \end{bmatrix} \ldots (5\text{-}5)$$

and for condition b by

$$\phi_b(t) = \begin{bmatrix} 1 & 0 \\ 0 & e^{2\sigma_b t} \end{bmatrix} \quad \ldots\ldots\ldots\ldots (5\text{-}6)$$

h(t), the control transition matrix is given by,

$$h_{a,c}(t) = \frac{\ell}{(\sigma_a^2+\omega_a^2)L_c} \begin{bmatrix} \frac{1-e^{\sigma_a t}\cos\omega_a t}{\tau_2} + (\sigma_a^2+\omega_a^2+\frac{\sigma_a}{\tau_2})e^{\sigma_a t}\frac{\sin\omega_a t}{\omega_a} \\ \frac{1}{C}\left\{1 + e^{\sigma_a t}\left(\frac{\sigma_a}{\omega_a}\sin\omega_a t - \cos\omega_a t\right)\right\} \end{bmatrix} \ldots (5\text{-}7)$$

and,

$$h_b(t) = \begin{bmatrix} 0 \\ 0 \end{bmatrix} \quad \ldots\ldots\ldots (5\text{-}8)$$

The eigenvalues, λ, are at $\sigma + j\omega$ and $\sigma - j\omega$, given by the solution of the characteristic equation,

$$\lambda^2 + \left(\frac{k}{\tau_1} + \frac{1}{\tau_2}\right) + \frac{k^2}{L_c C} + \frac{k}{\tau_1\tau_2} = 0 \quad \ldots\ldots\ldots (5\text{-}9)$$

i.e. $$\sigma = \frac{-1}{2}\left(\frac{k}{\tau_1} + \frac{1}{\tau_2}\right) \quad \ldots\ldots\ldots\ldots (5\text{-}10)$$

$$\omega^2 = \frac{k}{\tau_1\tau_2} + \frac{k^2}{L_c C} - \frac{1}{4}\left(\frac{k}{\tau_1} - \frac{1}{\tau_2}\right)^2 \quad \ldots\ldots\ldots\ldots (5\text{-}11)$$

In conditions 'a' and 'c' the circuit has a natural frequency ω_n and damping factor ζ, given by,

$$\omega_n^2 = \sigma_a^2 + \omega_a^2 = \frac{1}{L_c C}\left(1 + \frac{R_c}{R_L}\right) \quad \ldots\ldots\ldots (5\text{-}12)$$

$$\zeta = \frac{\frac{1}{\tau_1} + \frac{1}{\tau_2}}{2\omega_n} \quad \ldots\ldots\ldots\ldots\ldots\ldots (5\text{-}13)$$

i.e. $$\sigma_a = -\zeta\omega_n \quad \ldots\ldots\ldots (5\text{-}14)$$

and

$$\omega_a = \omega_n\sqrt{1-\zeta^2} \quad \ldots\ldots\ldots (5\text{-}15)$$

Note that R_c affects both ω_n and ζ. The constraint for oscillatory operation, in terms of R_L, is

$$\left(C - \frac{4\tau_1^2}{L_c}\right) CR_L^2 - 3\tau_1 C R_L + \tau_1 > 0 \quad \ldots\ldots\ldots (5\text{-}16)$$

Consider operation in mode A. Let the state vector after switching from condition 'b' to condition 'a' at time t_o be,

$$\underline{x}(t_o) = \begin{bmatrix} V_d \\ 0 \\ V_s \end{bmatrix} \quad \ldots\ldots\ldots\ldots (5\text{-}17)$$

V_s is the value of the voltage across the load below which the decision is taken to switch to condition 'a'. In condition 'a' the current is given by,

$$i_d(t) = \frac{V_d}{L_c(\sigma_a^2+\omega_a^2)}\left\{\frac{1-e^{\sigma_a(t-t_o)}\cos\omega_a(t-t_o)}{\tau_2}\right.$$

$$\left. + (\sigma_a^2+\omega_a^2+\frac{\sigma_a}{\tau_2})\, e^{\sigma_a(t-t_o)}\, \frac{\sin\omega_a(t-t_o)}{\omega_a}\right\} - V_d\, e^{\sigma_a(t-t_o)}\, \frac{\sin\omega_a(t-t_o)}{\omega_a}$$

$\ldots\ldots\ldots\ldots (5\text{-}18)$

and the voltage across the load is,

$$v_c(t) = \frac{V_d}{L_c C(\sigma_a^2+\omega_a^2)}\left\{1-e^{\sigma_a(t-t_o)}\cos\omega_a(t-t_o)+\frac{\sigma_a e^{\sigma_a(t-t_o)}}{\omega_a}\sin\omega_a(t-t_o)\right\}$$

$$+V_s\, e^{\sigma_a(t-t_o)}\left\{(\sigma_a+\frac{1}{\tau_1})\,\frac{\sin\omega_a(t-t_o)}{\omega_a}+\cos\omega_a(t-t_o)\right\} \ldots (5\text{-}19)$$

Let $t = t_1$ when $i_d(t)$ first falls to zero, then equation (5-18) could be solved for t_1.

Preferably damping should be low so t_1 and $v_c(t_1)$ may be given by the approximations,

$$\omega_a \triangleq \omega_n \qquad \ldots\ldots\ldots (5\text{-}20)$$

$$t_1 \triangleq t_o + \frac{\pi}{\omega_n} \qquad \ldots\ldots\ldots (5\text{-}21)$$

and

$$v_c(t_1) \triangleq \frac{2\,V_d}{\omega_n^2 L_c C} - V_s \qquad \ldots\ldots\ldots (5\text{-}22)$$

The state vector at time t_1 can be expressed as,

$$\underline{x}(t_1) = \phi_a(t-t_o)\,\underline{x}(t_o) \qquad \ldots\ldots\ldots\ldots (5\text{-}23)$$

After switching from 'a' to 'b', this becomes,

$$\underline{x}(t_1^+) = \begin{bmatrix} 0 \\ 0 \\ v_c(t_1) \end{bmatrix} \qquad \ldots\ldots\ldots (5\text{-}24)$$

and $v_c(t)$ is then given by,

$$v_c(t) = e^{-\frac{t-t_1}{\tau_2}}\, v_c(t_1) \qquad \ldots\ldots\ldots (5\text{-}25)$$

Let $t = t_2$ when $v_c(t)$ has fallen to V_s

then

$$t_2 = t_1 + \tau_2 \log\left(\frac{v_c(t_1)}{V_s}\right) \qquad \ldots\ldots\ldots (5\text{-}26)$$

The nominal thyristor switching frequency ω_s, for modes A and C, is determined by

$$\omega_s = \frac{2\pi}{t_2 - t_o} \qquad \ldots\ldots\ldots (5\text{-}27)$$

The first cycle following a change in mode will have a greater period

due to the different initial conditions.

Thus from (5-20) (5-21) (5-22) (5-26) and (5-27), if damping is low,

$$\omega_s \simeq \frac{2\omega_n}{1 + \frac{\omega_n \tau_2}{\pi} \log\left(\frac{2V_d}{\omega_n^2 L_c C V_s} - 1\right)} \quad \ldots\ldots\ldots\ldots \quad (5\text{-}28)$$

(ii) Operation with an inductive load.

With a load of inductance L_L and series resistance R_L, the state equations become,

$$\begin{bmatrix} \dot{v}_d \\ \dot{i}_d \\ \dot{v}_c \\ \dot{i}_L \end{bmatrix} = \begin{bmatrix} 0 & 0 & 0 & 0 \\ \frac{\ell}{L_c} & \frac{-k}{\tau_1} & \frac{-k}{L_c} & 0 \\ 0 & \frac{k}{C} & 0 & \frac{-1}{C} \\ 0 & 0 & \frac{1}{L_L} & \frac{-1}{\tau_2} \end{bmatrix} \begin{bmatrix} v_d \\ i_d \\ v_c \\ i_L \end{bmatrix} \quad \ldots\ldots\ldots\ldots \quad (5\text{-}29)$$

where,

$$\tau_1 = \frac{L_c}{R_c} \quad \ldots\ldots\ldots\ldots \quad (5\text{-}30)$$

$$\tau_2 = \frac{L_L}{R_L} \quad \ldots\ldots\ldots\ldots$$

for conditions 'a' and 'c'

$$\phi_{a,c}(t) = \frac{1}{(\sigma_a - \sigma_{al})^2 + \omega_a^2} \left\{ \left(\sigma_{al}^2 e^{\sigma_{al} t} + A_4 e^{\sigma_a t} \sin(\omega_a t + \alpha_4) \right) \begin{bmatrix} 1 & 0 & 0 \\ 0 & 1 & 0 \\ 0 & 0 & 1 \end{bmatrix} \right.$$

$$\left. + \left(\sigma_{al} e^{\sigma_{al} t} + A_3 e^{\sigma_a t} \sin(\omega_a t + \alpha_3) \right) \begin{bmatrix} \frac{1}{\tau_2} & \frac{-1}{L_c} & 0 \\ \frac{1}{C} & \frac{1}{\tau_1} + \frac{1}{\tau_2} & \frac{-1}{C} \\ 0 & \frac{1}{L_L} & \frac{1}{\tau_1} \end{bmatrix} + \ldots \right.$$

$$+ \left(e^{\sigma_{al}t} + A_2 e^{\sigma t} \sin(\omega_a t + \alpha_2)\right) \left\{ \begin{bmatrix} \frac{1}{L_L C} & \frac{-1}{L_c \tau_2} & \frac{1}{L_c C} \\ \frac{1}{C\tau_2} & \frac{1}{\tau_1 \tau_2} & \frac{-1}{C\tau_1} \\ \frac{1}{L_L C} & \frac{1}{L_L \tau_1} & \frac{1}{L_c C} \end{bmatrix} \right\} \quad \ldots\ldots (5\text{-}31)$$

and for condition 'b' by,

$$\phi_b(t) = e^{\sigma_b t} \left(\cos \omega_b t + \frac{\sigma_b}{\omega_b} \sin \omega_b t\right) \begin{bmatrix} 1 & 0 & 0 \\ 0 & 1 & 0 \\ 0 & 0 & 1 \end{bmatrix}$$

$$+ \frac{e^{\sigma_b t} \sin \omega_b t}{\omega_b} \begin{bmatrix} \frac{1}{\tau_2} & 0 & 0 \\ 0 & \frac{1}{\tau_2} & \frac{-1}{C} \\ 0 & \frac{1}{L_L} & 0 \end{bmatrix}$$

$$+ \frac{\omega_b + e^{\sigma_b t} (\sigma_b \sin \omega_b t - \omega_b \cos \omega_b t)}{\sigma_b^2 + \omega_b^2} \begin{bmatrix} \frac{1}{L_L C} & 0 & 0 \\ 0 & 0 & 0 \\ \frac{1}{L_L C} & 0 & 0 \end{bmatrix} \quad \ldots\ldots (5\text{-}32)$$

and the control transition matrices are given by,

$$h_{a,c}(t) = \frac{\ell}{((\sigma_a - \sigma_{al})^2 + \omega_a^2) L_c} \left\{ \left(\sigma_{al} e^{\sigma_{al} t} + A_3 e^{\sigma_a t} \sin(\omega_a t + \alpha_3)\right) \begin{bmatrix} 1 \\ 0 \\ 0 \end{bmatrix} \right.$$

$$\left. + \left(e^{\sigma_{al} t} + A_2 e^{\sigma_a t} \sin(\omega_a t + \alpha_2)\right) \begin{bmatrix} \frac{1}{\tau_2} \\ \frac{1}{C} \\ 0 \end{bmatrix} \right.$$

$$+\left(\frac{e^{\sigma_{al}t}-1}{\sigma_{al}}+A_1 e^{\sigma_a t}\sin(\omega_a t+\alpha_1)\right)\begin{bmatrix}\frac{1}{L_L C}\\ \frac{1}{C\tau_2}\\ \frac{1}{L_L C}\end{bmatrix}\Bigg\} \quad \ldots\ldots\ldots (5\text{-}33)$$

and,

$$h_b(t) = \begin{bmatrix}0\\0\\0\end{bmatrix} \quad \ldots\ldots\ldots\ldots (5\text{-}34)$$

where, in the above equations,

$$A_1 = \frac{\sqrt{(\sigma_{al}-2\sigma_a)^2+\left(\frac{\sigma_a^2-\sigma_a\sigma_{al}-\omega_a^2}{\omega_a}\right)^2}}{\sigma_a^2+\omega_a^2} \qquad \alpha_1 = \tan^{-1}\frac{\omega_a(\sigma_{al}-2\sigma_a)}{\sigma_a(\sigma_a-\sigma_{al})-\omega_a^2} \quad \ldots\ldots (5\text{-}35)$$

$$A_2 = \sqrt{1+\left(\frac{\sigma_a-\sigma_{al}}{\omega_a}\right)^2} \qquad \alpha_2 = \tan^{-1}\frac{\omega_a}{\sigma_{al}-\sigma_a} \quad \ldots\ldots (5\text{-}36)$$

$$A_3 = \sqrt{\left(\omega_a+\frac{\sigma_a(\sigma_a-\sigma_{al})}{\omega_a}\right)^2+\sigma_{al}^2} \qquad \alpha_3 = \tan^{-1}\frac{-\omega_a\sigma_{al}}{\omega_a^2+\sigma_a(\sigma_a-\sigma_{al})} \quad \ldots (5\text{-}37)$$

$$A_4 = \sqrt{\left\{\omega_a(\sigma_a+\sigma_{al})+\frac{\sigma_a^2}{\omega_a}(\sigma_a-\sigma_{al})\right\}^2+(\omega_a^2-2\sigma_a\sigma_{al}+\sigma_a^2)^2}$$

$$\alpha_4 = \tan^{-1}\frac{\omega_a(\omega_a^2-2\sigma_a\sigma_{al}+\sigma_a^2)}{\omega_a^2(\sigma_a+\sigma_{al})+\sigma_a^2(\sigma_a-\sigma_{al})} \quad \ldots\ldots\ldots\ldots\ldots (5\text{-}38)$$

The eigenvalues located at σ_1, $\sigma+j\omega$ and $\sigma-j\omega$, are given by the solution of the characteristic equation,

$$\lambda^3+\left(\frac{k}{\tau_1}+\frac{1}{\tau_2}\right)\lambda^2+\left(\frac{k}{\tau_1\tau_2}+\frac{1}{L_L C}+\frac{k^2}{L_c C}\right)\lambda+\frac{kR_c+k^2R_L}{L_L L_c C}=0 \quad \ldots\ldots\ldots (5\text{-}39)$$

The oscillatory form of equations (5-31) to (5-33) has been given since this form of response is necessary, thus the constraints for conditions 'a' and 'c'

$$27\,a_o^2 - a_2^2\,a_1^2 + 4\,a_1^3 + 4\,a_o\,a_2^3 - 18\,a_2 a_1 a_o > 0 \quad \ldots\ (5\text{-}40)$$

where a_1, a_2, a_3, a_4 are the coefficients of λ^n in equation (5-39)

i.e. $a_3 = 1$

$$a_2 = \frac{1}{\tau_1} + \frac{1}{\tau_2} = -\sigma_{al} - 2\sigma_a \quad \ldots\ (5\text{-}41)$$

$$a_1 = \frac{1}{\tau_1\tau_2} + \frac{1}{L_L C} + \frac{1}{L_c C} = \sigma_a^2 + \omega_a^2 + 2\sigma_{al}\sigma_a \quad \ldots\ (5\text{-}42)$$

$$a_o = \frac{R_c + R_L}{L_L L_c C} = -\sigma_{al}(\sigma_a^2 + \omega_a^2) \quad \ldots\ (5\text{-}43)$$

If R_L and R_c are assumed negligible then equation (5-39) reduces to a second order equation with $\zeta = 0$. Thus if R_L and R_c are small the natural frequency is,

$$\omega_{n_a} \simeq \sqrt{\frac{1}{C}\left(\frac{1}{L_L} + \frac{1}{L_c}\right)} \quad \ldots\ (5\text{-}44)$$

In condition b equation (5-39) is also of second order form and gives a natural frequency ω_{nb} and damping factor ζ_b of

$$\omega_{nb} = \frac{1}{\sqrt{L_L C}} \quad \ldots\ (5\text{-}45)$$

$$\zeta_b = \frac{R_L}{2}\sqrt{\frac{C}{L_L}} \quad \ldots\ (5\text{-}46)$$

If again damping is assumed to be low then the following approximations can be made.

$$\omega_a \triangleq \omega_{na} \qquad \ldots\ldots\ldots\ldots (5\text{-}47)$$

$$t_1 \triangleq t_o + \frac{\pi}{\omega_{na}} \qquad \ldots\ldots\ldots\ldots (5\text{-}48)$$

$$\omega_b \triangleq \omega_{nb} \qquad \ldots\ldots\ldots\ldots, (5\text{-}49)$$

i.e. $\sigma_1 \triangleq \sigma \triangleq 0$ ..... (5-50)

equations (5-31) to (5-33) then become,

$$\phi_{a,c}(t) \triangleq \begin{bmatrix} \frac{L_c+L_L \cos\omega_{na}t}{L_L+L_c} & -\frac{\sin\omega_{na}t}{\omega_{na}L_c} & \frac{L_L(1-\cos\omega_{na}t)}{L_L+L_c} \\ \frac{\sin\omega_{na}t}{\omega_{na}C} & \cos\omega_{na}t & -\frac{\sin\omega_{na}t}{\omega_{na}C} \\ \frac{L_c(1-\cos\omega_{na}t)}{L_L+L_c} & -\frac{\sin\omega_{na}t}{\omega_{na}L_L} & \frac{L_L+L_c\cos\omega_{na}t}{L_L+L_c} \end{bmatrix} \qquad \ldots\ldots\ldots (5\text{-}51)$$

$$\phi_b(t) \triangleq \begin{bmatrix} \cos\omega_{nb}t & 0 & 0 \\ 0 & \cos\omega_{nb}t & -\frac{\sin\omega_{nb}t}{\omega_{nb}C} \\ 0 & \frac{\sin\omega_{nb}t}{\omega_{nb}L_L} & \cos\omega_{nb}t \end{bmatrix} \qquad \ldots\ldots\ldots (5\text{-}52)$$

$$h_{a,c}(t) \triangleq \frac{\ell}{L_L+L_c} \begin{bmatrix} t + \frac{L_L}{L_c}\frac{\sin\omega_{na}}{\omega_{na}} \\ L_L(1-\cos\omega_{na}t) \\ t + \frac{L_L}{L_c}\frac{\sin\omega_{na}t}{\omega_{na}} \end{bmatrix} \qquad \ldots\ldots\ldots\ldots (5\text{-}53)$$

Let the state vector after switching from condition 'b' to condition 'a' (mode A) at time t_o be

$$\underline{x}(t_o) = \begin{bmatrix} V_d \\ 0 \\ v_c(t_o) \\ I_s \end{bmatrix} \qquad \ldots\ldots\ldots\ldots (5\text{-}54)$$

where I_s is the value of the load current below which the decision is taken to switch to condition 'a'.

When $i_d(t)$ falls to zero, at $t = t_1$, the state vector then becomes,

$$\underline{x}(t_1) = \begin{bmatrix} V_d \\ 0 \\ v_c(t_1) \\ i_L(t_1) \end{bmatrix} \qquad \ldots\ldots\ldots\ldots (5\text{-}55)$$

where $$v_c(t_1) = \frac{2\,V_d L_L}{L_L + L_c} - v_c(t_o) \qquad \ldots\ldots\ldots\ldots (5\text{-}56)$$

and $$i_L(t_1) = \frac{t_1 - t_o}{L_L + L_c}\, V_d - I_s \qquad \ldots\ldots\ldots\ldots (5\text{-}57)$$

At time $t = t_2$, i_d has again fallen to I_s and thus

$$i_L(t_2) = i_L(t_o) = I_s = \frac{\sin \omega_{nb}(t_2 - t_1)}{\omega_{nb} L_L} \cdot v_c(t_1) + \cos \omega_{nb}(t_2 - t_1) \cdot i_L(t_1) \qquad \ldots\ldots\ldots\ldots (5\text{-}58)$$

and solving for t_2 gives,

$$t_2 = t_1 + \frac{1}{\omega_{nb}} \sin^{-1}\left(\frac{I_s}{\sqrt{\left(\frac{v_c(t_1)}{\omega_{nb} L_L}\right)^2 + i_L^2(t_1)}} - \theta \right) \qquad \ldots\ldots\ldots\ldots (5\text{-}59)$$

where,

$$\theta = \tan^{-1} \frac{i_L(t_1)\,\omega_{nb} L_L}{v_c(t_1)} \qquad \ldots\ldots\ldots\ldots (5\text{-}60)$$

Equations (5-56) and (5-57) require the value of $v_c(t_o)$ in order to obtain t_2 from equations (5-59) and (5-60).

This is given by,

$$v_c(t_2) = v_c(t_o) = \cos \omega_{nb}(t_2-t_1).v_c(t_1) - i_L(t_1) \frac{\sin \omega_{nb}(t_2-t_1)}{\omega_{nb}\, C} \qquad \ldots\ldots\ldots\ldots (5\text{-}61)$$

using (5-56) and solving for $v_c(t_o)$,

$$v_c(t_o) = \frac{\frac{i_L(t_1)}{\omega_{nb}\, C} \sin \omega_{nb}(t_2-t_1) - \frac{2\, V_d L_L}{L_L+L_c} \cos \omega_{nb}(t_2-t_1)}{1 - \cos \omega_{nb}(t_2-t_1)} \qquad \ldots\ldots (5\text{-}62)$$

giving (5-59) and (5-62) as simultaneous equations in t_2 and $v_c(t_o)$. The nominal thyristor switching frequency ω_s is again given by equation (5-27).

5.3.2 Features of the Improved Cycloinverter

The main advantage of using the capacitors in a bridge arrangement, instead of across the load, as in ref.29, is increased reliability of commutation, for the following reasons.

(i) At instants when all thyristors are 'off' the load is no longer 'floating'. A capacitor is present for each thyristor to reduce the risk of damage by by-passing any spurious voltage transients which may occur.

(ii) When two thyristors, such as TH1 and TH4, are commutated they are effectively in series and the capacitors provide an equalising

network so that during 'turn on' and 'turn off' the thyristors share equal voltages.

(iii) The risk of false triggering of the thyristors is also reduced. Suppose TH1 turns 'on' faster than TH4. This could be due to devices having slightly different characteristics, or a difference of a microsecond or so in the application of the gate pulses. In the single capacitor circuit a high rate of rise of anode voltage may then trigger TH3 and short circuit the bridge.

(iv) The capacitors also assist to prevent a drop in bridge input voltage from hindering commutation due to the internal impedance of the supply. If this is not sufficient, additional capacitance may be required across the input to the bridge.

With both resistive and inductive loads satisfactory commutation can be achieved provided the circuit is underdamped. With a stepping motor load the main difference in circuit operation appears to be that this condition is no longer sufficient. The circuit was used with a permanent magnet machine and it was found that the e.m.f. due to the permanent magnet can occasionally interfere with the commutation. If the current through TH1 and TH4 ever fails to reach zero before TH2 and TH3 are turned on, commutation can fail. This can be avoided by having a high mutual coupling between L_{c_1} and L_{c_3} and between L_{c_2} and L_{c_4}. This does not effect the operation of the circuit, as described earlier.

Suppose the current through TH1 becomes non oscillatory and the thyristors remained conducting when TH2 and TH3 are turned on. The high rate of rise of current through TH3 will induce an e.m.f. in L_{c_1}. The voltage across C_1 will be low and most of the induced e.m.f. will appear as a reverse voltage across TH1, improving 'turn off time' to this thyristor and effecting commutation. This is a method of forced commutation, easily built into the circuit, which can 'take over' on instances of failure of natural commutation.

5.4 CLOSED LOOP STEPPING MOTOR SYSTEMS

5.4.1 Method of Phase Angle Control

The principle of phase angle control is to generate the input pulse sequence to the motor from the electrical angular position of the rotor (θ_e) and then synchronism is inherently maintained. This sequence, $F(\theta_e)$, may be shifted in phase by an angle γ giving the driving function $F(\theta_e + \gamma)$.

Analogue methods[20,30] have been used to control the angles of phase shift, but most methods employ digital techniques[31-35].

Consider the logic signals PA and PB and their inverses $\overline{PA}$ and $\overline{PB}$, as shown in Fig.5.12 and let these indicate quadrant information of the electrical angular position of the rotor of a two-phase machine. The fundamental components of these signals are

$$D(o)_1 = (\cos\theta_e \quad -\cos\theta_e \sin\theta_e \quad -\sin\theta_e) \qquad \ldots\ldots (5\text{-}63)$$

where the set D(o) is,

$$D(o) = F(\theta_e) = (PA\ \overline{PA}\ PB\ \overline{PB}) \qquad \ldots\ldots\ldots (5\text{-}64)$$

The windings each have three states of energisation E.

Let, E = 0, represent an unenergised state

E = 1, represent the winding energised, in one sense

E = -1, represent the winding energised, in an opposite sense.

Two bi-level logic signals D_1 and D_2 are required to define E as shown in Table 5.2.

E	D_1	D_2
0	0	0
1	1	0
-1	0	1

Table 5.2.

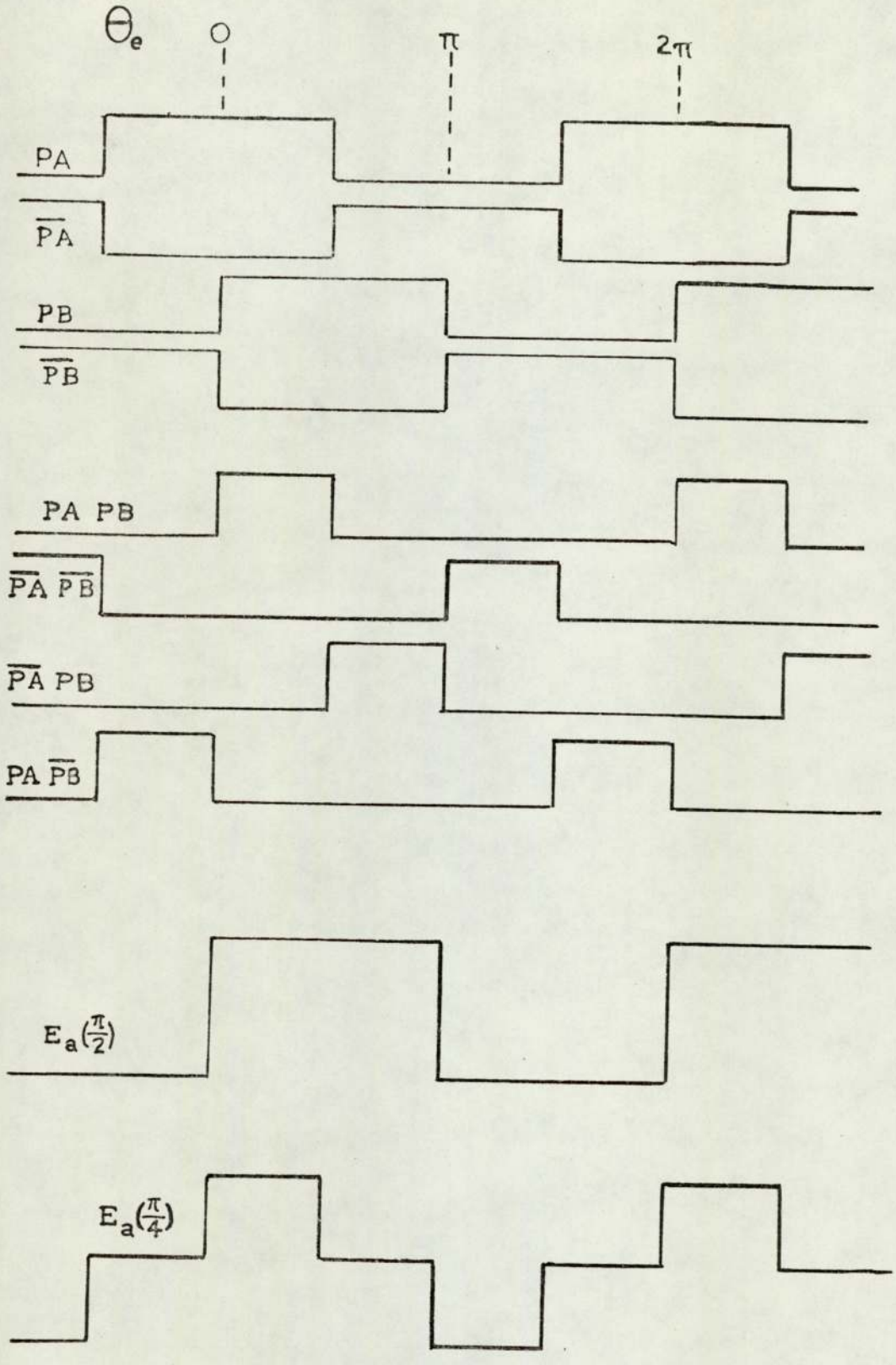

Fig.5.12 Typical signals for 2 phase and 1 phase moades, using Fredriksen method.

Thus the set of driving signals,

$$D = (D_{a_1}\ D_{a_2}\ D_{b_1}\ D_{b_2}) \quad \ldots\ldots\ldots (5\text{-}65)$$

defines the set,

$$E = (E_a\ E_b) \quad \ldots\ldots\ldots\ldots\ldots (5\text{-}66)$$

and hence the state of the input to the machine. A phase shift γ is easily obtained, if this is a multiple of $\pi/2$. e.g. to obtain $\gamma = \pi/2$,

let, $F(\theta_e + \pi/2) = D(\pi/2) = (PB\ \overline{PB}\ \overline{PA}\ PA) \quad \ldots\ldots\ldots (5\text{-}67)$

i.e. $D(\pi/2)_1 = (\sin\theta_e\ -\sin\theta_e\ -\cos\theta_e\ \cos\theta_e) \quad \ldots (5\text{-}68)$

Thus we have the driving circuit signals in terms of position signals for phase angles of even step multiples.

Control Modes	γ (steps)	D_{a_1}	D_{a_2}	D_{b_1}	D_{b_2}
CW	$-\pi/2$ (-2)	$\overline{PB}$	PB	PA	$\overline{PA}$
STOP	0 (0)	PA	$\overline{PA}$	PB	$\overline{PB}$
CCW	$\pi/2$ (2)	PB	$\overline{PB}$	$\overline{PA}$	PA
HS	π (4)	$\overline{PA}$	PA	$\overline{PB}$	PB

Table 5.3

The choice of four phase angles have been termed control modes by Fredriksen[31], as shown in Table 5.3. This method has been extended to give eight phase angles by deriving signals for the so called 'single-phase sense'. (Odd step multiples).

Control Modes	γ (steps)	D_{a_1}	D_{a_2}	D_{b_1}	D_{b_2}
CWMED	$-3\pi/4$ (-3)	$\overline{PA}\ \overline{PB}$	PA PB	PA $\overline{PB}$	$\overline{PA}$ PB
CWLOW	$-\pi/4$ (-1)	PA $\overline{PB}$	$\overline{PA}$ PB	PA PB	$\overline{PA}\ \overline{PB}$
CCWLOW	$\pi/4$ (1)	PA PB	$\overline{PA}\ \overline{PB}$	$\overline{PA}$ PB	PA $\overline{PB}$
CCWMED	$3\pi/4$ (3)	$\overline{PA}$ PB	PA $\overline{PB}$	$\overline{PA}\ \overline{PB}$	PA PB

Table 5.4

These sets can be related by observing that, for n = ± 1, ± 3 etc.

$$D\left(\frac{n\pi}{4}\right) = D\left(\frac{(n-1)\pi}{4}\right).\ D\left(\frac{(n+1)\pi}{4}\right) \qquad \ldots\ldots\ldots (5\text{-}69)$$

and for n = 0, ± 2, ± 4 etc.,

$$D\left(\frac{n\pi}{4}\right) = D\left(\frac{(n-1)\pi}{4}\right) + D\left(\frac{(n+1)\pi}{4}\right) \qquad \ldots\ldots\ldots (5\text{-}70)$$

Note that all phase angles do not give the same pulse width. By using more logic signals other pulse widths and a wider choice of phase angles is possible.

5.4.2 An Optical Method of Phase Angle Control

This method reduces the amount of hardware that would be involved with the previous method if a wide choice of phase angles is required. In the previous method, signals would usually be obtained optically and then processed electrically. With the alternative optical arrangement, processing is not required.

Consider four photo transistors T_1, T_2, T_3, T_4 and four light sources S_1, S_2, S_3, S_4 arranged either side of a slotted disc, as in Fig.5.13. Let the electrical angular spacing between transistors be $\pi/2$ and let the disc be positioned so that

$$d_t = d_s \qquad \ldots\ldots\ldots (5\text{-}71)$$

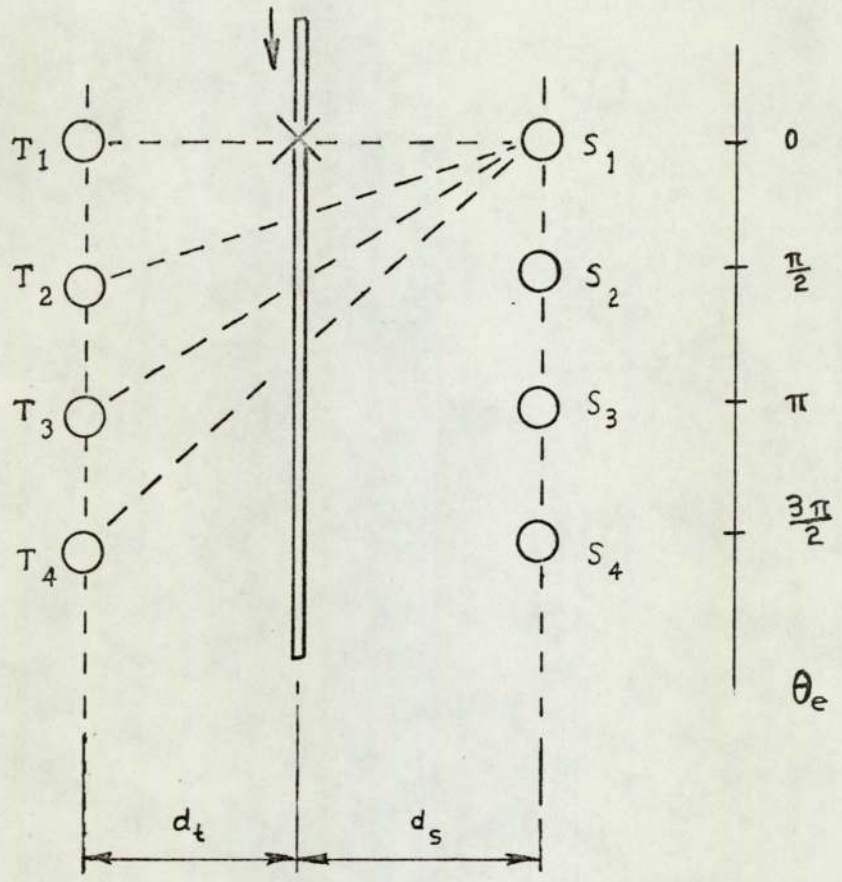

Fig.5.13 Arrangement for optical method.

Consider the edge of a slot, represented by point X on the disc, in line with T_1 and S_1 as it moves in the direction indicated. X will be in line with T_2 and S_1, T_3 and S_1, T_4 and S_1 when the disc has moved through $\pi/4$, $\pi/2$ and $3\pi/4$ respectively. Suppose the light from each source is able to radiate to all photo-transistors. If source S_1 only is active, the signals from the photo-transistors have a mutual phase displacement of $\pi/4$, as in Table 5.5.

θ_e	Transistors in Line with X (Active Source)			
	S_1	S_2	S_3	S_4
0	T_1	-	-	-
$\pi/4$	T_2	T_1	-	-
$\pi/2$	T_3	T_2	T_1	-
$3\pi/4$	T_4	T_3	T_2	T_1
π	-	T_4	T_3	T_2
$5\pi/4$	-	-	T_4	T_3
$3\pi/2$	-	-	-	T_4

Table 5.5

The signals are effectively shifted by $\frac{\pi}{4}$ using source S_3 and by $\frac{3\pi}{4}$ using source S_4 giving, in this case four phase angles. For any single active source S the phase of any transistor signal T is given by the mean electrical angular displacement of S and T from the reference position. The number of phase angles is determined by the number of sources and the width of the slot can be used to determine pulse width.

The edge of the slot should be machined radially since the transistors and sources are placed on an arc and not in a straight line. Clearly there are problems if this arc is large and, in its present form, the method is best suited to machines with a large number of poles.

The number of sources, and hence the number of phase angles is limited by physical constraints. In describing this method an accurately positioned point source was assumed, and errors could arise if this were not so. Using light emitting diodes (LED's) of small size (typically 1/16" diameter) this is a reasonable assumption and simplifies any problems with close-packing of sources. When used with inverter driving circuits the fast response of the LED eliminates the commutation problems which could otherwise arise due to lamp filament 'after glow' when changing phase angles. At present LED's are not the most economical light source, but the use of solid state devices is generally preferable in systems of this type where high reliability is desirable.

The optical characteristics of the photo-transistors and sources must be carefully matched to ensure that signals can be obtained from all transistors for every phase angle.

The signals at the photo-transistors would normally require amplification to levels suitable for either subsequent logic or the driving circuit. It would be more economical to use low power LED's, but the presence of noise can be a problem if low light levels are used. Various experimental arrangements have been tested in which the diodes have been pulsed. Such systems, using modulated light, need not be affected by wide changes in ambient light levels. A disadvantage however is that, for a given peak optical signal, the pulse frequency is limited by the rating of the diode, and this limits the response of the demodulated signal.

It is simpler not to pulse the diodes and the problem of obtaining suitable light levels at the transistors may be overcome by other means, without using 'high' power LED's. The problem is basically one of light utilisation. When wide optical angles are used, only a small part of the emitted light is used. The use of fibre optics could therefore provide a solution.

5.4.3 Systems Using Photo-thyristors

An important feature of the above optical method is that a single device could be used both to detect levels and be part of the driving circuit. If this is a photo-transistor the low power handling capabilities limit their use in this manner to very small machines.

Power-photo-transistors do not appear to be available and light-activated switches or other similar devices are unsuitable. However, if a photo-thyristor is used the reduction in the amount of hardware is such that it would often be feasible to mount all the components along with the disc inside an extended motor enshield. As an example, Fig.5.14 shows a McMurray-Bedford type of inverter and a bifilar wound stepping motor. The complete phase angle control system could be regarded as a single module. Protected from stray light and dust, with a minimum of circuitry, it would be well suited to an industrial environment and require little maintenance.

5.4.4 Combining Optical and Electronic Methods

By combining the optical and electronic methods, a wide choice of phase angles can be obtained with a reasonably simple system.

Suppose that the optical method could be used to give a choice of n phase angles and that the electronic method, when used separately, gives a choice of m phase angles. When combined, these methods can give a choice of up to nxm phase angles. The 'combined methods' is therefore considerably more effective than either method used separately.

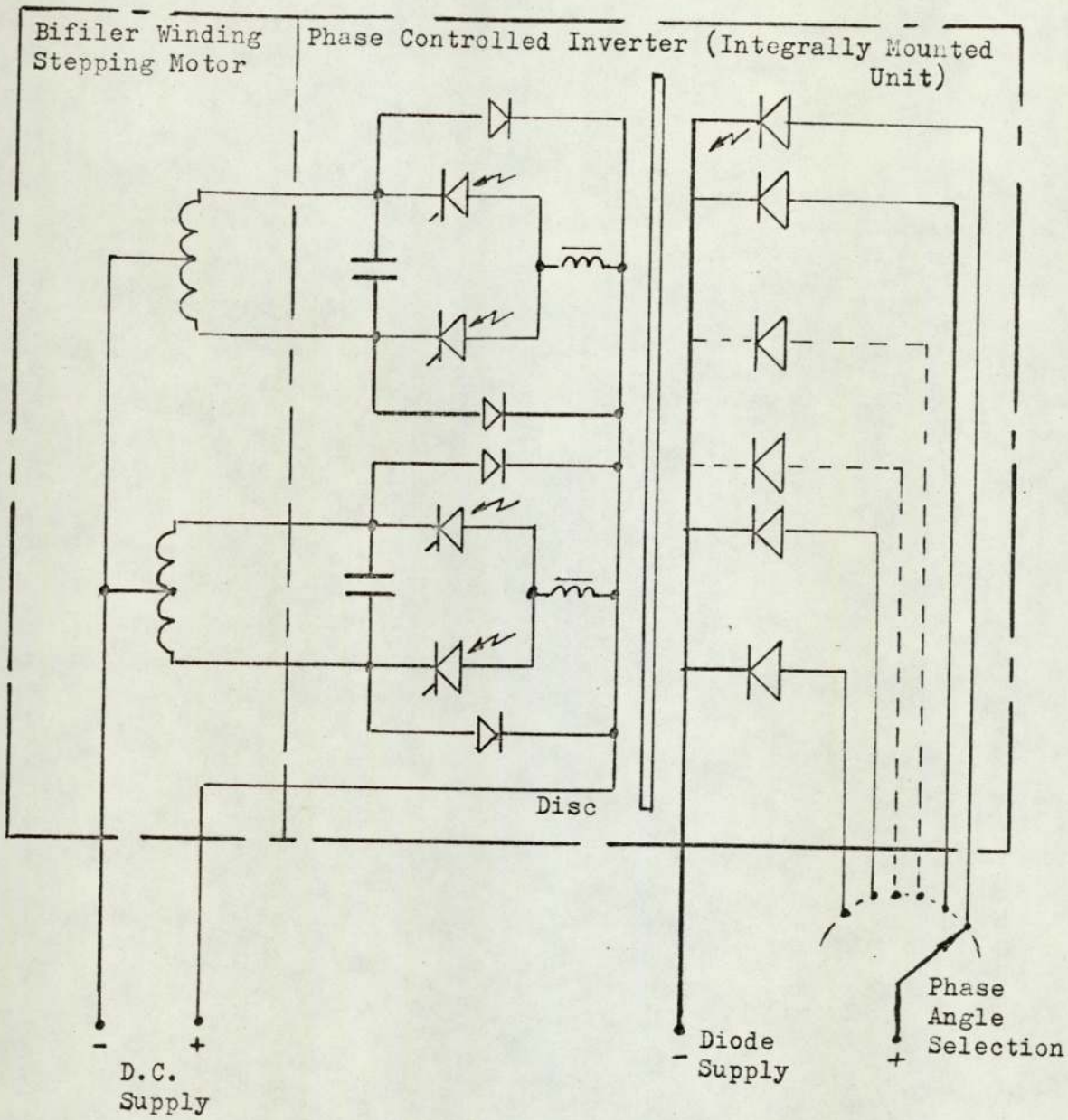

Fig.5.14 Modular Approach to Phase Angle Controlled Stepping Motor.

As an example, consider the combined method applied to the inverter circuit of Fig.5.3. 'E' is given in terms of the thyristor gate signals by Table 5.6.

With four position signals, as shown in Fig.5.15 eight phase angles are possible using logic.

G_1	G_2	G_3	G_4	E
0	0	0	0	0
0	0	X	X	0
X	X	0	0	0
1	0	0	1	1
0	1	1	0	-1

X = either state

Table 5.6

When the inverter was described, the driving signals used were,

$$D_1 = G_1 = G_4 \quad \ldots\ldots (5\text{-}72)$$

$$D_2 = G_2 = G_3 \quad \ldots\ldots (5\text{-}73)$$

For a pulse width of $3\pi/4$ in E the driving signals would have the form shown in Fig.5.16(a), but this is not the only way of producing the desired form of E. An alternative is to use the position signals, without processing, and to define,

$$D_1 = G_1 = \overline{G_3} \quad \ldots\ldots (5\text{-}74)$$

$$D_2 = G_2 = \overline{G_4} \quad \ldots\ldots (5\text{-}75)$$

Reference to Fig.5.16 and Table 5.6 will show that this alternative produces the same result. Table 5.7 shows the driving signal functions for both cases.

γ (steps)		$D_1 = G_1 = G_4$ $D_2 = G_2 = G_3$				$D_1 = G_1 = \overline{G_3}$ $D_2 = G_2 = \overline{G_4}$				γ BINARY		
		D_{a_1}	D_{a_2}	D_{b_1}	D_{b_2}	D_{a_1}	D_{a_2}	D_{b_1}	D_{b_2}	U	V	W
$-3\pi/4$	(-3)	$\overline{P_2}\ \overline{P_3}$	$P_2\ P_3$	$\overline{P_4}\ P_1$	$P_4\ \overline{P_1}$	$\overline{P_3}$	P_2	P_1	P_4	1	0	1
$-\pi/2$	(-2)	$\overline{P_3}\ \overline{P_4}$	$P_3\ P_4$	$P_1\ P_2$	$\overline{P_1}\ \overline{P_2}$	$\overline{P_4}$	P_3	P_2	$\overline{P_1}$	1	1	0
$-\pi/4$	(-1)	$\overline{P_4}\ P_1$	$P_4\ \overline{P_1}$	$P_2\ P_3$	$\overline{P_2}\ \overline{P_3}$	P_1	P_4	P_3	$\overline{P_2}$	1	1	1
0	(0)	$P_1\ P_2$	$\overline{P_1}\ \overline{P_2}$	$P_3\ P_4$	$\overline{P_3}\ \overline{P_4}$	P_2	$\overline{P_1}$	P_4	$\overline{P_3}$	0	0	0
$\pi/4$	(1)	$P_2\ P_3$	$\overline{P_2}\ \overline{P_3}$	$P_4\ \overline{P_1}$	$\overline{P_4}\ P_1$	P_3	$\overline{P_2}$	$\overline{P_1}$	$\overline{P_4}$	0	0	1
$\pi/2$	(2)	$P_3\ P_4$	$\overline{P_3}\ \overline{P_4}$	$\overline{P_1}\ \overline{P_2}$	$P_1\ P_2$	P_4	$\overline{P_3}$	$\overline{P_2}$	P_1	0	1	0
$3\pi/4$	(3)	$P_4\ \overline{P_1}$	$\overline{P_4}\ P_1$	$\overline{P_2}\ \overline{P_3}$	$P_2\ P_3$	$\overline{P_1}$	$\overline{P_4}$	$\overline{P_3}$	P_2	0	1	1
π	(4)	$\overline{P_1}\ P_2$	$P_1\ P_2$	$\overline{P_3}\ \overline{P_4}$	$P_3\ P_4$	$\overline{P_2}$	P_1	$\overline{P_4}$	P_3	1	0	0

Table 5.7.

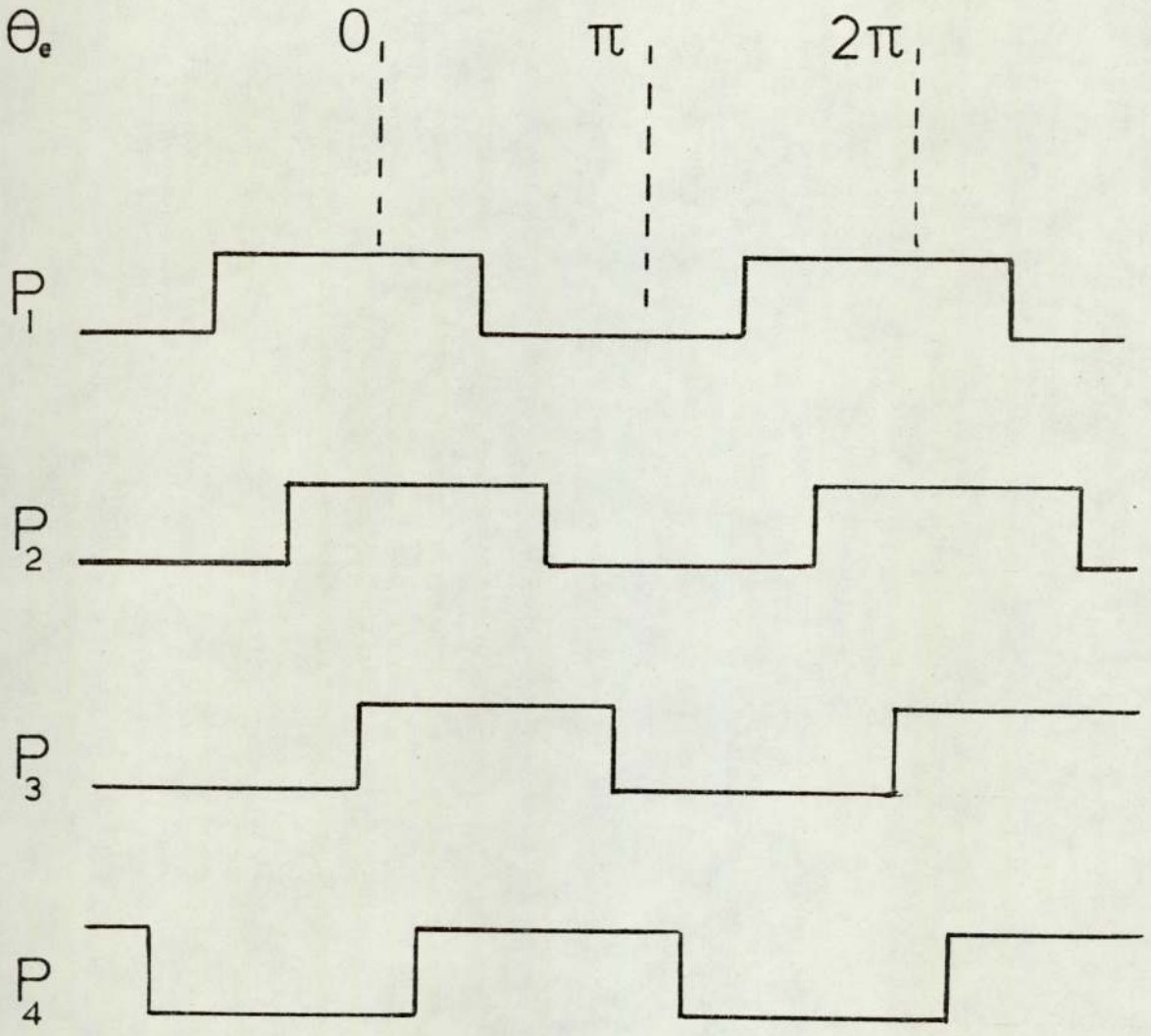

Fig.5.15 Position Signals for Combined Method.

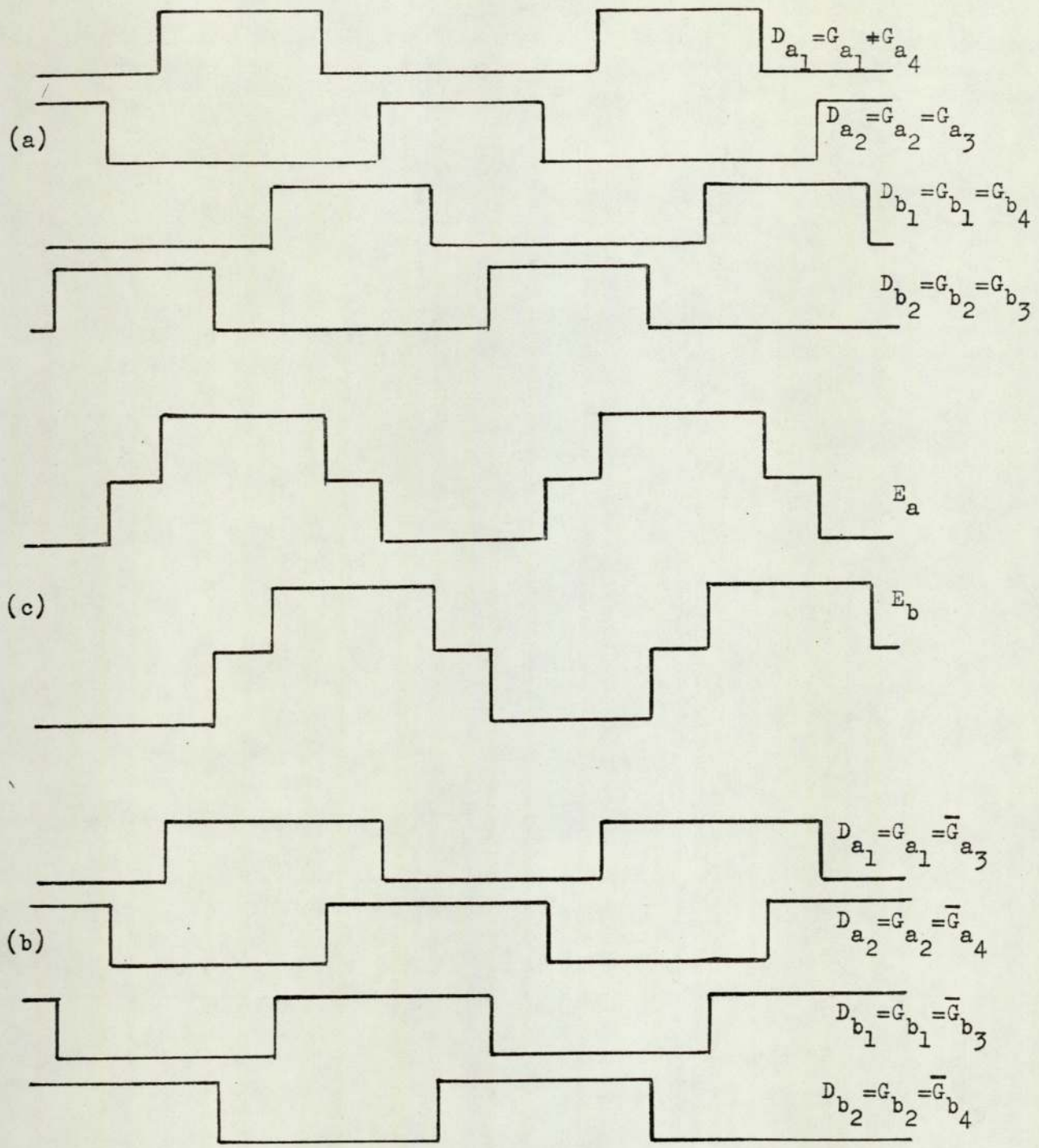

Fig.5.16 Alternative Driving Sequences (a) and (b) Producing same Energisation Sequence (c).

If U V W represent the electronically selected phase angle, then driving signals can be expressed as,

$$D_{a_1} = P_2 \bar{U}\bar{V}\bar{W} + P_3 \bar{U}\bar{V}W + P_4 \bar{U}V\bar{W} + \overline{P_1}\ \bar{U}VW$$

$$+ \overline{P_2}\ \bar{U}\bar{V}\bar{W} + \overline{P_3}\ \bar{U}\bar{V}W + \overline{P_4}\ UV\bar{W} + P_1\ UVW \qquad \ldots\ldots\ (5\text{-}76)$$

and similarly for D_{a_2}, D_{b_1} and D_{b_2}.

These functions are readily generated using MSI data selectors.

The position signals can be obtained using the optical method with four photo-transistors spaced as in Fig.5.13, and a single LED would give the above choice of eight phase angles.

A further diode placed at an angle 2δ from the previous diode would give a further eight phase angles, displaced from those above by the angle δ.

Using eight diodes spaced $\pi/16$ apart a full range of 64 phase angles can be obtained in increments of $\pi/32$. If that part of the phase angle which is obtained optically is represented by bits XYZ, then it is required that diodes 0 to 7 be selected according to the binary value of XYZ. This is readily achieved using MSI with a unit such as a 2-line to 4-line decoder connected to give "1 of 8" selection as shown in Fig.5.17.

Therefore using only five integrated circuits a choice of 64 phase angles is available by the setting of a six bit word at the interface.

5.5 CONCLUSIONS

The use of the thyristor as a driving circuit element has been discussed with reference to the probable development of power stepping motors. Some basic inverter circuits have been reviewed and their limitations for this application explained. A cyclo-inverter circuit that was developed for a closed loop stepping motor control

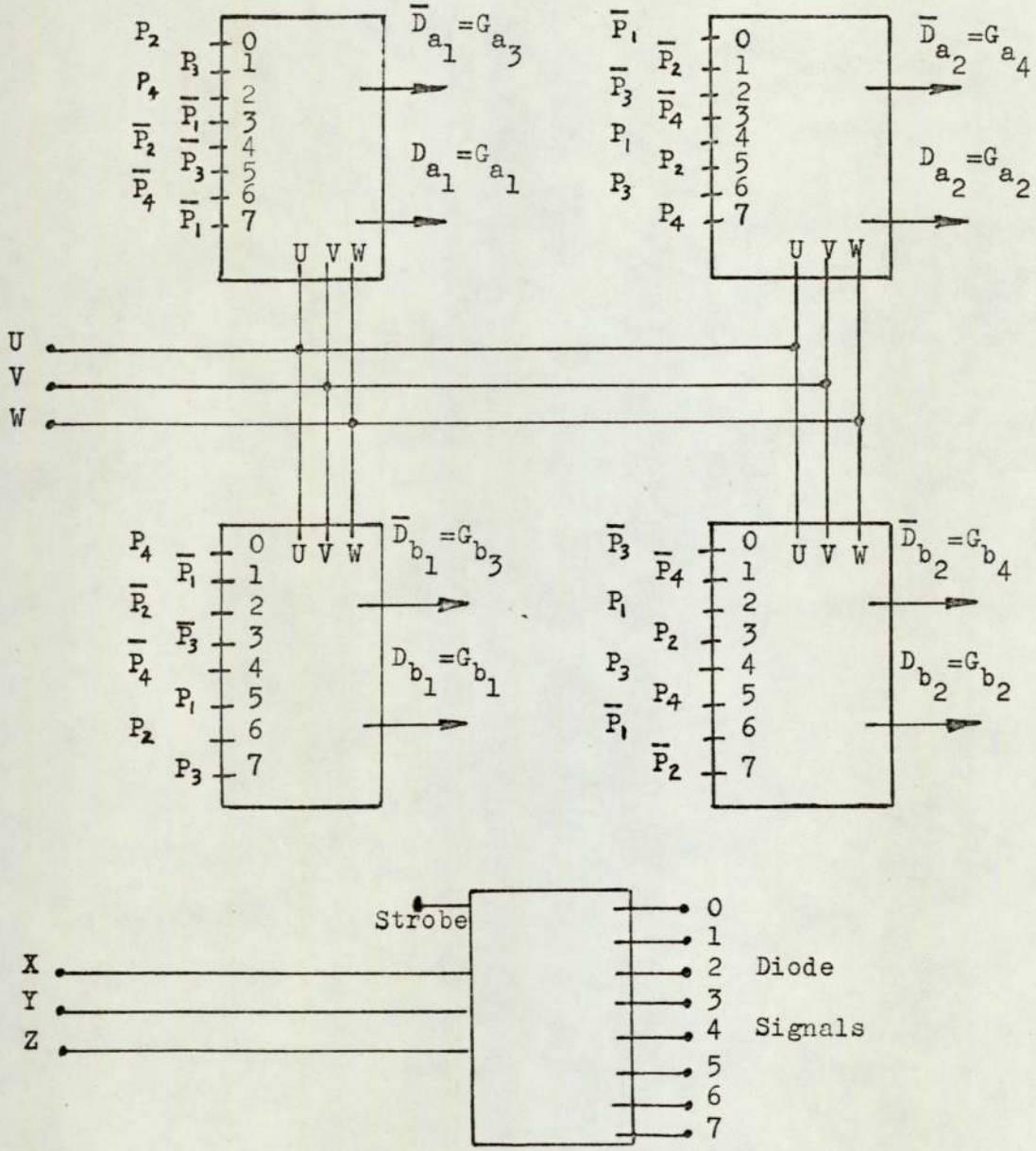

Fig.5.17 Phase Angle Control Circuit Using MSI.

system has also been described. The technique of phase angle control has been reviewed and a digital method of accurate phase control presented.

The above method of phase control was used with the inverter drive described in Section 5.3. The relevant optimum conditions are therefore derived in Section 3.3.3, but with θ_{wo} kept constant at 135^{o} as shown in fig.5.16(c) (compare with fig.3.3) This is convenient to achieve in practice and is very near the value of 133^{o} which was found to minimise P_{cu} as shown in equation (3-126) and to minimise P_{Fe} at high frequencies as shown in equation (3-131).

The closed-loop drive formed part of the computer controlled system described in the following section.

6. A COMPUTER CONTROLLED STEPPING MOTOR DRIVE SYSTEM.

6.1 INTRODUCTION

To obtain optimum performance it is essential that a closed loop stepping motor drive, such as that described in the previous Section, be effectively controlled by maintaining the correct phase angle and level of drive forcing at all times. In order to compute these it is necessary to determine shaft position, velocity and possibly torque or even winding temperature.

One of the duties of the controller is to estimate the time at which the transition from acceleration to deceleration should be made and to generate a 'directing signal' giving the demanded directions.

The controller is likely to take one, or both, of two forms:-

i) A small special purpose computer (i.e. 'wired logic circuits') or ii) If it is convenient to access a larger general purpose computer, this may be used on a time sharing basis. (i) is essentially a hardware approach, whilst (ii) requires software.

Although all the controllers duties may be carried out on a time shared general purpose computer, some of the operations can also be done by a certain amount of logic at a more local level, thus leaving the central processor free for more important duties.

The relative proportioning of the control function between central and local levels depends upon the relative cost of the hardware involved and upon the value of c.p.u time and will vary from one application to another. It is generally easier to estimate the cost of performing operations at a central level, than at a local level, once the number of required computations are realised. Thus, in order to decide upon the optimum configuration it is necessary for the user to be aware of, and to closely consider, operations that can be carried out locally without undesirable complexity.

The 'minor loop' function of deriving the driving signals from the encoder signals is simple to implement locally, as previously described in Section 5.4, at a cost that is probably less than the cost of linking these signals to a computer. It is therefore very unlikely that this will be performed at other than a local level, whatever the cost of c.p.u. time.

The task of keeping a record of position is also unlikely to be suitably assigned to a central control, since it would demand close monitoring and would require some c.p.u. time at each step change.

The operation of deriving phase angle and current level signals, in terms of the measured variables and the 'directing signal' is not generally suited to the local level of control. An exception to this is the case of a simple function derived from only one variable such as velocity[36].

The generation of the directing signal is an operation which can be carried out completely at the local level of control if a single approximate switching boundary is acceptable. Although this would be inadequate where wide changes in the load characteristics are present. In the system to be described, which is shown in Fig.6.1 the switching boundary may either be generated locally or from the central controller. When generated locally the characteristics of the switching boundary may be changed by the central controller as required. This gives a flexible system requiring a minimum of c.p.u. time and allowing adaptive features to be incorporated.

6.2 MEASUREMENT OF SYSTEM VARIABLES

6.2.1 Measurement of Position

The method of using the position signals from the optical encoder has been described in chapter 5.4. These signals alone do not uniquely define the position of the shaft. Further logic circuitry is

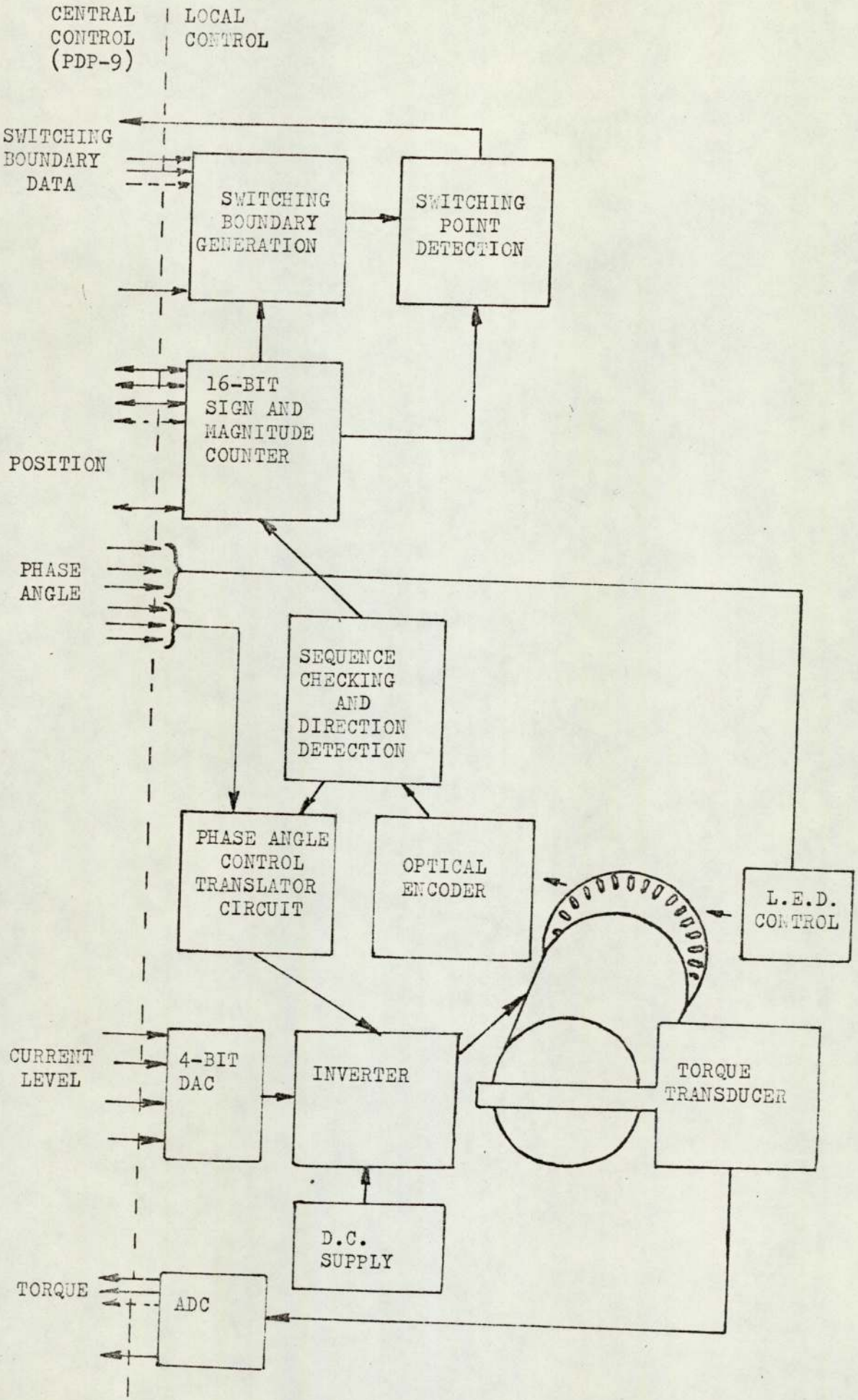

Fig.6.1 Block diagram of computer control system.

required to detect the direction and magnitude of shaft movement and to provide the necessary memory, in the form of a counter, to record the angular displacement relative to some given datum.

It is essential that the counter circuit is not affected by the presence of noise on the encoder signals. It is also desirable that the signals to the inverter, derived from the encoder, are free of noise. The circuit shown in Fig.6.2(b) using line drivers was finally adopted since this was found to give good noise rejection. Some hysteresis can be built into the encoder to take away much of the noise present when a change in light level occurs at the photo-transistors, and noise from the power circuit can be further reduced by suitable screening, but these methods are insufficient to guarantee reliability.

To measure position reliably, it is essential to check that the set of signals from the encoder are not only a 'legal' set but that they are the next in sequence to the previously accepted 'legal' set of signals. For each accepted set of signals it must also be determined whether it is the next legal set in a forward sequence or the next legal set in a reverse sequence, and the counter must be updated accordingly. Safegards must also be taken against the signals changing state during the short time between the stages of checking and acceptance.

The method shown in Fig.6.2(a) was devised to achieve these aims. Incoming signals PH1, PH2, PH3, PH4 derived from the photo-transistors are sampled and held on the latch L1 which is operated by phase 1 of a two phase clock at a relatively high frequency (100kHz in this case). The latched signals PL1, PL2, PL3, PL4 are then compared with the signals already stored on the second latch L2.

Legal sets of latched signals, according to the contents of latch L2, are shown in Table 6.1.

The sequences of legal sets are not only cyclic but each set is

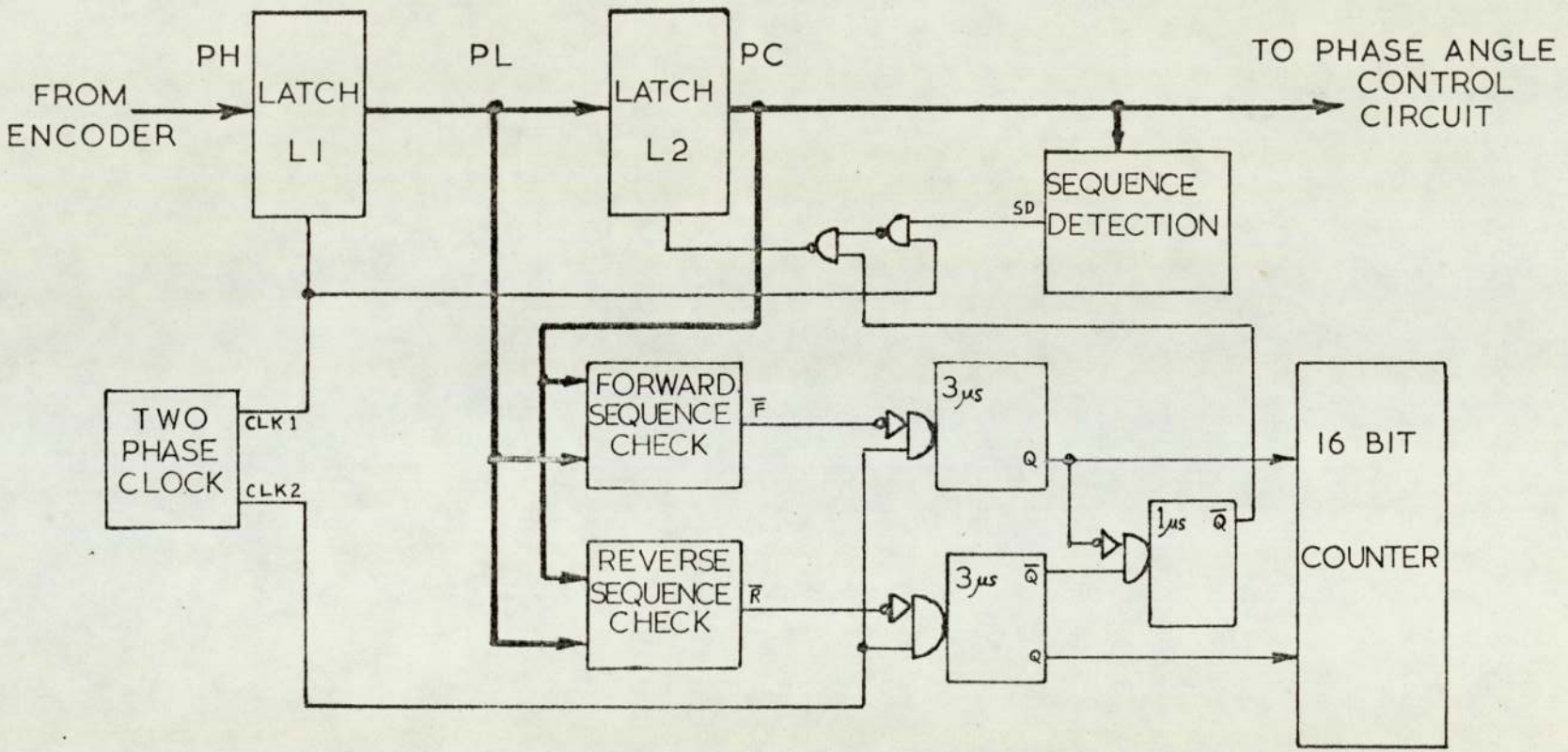

Fig.6.2(a) Position Measuring System

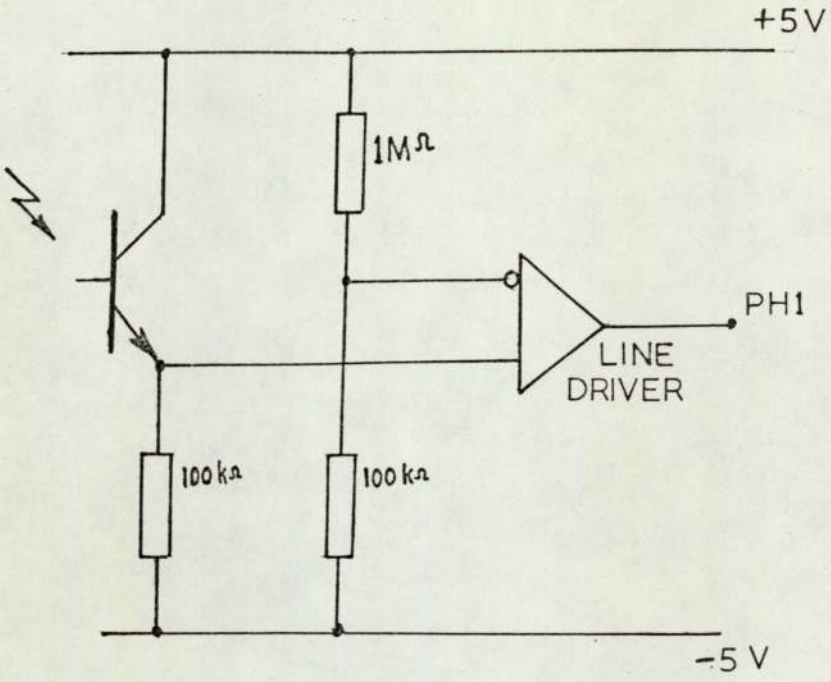

Fig.6.2(b) Optical encoder circuit (per photo-transistor) using line driver.

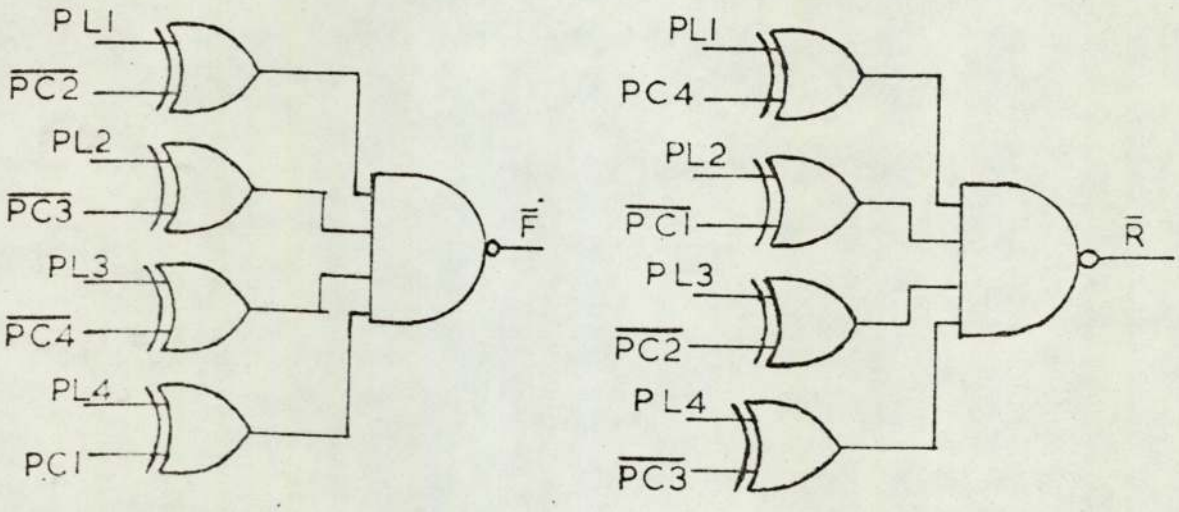

Fig.6.3 Forward and reverse sequence checking logic.

	CONTENTS OF LATCH L1	
CONTENTS OF LATCH L2	LEGAL SETS IN FORWARD SEQUENCE (F = 1)	LEGAL SETS IN REVERSE SEQUENCE (R = 1)
0 0 0 0	0 0 0 1	1 0 0 0
0 0 0 1	0 0 1 1	0 0 0 0
0 0 1 1	0 1 1 1	0 0 0 1
0 1 1 1	1 1 1 1	0 0 1 1
1 1 1 1	1 1 1 0	0 1 1 1
1 1 1 0	1 1 0 0	1 1 1 1
1 1 0 0	1 0 0 0	1 1 1 0
1 0 0 0	0 0 0 0	1 1 0 0

Table 6.1 LEGAL SETS OF LATCHED SIGNALS ACCORDING TO THE CONTENTS OF LATCH L2.

easily related to the next set in the sequence. The sequence checking logic is therefore very simple and is shown in Fig.6.3. Referring to Table 6.1, the signals PL are the next legal sets in a forward sequence (F = 1) if,

$$(PL1 \oplus PC2) + (PL2 \oplus PC3) + (PL3 \oplus PC4) + (PL4 \oplus \overline{PC1}) = 0 = \overline{F} \quad .... \quad (6\text{-}1)$$

and if the signals PL are the next legal set in a reverse sequence (R = 1) then,

$$(PL1 \oplus \overline{PC4}) + (PL2 \oplus PC1) + (PL3 \oplus PC2) + (PL4 \oplus PC3) = 0 = \overline{R} \quad .... \quad (6\text{-}2)$$

The signals $\overline{F}$ and $\overline{R}$ can also be expressed as

$$\overline{F} = \overline{(PL1 \oplus \overline{PC2})(PL2 \oplus \overline{PC3})(PL3 \oplus \overline{PC4})(PL4 \oplus PC1)} \quad .... \quad (6\text{-}3)$$

and

$$\overline{R} = \overline{(PL1 \oplus PC4)\ (PL2 \oplus \overline{PC1})(PL3 \oplus \overline{PC2})(PL4 \oplus \overline{PC3})} \quad .... \quad (6\text{-}4)$$

If F = 1 or R = 1 when a pulse occurs on phase 2 of the two phase clock an outgoing pulse is generated from a monostable on either the 'up' or 'down' lines to the counter, respectively. A pulse on either of these lines then causes a further pulse to be generated, operating the latch L2.

Data, checked and accepted, on latch L2 will now be the same as that on latch L1, setting F = 0 and R = 0 until a pulse from phase 1 of the clock causes a new set of data to appear at latch L1 and this is checked with the new contents of latch L2, and so on. Once latch L2 contains one of the legal sets of signals shown in Table 6.1 only adjacent sets in the series will be accepted as shown in the Karnaugh map in Fig.6.4. Such a system has a very high immunity to noise on the incoming signals.

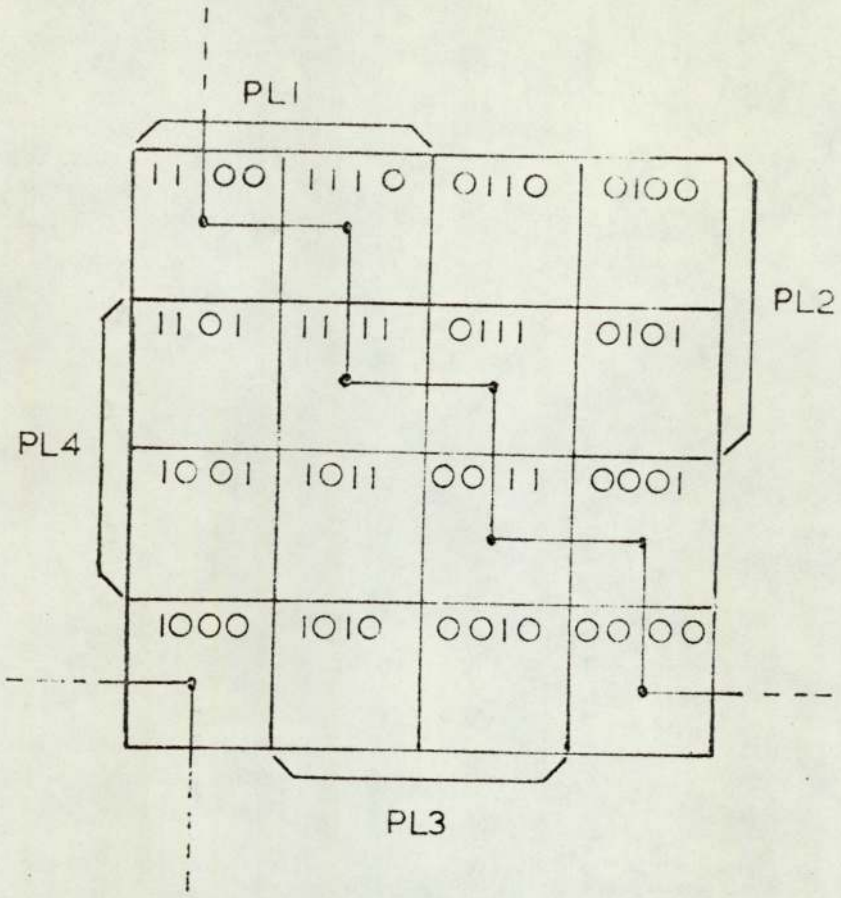

Fig.6.4 Karnaugh map showing legal sequence.

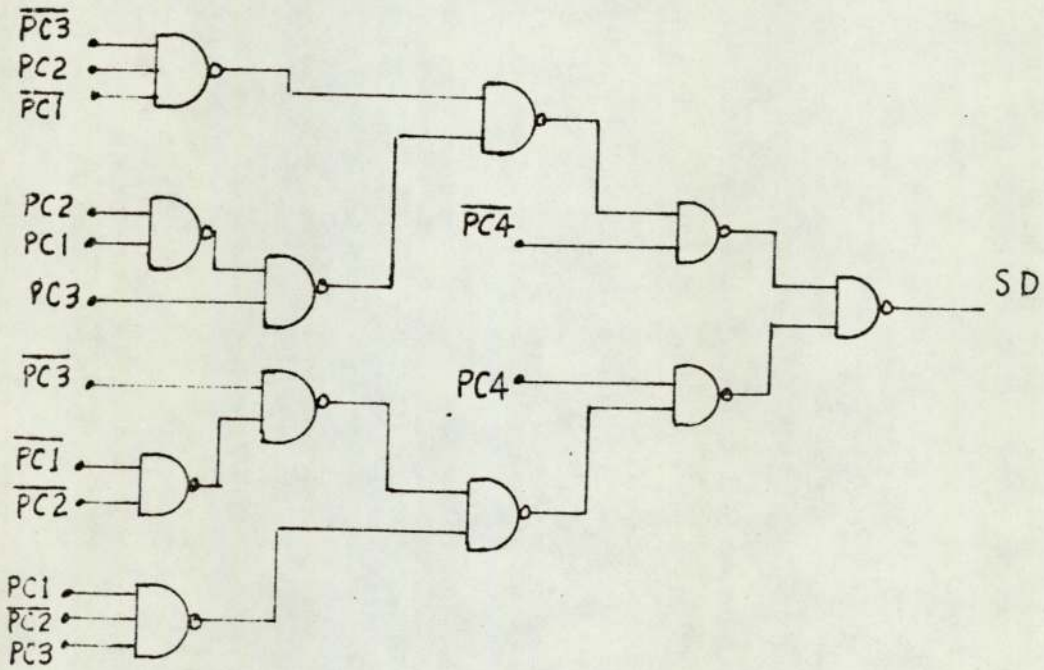

Fig.6.5 Sequence detection logic.

It is necessary that the initial contents of latch L2, when the apparatus is first switched on, is the same as the set of signals at latch L1, and that these are legal, before setting the counter to give the reference position.

If latch L2 ever contained any one of the eight illegal sets of signals then only further illegal signals, in a certain order, would be accepted. This is because the eight illegal sets when considered in a particular order give a closed sequence which can be 'passed through' the latches when checked by the logic using equations (6-1) to (6-4). Thus the logic accepts two sequences (covering all 16 states)

i) The legal sequence, given by any one of the columns in Table 1.

ii) The illegal sequence;-.... 0101, 1011, 0110, 1101, 1010, 0100, 1001, 0010, 0101 ....

The purpose of the sequence detection circuit shown in Fig.6.5 is to determine if latch L2 contains any one of the sets in the illegal sequence, and this is detected by the condition SD = 1, where,

$$SD = \overline{PC4}.(\overline{PC3}.\ PC2.\ \overline{PC1} + PC3(\overline{PC2} + \overline{PC1}))$$

$$+ PC4\ (\overline{PC3}\ (PC1 + PC2) + PC1.\ \overline{PC2}.\ PC3) \quad \ldots\ldots (6\text{-}5)$$

If SD = 1, then the following clock pulses from phase 1 of the clock operate both latches until the contents of latch L2 are legal.

Latch L2 could have been initialised manually and the sequence detection circuit should not be needed, but, its inclusion also safegards against the risk of a supply line transient changing the contents of latch L2 so as to lock the signals into the illegal sequence.

The circuit therefore only responds to legal sets of signals,

and only when in the correct sequence. If noise is present on the signals from a photo-transistor when a change in logic level takes place such as the series of samples

..... 0011, 0011, 0111, 0011, 0111, 0011, 0111, 0111 .....

then alternating 'up' and 'down' pulses are generated to the counter and cause the least significant bit to alternate but this finally settles at the correct level.

6.2.2 Measurement of Velocity

The most convenient methods of estimating shaft velocity is likely to make use of the positional information already available rather than to use a separate velocity transducer. There are two basic methods to determine velocity from the position signals;-

i) The position pulses are fed into a counter which is periodically reset. The contents of the counter immediately before resetting is proportional to the velocity. The constant of proportionality is the reset pulse frequency, which can be used as a scaling factor.

The disadvantage of this approach is that to obtain a high resolution requires a low reset pulse frequency and therefore the measurement has a slow response to changes in velocity. Consequently to obtain a faster response a reduction in resolution must be accepted.

ii) The time between successive position pulses can be determined. This can be done by feeding pulses from a high frequency clock into a counter and using the position pulses to reset the counter. The contents of the counter immediately before resetting is inversely proportional to the velocity.

The disadvantage of this method is that it is not simple to

obtain the reciprocal of the counter contents without using the c.p.u.

Resolution and speed of response however can be much higher than is possible with the previous method and is limited only by the frequency of the h.f. clock and capacity of the counter. The response time is that of the time between consecutive position pulses.

In the system to be described it was not necessary to measure velocity directly in order to generate the switching function.

6.2.3 Measurement of Torque.

Various methods of torque measurement are available but for control applications those methods that are restricted to the measurement of static torque are unsuitable. Dynamometer methods which introduce and measure a load on the machine are also unsuitable. Two ways of obtaining the torque developed by the motor are,

i) By mounting a transducer on the shaft or coupling.

This has the disadvantage of requiring slip rings or other means of transmitting the transducer signal.

ii) By cradle mounting the motor and measuring the reaction torque transmitted from the motor frame.

This would generally be the more convenient method.

Ideally measurements should be of the 'instantaneous' developed torque, requiring a transducer with a very fast response. For a step change in torque the transducer output should have a rise time of a millisecond or so. Four types of transducers to be considered are,

(i) Wire Strain Gauges. The response of a spring loaded linear variable displacement transducer is limited to frequencies that are much less than the natural frequency determined by spring stiffness and motor mass. Alternatively, wire strain gauges mounted in a load cell or load ring have responses which are typically limited to 100Hz or so.

(ii) Piezo-Electric Transducers have a very wide response, typically up to 20kHz. Unfortunately this does not include d.c. and therefore they are only suitable for transient torque measurement. To obtain instantaneous torques this transducer would have to be used in conjunction with another transducer giving steady state torques; a combined method would present some difficulties.

(iii) Piezo-Resistive transducers have a reasonably wide response, including d.c. and they were used for the torque measuring system to be described.

Fig.6.6 shows the type of piezo-resistive transducer used. They are commonly called 'pixies'[37] and are constructed of p-type silicon mounted on a substrate which simultaneously provides mechanical clamping and electrical connections. The maximum force 'F' shown in Fig.6.6 should be about 10 gm. and within this range the linearity is within 1%. A proof force of 40 gms. gives a generous overload capability compared to conventional wire strain gauges.

The compliance of the device is about 1.4 μm/gm at F so that if forces greater than 10 gm are involved the pixie must be mounted so that the movement of the substrate is about 14 μm, which is equivalent to a force of 10 gm directly applied to the substrate at 'F'. An example of this is shown in Fig.6.7 where two pixies are clamped either side of a beam, using printed circuit board for electrical connections. The non-clamped ends of the pixies are fixed to the beam using an epoxy resin.

Various schemes using this principle were tried with the beam either being rigidly fixed to, or forming the shaft torque bar. Great care must be exercised when mounting pixies. The flatness is not controlled to a close tolerance during manufacture and it is advisable to select those devices with a curvature which will not cause breakage by clamping. The gauges form two arms of a bridge circuit and when

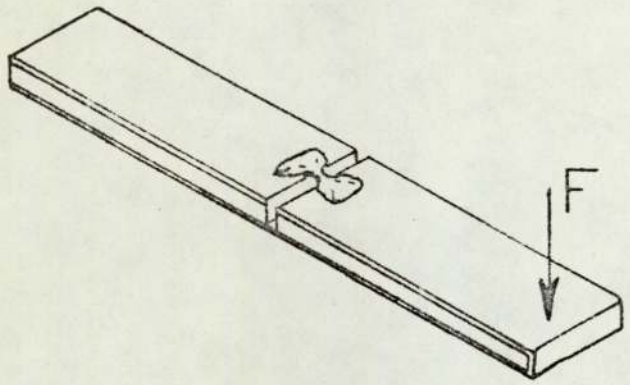

Fig.6.6 A 'Pixie' piezo-resistive transducer.

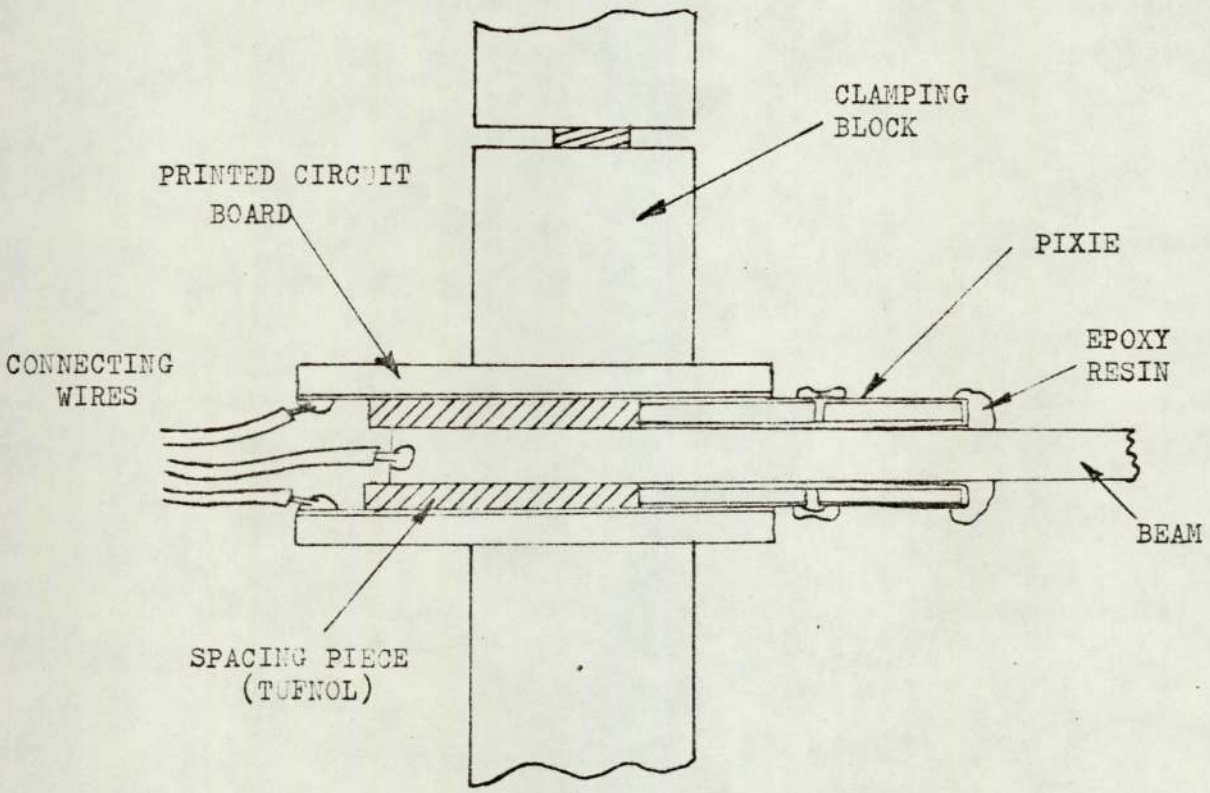

Fig.6.7 Possible transducer mounting arrangement.

one gauge is in tension the other is compressed, and visa-versa. Sensitivity was about 0.14 Ω/Ω for a full substrate movement of 14 μm.

The main limitations of these schemes were,

(i) The presence of resonance due to the natural frequencies of the mechanical structure.

(ii) Signals were obtained from the bridge when other forces/ movements occurred in almost any part of the mounting or adjacent structure.

These effects interact and the bridge output signal resulting from a step change in shaft torque becomes very complex to analyse.

The presence of resonances is unavoidable and to obtain a wide frequency response the natural frequencies must be designed to be as high as possible and electrical filtering used to minimise their effect. The resonant frequency of the substrate is about 6kHz but it is the mounting which determines the overall characteristics of the transducer output. If low natural frequencies are to be avoided a very rigid mechanical structure must be used. This means a reduction in sensitivity since there will be less movement for a given torque. The problem then becomes a compromise between a high rigidity and an output of a measurable level above that of any noise present.

The inherent thermal noise from the transducers is approximately 4 μVr.m.s. over the range 300Hz to 5kHz and this would normally set a lower limit for the sensitivity of about 100 μV/N-m. In view of the possible interference of electrical noise from other parts of the system screened leads are necessary and it is also advisable to raise the limit for minimum sensitivity to at least 1 mV/N-m.

Even at this level small variations in ambient temperature of 2°C or so can cause a 1mV change in output unless some temperature compensation is used and this is most difficult with low sensitivities.

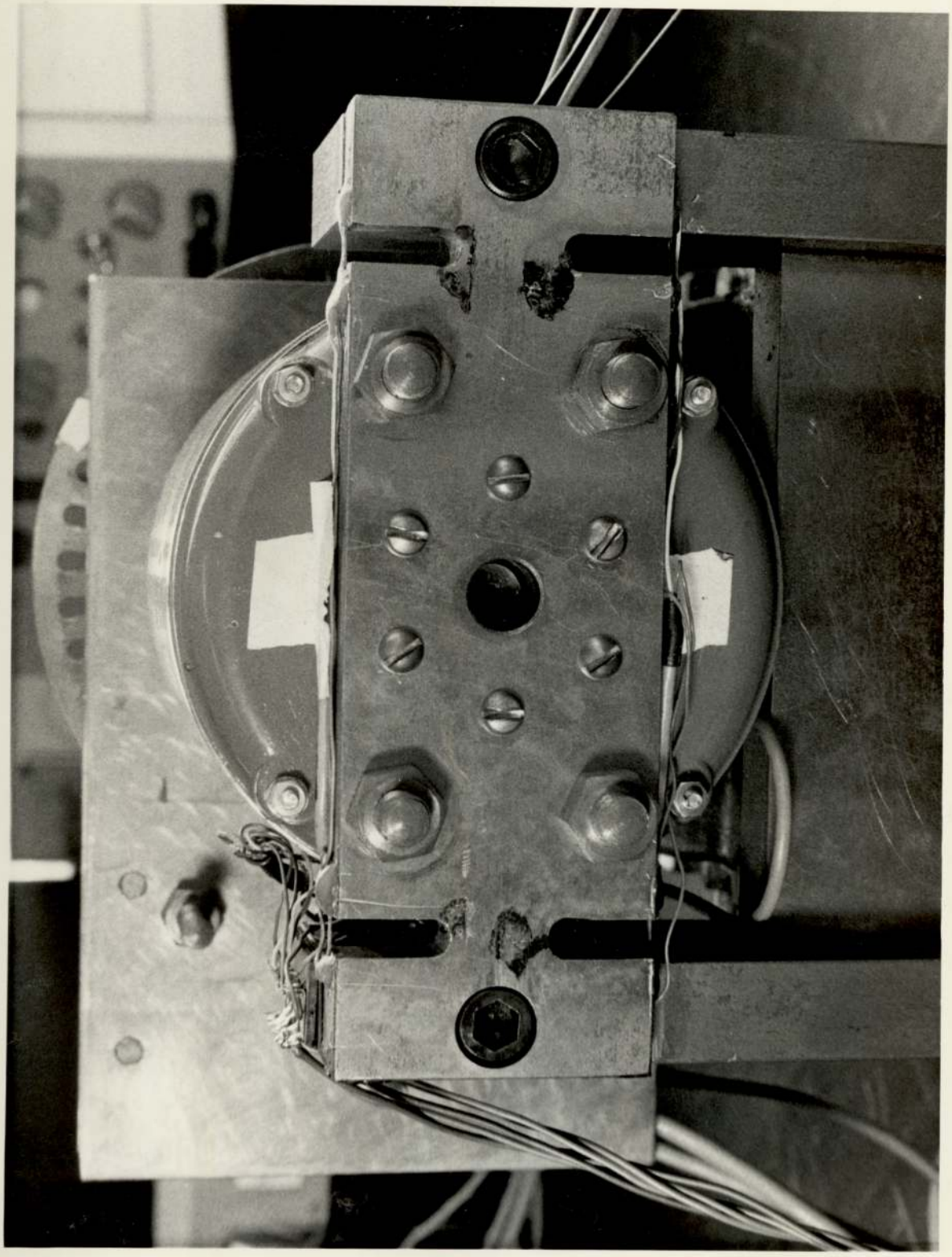

Fig.6.8 Photograph showing torque transducers.

A new arrangement, shown in Fig.6.8 largely overcame these limitations. One end of the motor was supported by bearings so that it was free to rotate whilst the other end of the motor was rigidly attached to a special torque bar which was supported at its ends and so limits perceivable rotation of the motor frame. The torque bar also supports the weight of the motor at this end, and on it were mounted four pixies in a bridge circuit.

By bonding each side of the pixies the main force applied to the pixie is along its length, instead of perpendicular to this, and a gain in sensitivity of greater than ten times can be achieved for the same movement. A lengthwise movement of 1 μm for one half of the pixie gauge, relative to the other half is equivalent to a movement of more than 10 μm at F in Fig.6.6.

Although pixies are not usually used in this way the only objection to this method seems to be that the input energy to the transducer needs to be far greater since the substrate must also be stressed. This is not a serious disadvantage in this application since the input energy required to stress the substrate is negligible in comparison to that required to stress the structure on which it is mounted.

Consider three mutually perpendicular forces acting separately as shown in Figs.6.9(i) to 6.9(iv). The resulting forces on the pixies is in every case such that no output is obtained from the bridge. In practice there is some output as a result of different sensitivities and unequal stressing of the individual gauges but thisis much smaller than with the earlier arrangements.

Likewise an external force acting upon the motor or the mounting framework, in any other direction will produce a similar result, since it can be resolved into these three components.

Now consider a turning movement about the axis of the motor as

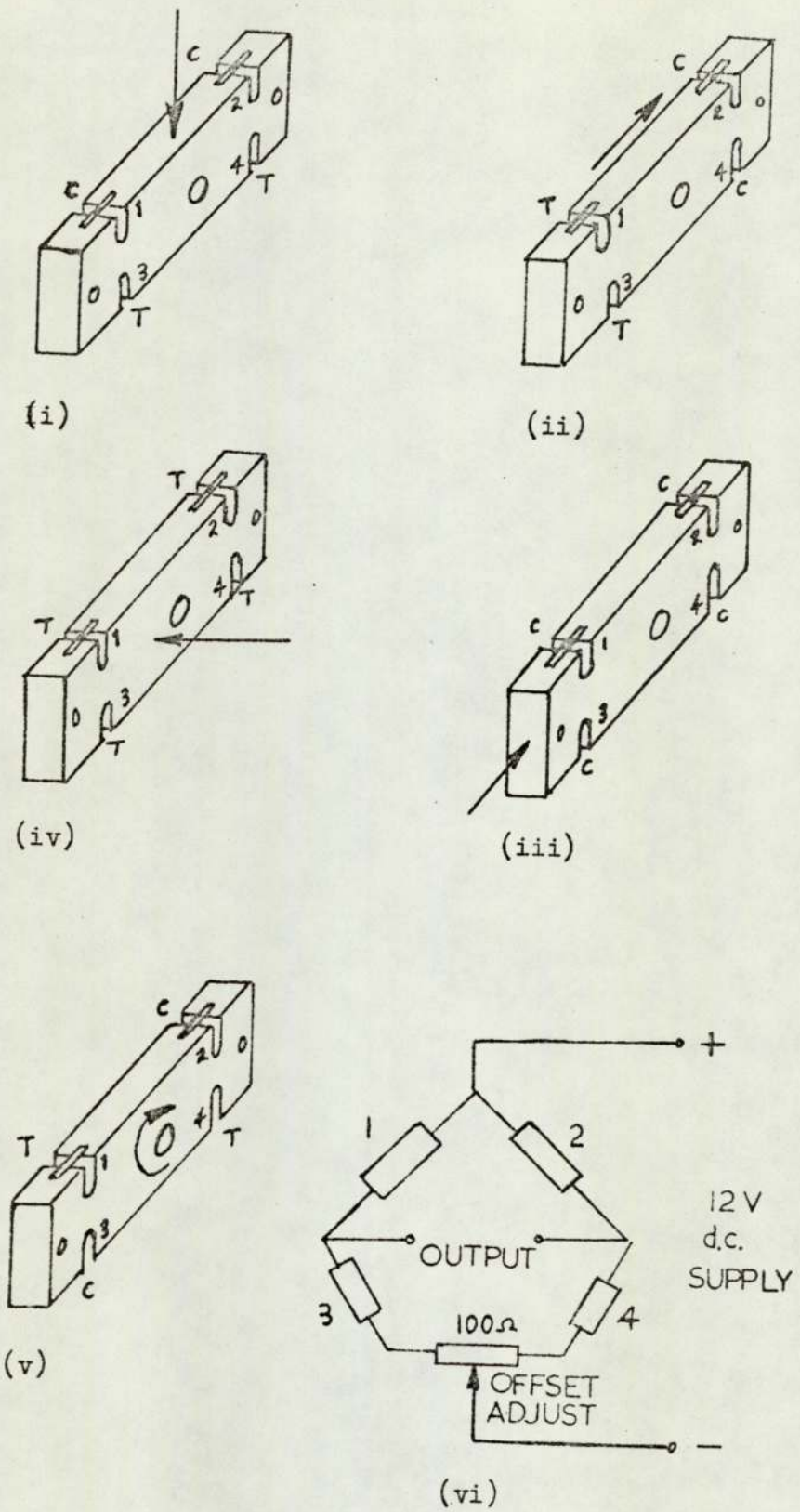

Fig.6.9 (i) to (v) Result of various forces on transducer mounting structure.

T = Tension C = Compression

(vi) Electrical arrangement of gauges.

shown in Fig.6.9(v). Gauges 1 and 4 will be in tension while gauges 2 and 3 will be in compression and this is the combination required to produce an output from the bridge circuit. The arrangement has a low sensitivity to all forces except those producing a turning moment about the motor shaft.

The response to a step in torque with a simple passive low pass filter is shown in Fig.6.10. To obtain the step in torque a weight was suspended by a single strand of cotton fastened to a stud on the motor frame. The stud was machined with a groove which was accurately positioned at a known distance (5 cm) from the axis of the shaft and was also used for calibration.

With the cotton at near-breaking strain, this eventually snapped and the bridge output was recorded on a storage oscilloscope. The rise time of about 1 ms was satisfactory and the sensitivity obtained was 71 mV/N-m. The range over which linearity is within 1% was up to about 3.5 N-m, which is far greater than the maximum motor torque. The maximum torque (equivalent to the movement produced by a proof force of 40 gms at F in Fig.6.6) is about 14 N-m, giving generous overload allowance.

The largest source of error was now due to creep and of the order of 10% when overloaded to 2.5 N-m for 10 minutes. A small error was also detectable due to changes in ambient light intensities, but this was easily overcome by surrounding the pixies by light shields as shown in Fig.6.11.

Otherwise accuracy was about 1% for torques up to 1 N-m and with moderate temperature variations of $\pm$ 5°C about 20° C. Due to the high sensitivity this was achieved without the need for temperature compensation.

(a)

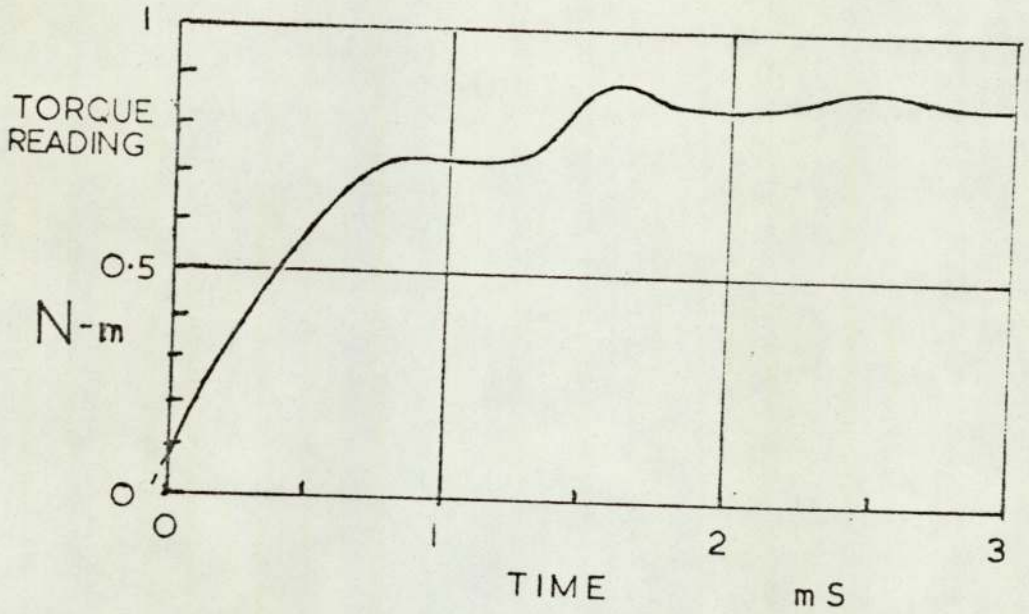

(b)

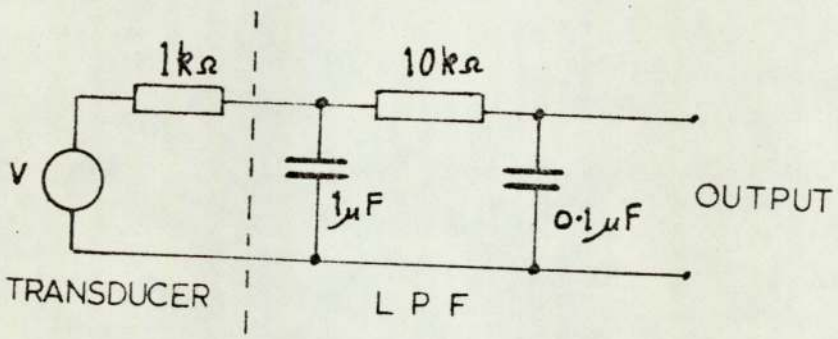

Fig.6.10 (a) Response to step in torque.
(b) Simple filter arrangement used.

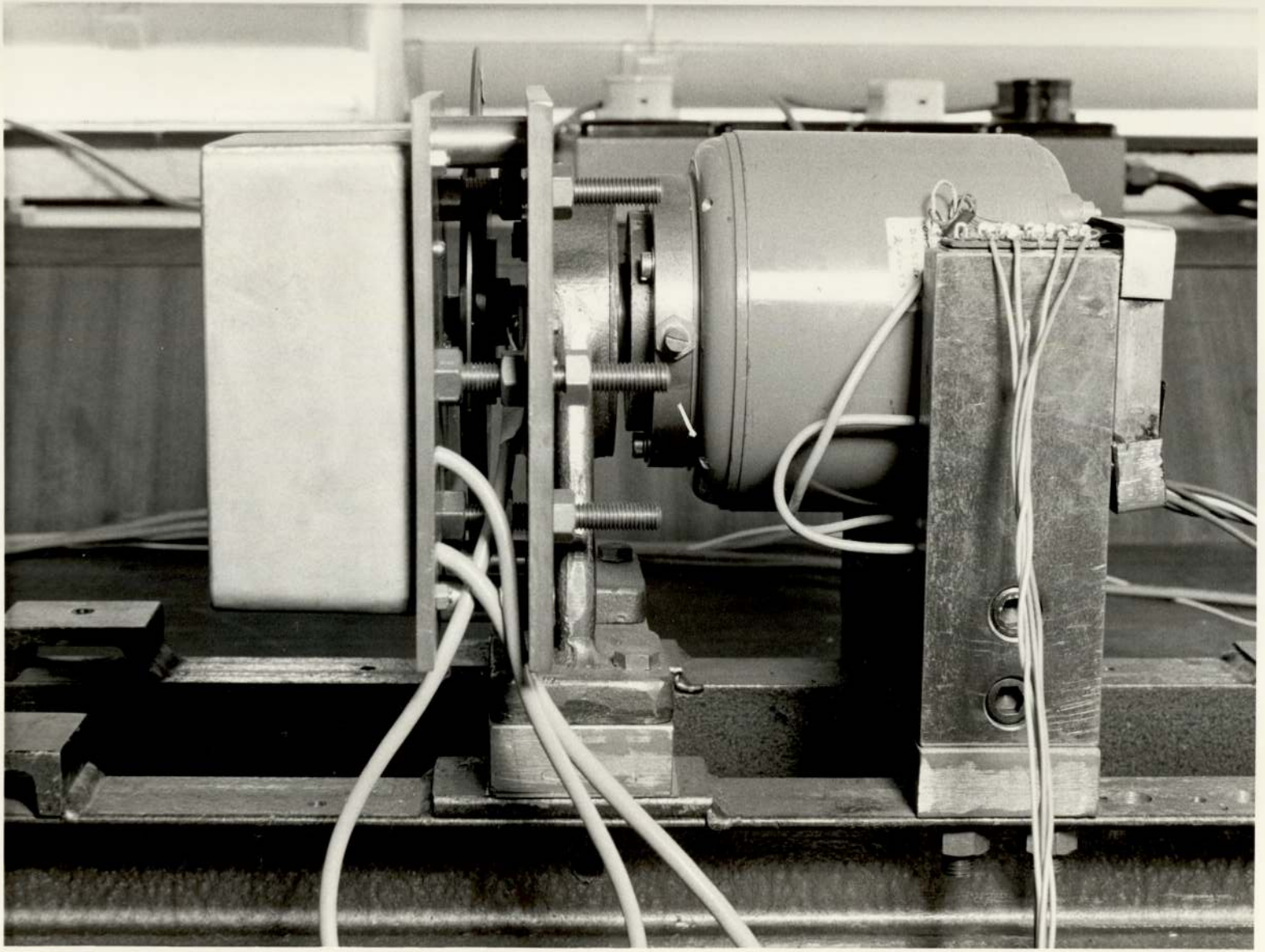

Fig.6.11 Side view of motor with torque transducer and optical transducer.

6.3 A DIGITAL SWITCHING FUNCTION GENERATOR.

6.3.1 Implementation of Optimal Switching.

The theory of optimal switching and of optimal control in general is far in advance of current practice and it is the development of methods for implementing the theory which is of concern here. It is assumed that some optimum driving function has already been derived and that this gives 'minimum time' conditions, i.e. time optimal control.

The optimal driving function will be derived from switching between two driving functions each derived from the state variables. One of these functions will produce maximum 'forward' torque giving maximum acceleration and the other function will produce maximum 'reverse' torque giving maximum deceleration.

We shall consider that the above switching strategy is to be adopted over the greater part of the slewing operation. When the final step position is closely approached, a slightly different strategy may be required to maintain the time optimal condition, though this largely depends upon how the acceptable final conditions are defined. If an exact formulation of the switching boundary is available, an approximation to this boundary may be most useful. This may be obtained either from practical results obtained by trial and error or from a simplified analysis. Although an exact formulation of the switching boundary may be available, the usefulness of incorporating this into the system becomes questionable.

Computing 'power', and speed, required are factors to be considered in the assessment of system cost when studying the feasibility of alternative systems. The practical and theoretical problems associated with implementing a switching boundary based upon an exact solution are immense. We will not dwell on these here since at present it seems

more important to study the much wider range of applications where 'near optimal' switching is required and where the cost of the controller is somewhat limited.

In such systems the optimal switching becomes that based upon an approximation to the otherwise ideal switching boundary. The classical example is the boundary given by,

$$\theta = k\,\omega\,|\omega| \qquad \ldots\ldots (6\text{-}6)$$

This has been used in practical systems and examples of this can be found in many textbooks. The switching function can be generated by methods using tachometers or resistor-diode networks (arranged to give a parabolic characteristic).

Although these analogue methods have been popular it would be appropriate in a digital system, to use a digital method. A computer could be used for this purpose but this may not be desirable if a simpler alternative is available.

The method to be described is a means of generating an approximate switching boundary using relatively simple logic circuitry. It therefore also has a more general application to a wide range of digital servomechanisms.

6.3.2 Digital Generation of the Switching Boundary.

Consider the circuit shown in Fig.6.12. The input S1 is taken from the second least significant bit of the position counter and each change in level represents an angular displacement of two steps. The least significant bit could have been used but this signal could have pulses due to noise as discussed at the end of Section 6.2.1.

Each alternate change in level of S1 enables the input to a binary rate multiplier BRM1 for a preset time t_e which must be shorter

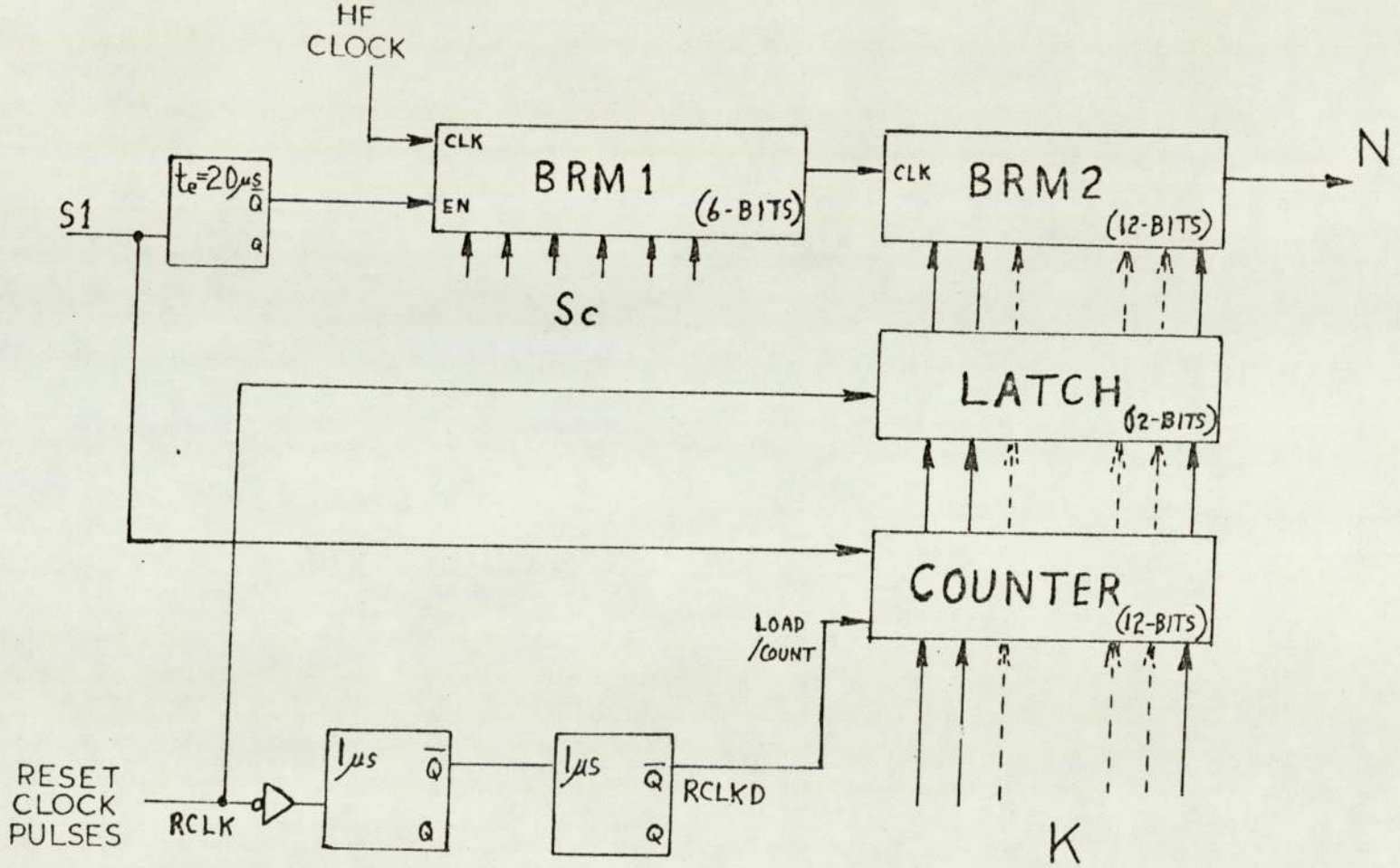

Fig.6.12 Switching boundary generation.

than the minimum period of S1. The input to BRM1 is from a clock with a preset frequency f_c which is high, so that each time BRM1 is enabled a number of pulses are accepted from the input. The other input to BRM1 is a per unit scaling factor Sc which defines the ratio of output pulse rate to input pulse rate. The pulses at the output of BRM1 are fed into a second binary rate multiplier BRM2 which has a scaling factor set on a latch. The latch is regularly reset with the contents of a counter at a frequency of $\frac{1}{t_r}$ which is relatively low in comparison to the stepping rate overall but the final step or so of slewing. The input to the counter is the signal S1 and the counter is reset to a value K shortly after the latch has been reset. This ensures that the latch contains the maximum count obtained during each period of t_r.

During the period t_r, between successive reset pulses, assume the motor has taken n steps in either direction. The stepping rate ω_s is therefore given by

$$\left|\omega_s\right| = \frac{n}{t_r} \qquad \ldots\ldots (6\text{-}7)$$

Let there be m pulses per step fed into BRM1, determined by t_e and f_c. Over a period t_r there will be m x n pulses fed into BRM1 and therefore

$$\text{Output of BRM1} = m\ n\ Sc \text{ pulses} \qquad \ldots\ldots (6\text{-}8)$$

while, over the same period,

$$\text{Contents of counter} = K + n \qquad \ldots\ldots (6\text{-}9)$$

and, the output of BRM2 is given by

$$N = m\ n\ Sc\ (K + n) \qquad \ldots\ldots (6\text{-}10)$$

using equation (6-7),

$$N = k_1 \left|\omega_s\right| + k_2 \omega_s^2 \qquad \ldots\ldots (6\text{-}11)$$

where,

$$k_1 = m\, t_r\, Sc\, K \qquad \ldots\ldots (6\text{-}12)$$

and,

$$k_2 = m\, t_r^2\, Sc \qquad \ldots\ldots (6\text{-}13)$$

Equation (6-11) represents the switching boundary in the form of the first two terms of a power series in $\left|\omega_s\right|$. Using additional circuitry a higher order switching boundary could be obtained.

When used in conjunction with direction detecting logic supplying the sign of ω_s, this can be used to obtain a switching boundary, expressed by a modified form of equation (6-11).

$$N = k_1 \omega_s + k_2 \omega_s \left|\omega_s\right| \qquad \ldots\ldots (6\text{-}14)$$

This is a more general form of boundary than of the form given by equation (6-6). The parabolic form of boundary is easily obtained by setting the condition K = 0.

The linear term is produced by setting the load inputs of the counter and as such does not involve any additional circuitry over that required to produce the parabolic boundary.

With the appropriate parameters a system generating the boundary of equation (6-14) should be at least as effective as one using a boundary of the form in equation (6-6).

6.3.3 Switching Point Detection.

The switching boundary generation circuits give an output with a total of N pulses after every t_r seconds. The switching point detection circuits must compare the value of N with the present position. The switching decision is taken with regard to the present quadrant of the phase plane, decided by the signs of position and

velocity, and as to whether N is greater than or less than the contents of the position counter.

This is the purpose of the circuit shown in Fig.6.13. A 16 bit counter is loaded with the inverses of the 16 bits of the position counter denoting magnitude. Over the period t_r the counter counts 'up' towards zero. Immediately before zero is reached the counter will be full and all the outputs will be high. If this occurs, further input pulses to the counter are inhibited and flip-flop FF1 is set denoting that N is greater than the contents of the position counter. This defines the switching point parameter SP = 0. FF1 remains set after the end of the period t_r, since the direct setting overides the clocked input.

If the counter zero is not reached by the end of this period the clock input to FF1 clears the flip-flop denoting SP = 1 and the counter is again loaded with the complement of the position magnitude and the sequence repeats.

The 'up' and 'down' inputs of the position counter are fed into flip-flop FF2 and the output of this gives the sign of velocity according to,

UD=1 denotes an 'up' count in position, therefore a positive velocity

UD=0 denotes a 'down' count in position, therefore a negative velocity

The sign of position is taken from the sign bit of the position counter and likewise,

SN=0 denotes a positive position

SN=1 denotes a negative position

Consider Fig.6.14 the switching function is given by

$$SB = UD.SN.SP + UD.\overline{SN} + \overline{UD}.\overline{SN}.\overline{SP} \qquad \ldots\ldots (6\text{-}15)$$

where,

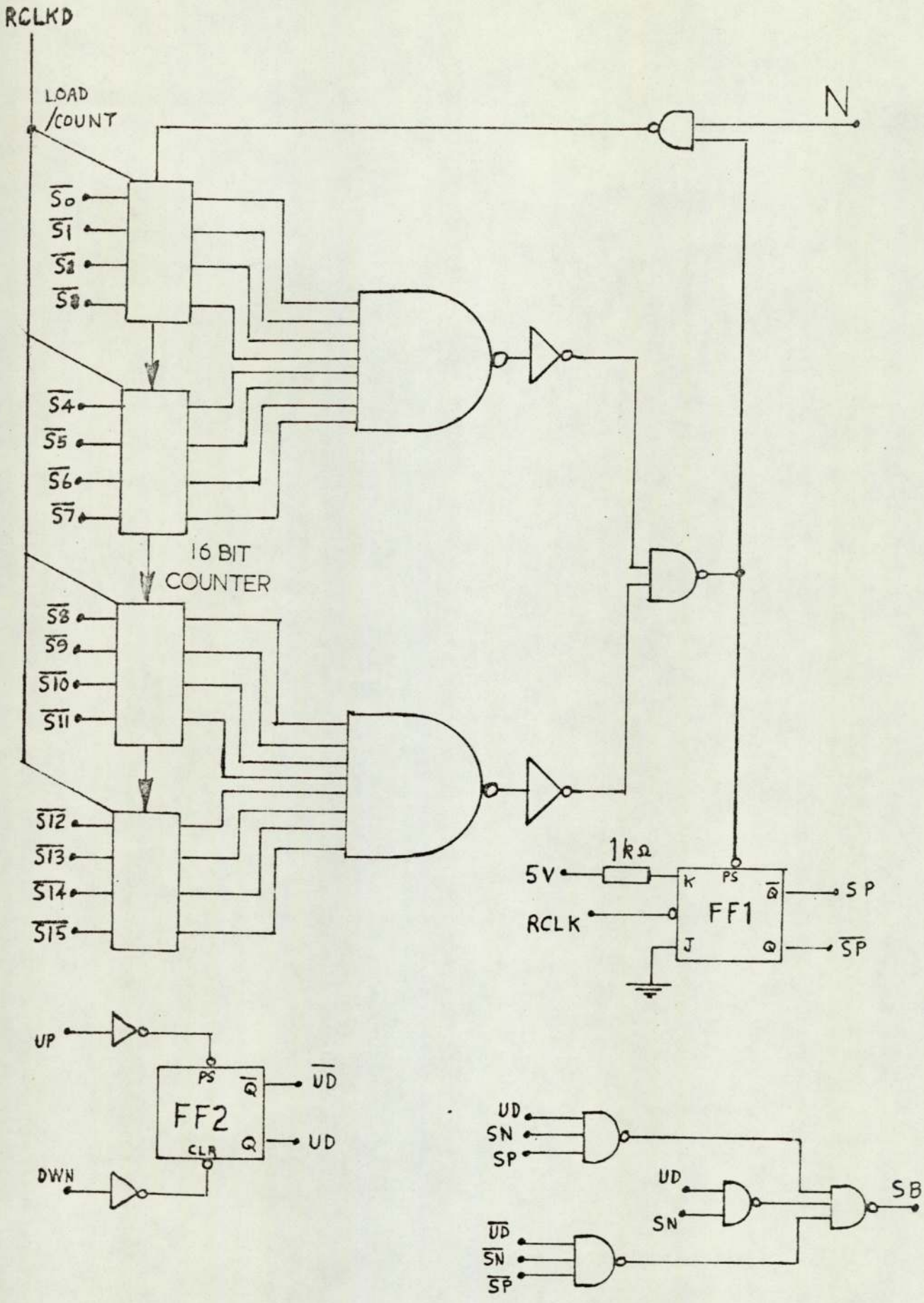

Fig.6.13 Switching point detection.

SB = 0 for maximum acceleration

and

SB = 1 for maximum deceleration shown by the shaded areas in Fig.6.14 and 6.15.

It is interesting to note that the eight sections of the phase plane diagram, defined by the spaces between the intersecting axes and parabolas, actually form a Karnough map with unconventionally shaped cells. Fig.6.15 may help to clarify the comparison.

6.3.4 Final Step Positioning.

When the final step is reached, indication of this is required so that appropriate action may be taken, such as switching to a phase angle of zero and for switching certain circuitry[38] which will give a good settling time for the final step.

In some applications associated equipment could be activated by this signal when the final step has been reached, without the need to wait for the next session of communication with the central controller.

The circuit of Fig.6.16 therefore gives this indication by making ZD = 1 when within one step of the final position. If the final positional accuracy is much less than one step then obtaining a good response for the final step will be important. Switching directly to a phase angle of zero can produce a response for the final step similar to that produced in open loop and under these conditions stepping motors can have a very oscillatory response with settling times up to about a second.

The settling of the final step will be a greater proportion of the total slewing time when slewing over a small number of steps.

The phase angle can alternate between positive and negative phase angles during the last step. This method is equivalent to 'electronic damping' methods already established.

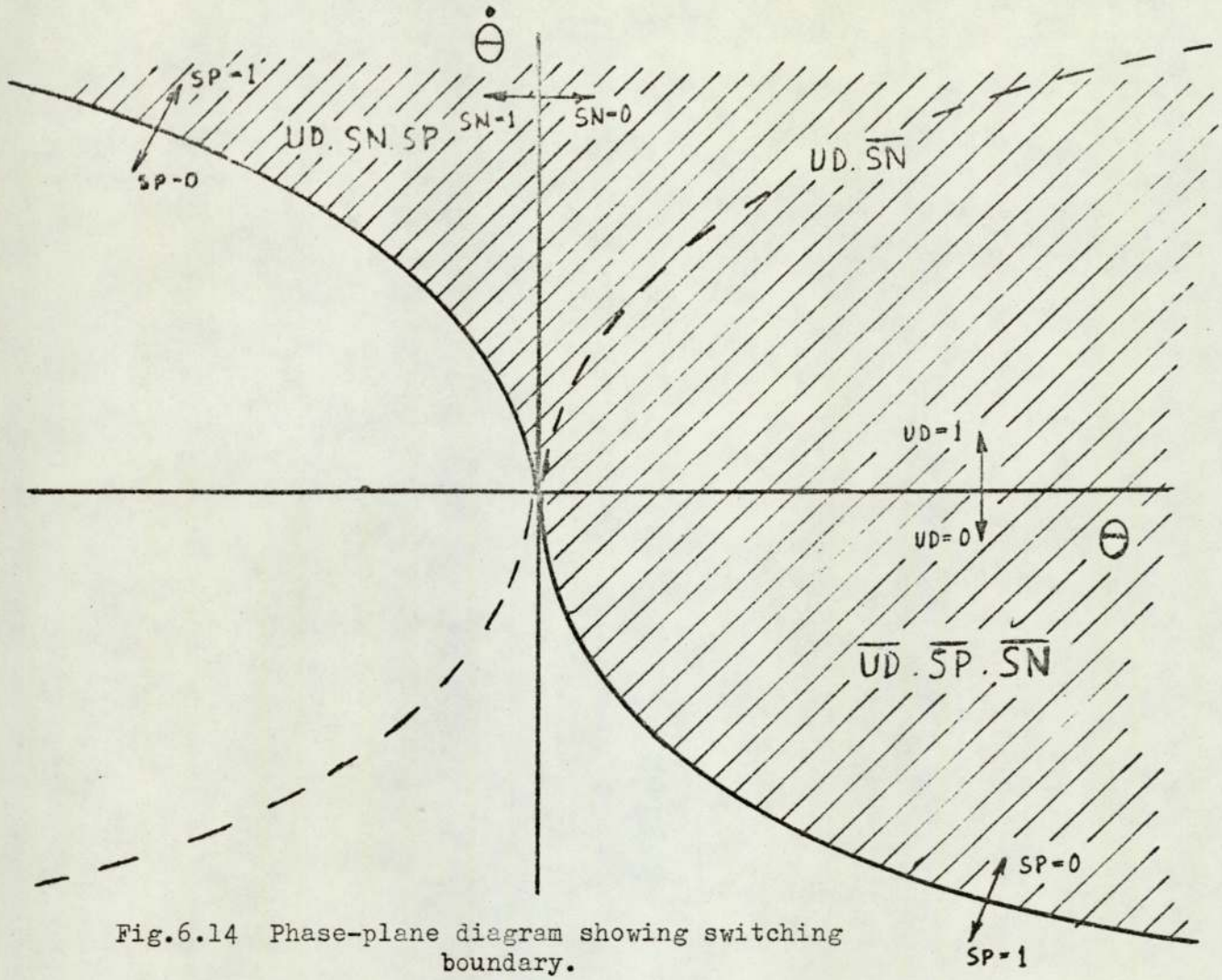

Fig.6.14 Phase-plane diagram showing switching boundary.

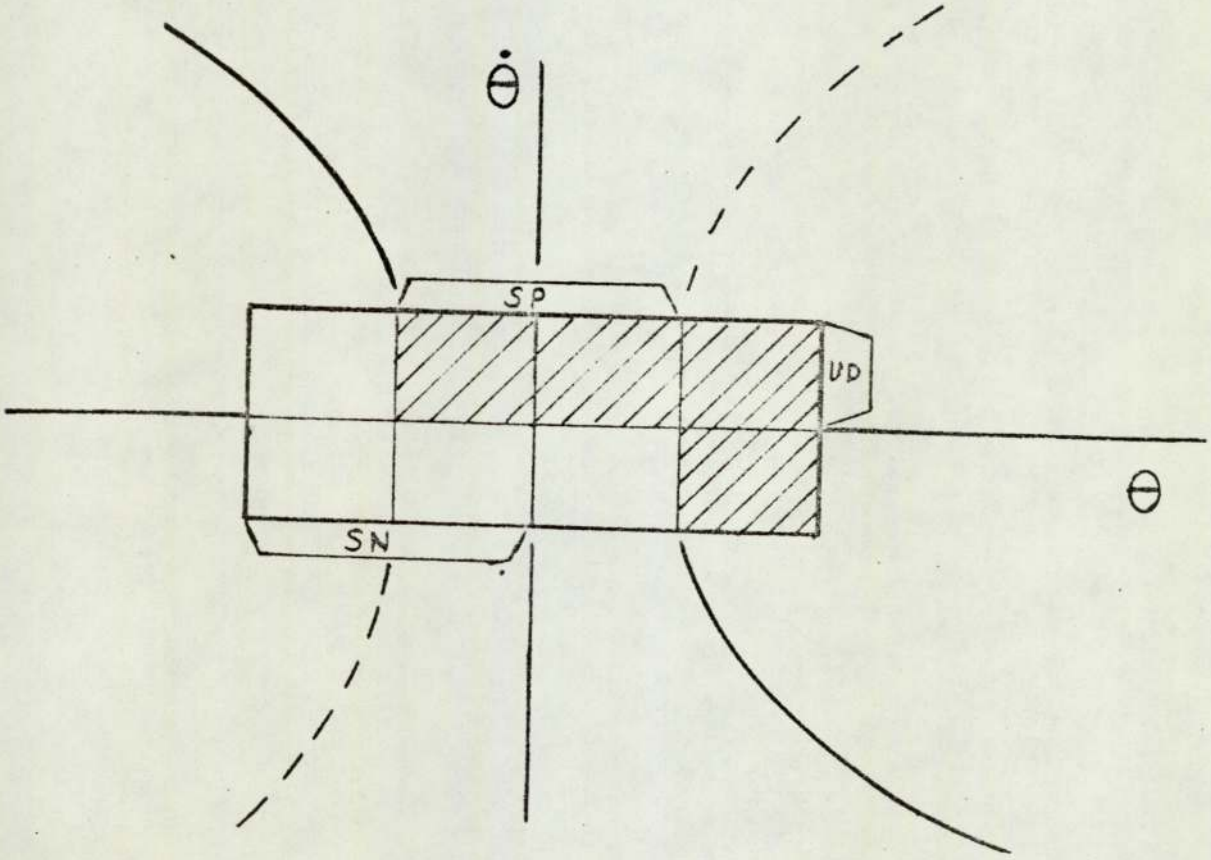

Fig.6.15 Karnaugh Map - arranged to correspond to phase plane.

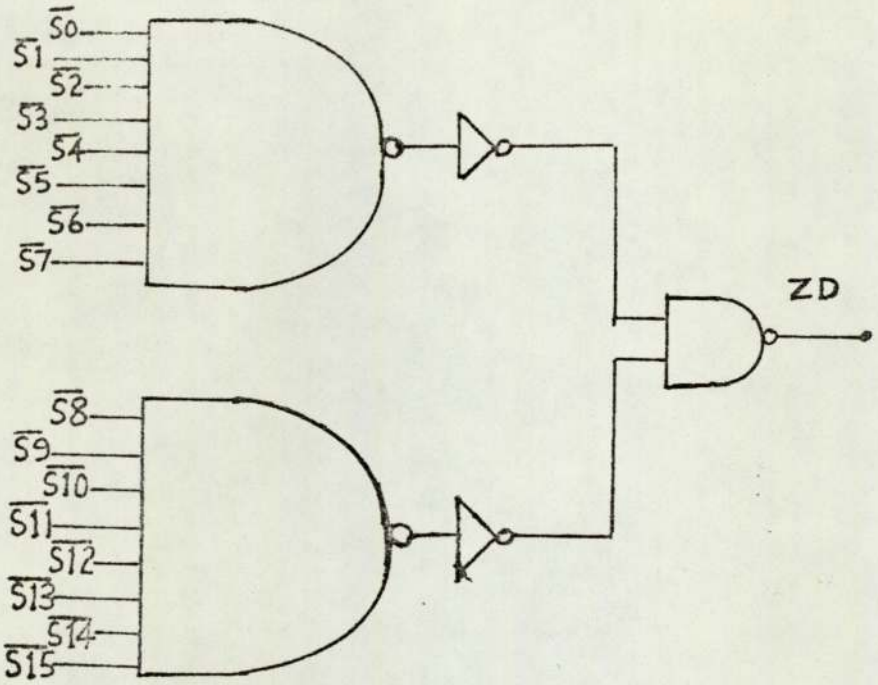

Fig.6.16 Zero Position Detection.

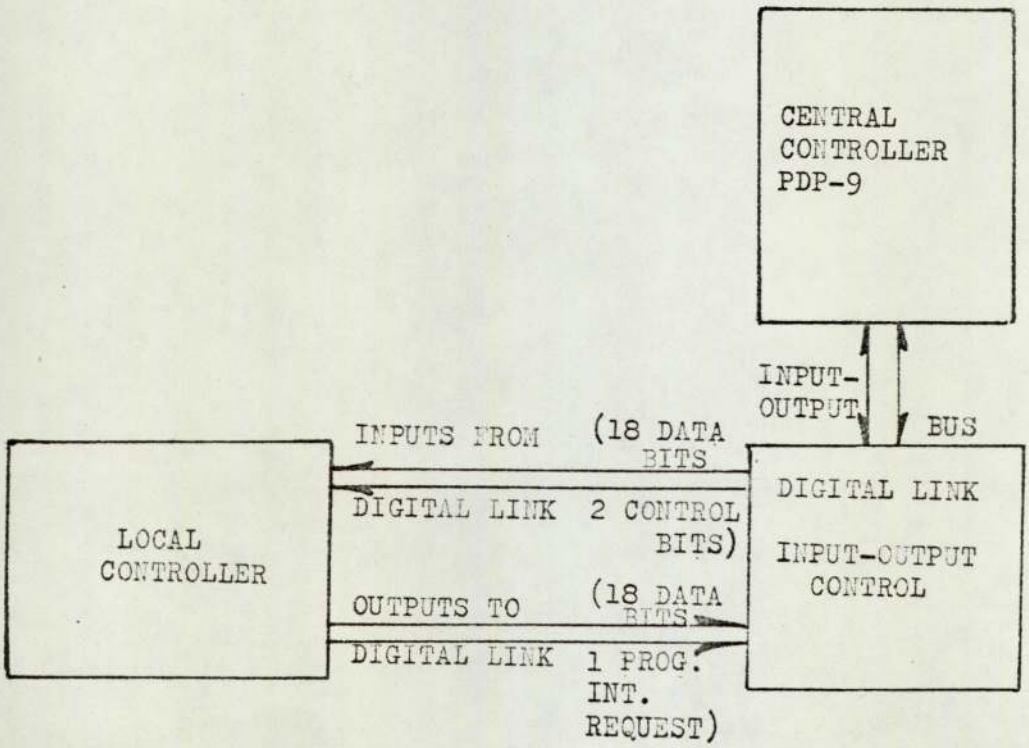

Fig.6.17 Outline of Digital Link.

Other methods of improving damping to obtain low settling times are currently being developed.

6.4 CONTROLLER-COMPUTER INTERFACE.

6.4.1 The Digital Link.

Information is exchanged between local and central controllers by means of a digital link. The parallel transmission of 18 data bits (one control word) can be carried out in either direction and takes only a few micro-seconds. The input-output control circuits for the digital link are outlined in Fig.6.17 and can be considered as a two-way buffer between the input and output lines of the local controller and the input-output bus of the PDP-9 computer. The circuitry provides for a program interupt request to be passed from the local controller to the PDP-9.

The PDP-9 addresses the digital link by sending appropriate device selection signals. These can transfer the input-output timing pulses to either the input or output circuits, depending upon the code used.

Signals from the local controller can be transferred to the input-output bus and read into the accumulator of the computer, or, the contents of the accumulator can be transferred by the I.O. bus to the output circuit register to be read by the local controller.

In addition two control bits CB1 and CB2 can be set by the appropriate code. The control bits and output register may be simultaneously cleared.

The digital link thus provides effective communication between local and central controllers. Alternatives to the form of link just described are,

(i) The serial transfer of data. Data transferred one bit at a time

requires more time than data transferred in parallel. This results in a saving in input output lines, but would use about the same amount of circuitry The increased speed obtained by the parallel transfer was therefore considered to be justified.

(ii) Direct memory access. This is the ideal method in terms of the possible rate of transfer of information. The contents of selected registers in the local controller could be transferred directly to a selected address in the memory, and visa-versa. This would have meant major modifications within the computer, and the transfer times achievable by the method adopted were considered adequate.

For experimental purposes the signals to the input of the local controller can be selected from two sources;-

(i) from the digital link when the central controller is used.

(ii) from the front panal (manually set switches) of the local controller when manual control is used.

Both sources use the same notation of coding and the input signals are then fed into input selection circuits.

6.4.2 Local Controller Input-Output Circuits.

The purpose of the input selection circuits is to decode the incoming 18 bits to the local controller in terms of one of the controller parameters and its value, and to assign this accordingly. The parameters to be controlled in this way, and the number of bits required to define the value are;-

(i) Position counter, sign and magnitude - 17 bits.

(ii) Phase angle - 6 bits

(iii) Current level - 4 bits

(iv) Boundary scale - 6 bits

(v) Boundary constant - 12 bits

The assignments used are shown in Table 6.2. The 18 bit word is composed of a memory address code, which is either 1 or 3 bits long, and the remainder of the word defines the value of the parameter.

The input selection circuit is shown in Fig.6.18. The parameter selection decoding circuit shown in Fig.6.19 operates the latching/loading signal and the value of the parameter is then placed in the appropriate store.

The parameters required to be sent as output data from the local controller are;-

(i) Switching boundary information, i.e. the switching decision - 1 bit.

(ii) Position counter, sign and magnitude - 17 bits.

This information is allocated as shown in Table 6.3, with no coding problems.

6.4.3 Input-Output Transfers.

If the computer is to be used to predict the state space trajectory it is likely that samples of position taken at regular intervals will be most useful as this will simplify any calculations involved.

It is assumed that the computer is working in a time sharing system and has some other work to do. More than one real-time programme introduces the need for priorities to be assigned to programme interrupt requests but for simplicity we shall assume that the other work is not being conducted on a real-time basis.

Sampling could be carried out using the computer to determine the timing but it would often be simpler to let the local controller issue programme interrupt requests at regular periods and to use these to initiate sampling. Control bit CB1 was used to enable the issuing of the interrupt request signals. Control bit CB2 was used

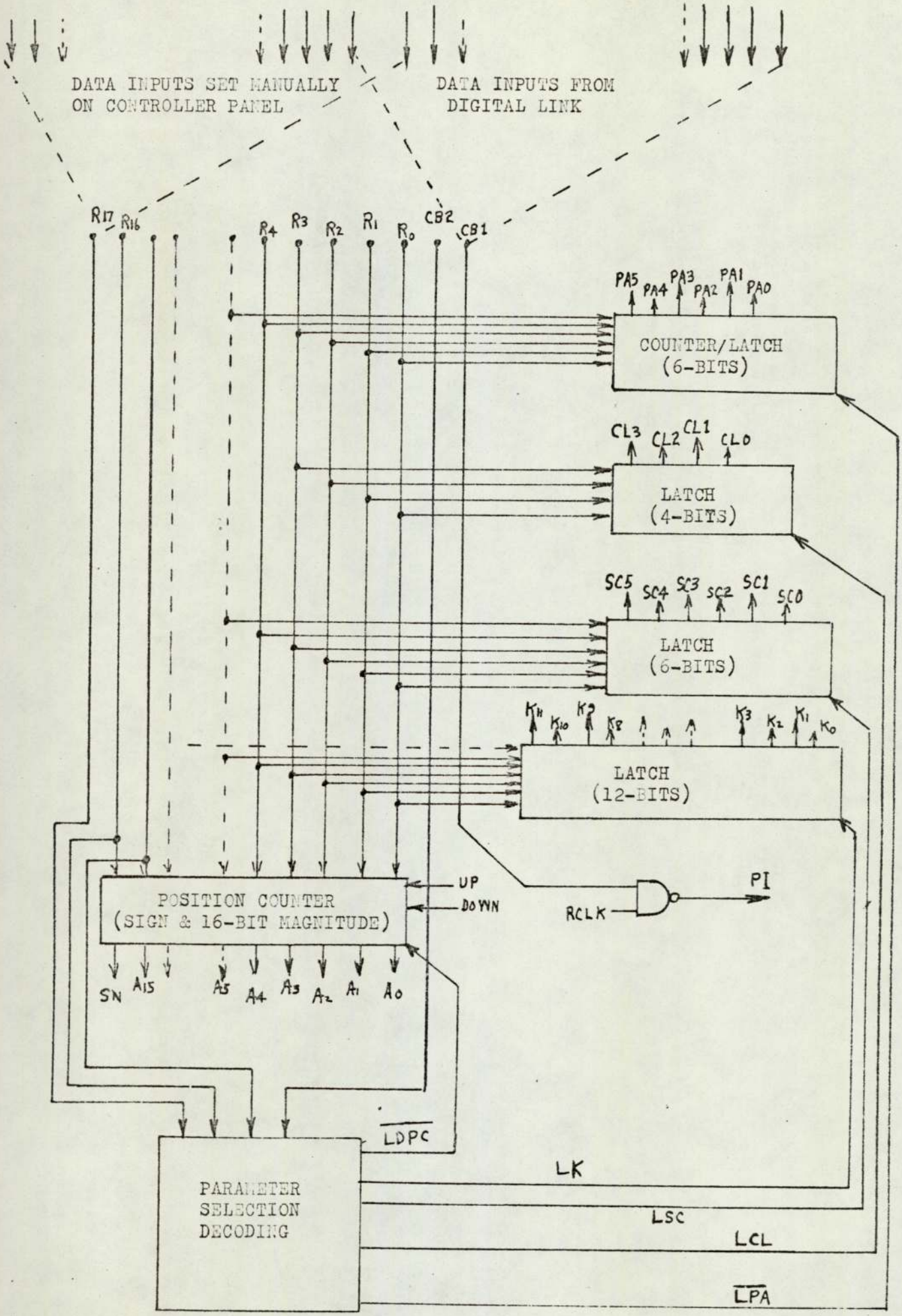

Fig.6.18 Input Selection Circuit.

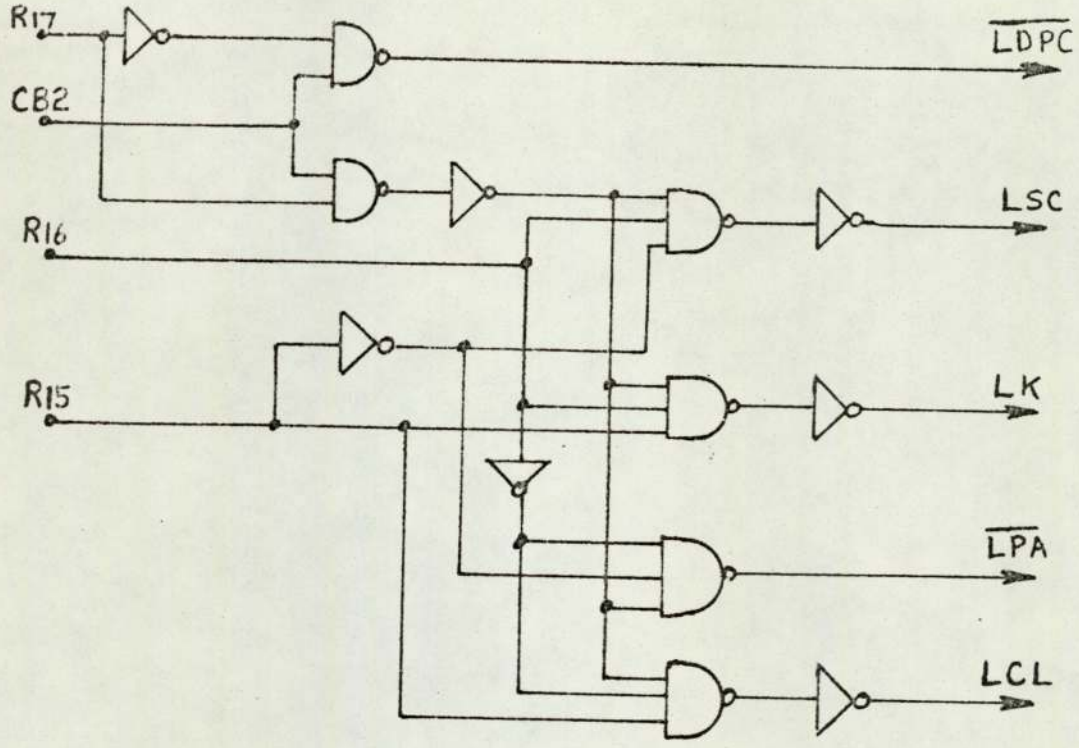

Fig.6.19 Parameter Selection Circuit.

	MEMORY ADDRESS CODE/REGISTER INPUT DATA (FROM LINK) (1 OR 3 BITS)										
INSTRUCTION	R17	R16	R15	R14	...	R5	R4	R3	R2	R1	R0
LOAD POSITION COUNTER	0	SN	A15	A14	...	A5	A4	A3	A2	A1	A0
LOAD PHASE ANGLE	1	0	0			U	V	W	X	Y	Z
LOAD CURRENT LEVEL	1	0	1					CL_3	CL_2	CL_1	CL_0
LOAD BOUNDARY SCALE	1	1	0			SC_5	SC_4	SC_3	SC_2	SC_1	SC_0
LOAD BOUNDARY CONSTANT	1	1	1		K_{11}..	K_5	K_4	K_3	K_2	K_1	K_0

TABLE 6.2. ASSIGNMENTS FOR DATA RECEIVED BY LOCAL CONTROLLER

OUTPUT DATA (TO LINK)									
SWITCHING BOUNDARY INFORMATION	RELATIVE ANGULAR POSITION (STEPS)								
S17	S16	S15	S14	....	S4	S3	S2	S1	S0
SB	SN	A15	A14		A4	A3	A2	A1	A0

TABLE 6.3. ASSIGNMENTS FOR DATA SENT BY LOCAL CONTROLLER.

MNEMONIC	CODE	OPERATION
SKIP	702201	Skip on link flag.
SETB	702204	Set link buffer.
READ	702212	Read data from local controller.
SETC1	702220	Enable interrupt request signals.
SETC2	702240	Request local controller to read link buffer.
CLEARB	702260	Clear buffer, CB1 and CB2.

TABLE 6.4.

to instruct the local controller to read data from the link.

A sub-programme INPUT was used to read the output data from the local controller upon receipt of an interrupt request and to allocate values to the two variables according to the information received. The variables, switching decision and position were then available for other programmes.

Sub-programmes LCNT, LPA, LCL, LBS, LBC were used to load into the local controller the position, phase angle, current level, boundary scale and boundary constant respectively. A variable was supplied, from another programme, to these sub-programmes to define the value to be transferred and each programme sent the appropriate code through the digital link and then instructed the local controller to accept it.

These sub-programmes were written in a low-level language MACRO-9[39] but can be used by programmes written in a high level language such as FORTRAN. A full listing of these programmes appears in the apprendix. In addition to the standard range of MACRO-9 instructions, the instruction codes to operate the digital link are required, as listed in Table 6.4.

The instruction code contains a general operation code 70_8, a device selection code (in this case 22_8) and information on sub-device selection and the programming of the input-output transfer pulses for function selection. In the programmes a mnemonic was used to carry out the MACRO instruction.

6.5 CONCLUSIONS

The duties of the controller have been discussed and the level of control most appropriate for each has been suggested.

Schemes for the measurement of the system variables have also been presented.

The circuitry described for the measurement of position used the signals from the optical encoder which were likely to contain noise. Sequence information was used to produce a similar set of signals, but with a higher reliability for the phase angle control circuitry, and to produce an accurate record of position.

The method of torque measurement can be used for transient or steady state torques. A fast response and good sensitivity were achieved. The particular arrangement in which the transducers were mounted minimised the undesirable effects of unavoidable interacting forces in the mounting framework.

The switching function generator circuitry obviated the need for separate measurement of velocity to define the switching boundary. It allowed the switching boundary to be defined as a second order equation in velocity and to be implemented at a local level of control, with the coefficients of the equation supplied either locally or from the central controller. This is of particular advantage where there are slow or occasional changes in the system characteristics, such as those due to changes in load or drift in the control circuits. With additional circuitry a higher order of equation could be represented but the simple circuitry used already represented a more general form than the equation accepted to be adequate in many analog 'optimally' switched systems.

Information such as phase angle, current level and position reference are supplied to the local controller either locally or from the central controller.

Additional function generators supplying phase angle and current level information at a local level, derived from velocity would add further flexibility to the system and if necessary it could then operate reasonably well when independent of central control.

Methods of transferring information between local and central

levels of control have been discussed and operation of the digital link used here has been briefly described.

Figs.6.20 and 6.21 indicate the size of the controller and the amount of hardware involved. This does not seem excessive and could be greatly reduced if this could be made using LSI.

All the various system elements so far described were built and were operational and although the closed loop drive was working, it was not run using computer control. A main Fortran program was to be used to control the data to the local controller, using the tested MACRO sub-programs, according to the calculated optimum values. It is unfortunate that this stage was not reached, due to lack of time, but there is no reason why this should have presented any special problems.

Many further enhancements to the system would then be possible and some of these are discussed, with some suggestions for alternative systems, in Section 7.1 that follows.

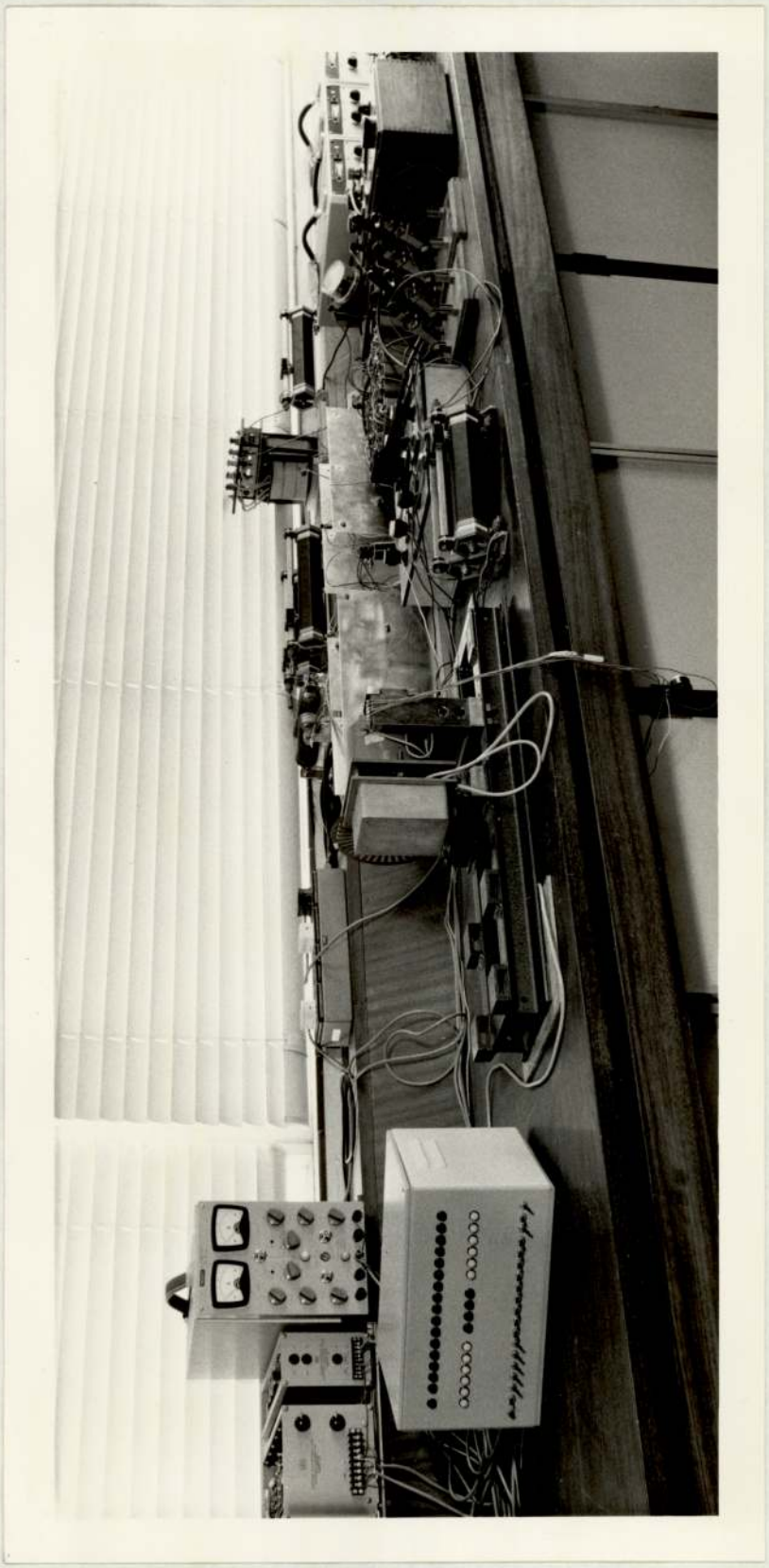

Fig. 6.20 Local controller and other apparatus.

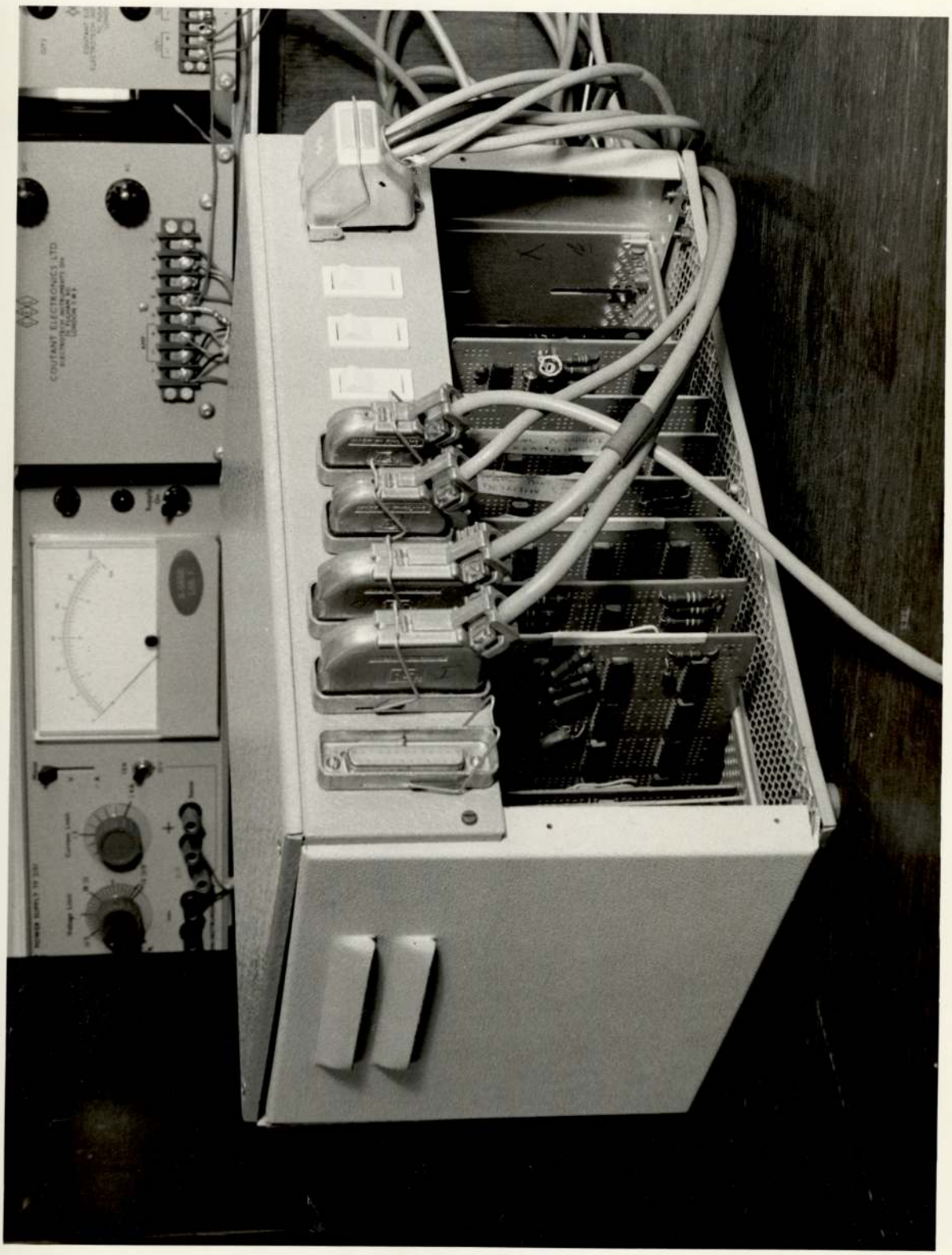

Fig.6.21 Rear view of local controller

7. CONCLUSION

7.1 Adaptive Systems.

Some of the control methods covered in the proceding sections are suitable for use in adaptive systems.

The changing of the switching boundary parameters to suit varying load conditions is an adaptive feature that has already been mentioned. These changes could be made by trial and error for a given load over a number of slewing operations using a 'hill climbing' approach. The slew time, or some other index of performance could be used to change the boundary parameters or other operating conditions.

Alternatively, the load could be identified by calculations based upon measurement of the system variables. The switching boundary or other operating conditions could then be adjusted accordingly to give an optimum response. This method of control is likely to require fewer slewing operations than the previous method before becoming effective and the response to a change in load should be better. Also a fixed load (initially unknown) could be accelerated, identified, and then brought to rest in an optimum manner in a single slewing operation. This would seem to be a very useful facility for many systems.

The main difference likely to be encountered in a model reference type of adaptive system is that of obtaining a real-time model of reasonable accuracy. Even the simplest models already presented are unsuitable for real-time simulation on present day digital computers.

Three other approaches are possible:-

(i) A hybrid computer, using analogue methods of integration may give a real-time model of adequate accuracy.

(ii) If a hybrid computer is inconvenient or considered to be too elaborate for the purpose then the motor could be represented by either analogue or digital function generators, giving the single output

variable - developed torque - in terms of the input variables of current, phase angle and velocity.

(iii) If a complex control strategy is to be used such that computer time is at an absolute premium, digital function generation may be considered too slow if accuracy is to be important, or too inaccurate if simplicity is important. The direct measurement of the developed torque may then be the best solution and a method such as that described in Section 6 2.3 is suggested.

Method (i) is a step by step solution and is unlikely to be essential, whilst method (ii) is a multi-stepping solution and does not provide information about 'inter-step transients'. Method (iii) is both a single and multi-step solution if the response of the transducer is adequate.

An interesting example of an adaptive system would be a temperature-adaptive controller where the motor temperature sets the control strategy.

A limitation in trying to force the machine performance is the maximum voltage. 'Current forcing' can cause over heating and is limited by the voltage available. Magnetic saturation is a further limit which ultimately restricts the torque that can be developed, yet operating well into saturation can produce a large amount of heat to be dissipated. At high stepping rates iron losses also produce considerable heat. All these effects combine to give high operating temperatures. The acceptability of these temperatures will depend upon the importance of particular slewing operations.

7.2 Evaluation of Optimal Systems.

The areas of work that have been covered in the preceding sections and those considered to make a contribution to the subject are:-

(i) Modelling by the development of electrical and magnetic equivalent circuits:- This is useful for optimising the design of the machine (which has not been covered) and for simulation studies of the machine and overall control system.

The model established is considered to be an improvement upon models proposed in previous papers. This section of the work was completed during the first year of the project and it is interesting to note that later papers[13,49] have confirmed the advantages of referring to the magnetic equivalent circuit in forming a model. The diversity of electromagnetic configurations for stepping motors means that unlike most other types of machine, a single simple electrical equivalent circuit is insufficient for all machines. It is therefore considered important to be able to interpret the duality in order to obtain an electrical equivalent circuit.

(ii) Optimisation of the operating conditions:- The examples given applied to unconstrained maximum torque and for the maximum torque constrained by given losses. Similar procedures could be used for other objectives.

(iii) Thyristor drive circuits:- A cycloinverter type of drive circuit has been presented that is considered to be suitable for stepping motors.

(iv) Closed loop control:- Optical, electronic and combined methods have been presented. These allow control of phase angle with various degrees of accuracy, and are considered to be simpler than previous methods. The combined method in particular is considered to be unique in providing a large number of digitally selected phase angles by simple means.

(v) Computer controlled drives:- Problems of measuring system variables have been discussed and a method of measuring instantaneous torque has been presented, and this is considered to be an improvement

over other methods. An example of a computer controlled drive has been given, with special reference to the problem of optimum switching. The digital generation of an 'adjustable' switching boundary using simple logic is considered to be a useful contribution to digital servomechanisms.

An evaluation of the degree of optimality of particular systems can only be made by reconsidering these aspects of the system. By making comparisons with alternative systems, according to his requirements, the user will eventually arrive at the optimal arrangement.

7.3 Suggestions for Further Work.

Much useful work can still be done in most areas, in particular the following.

i) Motor Design:-

a) To be competitive, manufacturers must constantly attempt to produce machines of higher performance. The ability to accurately model a machine can save valuable time in design development. A computer aided design package to do this would therefore be very useful.

b) Improvements in the use of materials appear to offer possibilities for higher performance.

For instance, the permanent magnet type of motor used here had solid rotor caps. These, together with the solid outer stator, account for most of the iron losses. The trend is now to laminated rotors.

Use could be made of improved magnetic materials such as the 'rare earth magnets' (samarium, mischmetal etc.) for the permanent magnet.

ii) Motor Control:-

a) The inverter drive circuit suggested here is suitable for stepping motors in that a wide operating frequency is possible. It is very likely that further improvements can be made in many other respects.

In particular the waveform (and the noise) produced at low frequencies is undesirable. This could be avoided by purposely introducing forced commutation at low frequencies.

b) A particular type of response (either for a single step, over a number of steps, or for just the final step of a multi-step operation) may be highly desirable.

The manner in which a few simple components, connected to the motor terminals, can be used to modify the response suggests that much can be done by investigating the use of filtering techniques to obtain an optimum response.

c) If the problem of developing a real-time model of reasonable accuracy can be overcome a wide range of control methods would be available.

The possibilities in these and other aspects of stepping motors means that the subject still has considerable scope for research.

8. ACKNOWLEDGEMENTS

The writer wishes to thank Dr. R.C. Johnson for the useful discussions and guidance given during the project.

Acknowledgement is made of the financial support given by the Science Research Council and by the University of Aston in Birmingham.

The assistance given by Mr. D. Paul in the practical work and that by my wife Margaret in typing the script is also appreciated.

9. REFERENCES

1. SPRACKLAN, S.G.: 'Standardisation of stepper motor terminology, configuration and test data', Proceedings of the International Conference on Stepping Motors & Systems, Leeds, 1974, pp 56-66.
2. HUGHES, A., LAWRENSON, P.J., STEELE, M.E., and STEPHENSON, J.M.: 'Prediction of stepping motor performance', Proceedings of the International Conference on Stepping Motors & Systems, Leeds, 1974, pp 67-76.
3. O'DONAHUE, J.P.: 'Transfer function for a stepping motor'. Control Engineering 1961, 8 No. 11, pp 103-104.
4. KIEBURTZ, R.B.: 'The step motor - the next advance in control systems', I.E.E.E. Trans 1964 AG9, pp 98-104.
5. DELGADO, M.A.: 'Mathematical model of a stepping motor operating as a fine positioner around a given step'. I. .E.E. Trans. 1969, AG14, pp.394-397.
6. GARNER, K.C.: 'Simulator study of optimal switching rates for stepping motor drive systems', Electron. Lett. 1967, 3 pp.491, 492.
7. DAILY, J.R.: 'Computer simulation of stepping motor performance, Electro-Technology (U.S.A.) 1967, 79, No.3 pp.60-64.
8. MATHAMS, R.F.: 'Phase-plane analysis of a permanent magnet stepping motor', Electron. Lett. 4, pp.103-104 1968.
9. ROBINSON, D.J. and TAFT, C.K.: 'A dynamic analysis of magnet stepping motors', I.E.E.E. Trans. 1969 ECI-16, pp.111-125.
10. VENKATARATNAM, K, SARKAR, S.C. and PALANI, S.: 'Synchronising characteristics of a step motor', I.E.E.E. Trans. 1969, AC-14 pp.510-517.
11. VENKATARATNAM, K. and MOULI, M.C.: 'Stability of a stepping motor' Proc. I.E.E., 1971, 118, pp.805-812.
12. POHL, R: 'Theory of pulsating field machines', J.I.E.E., 1946, 93, pp.37-47.

13. CHAI, H.D.: 'Magnetic circuit and formulation of static torque for single stack permanent magnet and variable reluctance step motors', Incremental Motor Control Systems, & Devices, Proc. 2nd Symposium, University of Illinois at Urbana-Champaign, 1973, pp.E1-18.

14. SNOWDEN, A.E. and MADSEN, E.M.: 'Characteristics of a synchronous inductor motor', Trans. Am. Inst. Elect. Eng. 1962, 81 pp.1-5.

15. SLEMON, G.R.:'Magnetoelectric devices' (Wiley 1966).

16. CHERRY, E.C.: 'The duality between interlinked electric and magnetic circuits and the formation of transformer equivalent circuits', Proc. Phys. Soc. 1949, 62, pp 101-111.

17. WHITNEY, H.: 'Non-separable and planar graphs', Proc. Nat. Acad. Sci. 1931 17, pp 125-127.

18. BLOCH, A.: 'On methods for the construction of networks dual to non-planar networks', Proc. Phys. Soc. 1946, 58, pp 677-694.

19. LAITHWAITE, E.R.: 'Magnetic equivalent circuits for electrical machines', Proc. I.E.E. 1967, 114, pp 1805-1809.

20. FIENNES, J.: 'New approach to general theory of electrical machines using magnetic equivalent circuits', Proc. I.E.E. , 1973, 120, pp. 94-104.

21. CHANG, S.S.L.: 'An analysis of the stepping motor - what can it do?, Proc. NEC, 1968, pp 36-41.

22. WAGNER, G.F.: 'Parallel inverter with resistive load', Trans. Ameri. Inst. Elect. Engrs. 1935, 54, p 1227.

23. WAGNER, G.F.: 'Parallel inverter with inductive load', ibid, 1936, 55, p 970.

24. McMURRAY, W. and SHATTUCK, D.P.: 'A silicon controlled rectifier inverter with improved commutation', ibid, 1961, 80, (Pt. 1), oo 531-542.

25. HAMUDMANOV, M.Z.: 'Variable frequency operation of synchronous motors using electronic frequency changer' in 'The technical problems of electric drives' USSR Academy of Science, 1957.

26. WARD, E.E.: 'Inverter suitable for operation over a range of frequency', Proc. I.E.E., 1964, 111, pp 1423-1434.

27. BRADLEY, D.A., CLARKE, C.D., DAVIS, R.M. and JONES, D.A.: 'Adjustable frequency inverters and their application to variable speed drives', Proc. I.E.E., 1964, 111, pp 1833-1846.

28. KING, K.G.: 'Variable frequency thyristor inverters for induction motor speed control' Direct Current, 1965, 10.

29. ROBERTSON, S.D.T. and HEBBAR, K.M.: 'A tuned circuit commutated inverter', Power thyristors and their applications, I.E.E. Conf. Publication 53, 1969, Pt.1, p 297-304.

30. ANDREW, P.: 'The stepping motor as a machine-tool actuator', Electronics and Power, 1972, Feb. pp 62-63.

31. FREDRIKSEN, T.R.: 'Closed loop stepping motor application', 1965 J.A.C.C. pp 531-538 and 1966 IFAC Congress, Paper 25C.

32. PAWLETKO, J.P.: 'Phase-locked oscillator supplies input pulses', Control Engineering, 1967, Vol.14, No. 8, pp 69-70.

33. GARNER, K.C.: 'Back e.m.f. controls stepping rate', ibid. p 71.

34. KENNEDY, D.W.: 'Digital methods fixes phase lag or lead', ibid, p. 72.

35. BALES, R.C.:'Rotary pulse generator provides all-digital feedback', ibid, p. 73.

36. FREDRIKSEN, T.R.: 'Direct digital process control of stepping motors', IBM Journal, March 1967, pp 179-188.

37. WILNER, L.B.: 'Piezo-resistive force gauges and their uses', Trans. I.E.E.E., Vol. ECI-16, 1969, 1, pp 40-43.

38. HUGHES, A and LAWRENSON, P.J.: 'Introduction to electromagnetic damping in stepping motors', Proceedings of the International Conference on Stepping Motors & Systems, Leeds, 1974, pp 135-47.

39. DIGITAL EQUIPMENT CORPORATION: 'PDP-9' Macro Manual.

40. DOUCE, J.L. and REFSUM, A.: 'The control of a synchronous motor', I.F.A.C. 3rd Congress 1966, paper 4A.

41. TOU, J.T.: 'Modern Control Theory', McGraw Hill.

42. MORREALE, A and IRANI, R: 'Stepping devices, introduction, types and variations', Proceedings of the International Conference on Stepping Motors and Systems, Leeds, 1974, pp.1-12.

43. BEATSON, C: 'Stepper Motors are making strides in the design field', The Engineer, 13th August 1970, pp.34-35.

44. FREDRIKSEN, T.R: 'Direct digital processor control of stepping motors', IBM Journal of Research and Development, 1967, 11, pp.179-188.

45. FREDRIKSEN, T.R: 'Stepping motors come of age', Electro-Technology, 1967, 80, No.5, pp.36-41.

46. FREDRIKSEN, T.R: 'The closed loop step motor an ideal actuator for process control', Proc. IFAC Symposium on Pulse rate and Pulse Number Signals in Automatic Control, 1968, pp.243-255.

47. FREDRIKSEN, T.R: 'Application of the closed loop stepping motor', IEEE Trans. Auto Control, 1968, AC-13 pp.464-474.

48. KUO, B.C, YACKEL, R and SINGH, G: 'Time-optimal control of a stepping motor', IEEE Trans. Auto Control, 1969, AC-14, pp.745-747.

49. SINGH, G and FOLKERTS, C: 'Computer-aided magnetic circuit analysis for performance prediction of step motors', Incremental Motion Control Systems and Devices, Proc. 3rd Symposium, University of Illinois at Urbana-Champaign, 1974, pp.M1-12.

50. KUO, B.C: 'A bibliography of publications and patents on step motors and controls', ibid., pp.Y1-21.

10. APPENDIX

10.1 MACRO Programme Listing.

```
PAGE   1      INPUT  SRC      INPUT


    1                                          .TITLE INPUT
    2                                          .GLOBL INPUT,.DA
    3          00000 R 740040 A      INPUT XX
    4          00001 R 120023 E              JMS* .DA
    5          00002 R 600005 R              JMP .+3
    6                  702201 A      SKIP=702201
    7                  702212 A      READ=702212
    8                  702220 A      SETC1=702220
    9                  702260 A      CLEARB=702260
   10          00003 R 000000 A      A       0
   11          00004 R 000000 A      B       0
   12          00005 R 700002 A              IOF
   13          00006 R 702220 A              SETC1
   14          00007 R 702201 A              SKIP
   15          00010 R 600007 R              JMP .-1
   16          00011 R 702212 A              READ
   17          00012 R 060004 R              DAC* B
   18          00013 R 744010 A              RCL
   19          00014 R 664000 A              GSM
   20          00015 R 740020 A              RAR
   21          00016 R 060003 R              DAC* A
   22          00017 R 702260 A              CLEARB
   23          00020 R 703344 A              DBR
   24          00021 R 700042 A              ION
   25          00022 R 620000 R              JMP* INPUT
   26                  000000 A              .END
               00023 R 000023 E *E
SIZE=00024      NO ERROR LINES
```

```
PAGE   1      LCNT   SRC      LCNT


    1                                          .TITLE LCNT
    2                                          .GLOBL LCNT,.DA
    3          00000 R 740040 A      LCNT  XX
    4          00001 R 120017 E              JMS* .DA
    5          00002 R 600004 R              JMP .+2
    6                  702204 A      SETB=702204
    7          00003 R 000000 A      A       0
    8          00004 R 220003 R              LAC* A
    9          00005 R 744000 A              CLL
   10          00006 R 742010 A              RTL
   11          00007 R 741400 A              SZL
   12          00010 R 740001 A              CMA
   13          00011 R 742020 A              RTR
   14          00012 R 741400 A              SZL
   15          00013 R 340020 R              TAD C1
   16          00014 R 702204 A              SETB
   17          00015 R 744000 A              CLL
   18          00016 R 620000 R              JMP* LCNT
   19                  000000 A              .END
               00017 R 000017 E *E
               00020 R 000001 A *L
SIZE=00021      NO ERROR LINES
```

```
PAGE    1       LPA     SRC     LPA

                                        .TITLE LPA
                                        .GLOBL LPA,.DA
    00000 R 740040 A    LPA     XX
    00001 R 120016 E            JMS*  .DA
    00002 R 600004 R            JMP  .+2
            702204 A    SETB=702204
            702240 A    SETC2=702240
            702260 A    CLEARB=702260
    00003 R 000000 A    A       0
    00004 R 200017 R            LAC (400000
    00005 R 260003 R            XOR* A
    00006 R 702204 A            SETB
    00007 R 740000 A            NOP
    00010 R 740000 A            NOP
    00011 R 702240 A            SETC2
    00012 R 740000 A            NOP
    00013 R 740000 A            NOP
    00014 R 702260 A            CLEARB
    00015 R 620000 R            JMP* LPA
            000000 A            .END
    00016 R 000016 E *E
    00017 R 400000 A *L
SIZE=00020      NO ERROR LINES
```

```
PAGE    1       LCL     SRC     LCL

                                        .TITLE LCL
                                        .GLOBL LCL,.DA
    00000 R 740044 A    LCL     XX
    00001 R 120016 E            JMS*  .DA
    00002 R 600004 R            JMP  .+2
            702204 A    SETB=702204
            702240 A    SETC2=702240
            702260 A    CLEARB=702260
    00003 R 000000 A    A       0
    00004 R 200017 R            LAC (500000
    00005 R 260003 R            XOR* A
    00006 R 702204 A            SETB
    00007 R 740000 A            NOP
    00010 R 740000 A            NOP
    00011 R 702240 A            SETC2
    00012 R 740000 A            NOP
    00013 R 740000 A            NOP
    00014 R 702260 A            CLEARB
    00015 R 620000 R            JMP* LCL
            000000 A            .END
    00016 R 000016 E *E
    00017 R 500000 A *L
SIZE=00020      NO ERROR LINES
```

```
PAGE    1       LBC     SRC     LBC


                                        .TITLE LBC
                                        .GLOBL LBC, .DA
    00000 R 600002 R                    JMP .+2
            702204 A            SETB=702244
            702244 A            SETC2=702240
            702260 A            CLEARB=702260
    00001 R 000000 A            A       0
    00002 R 240016 R                    LAC (700000
    00003 R 260001 R                    XOR* A
    00004 R 702204 A                    SETB
    00005 R 740000 A                    NOP
    00006 R 740000 A                    NOP
    00007 R 702240 A                    SETC2
    00010 R 740000 A                    NOP
    00011 R 740000 A                    NOP
    00012 R 702260 A                    CLEARB
    00013 R 620014 E                    JMP* LBC
            000000 A                    .END
    00014 R 000014 E *E
    00015 R 000015 E *E
    00016 R 700000 A *L
S
IZE=00017       NO ERROR LINES
```

```
PAGE    1       LBS     SRC     LBS


                                        .TITLE LBS
                                        .GLOBL LBS, .DA
    00000 R 740040 A        LBS     XX
    00001 R 120016 E                    JMS* .DA
    00002 R 600004 R                    JMP .+2
            702204 A            SETB=702204
            702240 A            SETC2=702240
            702260 A            CLEARB=702260
    00003 R 000000 A            A       0
    00004 R 240017 R                    LAC (600000
    00005 R 260003 R                    XOR* A
    00006 R 702204 A                    SETB
    00007 R 740000 A                    NOP
    00010 R 740000 A                    NOP
    00011 R 702240 A                    SETC2
    00012 R 740000 A                    NOP
    00013 R 740000 A                    NOP
    00014 R 702260 A                    CLEARB
    00015 R 620000 R                    JMP* LBS
            000000 A                    .END
    00016 R 000016 E *E

    00017 R 600000 A *L
SIZE=00020      NO ERROR LINES
```

10.2 SUPPORTING PAPERS

The following publications, presented at the International Conference on stepping motors and systems (Leeds 1974), are deemed to support this work.

(i) R.C. Johnson and M.E. Steele.

SOME ASPECTS OF INVERTER DRIVEN CLOSED LOOP STEPPING MOTOR SYSTEMS.

(ii) A. Hughes, P.J. Lawrenson, M.E. Steele and J.M. Stephenson.

PREDICTION OF STEPPING MOTOR PERFORMANCE.

(Also published in Electrical Review, 1974, Vol.195 No.5.)

SOME ASPECTS OF INVERTER DRIVEN CLOSED LOOP STEPPING MOTOR SYSTEMS

R C Johnson
University of Aston in Birmingham
Birmingham, England
and
M E Steele
University of Leeds
Leeds, England

1. INTRODUCTION

Present electrical stepping motors are considered to be small in comparison to most other types of electrical machine, but as improvements are made in stepping motor design, and as more effective driving methods are realised, it is likely that larger machines will be produced.

Manufacturers have not yet indicated such a trend, and some reasons that could account for this are:-

(i) The hydraulic stepping motor is already established for 'high-power' applications.

(ii) Instability due to resonance would be less acceptable in larger machines where it would be more important to maintain high overall efficiency.

(iii) Suitable drive circuits for electric power steppers are not yet sufficiently developed.

Given a suitable drive circuit the electric power stepping motor may offer some competition to its hydraulic counterpart.

The cycloinverter drive circuit presented here, although developed for a stepping motor has application in the control of other types of synchronous machine including the synchronous reluctance type which has been of much interest in recent years. It also is likely that some future designs for large stepping motors will stem from this type of machine, which is already well established and capable of being operated as a power stepper.

Drive circuits of the type proposed may also find application to machines of all sizes where relatively large amounts of energy are to be transferred for maximum possible acceleration in a closed loop system. The method of combining these circuits into a closed loop system will therefore also be discussed.

2. INVERTER CIRCUITS AND THEIR LIMITATIONS

2.1 Choice of Switching Device

Stepping motors can be operated from sinusoidal or switched supplies but the switched supply is the most common method of excitation. This is in accordance with operation as a digital device

and also results in less power dissipated in the driving circuit. The power requirements for most stepping motors can therefore be handled by transistors, and at present this is the standard method used. In applications involving large stepping motors, and in cases where considerable forcing is to be used, the thyristor may be found to be a more suitable device.

Since the invention of the thyristor in 1957 it has replaced other devices in a wide range of power circuits, including the control of many types of electrical machine. It is not surprising that the application of this device to the stepping motor has been somewhat neglected, since the basic transistor drive circuit is very simple. Provided with 'diode protection' the transistor can be safely turned 'on' or 'off' at any time, whereas thyristor circuits present special problems which require further discussion.

The price of power transistors is generally lower now than of a few years ago and devices of higher capability have become available, so the thyristor should not be expected to eventually replace the transistor entirely to drive small or medium sized machines. The thyristor is however capable of switching more power, for a single device, and is preferable where higher power levels are involved, especially commutation can be achieved with fairly simple circuitry.

2 Types of Inverter

For this application it is important to use an arrangement which will overcome the disadvantage of a limited frequency range generally associated with inverter circuits. The wide range of operating conditions for the stepping motor requires an inverter to operate from d.c. to several kHz. The facility to vary the output voltage to give similar driving currents at high and low frequencies may also be useful.

At low frequencies the parallel capacitor commutated inverter shown in Fig. 1 could be used. This circuit was known

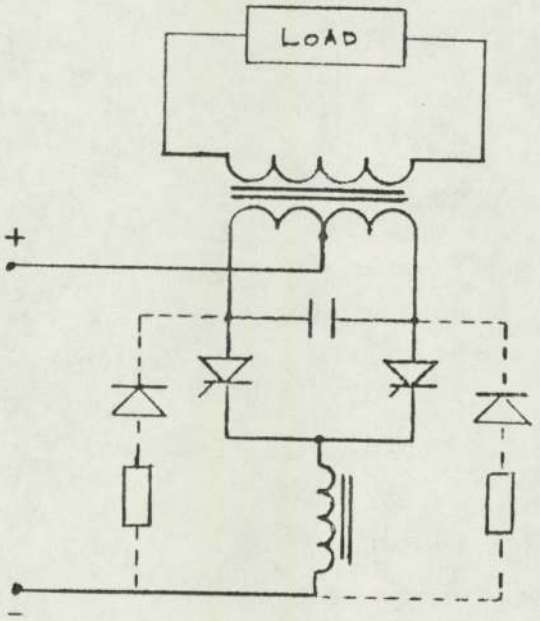

FIG. 1. Parallel Capacitor Commutated Inverter.

as early as 1932 using thyratrons and operation on resistive and inductive loads has been analysed by Wagner[1, 2] The circuit has many disadvantages. A large ballast inductance is required to maintain the continuous flow of direct current and to limit voltage overshoots, and in addition a large commutation capacitor is required for operation with inductive loads. The circuit has a limited load range and needs a minimum load to limit the peak voltage across the thyristors. Starting the inverter is also

difficult because of the time required to charge the large commutating capacitor.

As in many existing inverter circuits of the past, thyristors were directly substituted for thyratrons, but the better characteristics of the thyristor were not fully utilised by this direct replacement. The addition of diodes, shown dotted in Fig. 1, gave an improved circuit developed by McMurry and Bedford, which has been analysed by McMurry and Shattuck[3] The feedback diodes in the circuit return reactive energy associated with inductive loads to the d.c. supply. The capacitor and ballast inductor are no longer required to store this energy and may now be smaller. The improved inverter is less sensitive to changes in load or power factor and can operate over a wider, but still limited, frequency range.

It is necessary to remove the lower frequency limit for use as a stepping motor drive. This is easily achieved by simply omitting the transformer and using a centre tapped 'bifilar' motor phase winding.

Another desirable objective would be to increase the higher frequency limit, which is determined ultimately by thyristor turn-off time, but commutation losses reduce the efficiency at high frequencies and restrict useful operation to about 1 kHz.

The capacitor must be large enough to apply a reverse voltage across the thyristor during recovery but large currents will be delivered during the remainder of the cycle. It is possible to retain the charge on the capacitor until it is required for commutation by using the circuit of Fig. 2.

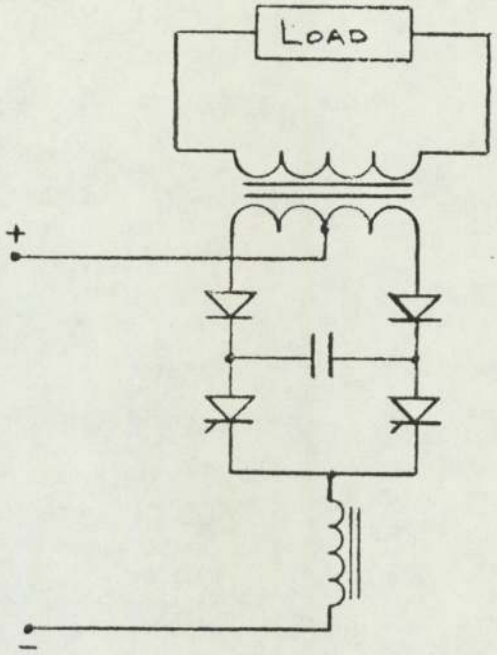

FIG.2 Improved Capacitor Commutated Inverter with Wide Frequency Range.

This technique[4] has been analysed by Ward[5] and has been shown to be suitable for operation over a wide range of frequency, particularly for drives where load resistance increases with frequency. Although this represents a further improvement, it was concluded that "adjustment of the capacitance as the frequency is varied must be accepted as a necessity and that there is the need to develop the means to do this automatically". No example was given to indicate what frequency range could be achieved in practice and so it may be of interest to consider the views of other later authors as to what constitutes a wide variable frequency.

To some[6], 150 Hz is considered to be a typical maximum frequency which will be improved upon by faster devices, rather than from circuit improvements. Another author[7] could see "no reason to suppose that frequencies up to say 400 Hz

re not practical with reasonable efficiency."

High frequency inverters have been eveloped which are self commutated by res- nating the load. These circuits are suit- ble for use above about 1 kHz because of e need for a resonant circuit which carries ll load current. The frequency may be as gh as 20 kHz but is basically fixed. Some ariation in frequency is possible by firing e thyristors at a lower rate than the res- nant frequency of the circuit and a frequency ange of 2 to 1 is about the maximum that can e achieved with a tolerable waveform.

One method, appearing to meet the equirements of operation over a wide requency, including d.c., is to use a cyclo- nverter fed from a high frequency supply. or many drives the cycloconverter is an lternative to the d c link inverter but for is application the d c link must remain ince the cycloconverter requires a high requency input. For operation from the .c. mains this implies three stages,) rectification, (ii) h.f. inversion and ii) cycloconversion, the latter two stages eing referred to as cycloinversion.

A circuit presented in 1969 by obertson and Hebbar[8], described as 'a uned circuit commutated inverter' operated s a block fired cycloinverter in which inver- ion and cycloconversion are not separable tages. It is this type of circuit which will e considered further.

A NATURALLY COMMUTATED CYCLO-INVERTER WITH WIDE FREQUENCY RANGE

1 Circuit Operation

Consider the circuit shown in Fig. 3, which operates as a cycloinverter.

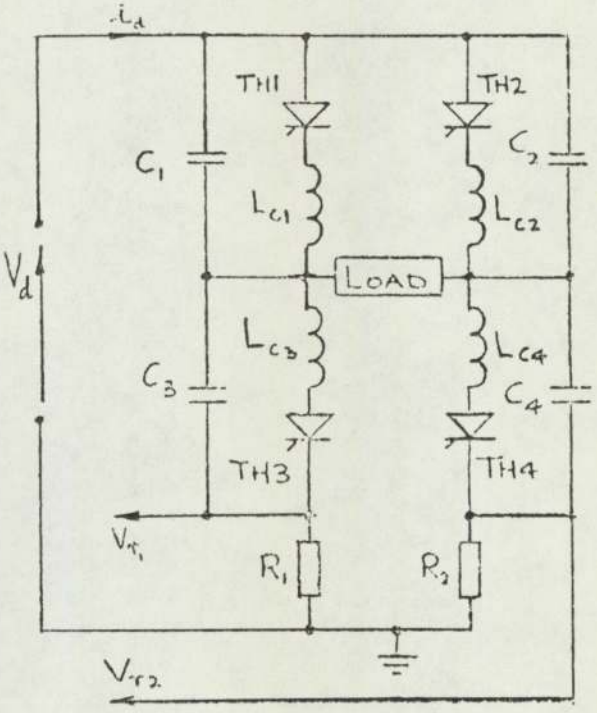

FIG. 3. Naturally Commutated Cyclo-inverter (one phase).

Let the capacitors have an initial voltage of $1/2\ V_d$. If pulses are applied to the gates of thyristors TH1 and TH4 current i_d flows through the commutating inductors L_{c_1} and L_{c4}, capacitors C_2 and C_3 charge and C_1 and C_4 discharge. The voltage across the load rises to a maximum value between V_d and $2V_d$, depending upon the type of load. The load current is then supplied from C_2 and C_3, which also charge C_1 and C_4, while the d.c. supply current i_d reduces to zero and TH1 and TH4 turn off. When the voltage across the load has fallen to a predetermined level, less than the supply, TH1 and TH4 are fired again and the cycle repeats. TH1 and TH4 may be fired a number of times in this manner.

The load current will be brought to

zero if no gate pulses are applied, or can be reversed by firing TH2 and TH3 for a number of cycles.

The inverter output can thus be 'modulated' at a frequency which is much lower than the natural frequency of the commutating circuit, and can easily be varied over a wide frequency range by simply altering the firing sequence. Fig. 4 shows the form of input current waveform produced by the firing sequence chosen, the output voltage being somewhat smoother.

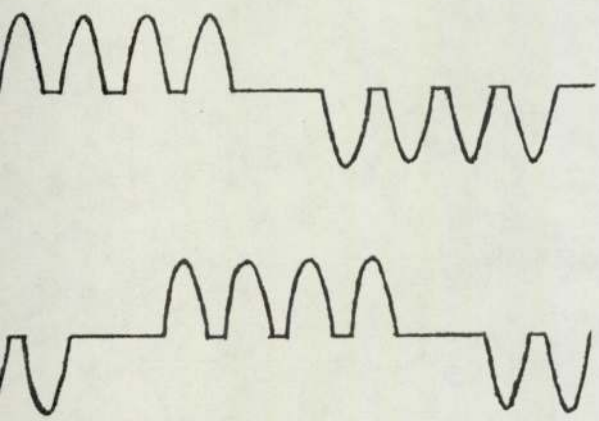

4. Sketch showing typical Input Current Waveform (two phases).

Other forms of modulation are possible which allow selected or general harmonic reduction such as pulse rate modulation. The circuit was used with a two-phase machine so that the sequence in Fig. 4 produces steps with alternately 'one phase on' and then 'two phases on.'

As the frequency varies, output voltage adjustment is required to give an approximately constant load current and this can be achieved by using a feedback signal proportional to the load current taken from $V_{r_1} - V_{r_2}$. If the firing signals are of a high frequency, these can be inhibited if the load current is greater than a preset value or enabled if it is less than this value. The thyristors then fire at a suitable frequency.

Fig. 5 shows the voltage waveform across a resistive load as the output frequency is increased, and Fig. 6 gives the corresponding inverter characteristics. Circuit values used are

$V_d = 50V$

Current reference level = 1A

$R_1 = R_2 = 1\Omega$

$C_1 = C_2 = C_3 = C_4 = 6\mu F$

$L_{c_1} = L_{c_2} = L_{c_3} = L_{c_4} = 14\mu H$

With an additional series load inductance of 10 mH the voltage and current waveforms are as shown in Fig. 7, and the characteristic given in Fig. 8.

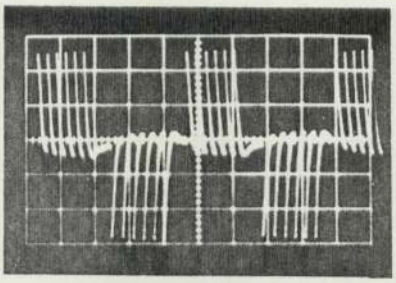

FIG. 5a.

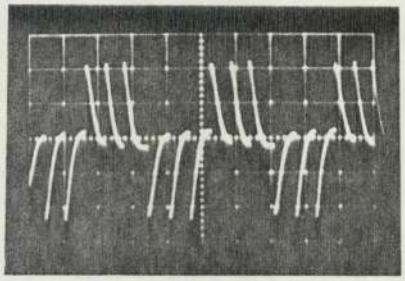

FIG. 5b.

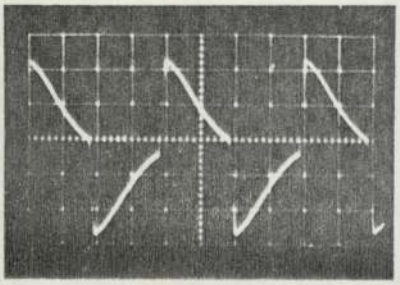

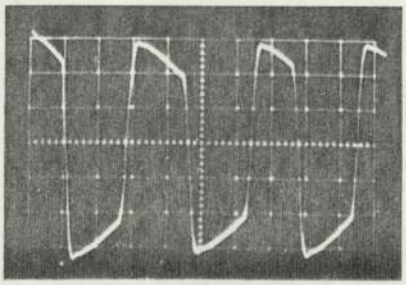

FIG. 5. Output Voltage Waveforms with Resistive Load.

	(a)	(b)	(c)	(d)
Output frequency, (Hz)	125	300	1,250	3,000
Time scale (ms/div)	2	1	0.2	0.1

V scale = 20V/div

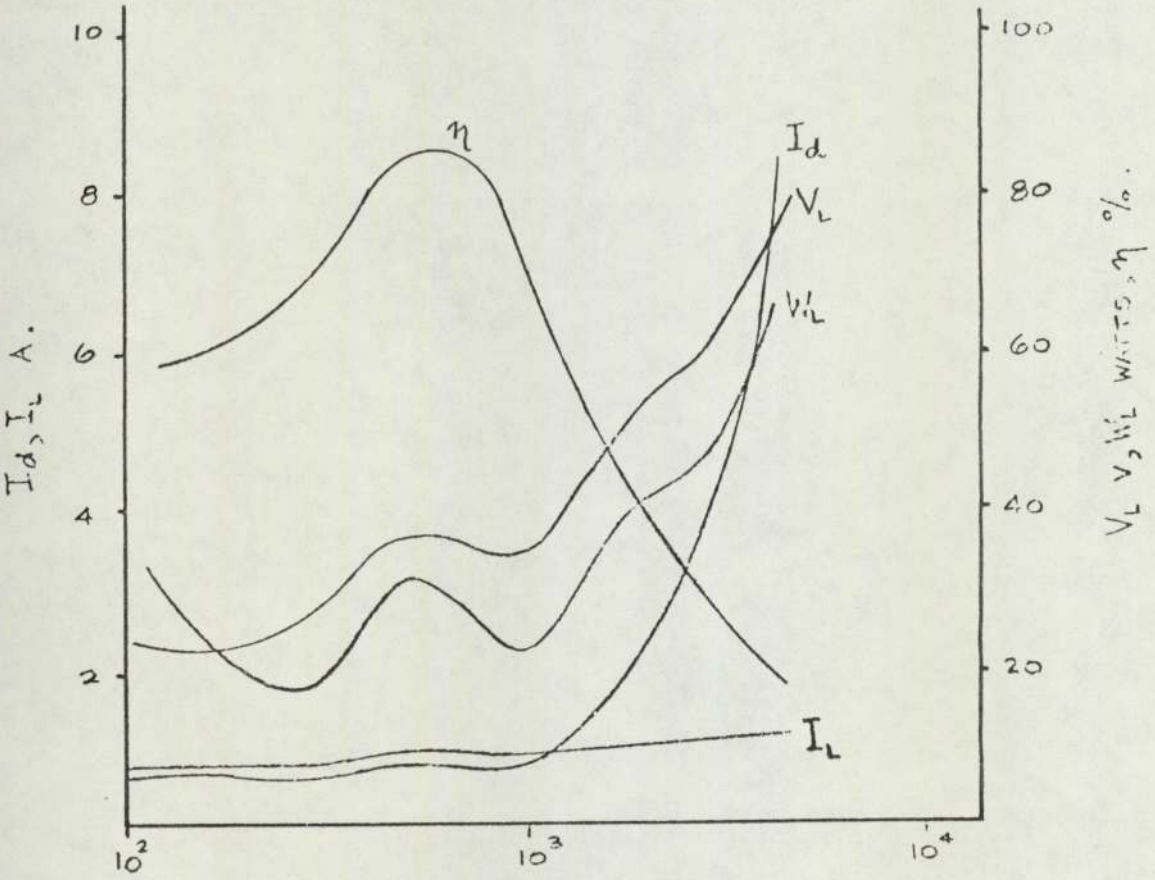

FIG. 6. Cycloinverter Characteristics with Resistive Load.

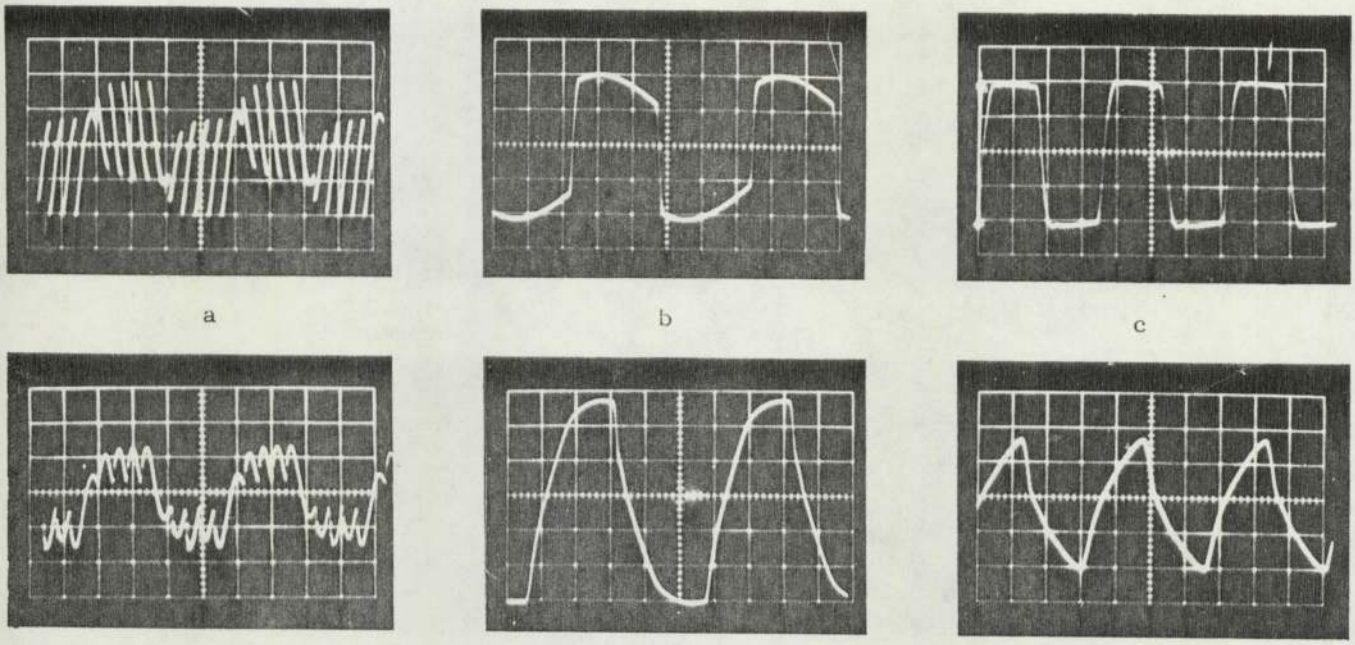

FIG. 7. Output Voltage and Current Waveforms with Inductive Load.

	(a)	(b)	(c)
Output frequency (Hz)	125	1,000	3,000
t scale (ms/div)	2	0.2	0.1
V scale (V/div)	20	40	40
I scale (A/div)	0.5	0.5	0.5

Upper Waveforms - Voltage
Lower Waveforms - Current

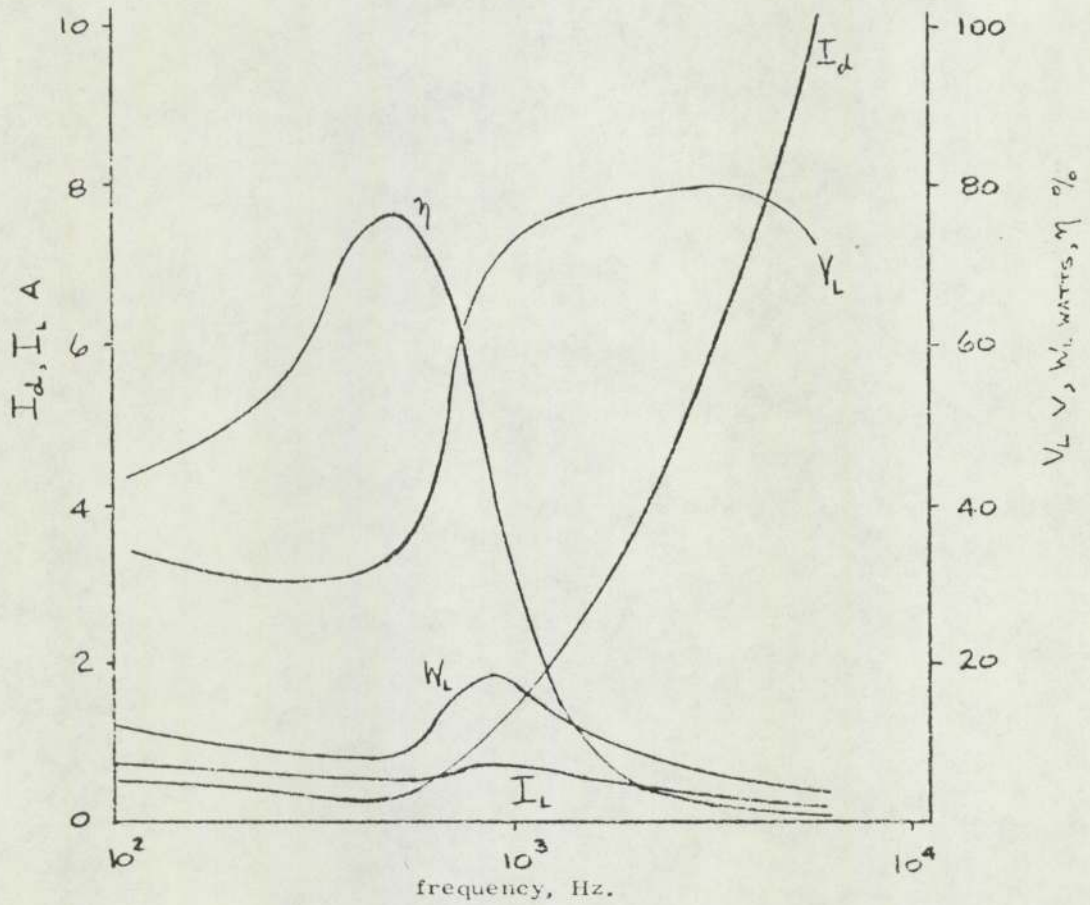

FIG. 8. Cycloinverter Characteristics with Inductive Load.

3.2 Features of the Improved Cycloinverter

The main advantage of using the capacitors in a bridge arrangement, instead of across the load, as in ref. 8, is increased reliability of commutation, for the following reasons.

(i) At instants when all thyristors are 'off' the load is no longer 'floating'. A capacitor is present for each thyristor to reduce the risk of damage by by-passing any spurious voltage transients which may occur.

(ii) When two thyristors, such as TH1 and TH4, are commutated they are effectively in series and the capacitors provide an equalising network so that during 'turn on' and 'turn off' the thyristors share equal voltages.

(iii) The risk of false triggering of the thyristors is also reduced. Suppose TH1 turns on' faster than TH4. This could be due to devices having slightly different characteristics, or a difference of a microsecond or so in the application of the gate pulses. In the single capacitor circuit a high rate of rise of anode voltage may then trigger TH3 and short circuit the bridge.

(iv) The capacitors also assist to prevent a drop in bridge input voltage from hindering commutation due to the internal impedance of the supply. If this is not sufficient, additional capacitance may be required across the input to the bridge.

With both resistive and inductive loads satisfactory commutation can be achieved provided the circuit is underdamped. With a stepping motor load the main difference in circuit operation appears to be that this condition is no longer sufficient. The circuit was used with a permanent magnet machine and it was found that the e.m.f. due to the permanent magnet can occasionally interfere with the commutation. If the current through TH1 and TH4 ever fails to reach zero before TH2 and TH3 are turned on, commutation can fail. This can be avoided by having a high mutual coupling between L_{c_1} and L_{c_3} and between L_{c_2} and L_{c_4}. This does not effect the operation of the circuit, as described earlier.

Suppose the current through TH1 becomes non oscillatory and the thyristors remained conducting when TH2 and TH3 are turned on. The high rate of rise of current through TH3 will induce an e.m.f. in L_{c_1}. The voltage across C_1 will be low and most of the induced e.m.f. will appear as a reverse voltage across TH1, increasing 'turn off time' to this thyristor and effecting commutation. This is a method of forced commutation, easily built into the circuit, which can 'take over' on instances of failure of natural commutation.

4. CLOSED LOOP STEPPING MOTOR SYSTEMS

4.1 Method of Phase Angle Control

The principle of phase angle control is to generate the input pulse sequence to the motor from the electrical angular position of the rotor (θ_e) and then synchronism is inherently maintained. This sequence, $F(\theta_e)$, may be shifted in phase by an angle γ giving the driving function $F(\theta_e + \gamma)$.

Analogue methods[9, 10] have been used to control the angles of phase shift, but most methods employ digital techniques.

Consider the logic signals PA and
and their inverses $\overline{PA}$ and $\overline{PB}$, as shown
Fig. 9 and let these indicate quadrant
ormation of the electrical angular position
the rotor of a two-phase machine.

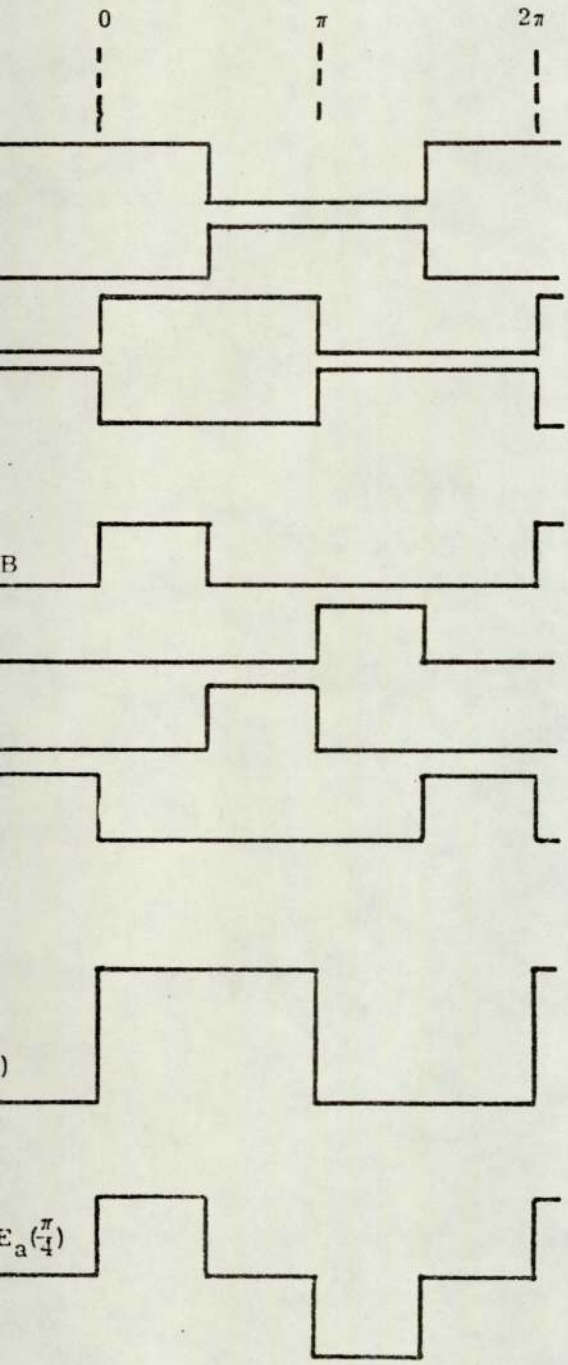

9. Typical signals for 2 phase and 1 phase modes, using Fredriksen method.

The fundamental components of these signals are

$$D(o)_1 = (\cos\theta_e \; -\cos\theta_e \;\; \sin\theta_e \; -\sin\theta_e) \quad (1)$$

where the set D(o) is,

$$D(o) = F(\theta_e) = (PA\ \overline{PA}\ PB\ \overline{PB}) \quad (2)$$

The windings each have three states of energisation E.

Let, E = 0, represent an unenergised state

E = 1, represent the winding energised, in one sense

E = -1, represent the winding energised, in an opposite sense..

Two bi-level logic signals D_1 and D_2 are required to define E as shown in Table 1.

E	D_1	D_2
0	0	0
1	1	0
-1	0	1

TABLE 1

Thus the set of driving signals,

$$D = (D_{a_1}\ D_{a_2}\ D_{b_1}\ D_{b_2}) \quad (3)$$

defines the set,

$$E = (E_a\ E_b) \quad (4)$$

and hence the state of the input to the machine.

A phase shift γ is easily obtained if this is a multiple of $\pi/2$. e.g. to obtain $\gamma = \pi/2$,

let, $F(\theta_e + \pi/2) = D(\pi/2) = (PB\ \overline{PB}\ \overline{PA}\ PA)$ (5)

i.e. $D(\pi/2)_1 = (\sin\theta_e \; -\sin\theta_e \; -\cos\theta_e \; \cos\theta_e)$ (6)

Thus we have the driving circuit signals in terms of position signals for phase angles of even step multiples. .

Control Modes	γ (steps)	D_{a_1}	D_{a_2}	D_{b_1}	D_{b_2}
CW	$-\pi/2$ (-2)	$\overline{PB}$	PB	PA	$\overline{PA}$
STOP	0 (0)	PA	$\overline{PA}$	PB	$\overline{PB}$
CCW	$\pi/2$ (2)	PB	$\overline{PB}$	$\overline{PA}$	PA
HS	π (4)	$\overline{PA}$	PA	$\overline{PB}$	PB

TABLE 2

The choice of four phase angles have been termed control modes by Fredriksen[11], as shown in Table 2. This method has been extended to give eight phase angles by deriving signals for the so called 'single-phase sense.' (Odd step multiples).

Control Modes	γ (steps)	D_{a_1}	D_{a_2}	D_{b_1}	D_{b_2}
CWMED	$-3\pi/4$ (-3)	$\overline{PA}\,\overline{PB}$	PA PB	PA $\overline{PB}$	$\overline{PA}$ PB
CWLOW	$-\pi/4$ (-1)	PA $\overline{PB}$	$\overline{PA}$ PB	PA PB	$\overline{PA}\,\overline{PB}$
CCWLOW	$\pi/4$ (1)	PA PB	$\overline{PA}\,\overline{PB}$	$\overline{PA}$ PB	PA $\overline{PB}$
CCWMED	$3\pi/4$ (3)	$\overline{PA}$ PB	PA $\overline{PB}$	$\overline{PA}\,\overline{PB}$	PA PB

TABLE 3

These sets can be related by observing that, for n = ± 1, ± 3 etc.

$$D\left(\frac{n\pi}{4}\right) = D\left(\frac{(n-1)\pi}{4}\right) \quad D\left(\frac{(n+1)\pi}{4}\right) \qquad (7)$$

and for n=0, ± 2, ± 4 etc.,

$$D\left(\frac{n\pi}{4}\right) = D\left(\frac{(n-1)\pi}{4}\right) + D\left(\frac{(n+1)\pi}{4}\right) \qquad (8)$$

Note that all phase angles do not give the same pulse width. By using more logic signals other pulse widths and a wider choice of phase angles is possible.

4.2 An Optical Method of Phase Angle Control

This method reduces the amount of hardware that would be involved with the previous method if a wide choice of phase angles is required. In the previous method, signals would usually be obtained optically and then processed electrically. With the alternative optical arrangement, processing is not required.

Consider four photo transistors T_1, T_2, T_3, T_4 and four light sources S_1, S_2, S_3, S_4 arranged either side of a slotted disc, as in Fig. 10.

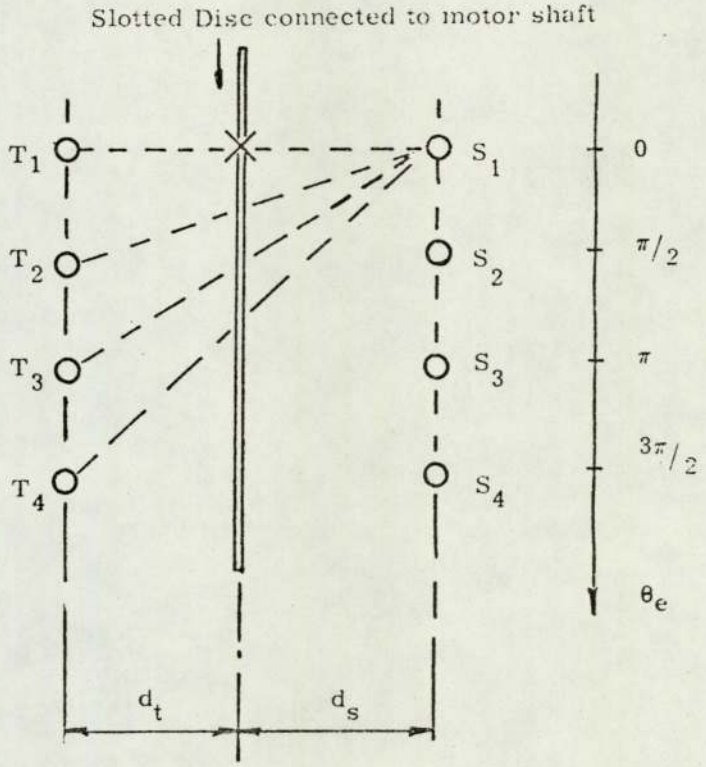

FIG. 10. Arrangement for Optical Method.

Let the electrical angular spacing between transistors be $\pi/2$ and let the disc be positioned so that

$$d_t = d_s \qquad (9)$$

Consider the edge of a slot, represented by point X on the disc, in line with T_1 and S_1 as it moves in the direction indicated. X will be in line with T_2 and S_1, T_3 and S_1, T_4 and S_1 when the disc has moved through $\pi/4$, $\pi/2$ and $3\pi/4$ respectively. Suppose the light from each source is able to radiate to all photo-transistors. If source S_1 only is active, the signals from the photo-transistors have a mutual phase displacement of $\pi/4$, as in Table 4.

	Transistors in Line with x			
	Active Source			
θ_e	S_1	S_2	S_3	S_4
0	T_1	-	-	-
$\pi/4$	T_2	T_1	-	-
$\pi/2$	T_3	T_2	T_1	-
$3\pi/4$	T_4	T_3	T_2	T_1
π	-	T_4	T_3	T_2
$5\pi/4$	-	-	T_4	T_3
$3\pi/2$	-	-	-	T_4

TABLE 4

The signals are effectively shifted by $\frac{\pi}{4}$ using source S_3 and by $\frac{3\pi}{4}$ using source S_4 giving, in this case four phase angles. For any single active source S the phase of any transistor signal T is given by the mean electrical angular displacement of S and T from the reference position. The number of phase angles is determined by the number of sources and the width of the slot can be used to determine pulse width.

4.3 Systems Using Photo-thyristors

An important feature of the above optical method is that a single device could be used both to detect levels and be part of the driving circuit. If this is a photo-transistor the low power handling capabilities limit their use in this manner to very small machines.

Power-photo-transistors do not appear to be available and light-activated switches or other similar devices are unsuitable. However, if a photo-thyristor is used the reduction in the amount of hardware is such that it would often be feasible to mount all the components along with the disc inside an extended motor enshield. As an example, Fig. 11 shows a McMurray-Bedford type of inverter and a bifilar wound stepping motor. The complete phase angle control system could be regarded as a single module. Protected from stray light and dust, with a minimum of circuitry, it would be well suited to an industrial environment and require little maintenance.

4.4 Combining Optical and Electronic Methods

By combining the optical and electronic methods, a wide choice of phase angles can be obtained with a reasonably simple system.

Suppose that the optical method could be used to give a choice of n phase angles and that the electronic method, when used separately, gives a choice of m phase angles. When combined, these methods can give a

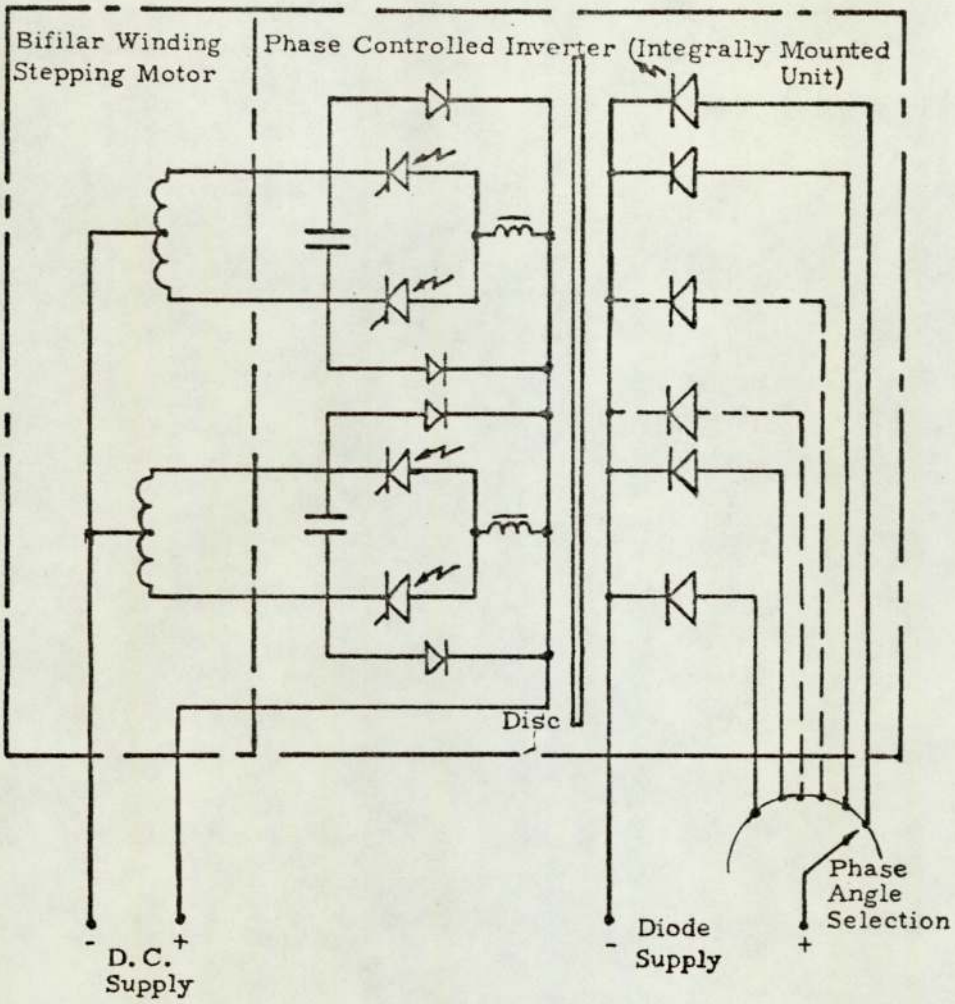

FIG. 11. Modular Approach to Phase Angle Controlled Stepping Motor.

oice of up to n x m phase angles. The ombined method' is therefore consider- ly more effective than either method us- separately.

As an example, consider the com- ned method applied to the inverter cir- it of Fig. 3. 'E' is given in terms of the yristor gate signals by Table 5.

With four position signals, as shown Fig. 12, eight phase angles are possible ing logic.

G_1	G_2	G_3	G_4	E
0	0	0	0	0
0	0	X	X	0
X	X	0	0	0
1	0	0	1	1
0	1	1	0	-1

X = either state

TABLE 5

When the inverter was described, the driving signals used were,

$$D_1 = G_1 = G_4 \quad (10)$$
$$D_2 = G_2 = G_3 \quad (11)$$

For a pulse width of $3\pi/4$ in E the driving signals would have the form shown in Fig. 13(a), but this is not the only way of producing the desired form of E. An alternative is to use the position signals, without processing, and to define,

$$D_1 = G_1 = \overline{G_3} \qquad (12)$$

$$D_2 = G_2 = \overline{G_4} \qquad (13)$$

Reference to Fig. 13 and Table 5 will show that this alternative produces the same result. Table 6 shows the driving signal functions for both cases.

and similarly for D_{a_2}, D_{b_1} and D_{b_2}.

These functions are readily generated using MSI data selectors.

The position signals can be obtained using the optical method with four photo transistors spaced as in Fig. 10, and a single LED would give the above choice of eight phase angles.

A further diode placed at an angle 2δ from the previous diode would give a further eight phase angles, displaced from those above by the angle δ.

		$D_1 = G_1 = G_4$ $D_2 = G_2 = G_3$				$D_1 = G_1 = \overline{G_3}$ $D_2 = G_2 = \overline{G_4}$				γ Binary		
γ	(steps)	D_{a_1}	D_{a_2}	D_{b_1}	D_{b_2}	D_{a_1}	D_{a_2}	D_{b_1}	D_{b_2}	U	V	W
$-3\pi/4$	(-3)	$\overline{P_2}\,\overline{P_3}$	$P_2\,P_3$	$\overline{P_4}\,P_1$	$P_4\,\overline{P_1}$	$\overline{P_3}$	P_2	P_1	P_4	1	0	1
$-\pi/2$	(-2)	$\overline{P_3}\,\overline{P_4}$	$P_3\,P_4$	$P_1\,P_2$	$\overline{P_1}\,\overline{P_2}$	$\overline{P_4}$	P_3	P_2	$\overline{P_1}$	1	1	0
$-\pi/4$	(-1)	$\overline{P_4}\,P_1$	$P_4\,\overline{P_1}$	$P_2\,P_3$	$\overline{P_2}\,\overline{P_3}$	P_1	P_4	P_3	$\overline{P_2}$	1	1	1
0	(0)	$P_1\,P_2$	$\overline{P_1}\,\overline{P_2}$	$P_3\,P_4$	$\overline{P_3}\,\overline{P_4}$	P_2	$\overline{P_1}$	P_4	$\overline{P_3}$	0	0	0
$\pi/4$	(1)	$P_2\,P_3$	$\overline{P_2}\,\overline{P_3}$	$P_4\,\overline{P_1}$	$\overline{P_4}\,P_1$	P_3	$\overline{P_2}$	$\overline{P_1}$	$\overline{P_4}$	0	0	1
$\pi/2$	(2)	$P_3\,P_4$	$\overline{P_3}\,\overline{P_4}$	$\overline{P_1}\,\overline{P_2}$	$P_1\,P_2$	P_4	$\overline{P_3}$	$\overline{P_2}$	P_1	0	1	0
$3\pi/4$	(3)	$P_4\,\overline{P_1}$	$\overline{P_4}\,P_1$	$\overline{P_2}\,\overline{P_3}$	$P_2\,P_3$	$\overline{P_1}$	$\overline{P_4}$	$\overline{P_3}$	P_2	0	1	1
π	(4)	$\overline{P_1}\,P_2$	$P_1\,P_2$	$\overline{P_3}\,\overline{P_4}$	$P_3\,P_4$	$\overline{P_2}$	P_1	$\overline{P_4}$	P_3	1	0	0

TABLE 6

If U V W represent the electronically selected phase angle, then driving signals can be expressed as,

$$D_{a_1} = P_2\,\bar{U}\bar{V}\bar{W} + P_3\,\bar{U}\bar{V}W + P_4\,\bar{U}V\bar{W} + \overline{P_1}\,\bar{U}VW + \overline{P_2}\,U\bar{V}\bar{W} + \overline{P_3}\,U\bar{V}W + \overline{P_4}\,UV\bar{W} + P_1\,UVW \qquad (14)$$

Using eight diodes spaced $\pi/16$ apart a full range of 64 phase angles can be obtained in increments of $\pi/32$. If that part of the phase angle which is obtained optically is represented by bits XYZ, then it is re-

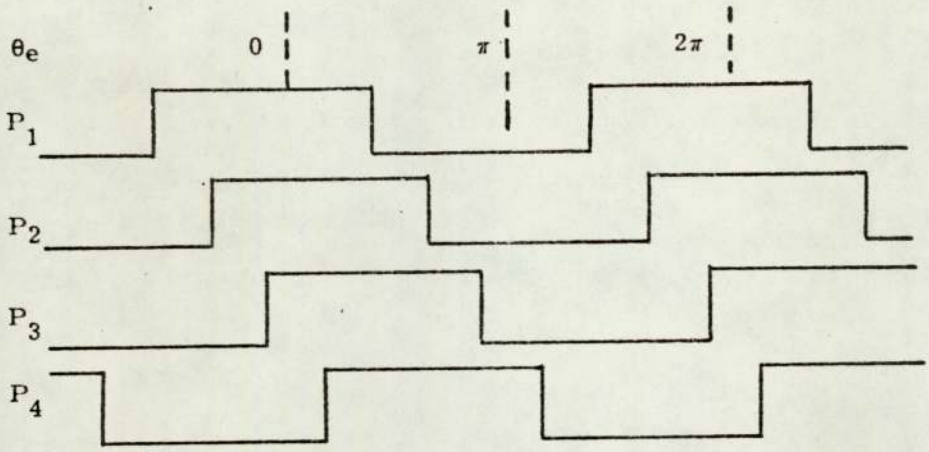

FIG. 12. Position Signals for Combined Method.

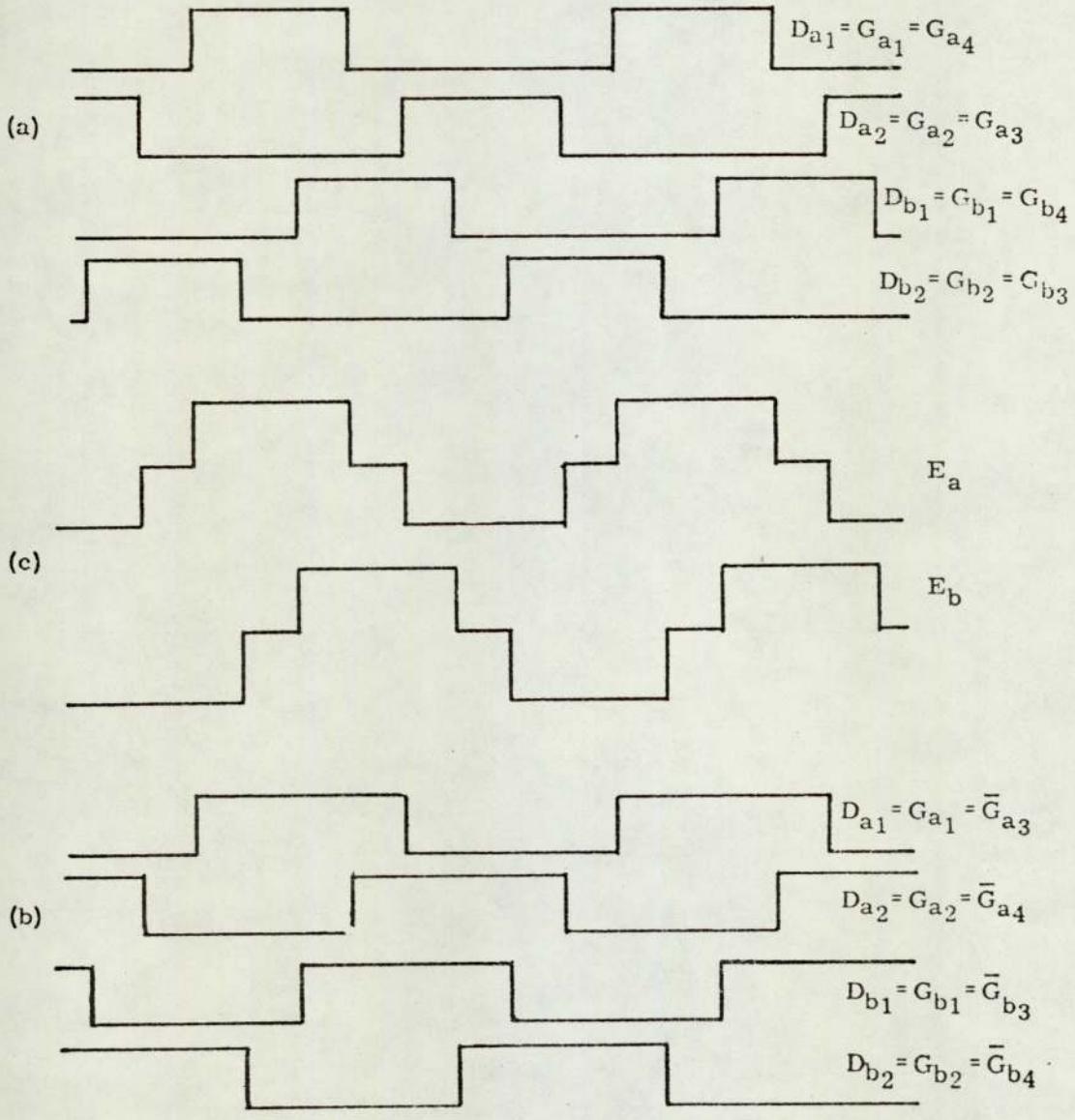

FIG. 13. Alternative Driving Sequences (a) and (b) Producing same Energisation Sequence (c).

uired that diodes 0 to 7 be selected accord-
g to the binary value of XYZ. This is
eadily achieved using MSI with a unit such
s a 2-line to 4-line decoder connected
give "1 of 8" selection as shown in Fig. 14.

5. CONCLUSIONS

The use of the thyristor as a driving circuit element has been discussed with reference to the probable development of power stepping motors. Some basic inver-

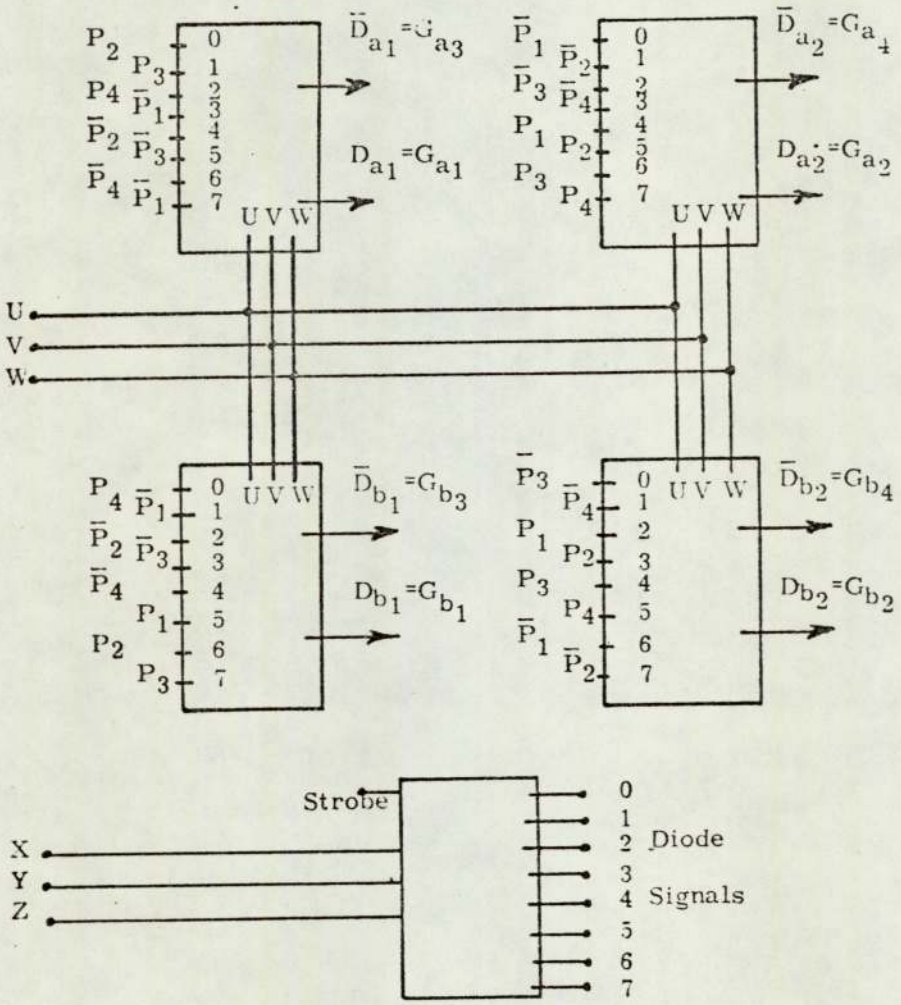

FIG. 14. Phase Angle Control Circuit Using MSI.

Therefore using only five integrated circuits a choice of 64 phase angles is available by the setting of a six bit word at the interface.

ter circuits have been reviewed and their limitations for this application explained. A cyclo-inverter circuit that was developed for a closed loop stepping motor control

stem has also been described.

Finally the technique of phase angle ntrol has been reviewed and a digital ethod of accurate phase control presented.

ACKNOWLEDGEMENT

M E Steele acknowledges the financial support given by the UK Science Research Council.

REFERENCES

WAGNER, G.F. : 'Parallel inverter with resistive load,' Trans.Amer.Inst.Elect. Engrs., 1935, 54, p1227.

WAGNER, G.F. : 'Parallel inverter with inductive load,' ibid, 1936, 55, p970.

McMURRAY, W. and SHATTUCK, D.P.: 'A silicon controlled rectifier inverter with improved commutation,' ibid, 1961, 80, (Pt.I), pp531-542.

HAMUDMANOV, M.Z.: 'Variable frequency operation of synchronous motors using electronic frequency changer' in 'The technical problems of electric drives' USSR Acadamy of Science, 1957.

WARD, E.E.: 'Inverter suitable for operation over a range of frequency,' Proc.IEE, 1964, 111, pp1423-1434.

BRADLEY, D.A.; CLARKE, C.D.: DAVIS, R.M. and JONES, D.A.: 'Adjustable frequency inverters and their application to variable speed drives,' Proc.IEE, 1964, 111 pp1833-1846.

KING, K.G.: 'Variable frequency thyristor inverters for induction motor speed control,' Direct Current, 1965, 10.

ROBERTSON, S.D.T. and HEBBAR, K.M.: 'A tuned circuit commutated inverter,' Power thyristors and their applications, IEE Conf. Publication 53, 1969, Pt.1, pp297-304.

9. DOUCE, J.L. and REFSUM, A.: 'The control of a synchronous motor,' 1966 IFAC Congress Paper 4A.
10. ANDREW, P.: 'The stepping motor as a machine-tool actuator,' Electronics and Power, 1972, Feb, pp62-63.
11. FREDRIKSEN, T.R.:'Closed loop stepping motor application,' 1965 J.A.C.C. pp531-538 and 1966 IFAC Congress Paper 25C.

PREDICTION OF STEPPING MOTOR PERFORMANCE

A Hughes, P J Lawrenson, M E Steele and J M Stephenson
University of Leeds
Leeds, England

INTRODUCTION

There seems to be a surprisingly widespread ression that prediction of stepping motor per- mance presents substantial difficulties. This not the case; and it is the purpose of this er to outline the different approaches which available.

Possible reasons why special difficulties ht be thought to apply in the case of stepping ors (as compared with more conventional hines) are that (i) they are commonly applied er control sequences which may in themselves quite complex and (ii) the rotor motion is ays to some degree irregular (even when wing fast) because it is the coalesence of itional step responses which interact in ying degrees. Actually, however, neither of se factors lead, even in the most general e, to difficulties which are in any way grea- than those normally encountered in studying transient behaviour of a more conventional hine (for example, the oscillation of a large chronous generator following a sudden load nge, or the run-up from rest of an induc- n motor). In fact, because (in open-loop es, particularly) the motion is continuously ined (and monitored) in distinct quanta, per- mance calculations can often be easier than more conventional machines (see approach 2 ow).

In making the above statement, it has been umed that the starting information for the culation consists of measured motor data. s data might relate to torque/displacement ves, torque/speed curves or inductance or x linkage/position curves, depending upon the ree of refinement of the study. It is not ng suggested that it is a straightforward matter, at the present time, to predict perfor- mance starting from a knowledge of the design dimensions of the motor. But again, this situa- tion is largely the same for conventional machines, although somewhat greater confidence in wholly theoretical studies is possible with the latter because of the much longer experience with them.

There are basically three different starting points, leading to three approaches which provide varying degrees of completeness and reliability of solution.

1. Starting with the steady-state, synchronous pull-out torque against speed (or pulse rate) characteristic it can be judged immediately in broad terms if a motor is adequate to deal with a particular load; and, merely by a single inte- gration of the mechanical equation for the system, it is possible to estimate acceleration and deceleration times. A further integration enables the number of steps associated with acceleration and retardation sequences to be cal- culated. This method is essentially the same one used with conventional machines, for example, to calculate the run-up time for a d.c. or induction motor, from steady-state characteristics (though an important distinction must be made as dis- cussed below). It gives rather rough and ready guidance only.

2. Starting with the torque/displacement curve, a suitable double-integration procedure on the mechanical equation can lead to quite detailed and quite reliable prediction of complete per- formance. This includes instantaneous positional information which is impossible by approach (1). There is no direct equivalent of this method in normal use for more conventional machines. It is adequate for many application studies.

Neither this method nor that above involve calculation of the changes taking place in the electrical circuits. (This second method implies a second-order-system model of the motor.)

3. Starting with a knowledge of the electrical impedances, including the dependance of inductance or flux linkage on position (and in a complete model, on the instantaneous currents and voltages) all aspects of performance can be fully studied. The procedure involves the integration of the simultaneous equations for the electrical circuits and the mechanical equation. The level of approach corresponds with that normal in full transient studies of other types of machine. It is necessary for serious motor-design work, and to estimate the reliability of the simpler approaches.

In all practical cases, integration has to be carried out numerically (sometimes graphically) but there are many well established techniques for doing this with the above types of problem. All of the foregoing may be most readily visualised in terms of open-loop operation, but it applies equally to closed-loop operation. In either case the crucial controlling features are the same - the location and timing of the drive impulses.

In the following sections each approach is outlined and a typical application indicated.

2. APPROACH USING STEADY-STATE TORQUE/SPEED CHARACTERISTICS

2.1 General

A problem which is often encountered is to establish how quickly a motor can accelerate its load up to a certain speed, or, conversely, how quickly it can be decelerated. The steady-state torque vs. speed (or pulse rate) curve offers a simple way of calculating the minimum theoretically possible acceleration and deceleration times, though, as explained below, the motor will not usually be able to reach these times when operated in an open loop.

The torque vs. pulse rate curve is generally of the form shown in Fig. 1(i), the pull-out-torque falling off at high stepping frequencies.

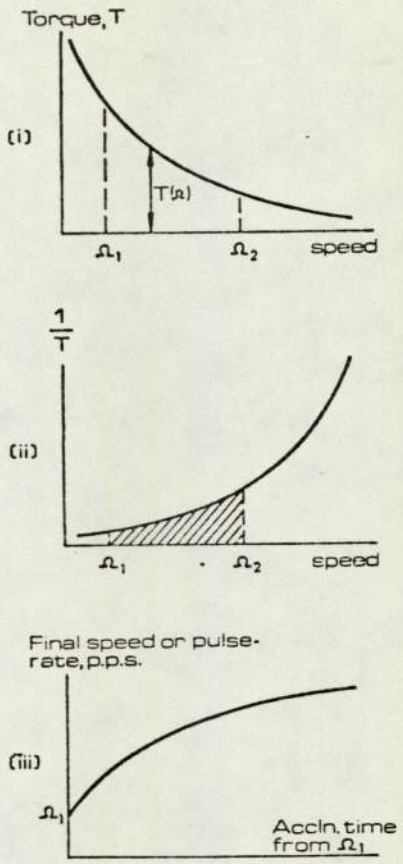

FIG. 1 Calculation of acceleration time using steady-state pull-out torque/speed curve

In practice resonance effects of varying magnitudes will be present, as discussed in section 2.4. (It ought to be emphasised here that a particular curve applies to a given motor together with a particular drive circuit, and that a quite different curve may be obtained from the same motor with a different drive circuit. Strictly speaking, a given curve is only correct for the particular inertia used when the test results were obtained, and, although the overall envelope of the curve is relatively insensitive to changes in inertia, the resonance regions can alter considerably.)

In practice the torque predicted by this curve would only be available if the load angle of the motor was continuously maintained at pull-out, a situation which can only be achieved exactly using a closed-loop control. It can be approached on open-loop using a well chosen

ping function. Thus, altho·gh calculations ed on the curve are optimistic for an open o scheme, it does enable a lower limit on the eleration time to be estimated.

Inertia Load

Consider first the simplest case in which re is no friction or other torque load. pose it is required to find the minimum time which the motor can accelerate from an initial eady) speed of Ω_1 (corresponding to a stepping quency, or pulse rate, of p_1 p.p.s.), to a new ed of Ω_2 (pulse rate p_2) in the absence of any d torque. At any intermediate speed Ω, the imum possible electromagnetic torque developed the motor is given by the corresponding value torque taken from the torque-speed curve, ch may be written as $T(\Omega)$.

All the torque $T(\Omega)$ is available to produce eleration and the equation of motion is simply

$$= J \frac{d^2\theta}{dt^2} = J \frac{d\Omega}{dt} \qquad (1)$$

re J is the total inertia referred to the or shaft. Integrating equation (1), the e taken to accelerate from speed Ω_1 to Ω_2 is en by

$$= J \int_{\Omega_1}^{\Omega_2} \frac{d\Omega}{T(\Omega)} \qquad (2)$$

the acceleration time is obtained by inteting the inverse of the torque with respect speed between the initial and final speeds. is shown graphically in Fig. 1(ii), where shaded area is the value of the integral

$$\frac{d\Omega}{T(\Omega)}$$

curve of $1/T(\Omega)$ being derived directly from curve of T. The integration can be perforgraphically, or by means of a simple comr integration routine.

By performing the integration for a range $_2$, a graph of time against final pulse rate be constructed as shown in Fig. 1(iii) and a further integration then gives the total angle turned through and, hence, the number of steps associated with a given acceleration sequence.

With purely inertial loads, the times to accelerate and decelerate between two given speeds are the same.

2.3 Torque Load

The effect of load and friction torques is to increase the acceleration time and reduce the deceleration times. The load torque, T_L, opposes the motor torque during acceleration, leaving $(T-T_L)$ as the torque available for acceleration, as shown in Fig. 2(i). The acceleration time is

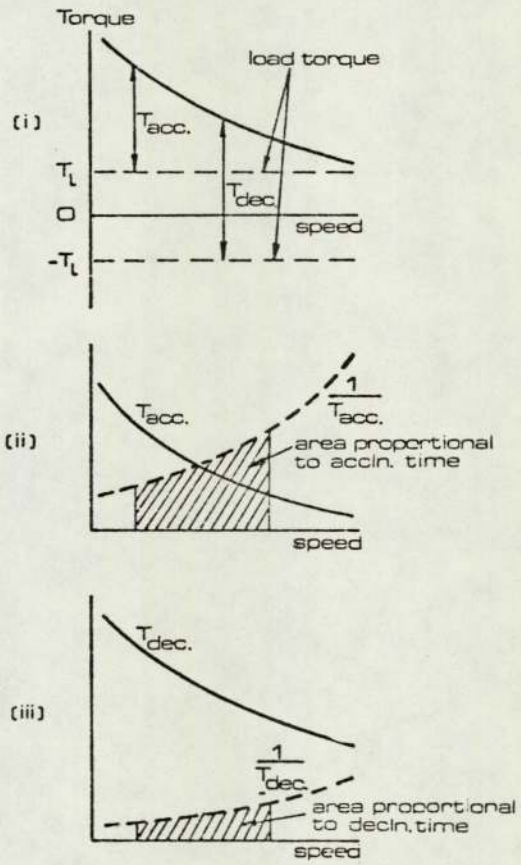

FIG. 2 Effect of load torque on acceleration time

thus proportional to the area under the graph of $1/(T-T_L)$ vs. Ω, as shown in Fig. 2(ii).

On the other hand, during deceleration the load torque assists the motor torque, giving a total decelerating torque of $(T+T_L)$. The deceleration time is proportional to the area under the curve of $1/(T+T_L)$, as shown in Fig. 2(iii).

In either case $(T \pm T_L)$ is used in place of T in equation (2).

If in addition there is a viscous friction term, the equation of motion is

$$T(\Omega) = J \frac{d\Omega}{dt} + K_v \Omega \qquad (3)$$

where the viscosity constant K_v is expressed in units of torque/velocity. K_v usually has to be estimated. The acceleration time is then obtained from the integral

$$t = J \int_{\Omega_1}^{\Omega_2} \frac{d\Omega}{T(\Omega) - K_v \Omega}$$

2.4 Resonances

In practice, the torque-speed curves are rarely as smooth as shown in Figs. 1 and 2, and there are often quite severe dips in the torque curve ('resonances'). Whether or not their effect on the acceleration time is significant depends on the 'depth' and 'width' of the dips. Even substantial torque reduction over a limited frequency range (say 5 p.p.s.) is likely to make little difference to the area under the curve of 1/Torque, but a more modest dip spread over a wide band of frequency, say 200 p.p.s., may have a significant effect on the acceleration time. Insofar as the present approach only aims to give the minimum theoretical time, it is fair to assume that the dips have been 'smoothed out' before performing the integration.

2.5 An example

The steady-state pull-out torque curve for a 200 step/rev. hybrid motor with a bi-polar constant-current drive is shown in Fig. 3(i). The load torque is 3000 gm.cm., and the total inertia referred to the motor shaft is 2000 $gm.cm^2$. What is the minimum time in which the speed can be increased from 500 p.p.s. to 2000 p.p.s.?

The graph of $1/(T-T_L)$ derived from (i) is shown in Fig. 3(ii). The area under the curve between 500 p.p.s. and 2000 p.p.s. is 0.135 $(gm.cm.sec)^{-1}$. Hence the minimum acceleration time for a total inertia of 2000 $gm.cm^2$ is

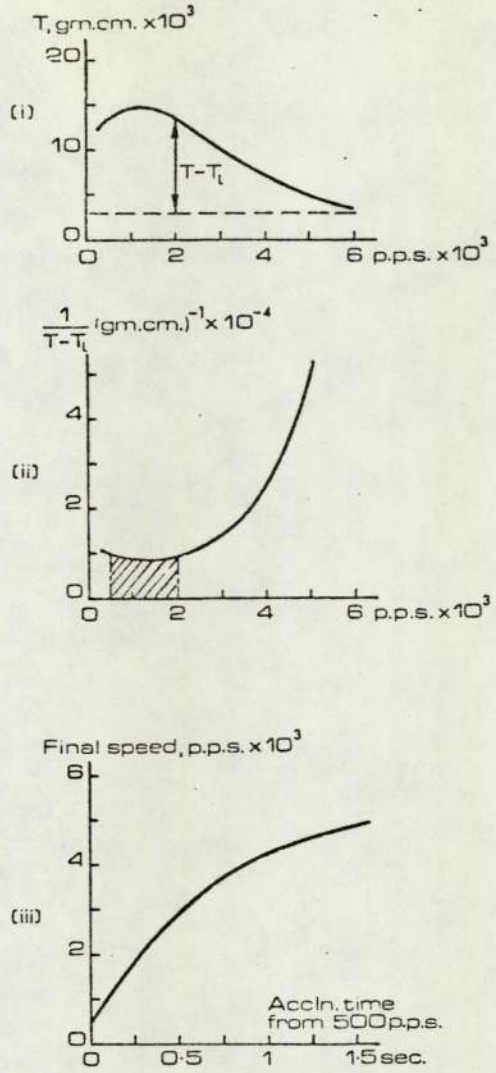

FIG. 3 Example of calculation of acceleration times for a 200 step/rev. motor

$$2000 \text{ gm.cm.}^2 \times 0.135 \text{ (gm.cm.sec}^{-1}) \times \frac{\text{sec}^2}{981 \text{ cm}} = \underline{0.28 \text{ seconds}}$$

The minimum times taken to accelerate to other speeds, derived in the same way as that above, are shown in Fig. 3(iii), and this curve therefore indicates the optimum manner in which the stepping frequency can be ramped in order to accelerate the given load inertia in minimum time.

3. APPROACH USING STEADY-STATE TORQUE/DISPLACEMENT CHARACTERISTIC

3.1 General

This approach is particularly useful when it

required to predict the shaft angle at any
tant of time following the application of a
p pulse or a series of step pulses, for
mple, to predict the starting rate under
ious load conditions.

For any stepping motor, the torque-
placement curve is periodic and has a shape
ilar to the curves shown in Fig. 4: the

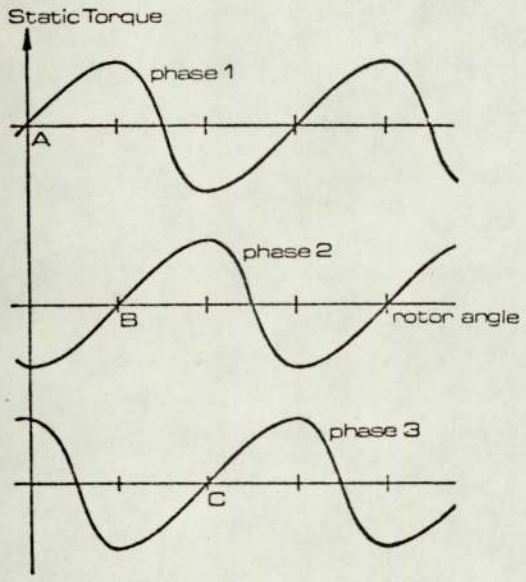

. 4 Torque-displacement curves for 3-phase, 3-stack VR motor

tantaneous electrically developed torque
rted on the rotor depends on the displacement
m equilibrium and the instantaneous stator
rent(s). If, in Fig. 4, phase 1 alone is
ited, the rotor will tend to settle in one of
stable equilibrium positions, such as 'A',
subsequent rotation to a new step position
caused by switching off phase 1 and switching
either phase 2 or phase 3, both of which have
que curves which are displaced relative to
se 1. If, for example, phase 2 is excited,
rotor experiences a forward accelerating
que and, in the absence of any steady load
que, the rotor will ultimately settle in the
ition B.

The torque curves for each phase are nomi-
ly identical and the motion of the rotor can
considered in terms of its response to a
gle torque curve which 'shifts' by one step
angle each time a switching operation is performed, i.e. each time a step command occurs. In practice the shift cannot be accomplished instantaneously, as a finite time is required for the current in one phase to decay and for the current in the next phase to build up, but in many cases the motor/drive-circuit time constant is small (or a constant current drive is used) and the curve can then be regarded as shifting instantaneously.

3.2 Method with Non-Linear Torque-Angle Curve

To be able to predict the rotor position at any instant of time, it is necessary firstly to know the time(s) at which the step pulses occur (and hence the times when the torque curve is shifted), and secondly it must be possible to solve the equation of motion for the rotor when the torque varies as shown in Fig. 4.

The general equation of motion of the rotor is

$$T(\theta_i-\theta) = J\frac{d^2\theta}{dt^2} + K_v\frac{d\theta}{dt} \qquad (4)$$

where θ is the angle turned through by the rotor and $T(\theta_i-\theta)$ is the torque developed at an angle $(\theta_i-\theta)$ from the currently effective equilibrium position which is given (assuming no loss of synchronism) by $\theta = \theta_i$, and acts in a direction such as to reduce $(\theta_i-\theta)$.

Equation (4) cannot usually be solved by an analytical method because $T(\theta_i-\theta)$ is usually a non-linear function of $\theta_i-\theta$. (If it was a linear function, it would be possible to write down a solution for angle $\theta_i-\theta$ in terms of time t, see section 3.4.) The solution for $\theta(t)$ can, however, be computed numerically, using for example the well-known Runge-Kutta process, for which the second-order equation (4) is split into two first order equations:

$$\frac{d\Omega}{dt} = \frac{T}{J}(\theta_i-\theta) - \frac{K_v}{J}\Omega \qquad (5)$$

$$\frac{d\theta}{dt} = \Omega \qquad (6)$$

subject to specified initial conditions for θ and Ω. The shape of the T vs. $(\theta_i-\theta)$ curve is specified either by means of a polynomial or a series

of data points. (It ought perhaps to be mentioned that the integrations required to solve equations (5) and (6) - a process analagous to that of obtaining the area under a curve - are easily adapted to be performed on a digital computer. In fact the solution of this type of differential equation is so often required that standard programs are readily available.)

Starting from a given state, for example the rotor at rest at position 'A', say $\theta = 0$, when the first shift occurs (at $t = 0$), the position of the rotor at any subsequent time t is computed from equations (5) and (6), with the initial conditions $\Omega = 0$, $\theta = 0$, and $\theta_i = \theta_s$, where θ_s is the step angle. Typically the response of rotor position as a function of time will be as shown in Fig. 5, and the rotor would ultimately settle in position B. If the next shift occurs at time t_1 however, the initial conditions for the next stage of the solution are the values of θ and Ω ($= d\theta/dt$) at t_1 obtained from the first stage of the solution, which need not therefore be continued beyond time t_1. Note that when the second shift occurs, an instantaneous change θ_s is made in θ_i and $\theta_i - \theta$ increases correspondingly. The computation process can be continued for any number of steps, the initial conditions for each step being obtained from the solution during the previous step. In this way a complete position-time curve can be predicted very simply. Once the torque-angle data and the load parameters J and k_v have been specified, the times t_1, t_2 etc. at which the step pulses occur completely define the response.

The optimum switching times needed to minimise the total response time for the two-step sequence in Fig. 5 could easily be obtained, or the so-called electronic damping techniques could be studied by obtaining the response when 'braking pulses' are used to bring the rotor rapidly to rest.

.3 Variation in exciting current

Throughout the preceding discussion it has been assumed that the stator currents can be switched on and off instantaneously. The finite

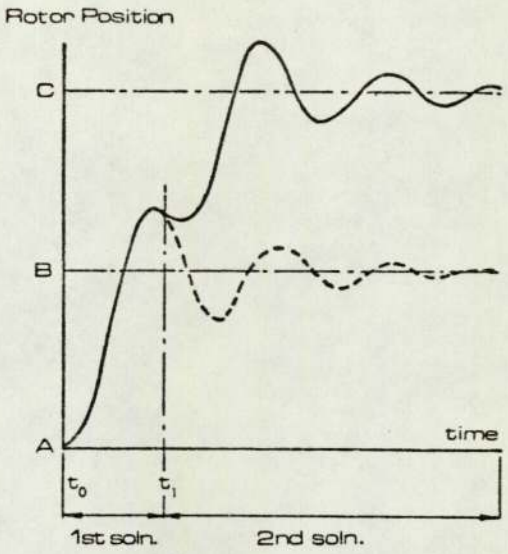

FIG. 5 Typical position/time curve for 2-step sequence

rise and fall times of the stator current must, however, be allowed for if these times are comparable with the time period being studied. For example, if the stator time constant is 2msec, it could be ignored if the study was of a single-step response which lasted for 150msec. But if a second switching occurred after say 5msec, then it becomes important to take account of the stator time constant.

The simplest way to account for this effect is to introduce a factor $(1 - e^{-t/\tau})$ which multiplies the torque term $T(\theta_i - \theta)$ in equation 4. This allows for the torque increasing in proportion to the stator current (which rises with a time-constant τ). For the decay condition, the factor is $e^{-t/\tau}$. Strictly speaking this treatment is only valid if (i) the shape of the torque-angle curve is independent of the current, and (ii) the peak magnitude is proportional to the current. Neither of these limitations are fulfilled in general, though P.M. motors and highly saturated V.R. motors usually satisfy requirement (ii). There is thus some approximation involved in simply multiplying by an experimental term and it is better, though more complicated, to use data defining the torque/angle curves as non-linear functions of both θ

stator current. The torque at any instant of and any position θ is then obtained directly, eing assumed that the current rises and ys exponentially. (It often happens that rise and decay time constants are different, this difference must be accounted for by s of two time-constants, one for switch-on one for switch-off.)

Approximate (Linearised) Method

It is sometimes useful, for example in mating the natural frequency of oscillation, ne single-step time, to make the assumption the torque-angle curve is linear about the librium point.[1] It is then possible to in an analytical solution of the equation of on, i.e. the solution for θ as a function of n be expressed directly in terms of the meters of the motor and its drive system. effect of changes in the parameters can then asily seen.

If the slope of the torque-angle curve umed constant) is k_T, the equation of motion

$$\frac{\theta}{2} + K_v \frac{d\theta}{dt} + k_T\theta = 0 \qquad (7)$$

h is the equation of a simple second order em. By writing the equation in the standard

$$+ 2\xi\omega_n \frac{d\theta}{dt} + \omega_n{}^2\theta = 0 \qquad (8)$$

e

$$= \sqrt{\frac{k_T}{J}} \qquad (9)$$

$$\frac{K_v}{2\sqrt{k_T J}} \qquad (10)$$

system is characterised by two simple meters, ω_n, the natural frequency, and ξ, damping ratio. The response of the system, any given set of initial conditions, is ly expressed in terms of exponentially ying oscillatory terms and the standard tions are available in many textbooks.

The accuracy of the linearised analysis obviously depends on how well a straight-line approximation fits the actual torque curve. Fortunately, most stepping motors are operated with torque curves which are fairly linear over the region of operation, i.e. from equilibrium up to near the peak torque, though an element of judicious approximation is involved in deciding just where to put the straight line. For example, in Fig. 6, which relates to a 3-phase

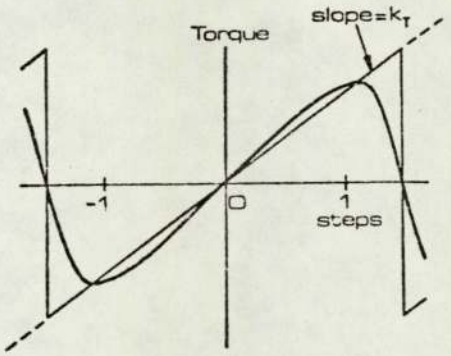

FIG. 6 Linearised representation of torque-displacement curve

VR motor, the torque curve is almost straight for displacements up to 1 step on either side of equilibrium. Beyond the peak point, however, the straight line approximation indicates increased restoring torque, while in reality the torque falls off towards the unstable equilibrium position. If operation in this region is involved, it becomes necessary to truncate the linear curve, as shown. This general question is discussed in reference 2, where the linearised representation is used to predict 'resonances'.

4. APPROACH USING COMPLETE MODEL OF MOTOR

4.1 General

Sections 2 and 3 have described simple methods for obtaining an approximate prediction of motor dynamic behaviour in which the changes taking place in the electrical circuits are neglected. The designer and research and development engineer may well require a more sophisticated mathematical model of the machine

d its drive circuits which can be used to plot y of the system variables (e.g. motor speed, gle or currents) as time functions for any sired mode of operation. With such a model it comes possible to investigate the effect on tor performance of changes in different system arameters, to test the performance of a pro-sed new design, or to check the reliability of impler, quicker, performance calculations for ypical situations, so that these may be used ith greater confidence.

The development of such a model of the tepping-motor system follows the same pattern nd uses the same technique as has been followed or conventional machines.[3]

.2 Form of the mathematical model

Any motor can be described by a set of ifferential equations for the electric circuits lus an equation for the electrically developed orque and the mechanical differential equations elating torque, friction, inertia, acceleration, peed and angular displacement. These equations onstitute a mathematical model of the system hich, when the appropriate numerical data for he resistances, inductances, currents, po-itions, etc. have been inserted, can be used o predict any required mode of behaviour.

For simplicity, consider first a machine ith only one winding. This is described, elec-trically, by the single differential equation

$$V = RI + \frac{d\psi}{dt} \tag{11}$$

where

$$\psi = LI \tag{12}$$

is the flux linkage with the winding of induc-tance L. Thus

$$V = RI + L\frac{dI}{dt} + I\frac{dL}{dt}$$

$$= RI + L\frac{dI}{dt} + I\Omega\frac{dL}{d\theta} \tag{13}$$

where $\Omega(= d\theta/dt)$ is the speed of rotation, as in the previous sections, and therefore

$$\frac{dI}{dt} = -L^{-1}\left(\Omega\frac{dL}{d\theta} + R\right)I + L^{-1}V \tag{14}$$

If it is assumed that the inductance depends only upon θ, not on the current (i.e. if saturation is neglected), then the electrically developed torque is simply given by

$$T = \tfrac{1}{2} I \frac{d\psi}{d\theta} = \tfrac{1}{2} I^2 \frac{dL}{d\theta} \tag{15}$$

It remains to add the mechanical equations, which are the same as in the previous method (equations 5 and 6):

$$\frac{d\Omega}{dt} = \frac{1}{J}(T - F_v\Omega) \tag{16}$$

$$\frac{d\theta}{dt} = \Omega \tag{17}$$

It will be observed that these equations have been arranged as in section 3.2 as a set of first-order simultaneous differential equations and that here they are three in number, compared with the two of the previous method (because of the addition of the electric circuit equation).

In a practical stepping motor there is more than one winding, but it is simply necessary to add the additional circuit equations (including the effects of mutual coupling). The flux linkages are then given by a set of simultaneous algebraic equations which for a machine with n coils are

$$\begin{bmatrix}\psi_1\\ \psi_2\\ \vdots\\ \psi_n\end{bmatrix} = \begin{bmatrix}L_{11} & L_{12} & \cdots & L_{1n}\\ L_{21} & L_{22} & \cdots & L_{2n}\\ \vdots & \vdots & & \vdots\\ L_{n1} & L_{n2} & \cdots & L_{nn}\end{bmatrix}\begin{bmatrix}I_1\\ I_2\\ \vdots\\ I_n\end{bmatrix} \tag{18}$$

or

$$[\psi] = [L][I] \tag{19}$$

where the matrix notation has been used for convenience.

The equations can be written down in the form ready for solution in exactly the same way as for the simple one-coil case discussed above:

$$\left.\begin{aligned}
\frac{[\quad]}{t} &= -[L]^{-1}\left(\frac{d[L]}{\Omega\, d\theta} + [R]\right)[I] + [L]^{-1}[V] \\
T &= \tfrac{1}{2}[I_t]\frac{d[\psi]}{d\theta} = \tfrac{1}{2}[I_t][I]\frac{d[L]}{d\theta} \\
\frac{d\Omega}{dt} &= \frac{1}{J}(T - F_v\Omega) \\
\frac{d\theta}{dt} &= \Omega
\end{aligned}\right\} \quad (20)$$

e. a set of n + 2 simultaneous, first-order fferential equations.

3 Solution of the equations

In order to specify the problem to be lved it is necessary to give the circuit resisnces and inductances (as functions of disacement θ), the inertia and viscous damping nstant, the voltage waveforms to be applied .e. the voltage level(s) and switching sequence) d the initial conditions at the start of the lution. The inductance functions will be tained by measurements (or in some cases calIations may be possible) and can be expressed ther in tabular form, to be referred to with opropriate interpolation during the computaon, or in Fourier-series form. As a simple ample, for a machine having an equal number of ator and rotor teeth (N_R), the idealised riation of self inductance of a coil is

$$= L_o + \hat{L}\cos N_R(\theta - \theta_o)$$

ere θ_o takes account of the initial rotor sition. Strictly, to allow for harmonics,

$$= \sum_{r=0}^{n} \hat{L}_r \cos N_R\, r\,(\theta - \theta_o)$$

d a similar expression applies to mutual inducnces in a multi-coil situation.

Having specified all the above data, the uations can be solved using one of a number of ll known numerical integration routines[4] (of e same kind as used in the section 3.2) and e transient behaviour of the motor obtained as set of curves (or sets of numbers) showing the riation with time of any of the variables.

An example of this kind of solution for the displacement, θ, as a function of time following the sudden switch-on of a variable-reluctance stepping motor is shown in Fig. 7, together with

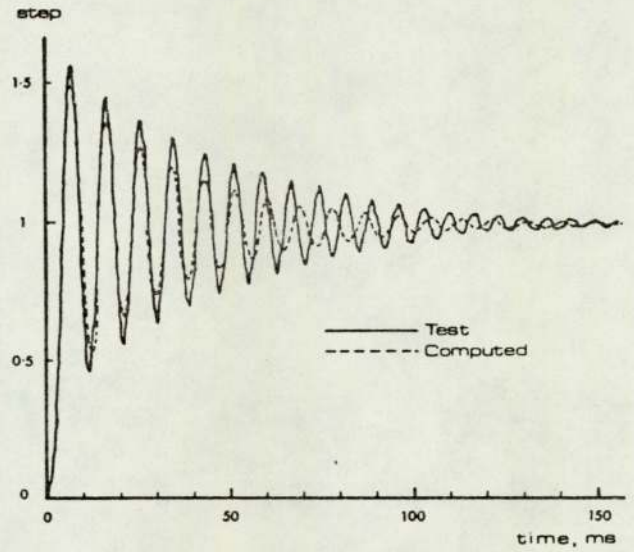

FIG. 7 Experimental and computed single-step response of a variable-reluctance stepping motor

the corresponding experimental curve, measured using the same motor. The data for the program consisted of measured resistances, inductances and viscous damping coefficient. The inductances were represented by a Fourier series in θ but only the first two terms in the series were used because for this particular motor they were found to give sufficient accuracy.

The numerical integration method used for this solution was a Runge-Kutta 4th-order, fixed-step-length method with deferred approach to the limit.[4] (This technique gives an accuracy comparable with that of a 5th-order Runge-Kutta method and is useful when an estimate of the error per integration step is required. For repeated calculations using a step length which is known to give sufficient accuracy, it is more efficient to use the faster, simple 4th-order Runge-Kutta method.) The time taken for the solution using an ICL 1906A computer was 24 secs. The time required for the computation increases with the number of coils, the number of harmonics in the

Fourier series and the length of the computation and inversely with the computational step length specified.

4.4 The complete model

In the form described above, the model does not allow for the effect of magnetic saturation, which makes all the inductances functions of the instantaneous currents in all the various windings (or permanent magnet characteristics). When including saturation it is helpful to work in terms of the flux linkages rather than the inductances and the equation for the electromagnetic torque must then be expressed in terms of the co-energy of the system, i.e.

$$T = \frac{\partial W'}{\partial \theta} \qquad (21)$$

It is now necessary to read in and to store in some form the necessary information relating flux linkages to both displacement and currents. The amount of data to be handled in describing the saturation depends on the accuracy of this description and on the complexity of the stepping motor system, i.e. the number of coils simultaneously excited. It can be used either in the form of equations describing the appropriate functions relating flux linkage to displacement and current(s) or in tabular form.

Clearly the technique described here is extremely powerful and all aspects of system dynamic behaviour can be represented providing they can be quantified and expressed as algebraic or differential relationships. For example the electrical driving circuits can be represented in detail in the model as also can the dynamic equations of the load. Parameter variations, such as those due to temperature rise, can also be allowed for.

5. ACKNOWLEDGEMENTS

The authors are much indebted for financial support to the Science Research Council and to Westool Ltd.

6. REFERENCES

1 Hughes A and Lawrenson P J: 'Introduction to Electromagnetic Damping in Stepping Motors', these Proceedings.

2 Lawrenson P J and Kingham I E: 'Low-Frequency Resonances', these Proceedings.

3 Lawrenson P J, Mathur R M and Stephenson J M: 'Transient Performance of Reluctance Machines', Proc IEE, 1971, 118, (6), pp 777-783.

4 Fox L and Mayers D F: 'Computing methods for scientists and engineers', O.U.P., 1968, p 176.